SR-Site – hydrogeochemical evolution of the Forsmark site

Joaquín Salas[1], Maria José Gimeno[2], Luís Auqué[2]
Jorge Molinero[1], Javier Gómez[2], Iker Juárez[1]

[1] Amphos 21
[2] University of Zaragoza

December 2010

SKB

SR-Site – hydrogeochemical evolution of the Forsmark site

Joaquín Salas[1], Maria José Gimeno[2], Luís Auqué[2]

Jorge Molinero[1], Javier Gómez[2], Iker Juárez[1]

[1] Amphos[21]

[2] University of Zaragoza

December 2010

Update notice

The original report, dated December 2010, was found to contain factual errors which have been corrected in this updated version. The corrected factual errors are presented below.

Updated 2013-11

Location	Original text	Corrected text
Page 29, section 3.4.3, third bullet	(NW: 1,628,519 m / 6702421; SE: 1,636,272 m / 6694615)	(NW: 1,628,263 m / 6,703,763; SE: 1,637,263 m / 6,694,763)
Page 37, Table 4.2, column "Deep Saline", row Stot	$1.000 \cdot 10^{-4}$	$1.067 \cdot 10^{-4}$
Page 37, Table 4.2, column "Deep Saline", row S(VI)	$1.000 \cdot 10^{-4}$	$1.067 \cdot 10^{-4}$
Page 37, Table 4.2, column "Littorina", row Stot	$9.385 \cdot 10^{-3}$	$9.391 \cdot 10^{-3}$
Page 37, Table 4.2, column "Littorina", row S(-II)	$8.245 \cdot 10^{-6}$	$1.423 \cdot 10^{-5}$
Page 48, Figure 6-4	Wrong data used in figure	Figure updated with correct data
Page 52, Figure 6-9	Wrong data used in figure	Figure updated with correct data
Page 57, Figure 6-16	Wrong data used in figure	Figure updated with correct data
Page 58, Figure 6-17	Wrong data used in figure	Figure updated with correct data
Page 59, Figure 6-18	Wrong data used in figure	Figure updated with correct data
Page 61, Figure 6-20	Wrong data used in figure	Figure updated with correct data
Page 62, Figure 6-21	Wrong data used in figure	Figure updated with correct data
Page 63, Figure 6-22	Wrong data used in figure	Figure updated with correct data
Page 64, Figure 6-23, plot Eh (mV), S(-II) (mol/L) and Fe (mol/L)	Wrong data used in figure	Figure updated with correct data
Page 65, Figure 6-24, plot Fe (mol/L), S(-II) (mol/L) and Eh (mV)	Wrong data used in figure	Figure updated with correct data
Page 67, Figure 6-25, plot Fe (mol/L), S(-II) (mol/L) and Eh (mV)	Wrong data used in figure	Figure updated with correct data
Page 71, Figure 7-2, plot to the right	Wrong data used in figure	Figure updated with correct data
Page 72, Figure 7-3	Wrong data used in figure	Figure updated with correct data
Page 78, Figure 7-9	Wrong data used in figure	Figure updated with correct data
Page 81, Figure 7-12	Wrong data used in figure	Figure updated with correct data
Page 83, Figure 7-15, plot to the right	Wrong data used in figure	Figure updated with correct data
Page 85, Figure 7-16, plot to the lower-right	Wrong data used in figure	Figure updated with correct data
Page 112, Figure 9-1, plots at the bottom	Wrong data used in figure	Figure updated with correct data
Page 126, Reference Pedersen 1997b	SKB TR-07-22	SKB TR 97-22
Page 126, Reference Selnert et al. 2008	SKB P-07-39	SKB P-07-139
Page 149, section A1.9.1, SOLUTION 1 Deep Saline	S(6) 906	S(6) 10
Page 153, section A1.9.2, SOLUTION 1 Deep Saline end-member	S(6) 906	S(6) 10
Pages 167 to 172, Appendix 4, Table A4.1–A4.5	Wrong data used in tables	All tables updated with correct data

The PHREEQC database "TDB_SKB-2009_Amphos21.dat" (SKBdoc nbr.1261302) used in the calculations reported in Salas et al (2010), SKB-TR-10-58, had at some stage a missing "+" sign in the reaction: $Fe^{2+} + HS^- \leftrightarrow FeS(aq) + H^+$. The error was detected and the database was corrected.

After the publication of the report it was discovered that some of the calculations had been performed with the earlier erroneous version of the database. This error affected the calculation results for iron and sulphide, and as a consequence, the calculated Eh values were slightly affected.

In addition, the saturation with hydroxyapatite, which was used to calculate the concentration of phosphate, included a temperature correction (from 25 to 15°C) in all the Laxemar calculations reported in Gimeno et al (2010), SKB-R-10-60, but this was only included in some of the Forsmark calculations. To make all calculation results consistent, a value of $\Delta H = -36.155$ kcal/mol for the reaction listed in page 36 of Salas et al. (2010) was added to all Forsmark calculations. The new Appendix 4 and the new Figure 6-9 show the calculated phosphate concentrations corrected when necessary.

Abstract

The present work has involved the development of a methodology in order to simulate the evolution of the groundwater composition within the candidate repository site of the Forsmark area. A series of climate periods is expected to be probable after the repository closure (temperate, periglacial and glacial) and, eventually, the area could be submerged under seawaters or under a lake of glacial melt waters. These environmental conditions will affect groundwater flow and composition around of the candidate repository volume. The present report summarizes the results obtained by the calculations which reproduce the hydrogeochemical evolution in the Forsmark area, and within the candidate repository volume.

The hydrogeochemical evolution of groundwaters is one of the key factors affecting the chemical stability of the buffer and the canister. In this way, the main objective of the hydrogeochemical simulations is to assay the evolution of a series of safety assessment factors, such as salinity, redox potential, pH, and concentrations of iron, sulphide and potassium, among others.

Using ConnectFlow, previous hydrological calculations have provided the transport of (1) the fractions of selected reference waters (Deep Saline, Old Meteoric, Glacial, Littorina and Altered Meteoric groundwaters), or (2) salinities, depending on the working team (Serco or Terrasolve). The results of the regional-scale groundwater flow modelling for each specific climate period are used as input of the geochemical models. Groundwater compositions have been modelled using PHREEQC, through mixing and chemical reactions between the waters obtained from the hydrogeological models and the reactive fracture-filling minerals. Both models (hydrological and geochemical) are not fully coupled, and it allows a description of the geochemical heterogeneity, which otherwise would be hard to attain.

The stage of the open repository has been non-numerically analysed. Aspects as salinity, redox conditions, oxygen consumption in backfill, precipitation and/or dissolution of minerals, and the effects of grout, shotcrete and concrete on pH values, have been extensively discussed.

The main hydrogeochemical process reproduced during the temperate period has been the infiltration of the recent meteoric water (Altered Meteoric end-member), generating a front which progressively reaches the repository depth. As a consequence, salinities decrease within the candidate repository volume. However, the safety criterion in reference to the summation of the cationic species ($\sum q[M^{q+}]$ > 4 mM) remains higher than 10 mM, whereas pH is maintained in a range of 6.5–8.0, in equilibrium with respect to calcite. The maximum iron and sulphide concentrations computed under these hydrogeological conditions are limited by values of 10^{-4} and 10^{-5} mol/L, respectively. On the other hand, the calculated Eh values remains below –125 mV during most of the temperate period.

During the glacial cycle, (1) infiltration of Glacial melt waters, (2) upconing of Deep Saline waters, and (3) the hydrological and the geochemical effects of a frozen soil under the ice sheet, have a strong influence controlling the hydrogeochemical evolution within the candidate repository volume. The calculated safety function $\sum q[M^{q+}]$ is lower than 4 mM in a wide period of the glacial cycle, whereas the computed pH values remains below 9.75. On the other hand, the computed Eh values range between –25 and –375 mV.

The results computed under the submerged saline period (assumed to be similar to the Littorina Sea stage, 3,000 years ago) show that the hydrogeochemical characterization of groundwaters within the candidate repository volume are similar to those calculated for the initial temperate period. However, groundwaters are slightly less saline because the front of the marine waters is above the candidate repository volume.

An assessment of the possible amount of certain components in the future evolution of the groundwater system at Forsmark has been performed (such as colloids, dissolved and total organic carbon, nitrite, ammonia, acetate, methane and molecular hydrogen). Pernicious effects of these components are mainly related to canister corrosion as many of them are corroding agents, or can enhance contents of such agents through different metabolic processes. This apparently heterogeneous group of parameters include components for which either the available information is not sufficient for a precise quantitative evaluation of their future evolution, or cannot be modelled with the same methodology as the rest of the geochemical parameters. Most of them are intimately related to the microbial activity conditioning, or being conditioned by different redox processes. This fact makes their evaluation a difficult task, as a consequence of the knowledge of microbial processes in the groundwaters of crystalline systems.

Contents

1   Introduction

With the objective of sitting a final repository for spent nuclear fuel according to the KBS-3 concept (see Section 1.3), the Swedish Nuclear Fuel and Waste Management Company (SKB) has conducted site investigations at the Forsmark area. The present study has been performed in the framework of the Safety of the final Repository (SR Site) exercises.

Hydrochemical conditions are crucial in the safety assessment of an underground repository for spent fuel. The Swedish concept for a deep geological repository foresees a geological environment that must fulfil a number of hydrochemical parameters and safety functions related with pH, Eh, dissolved oxygen, sulphide, calcium, sodium and phosphate concentrations, among the most relevant (see Section 1.3).

The hydrogeochemical changes and evolution at repository depth will be strongly conditioned by the hydrogeological conditions of the site. In this way, the estimation of the hydrochemical evolution at repository depth during a series of climatic periods is of importance for SKB. The hydrochemical calculations summarized in the present work are based on sophisticated hydrogeological models simulating groundwater evolution in the Forsmark area during temperate, periglacial, glacial, submerged (under a lake of glacial melt waters and under seawaters), and CO_2-rich atmosphere periods.

1.1   Objectives and scope

The main objective of the present work is to estimate the hydrogeochemical evolution of the Forsmark site along different climatic periods of interest in the SR Site assessment (Figure 1-1). With this aim, a
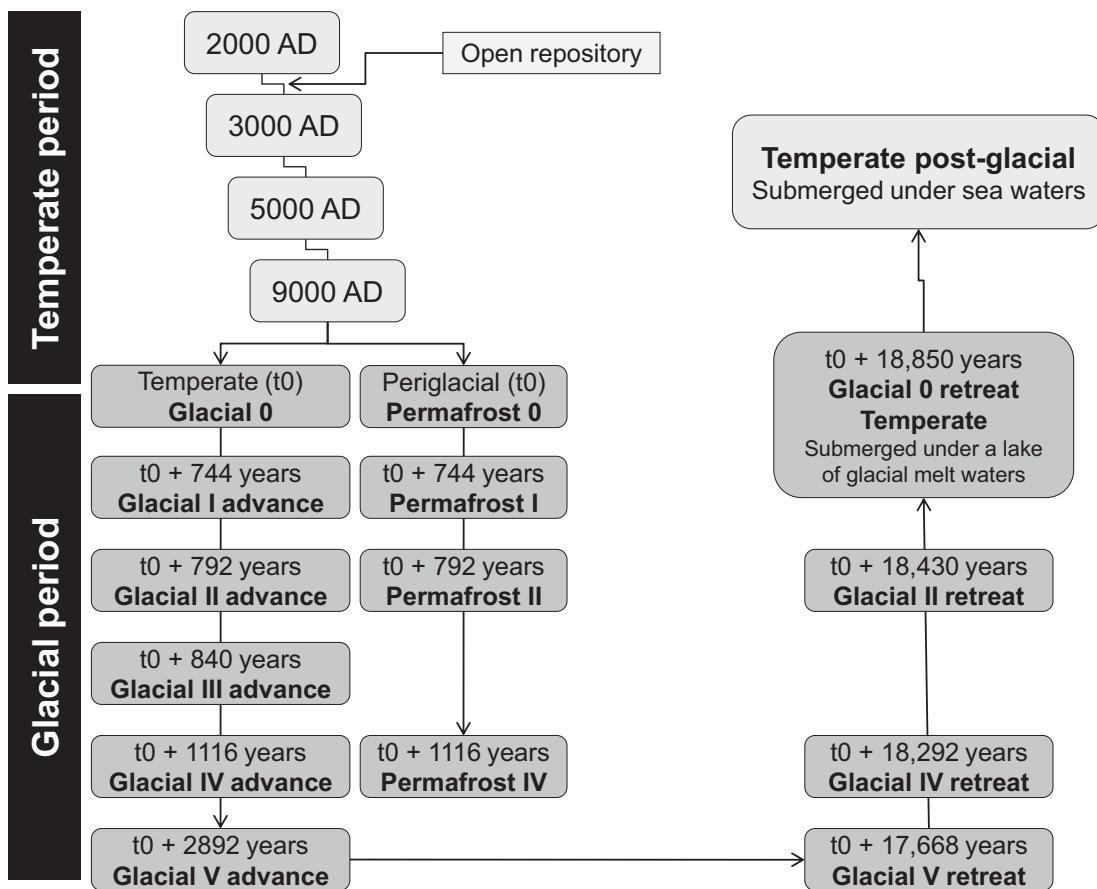
Figure 1-1. *Scheme of the sequence of the climatic and hydrological periods modeled and discussed in the framework of the present study.*

numerical methodology has been developed, based on the input of hydrogeological data estimated in previous calculations. In this way, the groundwater evolution has been simulated during:

1. A temperate period of 7,000 years, from the present day. The influences of a CO_2-rich atmosphere and the stage of open repository have been also discussed.

2. A complete glacial cycle (ice advance and retreat) of 18,850 years. Additionally, four alternative stages considering on the permafrost development during the ice advance have been also evaluated.

3. The last stage of the glacial cycle is represented by two submerged periods: first under a lake of glacial melt waters (fresh waters) and, later, under seawater.

No calculations have been performed in order to simulate the operation phase of the repository. This period has been conceptually discussed.

The most relevant data needed for this investigation are the geological structure of the site, the hydrogeological data and associated conceptual assumptions, the hydrogeochemical and mineralogical data from the Forsmark Site Descriptive Model (SDM) work, and the thermodynamic data used in the geochemical calculations.

1.2   Approach

In order to evaluate the evolution of the safety function criteria indicators around the candidate repository domain (see Section 1.3), a series of groundwater flow and geochemical simulations have been performed. They reproduce the hydrogeological environment in each climate period affecting the Forsmark area, at present and in the future. The hydrogeochemical calculations are described and discussed in this report.

The input data used in the hydrogeochemical calculations are:

1. Hydrogeological data provided by Serco, TerraSolve and computed aided Fluid Engineering AB and SF GeoLogic AB (see Section A1.1), described in Section 3.4 and Appendix 1. They are the fractions of the 5 end-member (temperate and submerged periods) and salinities (remaining glacial cycle).

2. Hydrochemical data described in Chapter 4. They consist in:
    •   chemical composition of the end-member waters, Deep Saline, Old Meteoric, Glacial, Littorina and Altered Meteoric (Section 4.4 and Section A1.7.1),
    •   thermodynamics database (Section 4.3),
    •   and the definition of the mineral equilibriums: calcite, quartz, hydroxyapatite and Fe(III) oxyhydroxides and/or amorphous Fe(II) sulphides (Section 4.1).

The methodology of the calculations has been explained in sections 4.1 and 4.5, and summarized in Appendix 1.

Hydrological models results (by the teams of Serco, using ConnectFlow, and TerraSolve or computer-aided Fluid Engineering, using DarcyTools) have provided groundwater composition as fractions of selected reference waters (Deep Saline, Old Meteoric, Glacial, Littorina and Altered Meteoric groundwaters, in the case of the temperate and submerged periods), or salinities (in the case of the operation period and the glacial and periglacial periods). When salinities have been provided (TerraSolve and computer-aided Fluid Engineering), they have been transformed to end-members fractions. These spatial and time distributions of the fractions of the end-member groundwaters have been used as inputs for hydrogeochemical calculations.

Hydrogeological models are constructed to simulate complex three-dimensional geological conditions, including main hydraulic conductor domains and heterogeneous hydraulic properties based on the upscaling of discrete fracture network models. Such hydrogeological models solve the groundwater flow equation (accounting for variable density driven flow), and the classical advection-dispersion transport equation. Also, matrix diffusion is accounted for. This not only allows accounting for density driven flow. The most important impact is on the exchange of solutes between the porewater in the matrix and the mobile water in the fractures.

The results of the regional-scale groundwater flow modelling are used as input data for the geochemical models. Groundwater compositions have been calculated using PHREEQC /Parkhurst

and Appelo 1999/, and considering the mixing fractions obtained by the hydrogeological models (considering different end-member waters), and the chemical reactions between the resulting aqueous solutions and the reactive fracture-filling minerals. A methodology has been developed in order to combine the hydrogeological model results with hydrogeochemical calculations (Figure 1-2). This methodology is able to evaluate the most likely hydrochemical evolution of the sites taking into account the computed hydrogeological framework. This approach has already been applied in the previous safety assessment exercise (SR-Can, /Auqué et al. 2006/). A procedure was developed in order to implement the methodology semi automatically.

The chemical composition of end-member waters is known from the Site Descritive Models (SDM) reports /Gimeno et al. 2008, 2009/, although several adjustments have been done for this task (see Section 4.1). Then, theoretical conservative compositions of the groundwater are computed with PHREEQC by using the mixing fractions obtained from the results of the hydrogeological models. Finally, chemical speciation and geochemical water rock interaction calculations are performed (with PHREEQC) in all the selected nodes over the selected times, in order to evaluate the hydrogeochemical conditions of the sites.

A series of geochemical constraints has been applied in the calculations. The aqueous solutions have been assumed to be in thermodynamics equilibrium with calcite, quartz, hydroxyapatite and Fe(III) oxyhydroxides (hematite). However, other geochemical assumptions have been evaluated, such as equilibrium with respect to amorphous Fe(II) sulphides instead of hematite, and uncoupling the redox reactions between S(VI) and S(-II) species (see Section 4.5.2).

For the statistical treatment of the results, a so-called "Base Case" has been defined. Within the candidate repository volume, the statistical distributions of the redox potential and the iron concentrations consider the results obtained assuming equilibrium with respect to amorphous Fe(II) sulphides and those obtained assuming equilibrium with respect to Fe(III) oxyhydroxides.

HYDROGEOLOGICAL RESULTS
Mixing proportions (3 or 5 end-members) in each point of the rock volume.
Selection of the points where geochemical calculations will be performed
(repository depth layer and vertical cross sections)

PHREEQC INPUT
pqi file with mixing proportions (and the chemical composition of the end-members)
+ equilibrium reactions with a set of minerals for each point

PHREEQC CALCULATIONS
Mixing and reaction simulations with PHREEQC

PHREEQC OUTPUT
pqo file with the chemical composition, including pH, Eh, molalities and activities
of the chemical components and the saturation indexes

SELECTION OF THE OUTPUT DATA
Selected output with the key parameters

RESULTS TREATMENT
Statistical calculations and representation (box-and-whiskers plots), and
graphical representation of the results (Surfer and Voxler interpolations)

Figure 1-2. *Scheme of the methodology applied for the evaluation of the chemical composition of the groundwaters under the climatic and the hydrologic periods shown in Figure 1-1.*

1.3 Key geochemical parameters in the analysis of the safety assessment of the candidate repository

In order to assess the safety of the future repository, a series of geochemical safety functions have been defined as requirements of the groundwater composition. In this way, the computed evolution of some geochemical parameters has been especially analyzed.

The primary safety function of the KBS-3 concept is to completely isolate the spent nuclear fuel within copper canisters over the entire assessment period. Should a canister be damaged, the secondary safety function is to retard any releases from the canisters. For the part of the geosphere surrounding the repository, most of the function indicators (Figure 1-3) concern the compositions of groundwaters in the fracture network; several of the groundwater characteristics are essential for providing a chemically favourable environment for the repository.

1.3.1 Salinity and concentration of solutes

The salinity of the groundwater should neither be too high, nor too low. Groundwaters of high ionic strengths would have a negative impact on the buffer and backfill properties, in particular on the backfill swelling pressure and hydraulic conductivity. In general, ionic strengths corresponding to NaCl concentrations of approximately 1.2 M are a safe limit for maintaining backfill properties, whereas the corresponding limit for the buffer is around 1.7 M /SKB 2006a/. The limit of tolerable ionic strength is however strongly dependent on the material properties, in particular for the backfill.

Safety functions related to containment

Canister

Can1. Provide corrosion barrier
Copper thickness > 0

Can2. Withstand isostatic load
Load < 45 MPa

Can3. Withstand shear load

Buffer

Buff1. Limit advective transport
a) Hydraulic conductivity < 10^{-12} m/s
b) Swelling pressure > 1 MPa

Buff2. Reduce microbial activity
Density; high

Buff3. Damp rock shear
Density < 2,050 kg/m³

Buff4. Resist transformation
Temperature < 100°C

Buff5. Prevent canister sinking
Swelling pressure > 0.2 MPa

Buff6. Limit pressure on canister and rock
a) Swelling pressure < 15 MPa
b) Temperature > −4°C

Deposition tunnel backfill

BF1. Counteract buffer expansion
Density; high

Geosphere

R1. Provide chemically favourable conditions
a) Reducing conditions; Eh limited
b) Salinity; TDS limited
c) Ionic strength; $\Sigma q[M^{q+}]$ > 4 mM charge equiv.
d) Concentrations of HS^-, H_2, CH_4 organic C, K^+ and Fe; limited
e) pH; pH < 11
f) Avoid chloride corrosion; pH > 4 and $[Cl^-]$ < 2 M

R2. Provide favourable hydrologic and transport conditions
a) Transport resistance in fractures, F; high
b) Equivalent flow rate in buffer/rock interface, Q_{eq}; low

R3. Provide mechanically stable conditions
a) GW pressure; limited
b) Shear movements at deposition holes < 0.05 m
c) Shear velocity at deposition holes < 1 m/s

R4. Provide favourable thermal conditions
a) Temperature > −4°C (avoid buffer freezing)
b) Temperature > 0°C (validity of can shear analysis)

Figure 1-3. *Safety functions (bold), safety function indicators and safety function indicator criteria. When quantitative criteria cannot be given, terms like "high", "low" and "limited" are used to indicate favourable values of the safety function indicators. The colour coding shows how the functions contribute to the canister safety functions Can1 (red), Can2 (green) or Can3 (blue).*

In general, the evolution of salinities is strictly controlled by the evolution of the diluted groundwater (altered meteoric and/or glacial origin groundwaters). The groundwater salinities in the Forsmark area are mainly controlled by the chloride concentration, and sodium and calcium.

Chloride and divalent cation concentrations

Chloride is not listed among the safety functions indicator criteria, but it is used when selecting radionuclide transport properties (sorption coefficients). It behaves almost conservatively and it rarely participates in chemical reactions between solutes and the solid phases. The salinity distribution may be initially affected during repository operation by perturbations in the hydraulic conditions, although in the case of Forsmark this perturbation is negligible /Auqué et al. 2006, Svensson and Follin 2010/. Salinities during the first temperate period following repository closure will remain limited, ensuring that the swelling properties of the buffer and backfill are not negatively affected. Afterwards, groundwaters will be affected by increasing amounts of waters of meteoric origin, which will produce a gradual decrease of the groundwater salinity, especially in the upper part of the modelled domain.

The concentration of cations is important in that their presence decreases the stability of colloids. In groundwaters that are too dilute, colloids might enhance the transport of radionuclides. In addition, as the buffer swells into fractures, montmorillonite colloids may be transported away by dilute groundwaters. Despite the criteria for order of 1 mM for divalent and 100 mM for monovalent cations have been published by many other researchers over the years, the criterion proposed by SKB for the safety function indicator is $2 \cdot \Sigma[M^{2+}] + \Sigma[M^+] = \Sigma qM^{q+} \geq 2\text{–}4$ mM, where $\Sigma[M^{2+}]$ and $\Sigma[M^+]$ are the summation of the concentrations of the divalent and monovalent cationic species, respectively, and q is the cation charge. In this way, available experimental data suggests that montmorillonite colloids are not stable at concentrations above this limit.

Calcium participates in water-rock interactions such as calcite dissolution and precipitation, feldspars weathering and cation exchange. However, deep saline groundwaters are quite rich in calcium and they are in equilibrium with gypsum /Gimeno et al. 2009/. Moreover examination of the groundwaters at depths below 100 m shows that calcium concentrations are also significantly controlled by mixing processes. The other major divalent cation is magnesium, which is a trecer of marine inputs in the studied systems and, therefore, is basically controlled by mixing when marine intrusions occur /Laaksoharju et al. 2008/ but also modulated by cation exchange /Gimeno et al. 2009/. Magnesium is also regulated in granitic groundwaters by the precipitation and dissolution of chlorite, a mineral that may have a wide range of compositions. In general, magnessium concentrations in groundwaters are much lower than those of calcium, and because of the low solubility of chlorites and the uncertainty in the composition of this mineral, the modelling of magnessium concentrations is much more uncertain than that of calcium.

Detrimental agents: sulphide, iron and potassium

Regarding canister corrosion, it is desirable to have low groundwater concentrations of agents detrimental to long-term stability of the buffer and backfill, in particular sulphide, iron and potassium /SKB 2006b/.

Potassium concentrations are generally low in the groundwaters sampled in the Forsmark area. Solubility control by sericite or illitic clays has been proposed as a mechanism controlling the maximum concentrations of potassium /Nordstrom et al. 1989/, but ion-exchange processes cannot be ruled out. Even if the exact mechanism is not known all available groundwater data indicate that the increased infiltration of waters of meteoric origin will not increase the potassium concentrations found at present. In the models presented in this study, potassium concentrations have been approximated as conservative aqueous species during the mixing calculations.

For sulphide to pose a problem, considerably higher concentrations would be required (not observed in the Forsmark groundwaters). Sulphide concentrations are usually below the detection limit. Under oxidizing conditions, sulphide is quickly oxidized to sulphate. Under reducing conditions, dissolved Fe(II) is normally present, and the maximum sulphide concentrations are controlled by the precipitation of Fe(II) sulphides. In most the Forsmark groundwaters, Fe(II) concentrations are lower than 10^{-6} mol/L, which sets the maximum S(-II) concentrations in the range 10^{-4}–10^{-5} mol/L /Auqué et al. 2006, Gimeno et al. 2009/.

The concentration of Fe(II) is basically regulated by the slow dissolution of Fe(II) silicates, such chlorite and biotite, the precipitation of Fe(II) sulphides and, also, by redox reactions. Concentrations of the Fe(III) aqueous species are, in general, negligible in granitic groundwaters, as the Fe(III) oxy-hydroxides are quite insoluble and precipitate quickly. Moreover, under the reducing conditions identified in the groundwaters of the Laxemar area, hematite has been found in fracture fillings at all examiend depths /Drake and Tullborg 2009, Gimeno et al. 2009/. Thus, equilibrium with respect to hematite and redox equilibrium between Fe(II) and Fe(III) oxy-hydroxides are assumed (which is also controlled by pH).

pH values and carbonate species concentrations

The concentration of carbonates and the pH are mainly controlled by calcite precipitation/dissolution reactions. Regarding pH, values lower than 11 have been formulated from the point of view of buffer and backfill stability /SKB 2006b/. This is fulfilled for any natural groundwater in the Forsmark area. However, during the construction period, concrete and other materials could contaminate the groundwater, and high pH values could be reached. On the other hand, the input of glacial melt waters during the glacial period could give rise to higher pH values.

A further requirement is that the combination of low pH values and high chloride concentrations should be avoided in order to exclude chloride corrosion of the canister (pH > 4 or [Cl] < 3M).

Sulphate and phosphate concentrations

Sulphate and phosphate aqueous species may complex significant fractions of uranyl cations /Geipel et al. 1996, Sanding and Bruno 1992/. Soluble complexes not only limit sorption, but often result in enhanced transport of uranium /Choppin and Wong 1998, Gabriel et al. 1998, McCarthy et al. 1998/. Sulphate is also important when determining the solubility limits for radium. In the present study, the sulphate concentrations are computed from (1) the proposed mixing proportions and (2) the redox stability of the S(VI) aqueous species. The phosphate concentrations have been calculated assuming equilibrium with hydroxyapatite.

1.3.2 Redox conditions

A fundamental safety requirement is that reducing conditions should prevail in the chemical evolution of the groundwater system. A necessary condition is the absence of dissolved oxygen, because any evidence of its presence would indicate oxidizing conditions. The presence of reducing agents that react quickly with oxygen, such as Fe(II) and sulphide, is sufficient to indicate reducing conditions. Other indicators of redox conditions, such as negative Eh, are not always well defined or easily measured, and thus, less practical as a basis. Nevertheless, the redox potential is useful as a measure of the availability of all kinetically active oxidizing species in groundwaters.

This requirement ensures that canister corrosion due to oxygen dissolved in the groundwater is avoided. Furthermore, should a canister be penetrated, reducing conditions are essential to ensure a low dissolution rate of the fuel matrix

The hydrological model of the site shows how the proportion of waters of meteoric origin at repository depths will increase with time. This evolution is not expected to change the reducing characteristics of the groundwater, as infiltrating meteoric waters become depleted of oxygen by microbial processes in the soil layers or after some tens of metres along fractures in the bedrock. Evidence from the Äspö laboratory, and other Swedish sites, shows that anoxic conditions prevail in the host rock even at a short distance from tunnel walls or from the ground surface.

Calculations include alternatively equilibrium with respect to:

- crystalline Fe(III)-oxy-hydroxide /Grenthe et al. 1992/ (and redox equilibrium with Fe(II) aqueous species), $Fe(OH)_3(s) + 3H^+ + e^- \leftrightarrow Fe^{2+} + 3H_2O$, where the resulting redox potential is strongly correlated to pH,

and/or

- amorphous Fe(II) monosulphide, $FeS(am) + H^+ \leftrightarrow Fe^{2+} + HS^-$

Except for the case where reduction of sulphate to sulphide is not allowed (uncoupled database), the reaction $SO_4^{2-} + 9H^+ + 8e^- \leftrightarrow HS^- + 4H_2O$ also takes place. In this case, the dependency between Eh and pH shows a less pronounced slope.

1.3.3 Colloids and other geochemical parameters

The evolution of colloids and the concentrations of other geochemical components, as $H_2(g)$, $CH_4(g)$, NH_4^+, NO_2^-, CH_3COO^-, TOC and DOC, have not been included in our calculations. This apparently heterogeneous group of parameters include components for which either the available information is insufficient for a precise quantitative evaluation of their future evolution or cannot be modelled in the same way and with the same tools as the rest of the geochemical parameters in this work. Most of them are intimately related to the microbial activity conditioning or being conditioned by different redox processes. This fact makes their evaluation a difficult task due to the complexity and the present knowledge of microbial processes in the groundwaters of crystalline systems.

Pernicious effects of these components are mainly related to canister corrosion as many of them are corroding agents or can enhance contents of such agents through different metabolic processes. This is the case of dissolved sulphide, whose content in low temperature environments depends on the activity of sulphate reducing bacteria (SRB). This activity is in turn conditioned by the amount and availability of suitable substrates, which, in the case of SRBs, include dissolved organic carbon, acetate, methane and molecular hydrogen. Therefore, an assessment of the potential amounts of these components over the future evolution of the groundwater system at Forsmark has been performed and is presented below.

Other parameters like nitrite, ammonia and acetate are also metabolic by-products of different microbial processes and they may enhance some specific types of corrosion, like stress corrosion cracking (SCC). This type of corrosion may affect copper and copper alloys and is considered to be a potential canister corrosion failure mechanism. The activation of SCC requires that a susceptible metal be exposed to a large enough tensile stress in the presence of an SCC agent like the aforementioned nitrite, ammonia and acetate (e.g. /King 2007/ and references therein). Substantial experimental works have been done to assess copper SCC in nitrite-, ammonia- and acetate-containing environments, both at room /Arilahti et al. 2000, Ikeda and Litke 2000, Ikeda et al. 2004, Betova et al. 2005, Litke and Ikeda 2006/ and at elevated temperature (100–130°C; /Kinnunen 2006, Ikeda and Litke 2007/. Overall, the results indicate that copper SCC susceptibility decreases with decreasing concentrations of the SCC agents. Furthermore, SCC susceptibility appears to decrease with increasing chloride concentration and temperature (the inhibiting effect of chloride on SCC susceptibility also appears to be enhanced at elevated temperatures; /King 2007/).

In the Swedish and Finnish concepts, SCC is considered highly unlikely in repository conditions because of the low probability of the simultaneous occurrence of SCC-promoting factors in the repository /King et al. 2001, Pastina and Hellä 2006, SKB 2006b/. However, an evaluation of the possible amounts of SCC agents (nitrite, ammonia and acetate) during the evolution of the groundwater system at Forsmark has also been performed.

Finally, another important component, difficult to include in the predictive modelling, is the concentration of colloids (particles with diameters between 1 and 1,000 nm). Colloids are thermodynamically metastable and consequently their occurrence and stability cannot be approached from an equilibrium point of view /SKB 2010/. In groundwaters, natural colloids form by the erosion of rock-forming minerals and alteration products, the precipitation of mineral oxides and the degradation of organic material. In addition, the bentonite barrier may represent an additional source of colloids (bentonite is in itself colloidal) under certain conditions, mainly through interaction with dilute glacial melt waters.

There is a fairly large body of literature on the colloidal contents in the investigated sites and in other groundwater systems. Moreover, bentonite colloid generation, stability and transport in dilute water mimicking glacial water have been investigated in a number of projects (like the SKB Colloid Dipole Project or the SKB Colloid Transport Project) and research articles (see review by /Wold 2010/). As the concentration of natural and bentonite-derived colloids should remain low to avoid transport of radionuclides by colloids, the available information has been reviewed in order to assess the possible evolution of the colloidal contents in the Forsmark site.

All these parameters will be analysed in a separate chapter from the rest of the calculations (Chapter 8) using a common structure: a) Overview/general description, including the significance in the performance assessment, factors controlling their contents, available data from the studied sites (or other natural systems); and b) Estimated values over time, with the evaluation of their contents and uncertainties in each of the considered future stages (open repository, temperate period, glacial period and submerged period).

1.4   Report layout

The present report has been structured starting with the presentation of the hydrogeochemical conceptual model of the site (Chapter 2), with a summary of the main hydrogeochemical features and the processes controlling their evolution. In the Chapter 3, a short introduction to the hydrodynamics models performed by Serco and TerraSolve has been included, whereas the methodology used in the geochemical calculations has been especified in Chapter 4. Chapter 5 presents the discussions about the geochemical evolution during the stage of the open repository, and the results obtained by the geochemical simulations for the temperate and the glacial periods have been included in Chapter 6 and in Chapter 7, respectively. In Chapter 8, the evolution of geochemical parameters not included in the calculations has been described, such as DOC and the concentrations of acetate, methane, molecular hydrogen, nitrite, ammonia and colloids. Additionally, four appendices have been included to the end of the report, describing (1) an example of the calculation procedure and a description of the input and the output files, (2) the hydrological evolution of the site during the hydrological and climatic periods previously mentioned, (3) the estimation of the composition of the glacial reference water, and (4) the tables containing the results of the statistical calculations.

2 Hydrogeochemical conceptual model for the Forsmark site

2.1 Introduction

From the site descriptive model, a hydrogeochemical conceptual understanding of the site based on measurements and model contributions was described in /Smellie et al. 2008, Laaksoharju et al. 2008/. This model is a combination of a quantitatively-derived hydrogeochemical model (e.g. based on site measurements) and a qualitatively-derived hydrogeochemical model (e.g. more descriptive, process-oriented conceptual model). It describes the chemistry and distribution of the groundwater and porewater in the bedrock and the groundwater close to the interface between bedrock and the overburden. Additionally, it describes the evolution of the hydrogeochemical processes.

This description is based primarily on measurements of the groundwater composition, but also incorporates the use of available geological and hydrogeological site descriptive models. The description also serves as the basis for possible hydrogeochemical simulations of the palaeohydrogeochemical evolution of the site and, also, to predict future changes /Laaksoharju et al. 2008/.

2.2 Present status of hydrogeochemical understanding at the Forsmark site

The complex groundwater evolution and patterns at Forsmark are a result of many factors, such as: a) past changes in hydrogeology related to glaciation/deglaciation, land uplift and repeated marine/lake water regressions/transgressions, b) the present-day topography and proximity to the Baltic Sea and c) organic or inorganic alteration of the groundwater composition caused by microbial processes or water/rock interactions /SKB 2005a, 2006c, Laaksoharju et al. 2008/.

The predominant rock-types in this area are metamorphosed medium-grained granites and granodiorites and most of them were formed between 1,900 and 1,800 Ma ago suffering both ductile and brittle deformation. The majority of the fracture systems that are water conducting today were activated or reactivated during the Palaeozoic and have probably been water pathways ever since /Tullborg et al. 2008/. The topography of the Forsmark area is relatively flat and is characterised by low relief with local, small-scale recharge (downward flow) and discharge (upward flow) areas, involving groundwater flow systems restricted to the Quaternary deposits. These flow systems overlie the more large-scale flow systems associated with groundwater flow in the bedrock. The transition from near-surface to upper bedrock (0–150 m depth), referred to as the shallow bedrock 'aquifer' comprises horizontal/subhorizontal sheet joints and is considered to be hydraulically anisotropic due to a lattice of intersecting near-surface joints and gently dipping single fractures. Therefore, the groundwater flow field is considered horizontally anisotropic with high flow rates. When the meteoric recharge waters enter the subhorizontal fractures they mix with existing groundwaters in the fractures and are rapidly transported laterally to be discharged towards the Baltic Sea to the north-east of the candidate area. This shallow bedrock 'aquifer' therefore limits direct meteoric recharge to deeper bedrock levels. Nevertheless, some deeper recharge of meteoric water is likely to occur where outcropping, steeply dipping deformation zones coincide with higher surface elevations south-west of the candidate area /Follin et al. 2007a, b/.

Figure 2-1 shows a cross-Section through the centre of the tectonic lens of the Forsmark site. The illustration outlines some of the key features of the Forsmark structural model and consequently key features of the hydrogeology:

- the gently dipping ZFMNE00A2 deformation zone divides the bedrock inside the tectonic lens into a foot wall rock mass (target volume for a final repository in Forsmark) and a hanging wall rock mass,

- the foot wall rock mass has higher rock stresses than the hanging wall rock mass; it is divided into two different fracture domains, FFM01 and FFM02, where the latter is closer to surface and substantially more fractured located than the former, and

- the hanging wall rock mass is intersected by quite a few gently-dipping deformation zones.
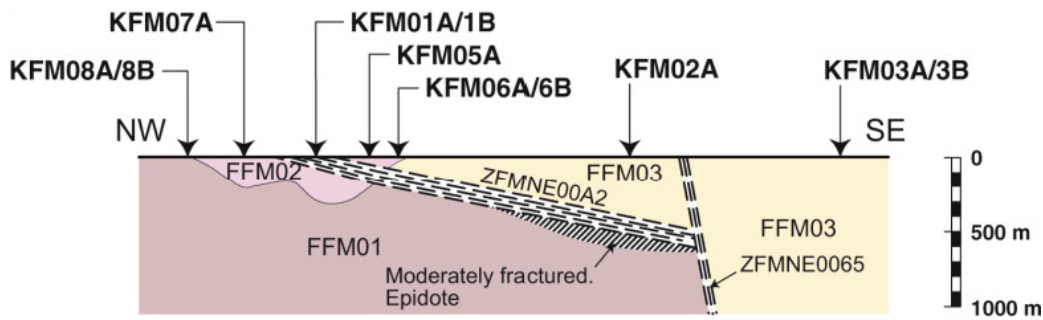
Fracture domain FFM01
Steeply dipping, minor fracture zones with sealed fractures,
low fracture frequency between zones, high in situ stress

Fracture domain FFM02
High frequency of sub-horizontal fractures with apertures

Fracture domain FFM03
High frequency of gently dipping, minor fracture zones
containing both sealed fractures and fractures with apertures,
low in situ stress relative to FFM01

Figure 2-1. The extensive and fairly transmissive gently dipping deformation zone ZFMNE00A2 divides the bedrock inside the tectonic lens into a foot wall rock mass (target volume for a final repository in Forsmark) and a hanging wall rock mass. FFM01–FFM03 are different fracture domains, cf. /SKB 2006c/.

The hydrogeology of the Forsmark site is determined by the presence of highly conductive gently-dipping fracture zones. Particularly, fracture zone ZFMNE00A2 plays a key role in the hydrogeological behaviour of the candidate area. The footwall of ZFMNE00A2 is relatively disconnected from the hanging wall due to the high transmissivity of the gently dipping fractures that concentrate most of the groundwater flow. Then, water of meteoric origin infiltrating through the top boundary (surface) does not reach the foot wall. In addition, the foot wall is dominated by a rock matrix with very few conductive fractures in it.

2.2.1 Post glacial evolution

Several water types which are now present in the bedrock can be associated with past climatic events in the late Pleistocene (from 120,000 years ago to 10,000 BP), including inter-glaciations, glaciations, deglaciations, and associated changes in the shoreline in connection with marine/non-marine transgressions and regressions. Among these, the last deglaciation and post glacial period is the most important for the groundwater development in the Fennoscandian shield, especially in terms of land uplift and shore-level displacement as well as the development of the Baltic Basin.

The post glacial development reveals that when the continental ice melted and retreated from the Forsmark area around 8,800 BC, glacial melt water was hydraulically injected under considerable head pressure into the bedrock. The exact penetration depth is unknown, but, according to hydraulic simulations depths exceeding several hundred metres are possible. Although the last deglaciation of the Forsmark region coincided with the end of the Yoldia period, there are no signs of Yoldia Sea water in the bedrock.

The Ancylus Lake (8,800 to 7,500 BC) was lacustrine and developed after the deglaciation. This period was followed by the brackish Littorina Sea (7,500 BC to 2,000 BC). During the Littorina Sea stage, the salinity was considerably higher than at present, reaching a maximum of about 15‰ in the period 4,500 to 3,000 BC. Dense brackish seawater from the Littorina Sea penetrated the bedrock, resulting in a density intrusion that affected the groundwater in the most conductive parts of the bedrock and, for example, becoming slightly diluted with fractions of glacial water.

The first parts of the Forsmark region emerged from the sea at ca. 2,500 years BC, and the recharge system of meteoric water circulation became established around 900 years ago forming a freshwater layer on top of the saline water because of its low density. As a result of the flat topography of the Forsmark area and of the short time period elapsed since the area emerged from the sea, the out-flushing of saline water has been limited, and consequently a freshwater layer remains at shallow depth.

Past Quaternary evolution has affected the groundwater chemistry at Forsmark, but this is not restricted to post glacial time since there is groundwater and porewater evidence that indicates a pre-Pleistocene warm-climate derived meteoric water component (before 2,59 Ma). The hydrochemistry of the Forsmark area cannot be explained without recognising this older component. The present groundwaters therefore are a result of mixing and reactions over a long period of geological time. The un-sharp interface between different water is also caused by molecular diffusion.

2.2.2   Summary of hydrogeochemical characters

The Forsmark site investigations have produced a good hydrogeochemical understanding of the site, both present and past, and have emphasised the different groundwater behaviour of the footwall bedrock to that of the hanging wall bedrock.

The main hydrogeochemical characters of groundwaters and porewaters in the Forsmark site are described below at different depth intervals: 0–20 m, 20–200 m, 200–600 m and > 600 m /Gimeno et al. 2008, Laaksoharju et al. 2008/.

Near-surface waters (0–20 m)

Within this 0 to 20 m depth interval, including the overburden, *Fresh groundwaters* (< 200 mg/L Cl or 5.6 mM) comprise the most recent recharge compositions. Therefore, their hydrogeochemical evolution is mainly determined by weathering reactions, in particular reactions influenced by limestone. The extensive presence of limestone blocks in the Quaternary overburden at Forsmark, a feature very uncommon in soils in other parts of Sweden, promotes an overall distinctive character to the near-surface groundwaters with respect to that observed in other areas (e.g. Laxemar). Properties include variable but higher pH values (usually higher than 7) and variable but high calcium concentrations (mostly between 50 and 200 mg/L; 1.25–5.00 mM) depending on the biogenic carbon dioxide input. This fact, together with the kinetically much slower weathering of the aluminosilicates (which otherwise would consume carbon dioxide) and the localised presence of especially intense biogenic input, contribute to the high bicarbonate values observed (between 200 and 900 mg/L; 3.3–14.7 mM). Groundwater redox conditions at these shallow levels are variable, both oxidising and reducing in character. No matrix porewater data are available from these very shallow levels.

Shallow groundwaters (20–200 m)

This depth interval in the upper part of the footwall bedrock includes the shallow bedrock aquifer, which rapidly transports recharging meteoric groundwaters laterally towards the north-east and effectively limits further recharge to deeper levels. This shallow bedrock aquifer is not developed in the hanging wall bedrock segment. In the footwall bedrock, these shallow groundwaters consist of a large percentage of "Fresh groundwater" that has persisted to the depths of the shallow bedrock aquifer. In the hanging wall bedrock, fresh groundwaters persist to varying depths to around 200 m depending on whether recharge or discharge conditions dominate the gently dipping deformation zones that intersect the bedrock surface. The hydrogeochemical evolution of those fresh groundwaters is mainly determined by water-rock interaction processes.

This uppermost 20 to 200 m in the footwall and the hanging wall bedrock are also characterised by the presence of "Mixed Brackish groundwaters" with a wide chemical variability (e.g. chloride contents in the range 200 to 2,000 mg/L; 5.64 to 56.4 mM) probably due to natural mixing of fresh recharging waters and discharging (or flushed out) saline groundwaters (i.e. recent Baltic or old Littorina Sea relicts). However mixing resulting from anthropogenic effects, related to drilling and sampling activities, is also possible. These shallow mixing processes occur throughout the Forsmark area, but are much more prevalent in the hanging wall segment where the shallow bedrock aquifer is virtually absent and variable discharge and recharge is occurring along the gently dipping deformation zones.

These hydrogeochemical and hydrogeological observations are supported by environmental isotope studies which show that recent to young fresh groundwaters, some showing signs of mixing, characterise the upper approximately 100–200 m of bedrock. This is shown by tritium and carbon-14 which indicate that near-surface groundwaters have short residence times mainly in the order of only a few decades to a few hundred years. This is in agreement with palaeohydrogeological evidence which indicates that the regional area at Forsmark started to emerge from the sea about 2,500 years ago with subsequent land uplift establishing meteoric water recharge some 900 years ago.

The redox characterization of this shallow groundwater system suggests the existence of a generalised anoxic state with possible episodic inputs of oxidising waters. At present, the contents of dissolved ferrous iron are high and represent post-oxic environments in which iron-reducing bacteria (IRB) activity seems to be dominant /Hallbeck and Pedersen 2008a/. Locally, sulphide environments with high contents of dissolved sulphide, probably active precipitation of amorphous monosulphide and, therefore, important sulphate-reducing bacteria (SRB) activity, are also found. The mineralogical results and uranium-decay series analyses of fracture filling materials indicate that redox conditions have varied both in time and space within the uppermost part of the bedrock. However, there are enough data to suggest that these oxidising episodes have not been intense enough to exhaust the reducing capacity of fracture filling minerals which are still present in the shallow system (e.g. Fe(II) chlorite or pyrite).

Only few porewater data are available from the rock matrix within this depth interval, and generally these suggest that close to steady-state conditions have been achieved in the hanging wall but not in the footwall bedrock.

Intermediate depth groundwaters (200–600 m)

Two types of groundwaters appear at this intermediate depth: *Brackish Marine groundwaters* (2,000 to 6,000 mg/L Cl; 56.4 to 169 mM Cl) and older *Brackish Non-marine groundwaters* of similar to higher salinity (4,000 to 10,000 mg/L Cl; 113 to 282 mM Cl) whose major chemical composition and distribution is mainly controlled by mixing processes among various end-members. The mixing proportions are different in the two main groundwater systems at Forsmark, (i.e. fracture groundwaters in the hanging wall bedrock compared to fracture groundwaters in the footwall bedrock).

Groundwaters from the footwall bedrock have a lower Littorina proportion and a larger contribution of *Brackish Non-marine groundwater* (or the Old meteoric ± Glacial + Saline end-member) at shallower depths (around 300 m). The same could be said for the influence of the deeper *Saline groundwater* component (10,000 to 20,000 mg/L Cl; 282 to 564 mM Cl). During the Littorina Sea transgression, the shallow bedrock aquifer subsequently became saturated by Littorina Sea water which persisted until recent uplift stimulated an increase in the local hydraulic gradient. The bulk of the Littorina waters then were flushed out by recharging meteoric waters, a process which is still on-going, contributing to the observed low Littorina proportions in these groundwaters.

This contrasts with the groundwaters from the series of gently dipping, highly transmissive deformation zones in the hanging wall where the shallow bedrock aquifer does not exist. The Littorina seawaters preferentially entered the bedrock through these deformation zones which have a much higher proportion (almost double) of the Littorina end-member down to greater depths (around 600 to 700 m). A higher Littorina component generally also results in higher sulphate and magnesium contents.

Radiocarbon studies of organic/inorganic carbon phases support a Holocene origin of the brackish marine (Littorina) groundwaters. This is in accordance with palaeohydrogeological estimations suggesting an age of approximately 5,000 to 6,000 years covering the period of maximum salinity during the Littorina Sea stage (4,500 to 3,000 BC).

Even though the compositional characteristics of these intermediate groundwaters are mainly determined by mixing processes, the quickly responding pH and Eh are controlled to a large extent by chemical reactions and microbial activity and, for example, thereby also the sulphur and carbon species. The pH is mainly controlled by calcite dissolution-precipitation reactions. Of secondary importance is the influence of other common chemical processes, such as aluminosilicate dissolution or cation exchange. Most of the Eh values determined in these brackish groundwaters (at depths between 110 and 646 m) are clearly reducing in spite of the disturbances in the redox pristine conditions. The dissolved ferrous iron contents are generally lower than in the shallow groundwater

system. Dissolved sulphide concentrations are systematically low and may be locally controlled by the precipitation of amorphous Fe(II) monosulphides, linked to the activity of SRB. Presently, the sulphide values are subjected for further monitoring to better assess their behaviour and the effects of drilling and sampling procedures /Tullborg et al. 2010/.

The available porewater data indicate the existence of greater disparity between the porewater chemistry and the adjacent groundwater compositions (the former being significantly more dilute) from approximately 300 to 650 m depth in the footwall bedrock below the shallow bedrock aquifer (where there is a marked decrease in open fracture frequency and transmissivity).This depth interval represents transient conditions where the porewater has retained a very old, dilute and warm-climate water signature. This signature is much older than the surrounding fracture groundwaters which have been dated to at least 1.5 Ma. Oxygen-18 is enriched and therefore indicates no obvious cold climate signature, which contrasts with the adjacent groundwaters. In the hanging wall, an overall transient state also is established down to about 650 m. The lower chloride contents and an isotope signature increasingly depleted in oxygen-18 with increasing depth, indicate that the porewater in these zones stores a dilute water signature with a probable cold-climate signature. The significantly negative $\delta^{18}O$ values (–13‰ V-SMOW) preserved far from the water conducting fractures indicates that this cold-climate signature was a glacial water circulating for a considerable time period in the fractures at these depths. Since the last deglaciation, the porewater signature has become overprinted with a Littorina and/or a Baltic-type signature, as indicated by chloride, magnesium and oxygen-18 in porewaters sampled closer to the conducting fracture.

Deep groundwaters (> 600 m)

Under this heading are included the *Brackish Non-marine groundwaters* and the *Saline groundwaters* previously referred to as potential mixing components with the brackish marine (Littorina) groundwater at shallower levels. In the hanging wall bedrock, the transition from brackish marine (Littorina) fracture groundwaters to brackish non-marine groundwaters is quite sharp and occurs at around 550 to 600 m depth. From 600 to 930 m depth, the chloride content increases steadily from 5,500 to 8,500 mg/L (155 to 240 mM) before levelling out at values just below 10,000 mg/L (282 mM) at 1,000 m depth, i.e. the transition to the saline groundwater member.

With respect to the overall redox conditions in the candidate volume, the dissolved sulphide concentrations increase at depths greater than 600 m. This is consistent with the occurrence of sulphate-reducing bacteria (SRB) and with the active precipitation of Fe(II) monosulphides. The iron system seems to be limited by crystalline oxides (mainly hematite), reflecting the pristine conditions of the geochemical system. This is coherent with the reducing character and long residence time of these groundwaters, where low crystallinity oxides are not expected. As stated above, the sulphide values are a subject for further monitoring to better assess their behaviour.

Hydrochemical observations of fracture groundwaters and porewaters show that the brackish to saline non-marine groundwaters become more mineralised with increasing depth (to saline in type) by water/rock interaction and exchange with the rock matrix porewater. Consistent with the indications of low-conductive bedrock at these depths (> 600 m), all qualitative and quantitative evidence points to groundwater residence times that are significant. This indicates that these brackish to saline non-marine groundwaters represent part of the salinity gradient that existed prior to the last deglaciation. This hypothesis is further strengthened by the transient composition of the rock matrix porewater present in the 300 to 600 m depth interval, which has around 2,000 mg/L Cl (56.4 mM Cl) as compared with around 6,000 mg/L Cl (169 mM Cl) in the fracture groundwaters. This porewater falls under the general heading of 'Old Meteoric ± Old Glacial +Saline' in type, in this case with no glacial component, and is considered to represent a snap-shot of the salinity profile at this depth prior to the last deglaciation.

Thus, transport of water volumes and mixing (both advection-dispersion and molecular diffusion) are major processes giving rise to present-day groundwater compositions. However, mixing also induces reactions and therefore the separation of these two processes is not only very challenging, but also important for the site understanding in order to indicate effects from past/present transport and reactions. Reactions involve interaction with the bedrock and fracture minerals, and in particular the alkalinity, pH and redox buffering capacity of the bedrock are of key importance for groundwater composition and predicting future changes.

3 Hydrodynamics numerical model setup

In order to evaluate the evolution of the safety factors around the candidate repository domain, a series of groundwater flow simulations has been performed in order to reproduce the solute transport mechanisms in the Forsmark area (during the climate periods specified in Figure 1-1). These models have provided the initial distribution of groundwaters (as salinities or as mixing ratios of five end-member solutions), which will be the previous step for the geochemical calculations.

Hydrogeological descriptions needed have been selected from published SKB reports from the site characterization. In particular, SKB R-08-23 "Hydrogeological conceptual model development and numerical modelling using ConnectFlow, Forsmark modelling stage 2.3" has been used /Follin et al. 2008/. This hydrogeological conceptual model has been updated accordingly to the results obtained by the hydrogeological team along the process of the Safety of the Final Repository (SR-Site) hydrogeological modelling. Updates have been provided by SKB and through the Trac system.

Hydrogeological model results have been provided by the hydrogeological team of SKB, through the standard QA procedures determined for SR-Site.

In the present chapter, only the most significant concepts will be introduced. More detailed descriptions of the methodologies and results can be consulted in /Rhén et al. 2003, Joyce et al. 2010, Vidstrand et al. 2006, 2010/ and /Hartikainen et al. 2010/.

3.1 Methodology

Two technical manager teams have provided the hydrological results from which the hydrogeochemical calculations have been performed (see Section A1.1):

- Serco /Joyce et al. 2010/ has simulated the hydrodynamics evolution of the site during (1) the temperate and (2) the submerged under seawater periods, and

- Terrasolve AB /Vidstrand et al. 2010/ has studied the hydrodynamics evolution of the site during (1) a periglacial period, (2) a hypothetical glacial cycle, and (3) when the candidate site is submerged by a glacial melt water lake.

The results of the regional-scale groundwater flow modelling (see Appendix 2) are used as input to a geochemical mixing and reaction model. The aim has been to obtain equivalent groundwater models for hydrology and geochemistry.

Hydrogeological models are solved usually with ConnectFlow version 9.6 of DarcyTools software, which allowed modelling on different scales to be carried out using both continuum porous medium and discrete fracture network concepts.

On the other hand, Computed-aided Fluid Engineering AB and SF GeoLogic AB /Svensson and Follin 2010/ have developed a series of works in order to determine the hydrogeological environment of the site during the stage of the open repository.

3.1.1 The open repository

This stage has been conceptually treated in the present report from the works performed by /Svensson and Follin 2010/. The fluid flow simulations were carried out with DarcyTools, and they provide inflow rates, drawdown of the groundwater table and upconing of deep saline water for an open final repository for spent fuel. Besides informing about possible effects of the excavation and operational periods, they also present tentative modelling results for the saturation phase, which starts once the completed parts of the repository are being backfilled.

The geometries and hydraulic properties of the discrete features, such as fractures, deformation zones and repository layout components (shafts, ramp, tunnels and deposition holes), were imported from a quality assured database managed by SKB, whereas other modelling issues, such as initial

and boundary conditions, followed the prerequisites for modelling outlined in /Selroos and Follin 2010/. Present-day surface waters (areas and flow rates), and groundwater chemistry were loosely used as "calibration targets" for the modelled evolution of the hydrological and hydrochemical conditions during Holocene time (8,000 BC to 2,000 AD). The simulated conditions at 2,000 AD were used as reference for the identification of disturbances caused by the subsequent flow modelling of the excavation and operation periods /Svensson and Follin 2010/.

3.1.2 Temperate and submerged saline periods

One of the processes modelled during the temperate period /Joyce et al. 2010/, and during the period submerged under seawater (Littorina Sea, 3,000 BC), has been the transport of the selected reference waters (a present meteoric recharge, marine waters, glacial melt waters, pre-existing saline waters and an older meteoric water). This approach calculates the mixing proportions of these waters at any time for the different parts of the studied rock volume.

Hydrogeochemical compositions of the end-members are based on the studies performed for the Site Descriptive Model /Gimeno et al. 2008, 2009/ and the estimations already used for the SR-Can exercise /Auqué et al. 2006/. Here they have been updated to include an additional end-member (see Section 4.4).

The following cases has been analyzed:

- groundwater composition for 2,000 AD, 3,000 AD, 5,000 AD and 9,000 AD ("temperate period"), and

- groundwater composition when the Littorina Sea was placed on the Forsmark site (3,000 BC; "submerged marine period").

It is assumed that there is some correlation between the size of fractures and their transmissivity (see next section). In this way, a series of hydrological variants have been considered in two additional variant cases, examining alternative relationships (fully correlated and uncorrelated):

- groundwater composition for 2,000 AD, 3,000 AD, 5,000 AD and 9,000 AD, considering a evolution which enhanced the effect of the heterogeneity induced by the presence of fracture and deformation zones ("extended spatial heterogeneity" case), and

- groundwater composition for 2,000 AD, under two hydrological characterizations ("case 5" and "case 9"), where no relationship between fracture radius and transmissivity has been considered.

3.1.3 Remaining part of the glacial cycle

The modelling for the remaining part of the reference glacial cycle is similar to that performed for the initial temperate period. One of the processes modelled is the transport of salts. Contrary to the modelling of the initial temperate period, the models for the periglacial and glacial periods have not included the fractions of selected reference waters. As a result of their calculations, the Terrasolve AB team has provided an estimated salinity evolution in the Forsmark area during a periglacial period, a hypothetical glacial cycle, and when the candidate site is submerged by a glacial melt water lake. The presence of a frozen soil (permafrost) in the most superficial areas during the first stages of the glacial cycle has been also simulated /Vidstrand et al. 2010/.

A process that must be evaluated is the out-freezing of dissolved salts when ice builds up underground during periglacial periods. However, the Darcy Tools model does not include the out-freezing of salts. This process has instead been evaluated using a two-dimensional model set-up. In the same line, /Hartikainen et al. 2010/ have also developed permafrost simulations at the Forsmark site, using a numerical two-dimensional thermo-hydro-chemical model.

For these stages, as already indicated above, the only information provided by the hydrological models is salinity (assumed to be equivalent to chloride) and, therefore, the problem is largely unconstrained to consider the involvement (known to exist) of all the possible end-members used for the previous cycle (temperate and submerged periods). Therefore, the following simplification was done: the rock volume is assumed to initially contain a mixture of two clearly different groundwaters, a saline groundwater (represented here as the Deep Saline end-member, but including also the salinity given by the input of the Littorina waters), and a dilute groundwater (represented here as the

Altered Meteoric end-member, but corresponding to all the dilute groundwaters previously presented in the system, old meteoric, glacial and the own present meteoric recharge). With the advancement and retreat of the glacier, the proportion of a third mixing end-member, glacial melt water, is calculated from the decrease of salinity in any point in space.

3.2   Physical model

The main objective of the modelling work carried out by Serco is to reproduce the hydrogeology of the Forsmark site during the temperate period (from 8,000 BC to 12,000 AD), and to calculate performance measures for the intended repository. These mechanisms are also implemented in the glacial cycle and the open repository calculations.

The Serco team studied different aspects as (1) exit locations and performance measures for particles released from the canister locations in the repository, (2) the effect of the heterogeneity of the hydraulic conductor domain, and the effect of stochastic properties, and (3) the statistic effects of different fractures and deformation zones. As a result, a series of numerical files have been provided, containing the spatial location of 2,022,911 discrete points with the proportions of the five reference waters (in the fractures and in the solid matrix), and salinity.

The physical model of the area has been performed by a complex methodology. Figure 3-1 illustrates schematically the division of the groundwater system into hydraulic domains used by SKB in the SDM work. The hydrogeological model consisted of three hydraulic domains /Joyce et al. 2010/:

- Hydraulic Conductor Domain (HCD) represents deformation zones,
- Hydraulic Rock mass Domain (HRD) represents the less fractured bedrock in between the deformation zones, and
- Hydraulic Soil Domain (HSD) represents the Quaternary deposits.

The division in hydraulic domains constitutes the basis for the conceptual modelling. On the other hand, the groundwater flow to the granitic bedrock at Forsmark can be simulated by considering two conceptual models: (1) continuum porous medium, or equivalent continuum porous medium, that considers the cristalline rocks as a continuum characterised by quantities defined at all points in a three-dimensional region, and (2) discrete fracture network, where the groundwater flows along fractures, and is characterised by quantities associated with the fractures. Typically, for crystalline hard rocks, groundwater flow generally takes place through an interconnected network of fractures.

Three different scales of model have been used in the SR-Site temperate period modelling /Joyce et al. 2010/. Each scale of model was chosen to focus in on parts of the model of interest, with
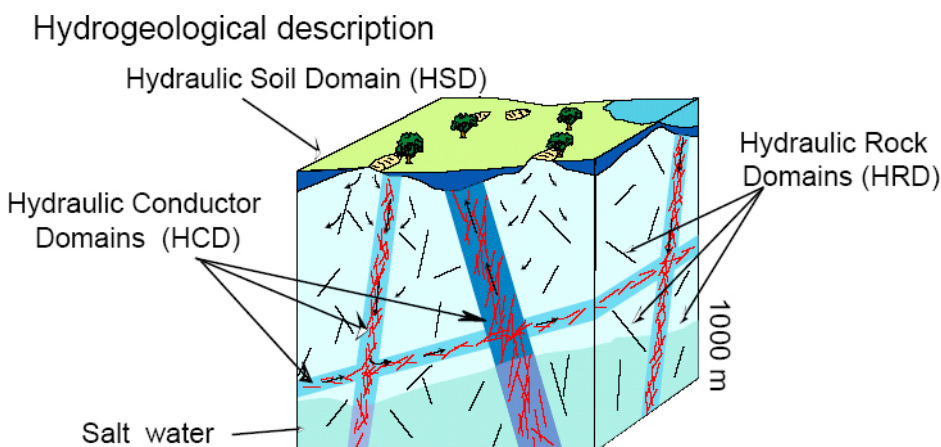
Figure 3-1. *Representation of the division of the crystalline bedrock and the Quaternary deposits into three hydraulic domains, HCD, HRD and HSD /Rhén et al. 2003/.*

consideration given to what was computationally feasible and which types of calculations were supported by the ConnectFlow software for different types of model.

(1) The regional-scale model corresponds to the SDM-Site model and covers the same domain. The model was used to calculate the transient evolution of coupled groundwater flow and reference water transport from 8,000 BC to 12,000 AD. The calculated pressure and fluid density values were exported from this model for particular times for use by the two other scales /Joyce et al. 2010/.

(2) The site-scale model replaced the part of the regional-scale equivalent continuum porous medium model local to the repository area. Fractures with appropriate hydraulic and transport properties were also used to represent the repository structures. Boundary conditions and initial conditions were imported from the regional-scale model. The site-scale model was primarily used to trace particles from the repository-scale model.

(3) The repository-scale model used a continuum porous medium representation of the main tunnels, deposition tunnels and deposition holes in the repository, embedded within a discrete fracture network representation of the hydraulic rock mass domain. Other repository features were represented by fractures with appropriate hydraulic and transport properties. The deformation zones and sheet joints were represented as fractures. The repository-scale model was divided into 3 blocks for computational efficiency /Joyce et al. 2010/.

3.2.1 Model variants

The hydrological model assumes that there is some correlation between the sizes of fractures and their transmissivity /Joyce et al. 2010/. In this way, a so-called "hydrological base case" has been defined, with a semi-correlated relationship between fracture size and transmissivity. Two alternative relationships have been also examined: fully correlated and uncorrelated.

The "hydrological base case" relates fracture radius to transmissivity according to the equation /Joyce et al. 2010/:

$$T = 10^{\log(ar^b) + \sigma N(0,1)} \qquad \text{(Equation 3-1)}$$

where a and b are the factor and exponent respectively of the power-law relationship between r and the mean of $\log_{10}(T)$, σ is the standard deviation of $\log_{10}(T)$, and $N(0,1)$ denotes a normally distributed random deviate with a mean equal to zero and a standard deviation of 1. The transmissivity is limited to two standard deviations either side of the mean by resampling values outside of this range. However, this resampling leads to a different random number sequence than that used in the correlated and uncorrelated variants and hence leads to a different realisation of the discrete fracture network. The correlated and uncorrelated variants have the same realisation of the discrete fracture network, and only differ in the fracture transmissivity values.

For the uncorrelated variant, there is no relationship between fracture radius and transmissivity. Instead, the transmissivity is based on the log-normal relationship given in the equation:

$$T = 10^{\mu + \sigma N(0,1)} \qquad \text{(Equation 3-2)}$$

where μ is the mean of $\log_{10}(T)$, σ is the standard deviation of $\log_{10}(T)$, and $N(0,1)$ denotes a normally distributed random deviate with a mean equal to zero and a standard deviation of 1.

For the fully correlated variant, the fracture transmissivity is completely determined by its radius according to equation /Joyce et al. 2010/:

$$T = ar^b \qquad \text{(Equation 3-3)}$$

where a and b are the factor and exponent, respectively, describing the power-law relationship.

Other than the different relationships between transmissivity and size, the fractures for the two variants are generated in the same way as for the hydro base case and used in the three scales of model in the same way.

The "hydrological base case" uses an hydraulic rock mass domain model from SDM-Site that covers the repository site area, based on the data available. Outside this area, the rock is modelled as a con-

tinuum porous medium with homogeneous and isotropic properties for each depth zone. However, this greatly reduces the effect of outcropping sub-vertical deformation zones on particle exit points.

Limited additional data from the ongoing investigations at SFR /Öhman and Follin 2010/ allowed for a tentative parameterisation of a discrete fracture network in the area currently modelled as a continuum porous medium. This variant keeps the "hydrological base case" discrete fracture network, but adds fractures, based on the additional data, to cover the area to the boundaries of the regional model. This is used to provide a full equivalent continuum porous medium for the regional-scale and site-scale models. In addition, the area of the discrete fracture network in the site-scale model was extended northwards beyond the Singö deformation zone, which may provide an important discharge location. Both models retain the existing hydraulic soil domain.

3.3   Transport of salts during the periglacial and the glacial periods

It is estimated that at Forsmark the ground will be frozen to a depth of 50 m or more for around 30 percent of the time in the glacial cycle of the reference evolution /Vidstrand et al. 2010/. According to these results, the permafrost will not occur over a continuous period of time, but rather thawing will occur between more or less short periods of permafrost. On the other hand, some of these permafrost periods will furthermore coincide with the time when the site is covered by an ice sheet. During these periods, a series of mechanisms can affect the distribution of groundwater salinities.

3.3.1   Salt rejection

When water freezes slowly, the solutes present in the water will not be incorporated in the crystal lattice of the ice. During this process, salts that have been present in the surface waters and groundwaters will tend to accumulate at the propagating freeze-out front. This front is, however, not necessarily sharp, because e.g. freezing will take place over a range of temperatures, depending on the salinity and on the ratio between "free" and tightly adsorbed water molecules. The freezing process can give rise to an accumulation of saline water at the depth to which the perennially frozen front has reached. The saline waters formed in this manner within fractures and fracture zones will sink rapidly due to density gradients.

The calculations made using a two-dimensional model set-up /Hartikainen et al. 2010/ illustrate this effect. When the freezing is extensive (down to several hundred metres depth) a salt front is developed in the calculations. The salinity of the unfrozen groundwater in the perennially frozen rock also increases substantially when the freezing front advances faster than the transport of salt. These results agree qualitatively with the previous generic calculations reported in /Vidstrand et al. 2006/.

The concentration of the out-frozen salt has been estimated in these calculations assuming that before the onset of the permafrost the salinity distribution is that found at present in Forsmark. Judging from the results /Vidstrand et al. 2006/, it may be that these initial salinities are overestimated, as the groundwaters will become gradually more diluted before the start of the permafrost.

Nevertheless the results of the 2D modelling /Hartikainen et al. 2010/ indicate a very moderate increase in salinities around the repository volume (not exceeding 1%) for the most extreme permafrost simulation. It corresponds to the dry variant of the repetition of the last glacial cycle with an air temperature decreased by 8 degrees. For the most extreme permafrost extent simulated, the calculated groundwater salinities in the repository volume do not exceed those found at present.

3.3.2   Upconing

The possibility of upconing of Deep Saline groundwater to repository depths during permafrost conditions was addressed in /King-Clayton et al. 1997/. This may possibly occur in the vicinity of permanent discharge features such as some taliks. Such discharge features mainly occur along more extensive conductive deformation zones. In Forsmark, where the topography is quite flat, the probable location of taliks is at some distance from the candidate repository area, as estimated from the forecasted landscape development following the shoreline displacement at Forsmark.

3.3.3 Permafrost decay

When the permafrost melts and decays there will be a release of dilute melt water from the upper highly permeable network of fracture zones. At this stage the low permeable matrix which has preserved (or accumulated) its salinity, especially at greater depths, will probably be more saline than the surrounding groundwaters. The resulting chemical gradient will then cause a gradual transfer of salinity to the more permeable rock mass. In all probability this will be a relatively slow process and dilution by mixing will occur also within the more permeable rock mass. The more dilute waters will tend to stay on the top layers of the rock mass due to their lower density.

3.4 Data files supplied by the hydrological models

The hydrogeological data files (see Section A1.1) provided by the Serco team (for the temperate and the submerged hydrodynamics models) and TerraSolve (for the remaining glacial cycle) include 2,111,649 points in the rock volume of Forsmark, representing the whole regional area of the site down to 2.3 km depth. For the temperate and the submerged periods, these files contain the X-Y-Z coordinates of each point together with the information on salinity (%) resultant from the hydrogeological model. Depending on the hydrogeological model used, this information is given also as mixing proportions of the five end-members (Deep Saline, Old Meteoric, Glacial, Littorina and Altered Meteoric;) in the fractures and in the matrix, or simply as salinity. The X and Y coordinates are given in metres in DarcyTools local coordinate system with the origin at x = 1,626,000 and y = 6,692,000. The Z coordinate is in metres above sea level. The three coordinates are referred to the DarcyTools cell centre.

3.4.1 Temperate and submerged saline periods

The hydrogeological data files provided by Serco /Joyce et al. 2010/ contain the X-Y-Z coordinates together with mixing proportions of the five end-members (Deep Saline, Old Meteoric, Glacial, Littorina and Altered Meteoric) for the groundwater in the fractures (indicated with an F) and in the matrix (indicated with an M) and a column with the salinity. The data are separated by columns and, as already said, there is a file for each year: 2,000 AD, 3,000 AD, 5,000 AD and 9,000 AD.

Once the data subsets with the mixing proportions for each data point are extracted, they are used to create input files for PHREEQC, using the software developed for SR-Can and updated for SR-Site, in order to obtain the chemical composition at each point as a result of the mixture between the reference waters.

3.4.2 Glacial and periglacial periods

For the periglacial and the glacial, instead of mixing proportions, the hydrogeological model results provided by TerraSolve /Vidstrand et al. 2010/ consist of salinities in a grid of points in the rock volume. These values must be converted into mixing proportions to be used in geochemical modelling and, therefore, a new software has been developed.

There is a file for each period including the advance and retreat of the ice front and different cases depending on the direction of the ice front movement (NW-SE, base case, or N-S, special case) and on the ice front angle (45º, base case, or 0º, special case). In all the cases the initial state (at time t = 0) and the model network are the same and correspond to the end of the Temperate period and therefore, free of ice and assuming that the Present day Baltic Sea is occupied by a fresh water lake. Table 3-1 summarises all the cases, giving the name of the hydrogeological file, the position of the Sea level, the real time in years, and the ice front location, movement, angle and coordinates.

In the hydrological "standard" case used in our calculations, the ice front has a frontal angle of 45 degrees, and moves over an unfrozen surface with a NW-SE direction. The periods include the advance of the ice front to different (x, y) locations: –5,300, 0 (Ice I), –2,900, 0 (Ice II), –500, 0 (Ice III), 13,000, 0 (Ice IV), and ice covering the entire model domain (Ice V; see Table 3-1 and Figure 1-1, where the time corresponding to these different episodes is also indicated). Then, its retreat, after 15,000 years of the domain covered by ice, to some of the previously considered positions: Ice Vr, IVr, IIr and 0r, ice-free again after a full glacial cycle (entire domain covered by 100 metres of fresh water).

As indicated above, there is a variant case in which the ice front moves in the N-S direction; the thickness profile is the same as for the base case but the ice front extends in 0 degrees. The temperate period (0) is the same as for the NW-SE case, and then, there are two files corresponding to the advance of the ice front to a position comparable to Glacial II and to a later position comparable to Glacial III. For more details see Table 3-1.

Another case corresponds to the development of Permafrost associated with the glacial period. There is an initial case of Permafrost corresponding to frozen conditions (periglacial period) and the existence of "taliks" before the ice advance ("xyzpss_IP_permIFL0.txt", see Table 3-1). Then the rest of the files correspond to progressive advances of the ice (Ice I, Ice, II and Ice IV) with permafrost development 2 km below the ice margin and with the presence of taliks ("xyzpss_IP_permI.txt", "xyzpss_IP2_permII.txt" and "xyzpss_IP4_permIV.txt", Table 3-1).

3.4.3   Data selection for the geochemical calculations

From the original hydrogeological data files, different data subsets are extracted:

- complete horizontal slice at the repository depth (450–490 m), with 111,900 and 67,795 points for the temperate and the glacial simulations, respectively,

- data points within the candidate repository volume, included in the domain inside the following coordinates: (1630.62,6701.17); (1633.37,6701.17); (1633.37,6698.9); (1630.62,6698.9). 65,237 and 24,425 points for the temperate and the glacial calculations have been selected within this domain, and

- a vertical slice approximately parallel to the shoreline (NW: 1,628,263 m / 6,703,763; SE: 1,637,263 m / 6,694,763), with 25,349 and 20,671 points for the temperate and the glacial simulations, respectively.

These subsets are then used to create input files for PHREEQC to obtain the detailed chemical composition at each point (see Appendix 1).

Table 3-1. Hydrogeological results obtained from Terrasolve for the glacial and permafrost cases. See report R-09-21 /Vidstrand et al. 2010/.

Name for the Hydrogeological File	Special Case	Sea Level	"Real" Time years	Ice Move-ment	Ice Front Angle	Ice Front Location	Ice Front Location Coordinates			
							Local DarcyTools		RT90	
							X (km)	Y (km)	X (km)	Y (km)
BASE CASE										
Chem_Forsmark_0.txt		0	0	-		Temperate	-42.5	0	1583.5	6692.0
Chem_Forsmark_I.txt		0	744	advance	-45	Ice I	-5.3	0	1620.7	6692.0
Chem_Forsmark_II.txt		0	792	advance	-45	Ice II	-2.9	0	1623.1	6692.0
Chem_Forsmark_III.txt		0	840	advance	-45	Ice III	-0.5	0	1625.5	6692.0
Chem_Forsmark_IV.txt		0	1116	advance	-45	Ice IV	13.0	0	1639.0	6692.0
Chem_Forsmark_Va.txt		0	2892	advance	-45	Ice Va				
Chem_Forsmark_Vr.txt		100	17668	retreat	-45	Ice Vr				
Chem_Forsmark_IVr.txt		100	18292	retreat	-45	Ice IV	13.0	0	1639.0	6692.0
Chem_Forsmark_IIr.txt		100	18430	retreat	-45	Ice II	-2.9	0	1623.1	6692.0
Chem_Forsmark_0r.txt		100	18850	-		Temperate	-42.5	0	1583.5	6692.0
ADVANCE OF THE ICE N-S DIRECTION										
Temperate case N-S siam.txt		0	0	-	0	Temperate	0	30.35	1626.0	6722.35
Chem_Forsmark_vNS_IIa.txt	NS	0	444	advance	0	Ice II	0	8.15	1626.0	6700.15
For_vNS_SDM_covered (iceIIIa).txt	NS	0	528	advance	0	Ice III	0	3.95	1626.0	6695.95
DEVELOPMENT OF PERMAFROST										
IP_permIFL0.txt	Perm_2km	-28	0	-	-	Frozen	-42.5	0	1583.5	6692.0
IP_permI.txt	Perm_2km	-28	744	advance	-45	Ice I	-5.3	0	1620.7	6692.0
IP2_permII.txt	Perm_2km	-28	792	advance	-45	Ice II	-2.9	0	1623.1	6692.0
IP4_permIV.txt	Perm_2km	-28	1116	advance	-45	Ice IV	13.0	0	1639.0	6692.0

The initial state (at time = 0) and the model network are the same in all cases.

4 Geochemical numerical model setup

Hydrochemical and mineralogical descriptions needed for the calculations have been selected from published SKB reports from the site characterization activities. In particular, the following reports have been used:

- Hydrochemistry: /Laaksoharju et al. 2008/ "Bedrock hydrogeochemistry Forsmark. Site descriptive modelling. SDM-Site Forsmark",

- Mineralogy: /Sandström et al. 2008/ "Fracture mineralogy of the Forsmark site SDM-Site Forsmark", and

- /Sandström and Tullborg 2006/ "Mineralogy, geochemistry, porosity and redox capacity of altered rock adjacent to fractures. Forsmark site investigation".

Hydrochemical data have been taken from the final version of ChemNet "datafreeze" deliveries. The last version of Forsmark hydrochemical data, according to the ChemNet group, is named "Forsmark_2_3_ updated_Dec30_2007.xls". This database is available at the ChemNet Project Place Forsmark site.

4.1 Conceptual model

The conceptual model on which the geochemical calculation strategies are based, assumes that the chemical characteristics of these groundwaters are the result of a complex mixing process driven by the input of different recharge waters during the palaeogeographic history of the sites, at least, since the last glaciation /Laaksoharju and Wallin 1997, Laaksoharju et al. 1999, SKB 2005b/. The successive penetration of dilute glacial melt waters and Littorina sea waters at different depths has triggered complex, density and hydraulically driven flows that have mixed them with long residence time highly saline waters (brines) present in the fractures and the rock matrix. The recent infiltration of meteoric and Baltic Sea marine waters has only affected the shallowest part of the aquifer system, about ≤ 200 m depth. As a result, from a purely geochemical viewpoint, mixing can be considered the prime irreversible process responsible for the chemical evolution of the Forsmark groundwater system. The successive disequilibrium states resulting from mixing conditioned the subsequent water-rock interaction processes and hence the re-equilibration pathways of the mixed groundwaters.

Mixing provides a satisfactory interpretation for several of the groundwater components partly because the rates of reaction between the rock and the circulating groundwater are relatively slow, as mentioned above. Besides, an important aspect is that there are large differences in concentrations between the mixing components, e.g. between the meteoric infiltrating waters and the Deep Saline end-member found at the deepest parts of the sites. Under such circumstances, the relative effects of water-rock interactions on the concentrations of main groundwater components are small when compared with the large effects caused by mixing. However, chemical reactions (homogeneous and heterogeneous) are needed to obtain the information about the non-linear parameters and the behaviour of other parameters mainly controlled by equilibrium reactions. This is why, instead of considering only the mixing proportions obtained by CONNECTFLOW, the coupling with a geochemical model has been implemented (Figure 1-2).

The importance of the ionic exchange processes in the hydrochemistry evolution of the Forsmark and Laxemar groundwaters has already been evidenced in the site descriptive models /Gimeno et al. 2008, 2009/. However, these processes have not been simulated for different reasons:

1. The very scarce available CEC values for the fracture fillings (basic parameter for this type of simulations) are subjected to important uncertainties due to the low sensitivity of the method used for their determination /Selnert et al. 2008/.

2. The thermodynamic data base imposed by SKB to be used for this exercise has not the capacity to deal with this type of exchange processes. To include the necessary data into this database would need a complete verification exercise as an indispensable QA requirement.

3. Due to the importance of these processes, the UZ group has developed the methodology and software necessary to deal with the exchange processes from the results provided by the hydroge-

ologists (mixing proportions). Scoping calculations with some "deduced" CEC values /Gimeno et al. 2008, 2009/ have been performed with the WATEQ4F.dat database (widely used to deal with exchange processes and previously used in the SR-Can exercise). The results suggest that no important differences with respect to the simulations without ionic exchange, are expected. However, some interesting indications on the qualitative effect of these processes over the main master variables have been found and deserve a thorough future study.

Over the Glacial and Permafrost periods the penetration at different depths of dilute glacial melt waters will produce important changes in the chemical composition of these waters. The assessment of the effects of future changes on the hydrogeochemistry of the site (including the effect of chemical reactions), is the main aim of these calculations.

Due to the fact that the hydrogeological results for the Glacial and Permafrost periods are given in the form of salinity values, and that the software that couples these results to the geochemical codes are based on mixing proportions (not on salinity; /Auqué et al. 2006/), the first step requires transforming salinities into mixing proportions for each time slice. Thus, the calculations over the glacial period follow the steps summarised below:

1. The initial state (at time t = 0) and the model network are the same in all cases (Figure 1-2). As the only data provided by the hydrogeologists are salinities, these are converted into chloride using the following relations:

$$\text{TDS (g/L)} = \rho \frac{S}{100} \qquad\qquad \text{(Equation 4-1)}$$

$$\text{Cl (g/L)} = \frac{\text{TDS (g/L)}}{1.646}, \qquad\qquad \text{(Equation 4-2)}$$

where S is percent salinity and $\rho = \rho_0 (1+\alpha S)$, with $\rho_0 = 1{,}000$ g/L and $\alpha = 0.00741$. The coefficient 1.646 has been estimated from the correlation of the analytical data as it has been illustrated in Figure 4-2.

2. With salinity (converted into chloride) as a starting point, (t0) we can only use two end-members (and their chemical compositions) with which, mixed in different proportions, obtain the calculated chloride content. Only with more information on other parameters (isotopes or magnesium, for example) could additional end-members be included in the transformation of chloride into mixing proportions.

3. So, from the salinity values, a new file with the mixing proportions of Deep Saline and Altered Meteoric is constructed. The rest of the end-members (in this case Glacial) have mixing proportions of zero at t0.

4. The hydrogeological results for the next period (Glacial I) will contain new salinity values calculated at the same grid points as before; so, they can be compared with the previous ones (Figure 4-3). Then, as the two main processes able to affect the groundwaters between the two time periods are the input of glacial melt waters and the upconing of saline waters, depending on the result of the comparison, the program calculates the new mixing proportion at each point in the following way: if the new salinity is lower than the t0 one, an amount of Glacial end-member water is added to the mixture (and the other two already existing proportions, DS and AM, are recalculated, keeping their ratio constant); if the new salinity is higher that the t0 one, an extra amount of Deep Saline water is added to the mixture (the AM proportion is recalculated and the proportion of Glacial remains at zero).

5. The next steps will follow the same procedure as step 4, that is, comparison of the salinities and addition of Glacial or DS proportions according to the differences found between the salinity in the previous period and the salinity in the period under consideration.

t0 First stage Glacial Cycle

HYDROGEOLOGICAL RESULTS
Salinity values for each point in the whole rock volume. Conversion in Cl

SALINITY CONVERSION
Cl transformed in mixing proportions of "diluted groundwater" (Altered Meteoric, Old Meteoric and Glacial), and "saline groundwaters" (Deep Saline)
% diluted groundwater + % Deep Saline

PHREEQC INPUT AND CALCULATIONS
pqi file with mixing proportions (and the geochemical composition of the End-members) + equilibrium reactions with a set of minerals for each point.
Mixing and reaction simulations with PHREEQC

PHREEQC OUTPUT
pqo file with the chemical composition, including pH, Eh, molalities and activities of the chemical components and the saturation indexes

SELECTION OF THE OUTPUT DATA
Selected output with the key parameters

RESULTS TREATMENT
Statistical calculations and representation (box-and-whiskers plots), and graphical representation of the results (Surfer and Voxler interpolations)

Figure 4-1. *Scheme of the methodology applied for the evaluation of the chemical composition of the groundwaters with the input data provided by Terrasolve (salinities in each point of space for the glacial period) for the first stage of the cycle, when salinities are attributed to the mixing between a saline and a diluted end-member (Deep Saline and Altered Meteoric, respectively).*
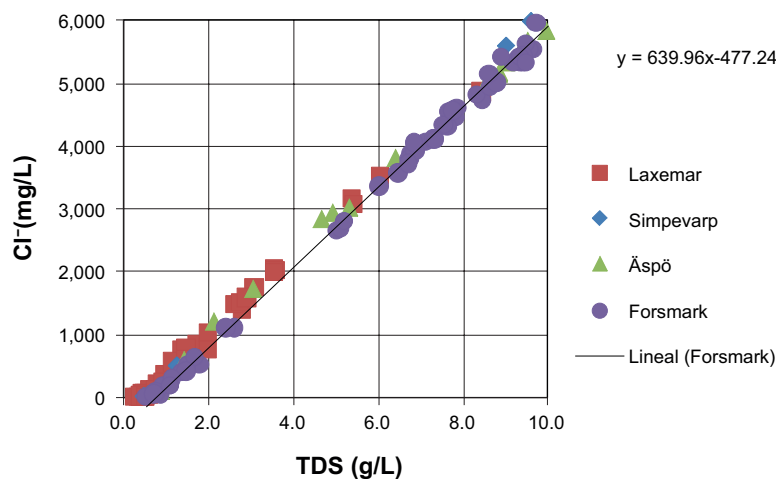
Figure 4-2. *Correlation between chloride concentrations and salinity for selected groundwaters.*

t_n Glacial Cycle (n=1,n)

HYDROGEOLOGICAL RESULTS
Salinity values for each point in the whole rock volume. Conversion in Cl (Cl_n)

SALINITY COMPARISON WITH t0 (Cl_0) FOR EACH POINT
If $Cl_n > Cl_{n-1}$ input of saline water
(addition of Deep saline to the mixing proportions calculated in t0)
New (%AM + %DS) + %DS

If $Cl_n < Cl_{n-1}$ input of dilute water
(addition of Glacial water to the mixing proportions calculated in t0)
New (%AM + %DS) + %Glacial

PHREEQC INPUT AND CALCULATIONS
pqi file with mixing proportions (and the geochemical composition of the
End-members) + equilibrium reactions with a set of minerals for each point.
Mixing and reaction simulations with PHREEQC

PHREEQC OUTPUT
pqo file with the chemical composition, including pH, Eh, molalities and activities
of the chemical components and the saturation indexes

SELECTION OF THE OUTPUT DATA
Selected output with the key parameters

RESULTS TREATMENT
Statistical calculations and representation (box-and-whiskers plots), and
graphical representation of the results (Surfer and Voxler interpolations)

Figure 4-3. *Scheme of the applied methodology for the evaluation of the chemical composition of the groundwaters with the input data provided by Terrasolve (salinities in each point of space for the glacial period) when calculations are not related to the first stage of the cycle (a decrease in salinities are attributed to an increase of the Glacial ratio in groundwaters).*

The same procedure explained above is also used for the Permafrost period. The conceptual difference with the previous case is in the initial state (at time t0) as in this case it corresponds to a frozen period, probably developed after the end of the temperate period. The procedure for this case is as follows:

1. Comparison of the initial state calculated for the glacial period (Glacial 0) with the initial state calculated for the Permafrost case (Permafrost 0).

2. Then, following the same procedure as for the glacial period, the mixing proportions of Deep Saline and Altered Meteoric end-members are calculated from the salinity values provided by the hydrogeologists.

3. The evolution over the Glacial + Permafrost period will be done in the same way as explained in steps 5 and 6 above.

The hydrogeological files expressed as mixing proportions are then used to create the input files for PHREEQC. However, the large number of points (i.e. water samples) on which PHREEQC calculations had to be performed, has led to the development of simple interface programs for the automatic import and export of data. This software (developed in-house by the GMG, /Gimeno et al. 2010/) accepts as input the hydro files with the mixing proportions and the file with the composition of the end-members to calculate the final chemical composition of the waters at each point. This interface allows also the selection of the processes that will be imposed on the waters. All this procedure is presented next and exemplified in Appendix 1.

4.2   Numerical tools

Hydrogeochemical calculations have been performed with PHREEQC /Parkhurst and Appelo 1999/. PHREEQC is a computer program written in the C programming language that is designed to perform a wide variety of low-temperature aqueous geochemical calculations. PHREEQC is based on an ion-association aqueous model and has capabilities for (1) speciation and saturation-index calculations; (2) batch-reaction and one-dimensional (1D) transport calculations involving reversible reactions, which include aqueous, mineral, gas, solid-solution, surface-complexation, and ion-exchange equilibrium, and irreversible reactions, which include specified mole transfers of reactants, kinetically controlled reactions, mixing of solutions, and temperature changes; and (3) inverse modelling, which finds sets of mineral and gas mole transfers that account for differences in composition between waters, within specified compositional uncertainty limits.

Other capabilities of the code are the possibility to simulate:

1. dispersion (or diffusion) and stagnant zones in 1D-transport calculations,

2. kinetic reactions with user-defined rate expressions,

3. formation or dissolution of ideal, multicomponent or non-ideal, binary solid solutions,

4. fixed-volume gas phases in addition to fixed-pressure gas phases,

5. the number of surface or exchange sites to vary with the dissolution or precipitation of minerals or kinetic reactants,

6. isotope mole balances in inverse modelling calculations,

7. automatically use multiple sets of convergence parameters.

On the other hand, the code is able to print user-defined quantities to the primary output file and (or) to a file suitable for importation into a spreadsheet, and to define solution compositions in a format more compatible with spreadsheet programs.

A detailed description of the use of PHREEQC in SR-Can safety assessment can be found in /SKB 2006d/.

Due to the fact that the geochemical calculations are not made with the actual chemical composition of the water at each point but with the time- and space-varying mixing proportions of several end-member waters, apart from the hydrogeological data file, the file containing the chemical composition of the end members is also needed. A more thorough description of this file will be seen in Section 4.3. With these two files, in house software developed for SR-Can, creates the input files for PHREEQC to calculate the chemical composition of each water in all the nodes and times selected from the hydrogeological models. X-Y plots for analysis of computed results will be made by standard software such as Microsoft Excel and Origin. Advanced visualization of data and computed results could be made by using different tools. Voxler and ModFlow 3D Model Builder will be evaluated and used in the current project. Visit software will be also tested in case the other proposed programs were not capable of visualizing all the desired geometrical objects and data.

4.3   Thermodynamic database

Consistency between the modelling in this work and other SR-Site geochemical models using thermodynamic data is an important issue. The thermodynamic database used in the simulations ("TDB_SKB-2009_Amphos21.dat") was obtained from SKB's Trac system. This database was developed by /Hummel et al. 2002/, with modifications related to thermodynamic data of radionuclides /Duro et al. 2006, Grivé et al. 2010/, and of some iron and sulphur species.

Some specific phases have been considered in order to establish mineral equilibrium with the groundwaters or with the reactive mixing. When these species are not included in the SKB-TDB, they are included as "Phases" in the PHREEQC input file[1]:

---

[1] See Appendix 1 where an example of the input and format files used in the developed software is shown.

- Albite: $NaAlSi_3O_8 + 8H_2O = Al(OH)_4^- + 3Si(OH)_4 + Na^+$ (log_k= –19.98)
- K-Feldspar: $KAlSi_3O_8 + 8H_2O = Al(OH)_4^- + 3Si(OH)_4 + K^+$ (log_k= –22.62)
- $Fe(OH)_3$(hematite_grenthe): $Fe(OH)_3 + 3H^+ = Fe^{3+} + 3H_2O$ (log_k= –1.10)
- FeS(ppt): $FeS + H^+ = Fe^{2+} + HS^-$ (log_k=–3.00)
- Kaolinite_G: $Al_2Si_2O_5(OH)_4 + 7H_2O = 2Al(OH)_4^- + 2H^+ + 2Si(OH)_4$ (log_k= –37.3)
- Hydroxyapatite: $Ca_5(PO_4)_3OH + 4H^+ = 5Ca^{2+} + 3HPO_4^{2-} + H_2O$ (log_k= –3.421)
- Rhodochrosite: $MnCO_3 = Mn^{2+} + CO_3^{2-}$ (log_k= –11.13)

The reasons for the selection of these phases and their equilibrium constants are described in /Auqué et al. 2006/ and /Gimeno et al. 2009/.

As in SR-Can, a series of calculations have been performed in order to evaluate the influence of the kinetic of the redox reaction between the pairs S(-II)/S(VI). In this way, a new database has been adapted, uncoupling the equilibrium reactions between the species with both oxidation states ("TDB_SKB-2009_Amphos21_no_S-redox.dat"). Calculations with this new "uncoupled" database have been performed as a geochemical variant case considering the case of hematite equilibrium (see Section 4.5).

4.4 Estimation of the end-member waters compositions

The chemical composition of the end-member waters (see Section A1.7.1) is a key issue that deserves a separate section. This is because, as stated above, the geochemical calculations are not made with the chemical composition of the water at each point but with the time- and space-varying mixing proportions of several end-member waters. Therefore, the chemical composition of the waters at each point (our main aim) can be greatly affected by the composition given to the end-members.

Chemical composition of end-members (Deep Saline, Old Meteoric, Glacial melt water, Littorina Sea water and Altered Meteoric) for the calculations has been provided in the site characterization models of both sites, and they are compiled in Table 4-1. For some end-members several fundamental parameters are not known (e.g. pH, Eh, Al, Fe, or S^{2-}) and mineral equilibrium reactions (with calcite, chalcedony, iron oxyhydroxides and/or monosulphides; /Auqué et al. 2006/) have been used to estimate them (see Section A1.9). These reactions are considered by expert judgment to have been affecting these waters over time.

- The **Deep Saline end-member** must have been in the rock for hundreds of thousands of years and therefore it must be in equilibrium with the rock-forming minerals and the fracture fillings. Therefore, the original composition of this water has been equilibrated with albite, K-feldspar, calcite, hematite (Grenthe's equilibrium constant), quartz (Rimdstidt's equilibrium constant), and with pH fixed at 8.0.
- **Glacial end-member** representing very dilute waters, have been equilibrated with calcite (SI= –1), quartz, kaolinite, and $Fe(OH)_3$(microcrystalline) (see Appendix 3 for more details in the estimation of the composition of this end-member).
- **Littorina end-member** as old marine waters that have pass through marine sediments, have been equilibrated with calcite, quartz, FeS(am) and kaolinite.
- The **Altered Meteoric end-member** corresponds to a real sample (sample #8335; Table 4-1). This sample represents dilute groundwater from the shallow parts of the aquifer system. The reactions assumed to have affected this water are equilibrium with calcite (SI= –0.5), kaolinite, quartz (using Rimdstidt's equilibrium constant) and $Fe(OH)_3$(microcrystalline).
- The SDM-Site Forsmark hydrogeochemical investigations showed that changes in the groundwater chemistry during the Quaternary were not restricted to post glacial time as there is groundwater and porewater evidence that indicates an old, warm-climate derived meteoric water component. Without recognising this older component the hydrogeochemistry (and hydrogeology) at both sites cannot be adequately explained. Therefore, in this new version of the hydrogeological model, the hydrogeologists have included a fifth end-member (not used in SR-Can calculations, "**Old Meteoricend-member**") and whose composition is on the Altered Meteoric end-member but with a longer residence time and therefore, longer interaction time with rock. This water has been equilibrated with calcite, hematite (Grenthe's equilibrium constant), kaolinite, quartz (Rimdstidt's equilibrium constant) and a $logP_{CO2}$ = –4.1.

Table 4-1. Original end-members used by the hydrogeologists (units in mg/L except to isotopes and pH). The equilibrated end-members, calculated with the coupled and the uncoupled database used for the geochemical calculations have been included in Section A1.8 and in Table 4-2.

	DeepSaline	Old Meteoric	Glacial	Littorina	Altered Meteoric
pH	8	7.91		7.6	7.91
Alkalinity	14.1	14.1	0.12	92.5	466.0
Cl	47,200	181	0.5	6,500	181
SO_4^{2-}	10	85.1	0.5	890	85.1
Br	323.66*	0.572		22.2	0.572
Ca	19,300	41.1	0.18	151	41.1
Mg	2.12	7.5	0.1	448	7.5
Na	8,500	274.0	0.17	3,674	274.0
K	45.5	5.60	0.4	134	5.60
Si	2.9	6.68	–	3.94	6.68
Fe	–			0.002	
δ^2H (‰)	–44.9	–50	–158.0	–37.8	–80.6
$\delta^{18}O$ (‰)	–8.9	–5	–21.0	–4.7	–11.1

Table 4-2. Equilibrated end-members, calculated with the coupled and the uncoupled databases (units in mol/L, except to pH, temperature, and pe). When numerical differences have been obtained with the uncoupled database, they have been specified in the grey rows. In the case of the sulphur aqueous species, S_{tot} is the parameter included in the input file when the coupled database is used. However, the S(VI) and the (S-II) concentrations have been included in the input file when the uncoupled database have been used in the calculations. Phosphate aqueous species are considered to be in equilibrium with respect to hydroxyapatite.

	DeepSaline	Old Meteoric	Glacial	Littorina	Altered Meteoric
T (ºC)	15	15	15	15	15
pH	8.000	8.500	9.300	7.951	7.314
	–	–	9.29	–	–
pe	–4.449	–4.925	–5.260	–4.422	0.554
	–5.909	–6.888	–2.622	–3.910	–
Al	$7.371 \cdot 10^{-9}$	$9.141 \cdot 10^{-7}$	$5.205 \cdot 10^{-6}$	$3.247 \cdot 10^{-7}$	$7.719 \cdot 10^{-8}$
	–	$9.143 \cdot 10^{-7}$	$5.087 \cdot 10^{-6}$	–	–
Br	$4.156 \cdot 10^{-3}$	$7.163 \cdot 10^{-6}$	–	$2.812 \cdot 10^{-4}$	$7.166 \cdot 10^{-6}$
C_{tot}	$3.678 \cdot 10^{-5}$	$5.222 \cdot 10^{-4}$	$8.515 \cdot 10^{-5}$	$1.627 \cdot 10^{-3}$	$7.230 \cdot 10^{-3}$
	$3.679 \cdot 10^{-5}$	$5.225 \cdot 10^{-4}$	$8.613 \cdot 10^{-5}$	–	–
Ca	$4.940 \cdot 10^{-1}$	$1.184 \cdot 10^{-3}$	$7.180 \cdot 10^{-5}$	$3.865 \cdot 10^{-3}$	$4.702 \cdot 10^{-4}$
	–	–	$7.229 \cdot 10^{-5}$	–	–
Cl	$1.366 \cdot 10^{0}$	$5.109 \cdot 10^{-3}$	$1.410 \cdot 10^{-5}$	$1.856 \cdot 10^{-1}$	$5.111 \cdot 10^{-3}$
F	$8.644 \cdot 10^{-5}$	$8.427 \cdot 10^{-5}$	–	$2.610 \cdot 10^{-5}$	$8.431 \cdot 10^{-5}$
Fe_{tot}	$2.525 \cdot 10^{-7}$	$8.744 \cdot 10^{-9}$	$8.002 \cdot 10^{-7}$	$8.262 \cdot 10^{-6}$	$1.793 \cdot 10^{-6}$
	$7.280 \cdot 10^{-6}$	$8.031 \cdot 10^{-7}$	$2.107 \cdot 10^{-9}$	$8.282 \cdot 10^{-6}$	–
K	$8.222 \cdot 10^{-4}$	$1.433 \cdot 10^{-4}$	$1.023 \cdot 10^{-5}$	$3.469 \cdot 10^{-3}$	$1.434 \cdot 10^{-4}$
Li	$6.861 \cdot 10^{-4}$	$2.018 \cdot 10^{-6}$	–	$1.021 \cdot 10^{-5}$	$2.019 \cdot 10^{-6}$
Mg	$8.952 \cdot 10^{-5}$	$3.088 \cdot 10^{-4}$	$4.114 \cdot 10^{-6}$	$1.865 \cdot 10^{-2}$	$3.089 \cdot 10^{-4}$
Mn	$2.615 \cdot 10^{-6}$	–	–	–	–
Na	$3.801 \cdot 10^{-1}$	$1.193 \cdot 10^{-2}$	$7.395 \cdot 10^{-6}$	$1.617 \cdot 10^{-1}$	$1.193 \cdot 10^{-2}$
P	in equilibrium with respect to hydroxyapatite				
S_{tot}	$1.067 \cdot 10^{-4}$	$8.854 \cdot 10^{-4}$	$5.305 \cdot 10^{-6}$	$9.391 \cdot 10^{-3}$	$8.858 \cdot 10^{-4}$
S(VI)	$1.067 \cdot 10^{-4}$	$8.854 \cdot 10^{-4}$	$5.205 \cdot 10^{-6}$	$9.377 \cdot 10^{-3}$	$8.858 \cdot 10^{-4}$
S(-II)	$1.026 \cdot 10^{-15}$	$1.001 \cdot 10^{-15}$	$1.000 \cdot 10^{-7}$	$1.423 \cdot 10^{-5}$	$1.001 \cdot 10^{-15}$
Si	$8.808 \cdot 10^{-5}$	$1.396 \cdot 10^{-4}$	$1.665 \cdot 10^{-4}$	$1.282 \cdot 10^{-4}$	$1.342 \cdot 10^{-4}$
	–	–	$1.657 \cdot 10^{-4}$	–	–
Sr	$3.947 \cdot 10^{-3}$	$4.340 \cdot 10^{-6}$	–	$3.096 \cdot 10^{-5}$	$4.341 \cdot 10^{-6}$

Once the main reactions have been established, the composition of each end-member was calculated using PHREEQC with the "TDB_SKB-2009_Amphos21.dat" thermodynamic data base. Additionally, as already done for SR-Can and stated above, the modification of this data base ("TDB_SKB-2009_Amphos21_no_S-redox.dat") has also been used to obtain the corresponding composition of end-members for the variant cases that use this modified data base. The obtained compositions for each end-member are specified in Table 4-2.

A full propagation of uncertainties, from the hydrogeological modelling into the geochemical calculations, has not been performed. In addition, the natural variability and other uncertainties in the compositions of the reference waters used for mixing (Deep Saline, Old Meteoric water, Glacial, Littorina and Altered Meteoric) have not been propagated to the mineral reaction calculations. It is, therefore, possible that the real variability in the chemical compositions of groundwater components is somewhat larger than that presented here.

4.5 Methodology of the geochemical calculations

Groundwater compositions are modelled through mixing and chemical reactions with fracture-filling and rock-forming minerals (see Appendix 1). The different components of the modelling are not fully coupled: the results of the regional-scale groundwater flow modelling are used as input to a geochemical mixing and reaction model. The aim has been to obtain equivalent groundwater models for hydrology and geochemistry. The loose coupling of the two models also allows a description of the geochemical heterogeneity, which otherwise would be hard to attain.

The geochemical calculations have been performed from the the data supplied by the hydrological calculations: salinities or % of the end-member solutions. Mineralogical description needed for the calculations will be selected from published SKB reports from the site characterization activities. In particular, the following reports will be used:

- /Sandström and Tullborg 2006/ "Fracture mineralogy of the Forsmark site SDM-Site Forsmark", and

- /Sandström et al. 2008/ "Mineralogy, geochemistry, porosity and redox capacity of altered rock adjacent to fractures. Forsmark site investigation".

The selected minerals are those present at the sites as fracture fillings, with fast kinetic compared to the simulated time intervals (calcite and Fe(III) oxyhydroxides; this last one with the equilibrium constant derived for deep Swedish groundwaters by /Grenthe et al. 1992/), or those with apparent equilibrium situations in present groundwaters (quartz, hydroxyapatite and amorphous Fe(II) monosulphides). The use of Fe(III) oxyhydroxides or Fe(II) monosulphides represents two alternative groundwater evolution: equilibrium with Fe(III) oxyhydroxide implies a situation where the redox state is not affected by sulphate-reducing bacteria, while equilibrium with Fe(II) monosulphides characterizes a situation with significant activity of sulphate-reducing bacteria. In this way, independent of the mineral equilibriums implemented to define the composition of end-member groundwaters (see Section 4.4), calcite, quartz and hydroxyapatite have been considered to be in thermodynamic equilibrium with the mixtures at all points in space and time. Additionally, crystalline Fe(III) oxyhydroxide or amorphous Fe(II) sulphide have been chosen as the Fe-bearing minerals that also are in equilibrium with the mixture.

The analytical data from the Forsmark area show that most groundwaters are undersaturated with respect to hydroxyapatite (Figure 4-4). In this way, the concentrations calculated by the equilibrium assumption will be the expected to be maximum concentrations. This is considered a pessimistic assumption, because phosphates can enhance radionuclide solubilities.

4.5.1 Definition of the "Base Case"

As it was previously commented, in order to evaluate the most probable Eh values and iron concentrations within the candidate repository volume, the numerical results obtained considering equilibrium of solutions with respect to Fe(III) oxyhydroxides or amorphous Fe(II) sulphides have been integrated in a so-called "Base Case" (Figure 4-5), for the statistic treatment of the results.
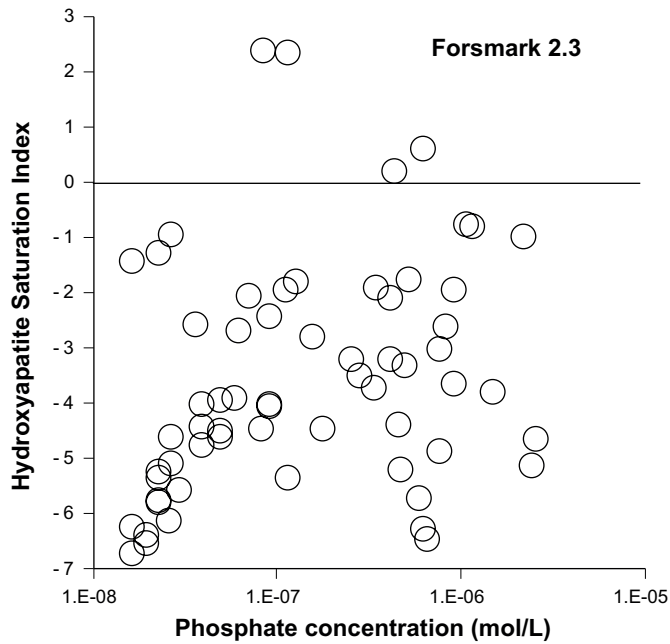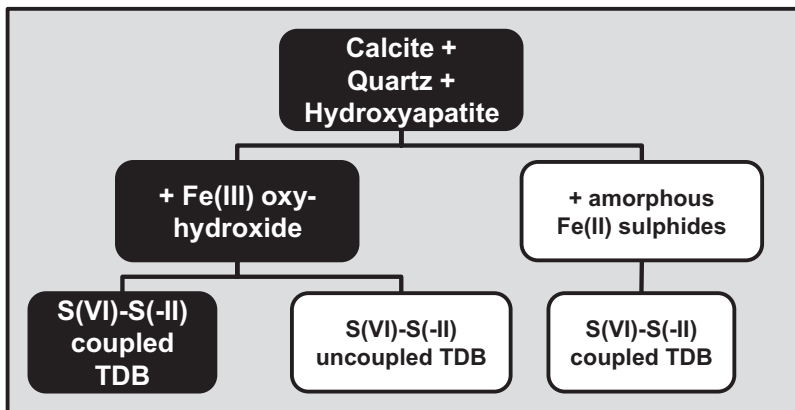
Figure 4-4. Distribution of the analytical phosphate concentrations related to the hydroxyapatite saturation index of the groundwater samples of the Forsmark area.
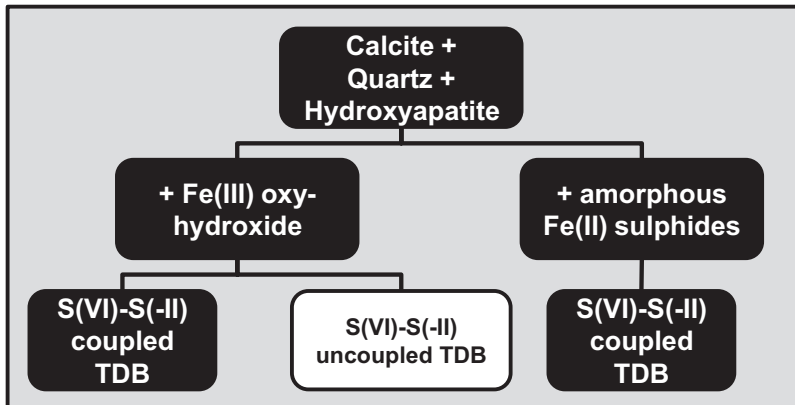

Figure 4-5. Scheme of the mineral equilibriums assumed in the calculations with the constrains applied in the "Base Case" (black squares) and for the geochemical variant cases (white square), for the statistical approaches.

Redox sensitive parameters, as Eh, iron and sulphide concentration, are strongly dependent on the Fe-bearing mineral chosen to be in thermodynamic equilibrium with the mixtures at all points in space and time. As the existence of and Fe(II) sulphides in the fracture fillings of the Forsmark area has been considered to be probable, both geochemical hypothesis have been evaluated in the statistical calculations.

The calculated pH values for both equilibrium models are practically identical. However, the sulphide concentrations are quite different. The simulated concentrations of S(-II) are strongly dependent on the chosen Fe-bearing mineral in equilibrium with the theoretical mixing solutions. When equilibrating the waters with the amorphous Fe(II) sulphides, very high concentrations of sulphide are calculated in almost all the points. Although the values obtained are similar to a few exceptionally high values measured in the Forsmark groundwaters, these high values only represent a very low percent of the real measurements, and not the 100% indicated by the simulations. Therefore, the concentrations selected for sulphide are those obtained when applying the equilibrium with the Fe(III) oxyhydroxide, whose values are closer to the ones obtained in the natural system.

4.5.2   Definition of the geochemical variant cases

A series of geochemical variant cases have been performed in order to check the influence of the solid phase selected to control the redox conditions: either the Fe(III) oxyhydroxide or amorphous Fe(II) sulphides. On the other hand, in order to test the influence of the kinetic processes in the redox reactions, a series of calculations have been implemented assuming no equilibrium between the pairs redox S(-II)/S(VI) and C(-IV)/C(IV). The sulphate reduction can be slow but can be speeded up by microbial activity. This analysis has been only performed in the case of the temperate period, and under the assumption of equilibrium with respect to Fe(III) oxyhydroxide.

Therefore, three different cases were proposed:

1. Equilibrium with quartz, calcite, hydroxyapatite and Fe(III) oxyhydroxides, and TDB coupled. With the coupled database, even if no concentration data for C(−IV) is specified in the input, PHREEQC assumes redox equilibrium between all redox pairs, and it calculates a value for the CH_4 concentration depending on the total carbon and on the Eh-pH values. If methane becomes stable then part of the input carbonate is reduced to CH_4, and as a consequence the alkalinity of the aqueous solution decreases. In this work the redox potentials are not low enough for methane to reach non-negligible values, as mentioned in Section 6.2.3.

2. Equilibrium with quartz, calcite, hydroxyapatite and Fe(III) oxyhydroxides, and TDB uncoupled. When the uncoupled database is used, the equilibrium between C(IV) and C(−IV) is not considered, and as a consequence methane generation is suppressed and the total concentration of carbonate remains unchanged.

3. Equilibrium with quartz, calcite, hydroxyapatite and amorphous Fe(II) monosulphides, and TDB coupled.

5 Geochemical evolution of groundwaters during the stage of the open repository

During the excavation and relatively long operational period, the hydraulic conditions of the Forsmark site will change and the hydraulic conditions may alter the groundwater composition around the repository. Some of these changes will be induced by the presence of the repository, but also shore-level displacements and climatic variations may cause more limited alterations. As a consequence, the salinity in some parts of the repository may decrease due to an increased infiltration of diluted waters of meteoric origin, whereas in other regions the corresponding upconing or the infiltration of Baltic seawater might instead induce an increase in salinity. This involves the safety function indicators R1b and R1c in Figure 1-3 and, in extreme cases it might affect the swelling of the backfill or enhance colloidal erosion of the buffer during deposition.

In addition to the groundwater changes caused by hydrological processes, other chemical aspects need to be considered during this period. It is to be expected that the excavation will be accompanied by grouting, and the chemical influence of the grout on groundwater must be considered. In general, cementitious grouts will increase the pH of the water, involving the safety function indicator R1e. During the operational phase, the role of stray materials must be assessed, as well as that of any other process that could possibly change the chemical conditions in the repository, such as the precipitation or dissolution of minerals and corrosion of metal in rock-bolts. These processes might, for example, affect the safety function indicators R2d and R2e in Figure 1-3, that is, the generation of colloids and the sorption properties of minerals.

When deposition tunnels are backfilled and plugged, air will be trapped in the porous buffer and back-fill, and processes consuming oxygen must be evaluated. Air will also cause some initial corrosion of the copper canisters until anoxic conditions are reached. All these chemical processes are related to the safety indicators Can1 (copper canister thickness) and R1a (reducing conditions) in Figure 1-3.

Other chemical processes taking place in the buffer and backfill occur on longer time scales than the relatively short operational phase.

5.1 Natural groundwater conditions at the sites

The chemical characteristics of groundwater at Forsmark prior to the construction of the repository are set out in detail in their corresponding SDM 2.3 /Laaksoharju et al. 2008/.

5.2 Salinity

The groundwater salinity and composition in the vicinity of the repository may be affected during this period because of the inflow into open tunnel sections. This will cause an unnatural infiltration of meteoric and Baltic seawater, and as a consequence, upconing may occur. This phenomenon has been observed for example in some boreholes at Äspö. In extreme cases, if the groundwaters at greater depth have high salinities, the upconing of these waters might decrease the swelling pressure of the backfill, safety function indicator R1b in Figure 1-3. However, no such highly saline groundwaters have been found at the deepest sampling points at Forsmark.

Once the repository has been backfilled and closed it is expected that groundwater salinities will return to normal conditions after some time. For example saline groundwaters that had moved upwards will then sink due to their higher density. Diffusion into the rock matrix might retain a certain amount of salts at repository depth during the operation period, and out-diffusion from the rock matrix into the fractures after closure will tend to restore the initial salinity distribution.

The inflow to the tunnels will be reduced by injecting grout into the surrounding fractures. This will prevent the depression of groundwater levels near the ground surface and the corresponding inflow of meteoric and seawaters as well as the upconing of saline waters into the excavations.

The effect of grouting has been modelled for the Forsmark site. The results using the code DarcyTools indicate that limited upconing and limited changes in salinities are to be expected during construction and operation of a repository located at Forsmark.

5.3 Redox conditions

Even with moderate inflows to the open tunnels, large amounts of superficial waters are predicted to percolate into the tunnels when considering the whole period of repository operation. Infiltrating waters will initially be equilibrated with oxygen in the atmosphere, whether they are of marine, lake, stream or meteoric in origin. It could be contended that the redox stability of the rock volume on top of the repository area might be challenged at the time of repository closure by the large amounts of infiltrating O_2-rich waters.

However, microbial oxygen consumption takes place already in the overburden and in the first metres of rock, as well as in lacustrine, fluvial and marine sediments. Therefore infiltrating waters are free of dissolved O_2. Oxygen consumption in saturated soils is well documented, see for example /Drew 1983, Silver et al. 1999, Pedersen 2006/. The Äspö Redox Zone experiment /Banwart 1999, Molinero-Huguet et al. 2004/ also showed that microbial respiration in the upper metres of a fracture zone effectively consumes the oxygen in infiltrating waters. In addition groundwater samples from Äspö and Stripa are always found to contain dissolved Fe(II) /Nordstrom et al. 1989/ indicating that groundwaters remain reducing even after prolonged periods of inflow into the tunnels.

In conclusion, the reducing capacity of transmissive fracture zones is not affected during the excavation and operation periods, because consumption of oxygen in infiltrating waters takes place already in soils, sediments as well as in the upper metres of fractures by microbial processes.

5.4 Oxygen consumption in backfill

Air will be trapped in the porous buffer and backfill when deposition tunnels are plugged. Most of the oxygen in this air will be in the backfill because of its larger volume. This oxygen can diffuse to the canister surface and cause some initial corrosion until anoxic conditions are achieved, and, therefore, it is valuable to estimate the reducing capacity of the backfill. Both chemical processes and microbial activities are expected to consume oxygen.

Numerical calculations /Grandia et al. 2006/ coupling chemical processes consuming oxygen with the hydrodynamic saturation of the backfill have been used to estimate the time scale for reaching anoxic conditions in the tunnels of the repository. These studies show that several inorganic O_2 consumption processes may take place with the accessory minerals present in the bentonite in the buffer and in the backfill. These reactions are, in order of decreasing rate, the dissolution of Fe(II) containing carbonates, the oxidation of pyrite, and the oxidation of Fe(II) bearing silicates such as mica and montmorillonite. The calculated oxygen consumption times are highly dependent on the postulated value for the surface area of the reacting minerals. Nevertheless, it may be concluded that anoxic conditions are likely to be reached after a period of the order of one month after the backfill becomes completely water saturated. The density of the backfill is low enough to allow microbial activities and the effect of microbial activities will be to shorten the time to reach anoxic conditions in the backfill. Diffusion of oxygen to the surrounding granite would be also an effective mechanism for oxygen consumption by aerobic bacteria populations that could develop in the backfill/granite interface. The REX experiment in the Äspö HRL showed that oxygenated water in contact with a granite surface will be reduced in a few weeks.

In the Prototype Repository Project at the Äspö Hard Rock Laboratory, a programme is in progress for sampling and analysing gases at different locations in the buffer and backfill. One of the specific aims is to monitor the consumption of oxygen /Pedersen et al. 2004/. The two sections of the Prototype Repository were sealed in September 2001 and September 2003, respectively. Results have been published for the samplings in 2004 and 2007. The resulting oxygen content in the gas phase ranged from almost zero to practically full air atmosphere, although there is a general decreasing trend with time. However, for technical reasons the backfill is not fully water saturated in all parts. These data, therefore, provides further indications that the oxygen consumption will be rapid.

In conclusion, both inorganic reactions and microbial processes will quickly consume O_2 in the air trapped in the backfill, which has the largest pore volume in the deposition tunnels. The majority of the oxygen in the backfill will react before it can diffuse into the buffer and reach the surface of a canister.

5.5 Effects of grout, shotcrete and concrete on pH

Injection of grout into fractures surrounding the repository tunnels might be necessary to avoid inflow of groundwater. Traditionally, cement-based grout is used when excavating tunnels. Standard Portland cement paste has porewater which is highly alkaline (pH ≈ 12.5). In order to avoid detrimental effects from porewater diffusing out of the cement matrix, cement recipes with porewaters having pH ≤ 11 will be used in the vicinity of deposition tunnels. It is to be expected that the development of recipes for such materials will be an ongoing process both at SKB and elsewhere during the whole period of repository operation. Although the effects of these porewaters are much smaller, they must be considered, because it is possible that relatively large quantities of cement will be used. Limited amounts of grouting will likely be needed at Forsmark due to the low permeability of the rock.

The distribution of shotcrete and concrete in the repository will be spatially limited and their potential impact during the excavation and operational phases will be restricted. Most of the leaking porewaters from these materials will be mixed with groundwater infiltrating into the tunnel and pumped away. A small part of the cement materials will be in contact with the backfill, and cement porewaters could migrate and diffuse into the bentonite. As long as low alkalinity cements are used, the consequences on the properties of the buffer and backfill may be neglected.

On the other hand, grout could have a large impact on the geosphere conditions, as it is widely and diffusely distributed in the fracture system. Grouting is, however, necessary to avoid a large groundwater drawdown (increased meteoric water influx) and the corresponding upconing of saline waters. Grouting is also needed for construction purposes; the ingress of water needs to be limited for the engineering installation and for worker safety. Two types of grout are envisaged in the vicinity of the deposition tunnels in the final repository: low alkalinity cement based grouts and suspensions of nano-sized silica particles (Silica Sol). The solidified Silica Sol grout is similar in its properties to the silica present in large quantities in the rock and fracture fillings, and may, therefore, be ignored in a long-term safety context. Cement-based grouts on the other hand have chemical properties quite different from the surrounding rock, and their effects have to be considered.

Boreholes crossing cement grouted fractures at the Olkiluoto site in Finland have yielded waters with elevated pH values since sampling started. The more limited experience from Äspö shows that a pulse of alkaline solutions may be detected in the immediate vicinity of the grouted fractures. This pulse of alkaline waters is believed to be due to two factors: pore water released while the liquid grout solidifies; and erosion and dilution of grout by flowing groundwater in the outer edge of the grouted volume. These effects in the non-grouted fractures at Äspö were transitory, and after a few days the chemical composition of the groundwater returned to its original state. The pH values were sufficiently low as to indicate that substantial dilution had occurred. The data from Olkiluoto indicates that the intensity of this short alkaline pulse will be decreased by the use of low alkalinity cement. Because of its short duration and its low intensity, its effects are negligible.

After this short period, grout will start to react with circulating groundwater, and a slightly alkaline plume will develop downstream in the grouted fractures /Luna et al. 2006/.

5.6   Precipitation/dissolution of minerals

During the operational phase, inflow of groundwater into the tunnel and mixing of groundwaters of different origin within rock fractures will probably result in precipitation or dissolution of minerals. These processes could only indirectly affect the safety function indicators listed in Figure 1-3. This process may be observed at the tunnel walls of the Äspö HRL, and it is believed to cause the observed decrease in the overall water inflow at Äspö. Simulations indicate that calcite and Fe(III) oxyhydroxide may precipitate at the tunnel/backfill boundary /Domènech et al. 2006, Acero et al. 2010/ and that this process does not influence the performance of the repository negatively.

5.7   Identified uncertainties and their handling in the subsequent analysis

Several uncertainties are identified when considering the different chemical aspects of the evolution of the repository during the operation period,

- There is a large degree of uncertainty in the detailed salinity distribution around the repository. However, the salinity changes will not become so high or so low as to affect the performance of the repository during this period or when considering its future evolution. The distributions of salinity, pH and other groundwater components obtained from the modelling of the temperate conditions at 2000 AD, described below, are wide enough to include the small changes caused by the operation of the repository.

- The degradation of organic materials is associated with a large degree of uncertainty. Man-made materials (plastics, lubricants, etc) have so slow degradation rates that they cannot be studied in the laboratory. The nature and the biodegradability of the organic matter in the bentonite is also unknown. The influence of the degradation of organic materials on repository performance is constrained by their limited amounts.

- The uncertainties on other chemical aspects, such as remaining oxygen, etc, have been established to be of no concern for the performance of the repository.

5.8   Summary of the excavation/operation phase

During the excavation/operation phase, the chemical evolution mainly arises from the disturbance to the natural conditions caused by the presence of the repository:

- the effects on salinity from upconing and groundwater draw-down are assessed to be negligible;

- a short alkaline pulse in the groundwater from low-pH cement, shotcrete and concrete is likely to form, but its effects will be negligible;

- an increased precipitation of calcite and Fe(III) oxyhydroxides will occur at the tunnel wall during operations, but this process is evaluated as being of no consequence for the performance of the repository;

- oxygen left in the repository will be consumed by either chemical processes or microbes; the majority of the oxygen in the backfill, which has the largest pore volume in the deposition tunnels, will react and thus not diffuse into the buffer and reach the surface of the canister.

The evolution of other key parameters is discussed in Chapter 8.

6 Hydrogeochemical numerical results from the temperate period calculations

During the initial temperate period after closure, the infiltration of meteoric waters, the displacement of the Baltic shore line and changes in annual precipitation will influence the hydrology of the site. These phenomena induce changes in the geochemical composition of groundwater around the repository.

One of the questions to be addressed for this period is whether the chemical environment will remain favourable after repository closure. The most important parameters are redox, pH and salinity. Other factors to consider are the groundwater content of potassium, sulphide and Fe(II), as they might affect the chemical stability of the buffer and the canister.

Results have been reproduced with vertical sections, cross-cutting the candidate repository volume, and in a horizontal surface located at the repository depth (–470 m) (Figure 6-1, Figure 6-7, Figure 6-11, Figure 6-13 and Figure 6-19). On the other hand, the statistical results obtained for the simulated points within the candidate repository volume have been represented by box-and-whisker plots, as it has been explained in each figure caption (Figure 6-2, Figure 6-3, Figure 6-4, Figure 6-6, Figure 6-8, Figure 6-12, Figure 6-16 and Figure 6-17)

6.1 Base Case

Groundwater compositions are modelled through advection, mixing and chemical reactions with fracture-filling minerals. We have assumed equilibrium with respect to calcite, quartz, hydroxyapatite and Fe(III) oxyhydroxides. Additionally, in the statistic calculations the "Base Case" assumes that redox sensitive parameters (as Eh and iron concentration) have to be evaluated considering the possibility of equilibrium with respect to amorphous Fe(II) sulphides at all points in space and time.

6.1.1 Salinity evolution

The gradient of salinities in the Forsmark domain is very significant by the presence of Deep Saline groundwaters (at depths below 600–700 m), and by the existence of diluted groundwaters resulting of the infiltration of meteoric waters in the shallowest zones of the fractured aquifer (Figure 6-1).

During the simulated temperate period, groundwaters are affected by increasing amounts of waters of meteoric origin. In this way, the evolution of salinities are basically controlled by the dilution from the infiltration of meteoric origin waters, and the convection of the corresponding front of salinities. On a regional scale this corresponds to a gradual decrease of the groundwater salinity, especially in the upper part of the modelled rock volume.

As a consequence of the hydrological structure of the lithological units in the vicinity of the repository area, the front of diluted groundwaters reaches the repository depth (470 m) after the year 9,000 AD. Before this (2,000, 3,000 and 5,000 AD), the average of the calculated salinities slightly decreases with time, increasing the range of the computed values (Figure 6-2). The minimum salinity calculated for the repository depth is around 1 g/L, which does not vary with respect to that obtained at the year 5,000 AD, indicating that in this time restricted areas within the repository volume are already affected by the arrival of the front of meteoric waters.

Towards the end of the modelled period (9,000 AD), approximately the 25% of the groundwaters within the repository volume have less than 0.3 g/L of dissolved salts, while all the groundwaters had salinities above 0.6 g/L at the start of the simulation, that is, at repository closure.

In conclusion, the salinities at Forsmark during the first temperate period following repository closure will remain at levels sufficiently low to ensure that the swelling properties of the buffer and backfill are not negatively affected.
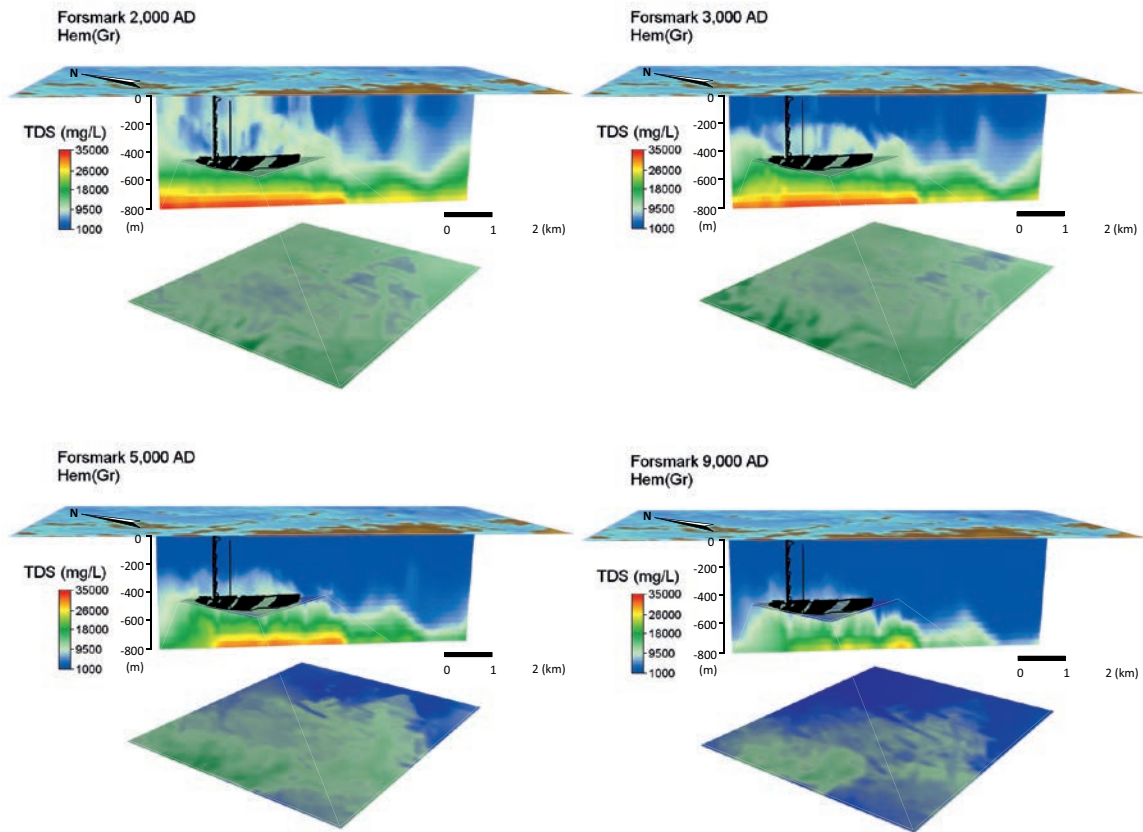
Figure 6-1. *Distribution of the computed salinity (TDS in mg/L), for Forsmark in vertical slices at times equal to 2,000 AD, 3,000 AD, 5,000 AD and 9,000 AD.*
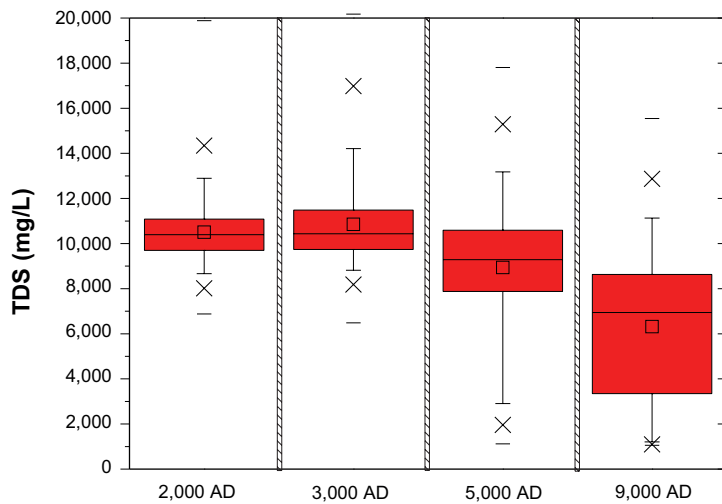
Figure 6-2. *Box-and-whisker plots showing the statistical distribution of the TDS for the "Base Case" defined in the text. The statistical measures are the median, the 25th and 75th percentile (box), the mean (square), the 5th and 95th percentile ("whiskers"), the 1st and 99th percentile (crosses) and the maximum and the minimum values.*

6.1.2 Evolution of concentrations of natural groundwater components

The increasing proportions of groundwaters of meteoric origin will decrease the overall salt content of the groundwaters, as discussed in the previous sub-section. However, the effects on the individual chemical constituents will depend on their reactivity. Some groundwater components behave as "conservative" (they do not participate to a large extent in chemical reactions), and their concentrations are mostly controlled by groundwater mixing.

Most of the groundwater chemical components are reactive: Fe(II) and Fe(III), H^+, bicarbonate and phosphate. Sodium and calcium may participate in ion-exchange processes, and calcium participates readily in the precipitation and dissolution of calcite. But, in spite of this, the high concentrations of the saline waters are such that these elements behave almost as conservative. Sulphate may be reduced to sulphide under hydrothermal conditions. At lower temperatures, as are applicable in this context, sulphate can only be reduced to sulphide by microbially mediated reactions with organic matter.

Cations

Showing the same trends of the salinity plot, the evolution of the computed concentrations of the cation are a result of dilution processes by the infiltration of the meteoric origin waters (see Appendix 2).

The concentration of cations is important in that their presence decreases the stability of colloids. In groundwaters that are too dilute, colloids might enhance the transport of radionuclides. In addition, as the buffer swells into fractures, montmorillonite colloids may be transported away by dilute groundwaters. The criterion for the safety function indicator is expressed in charge equivalents as $\sum q[M^{q+}]$. This value has to be higher than 4 mM, as available experimental data suggests that montmorillonite colloids are not stable at cation concentrations above this limit. Figure 6-3 shows the evolution of this safety function along the simulated temperate period. It may be concluded that for the whole temperate period following repository closure, cation concentrations at repository depth in the Forsmark site will remain higher than 4 mM, that is, above the limit where montmorillonite colloids start to become unstable. Even when meteoric origin waters are the major groundwater contributor in the mixing (9,000 AD), the safety function indicator $\sum q[M^{q+}]$ remains higher than 10 mM.

The cations contributing with the highest charge concentrations in the groundwaters at Forsmark are calcium and sodium and, to a much lower extent, magnesium and potassium (Figure 6-4). Because the concentration of calcium is duplicated in the safety function indicator, $\sum q[M^{q+}]$, calcium is the most important element in this context. Calcium participates in water-rock interactions as carbonates, and may be also released from the weathering of feldspar. It should be noted that the Ca concentrations in groundwaters found at present in the upper 200 m vary between 0.2 and 30 mM, according to the data shown in Figure 6-5. This spread of the data is not included in the meteoric reference water used in the mixing calculations, and, therefore, the variability is probably underestimated.
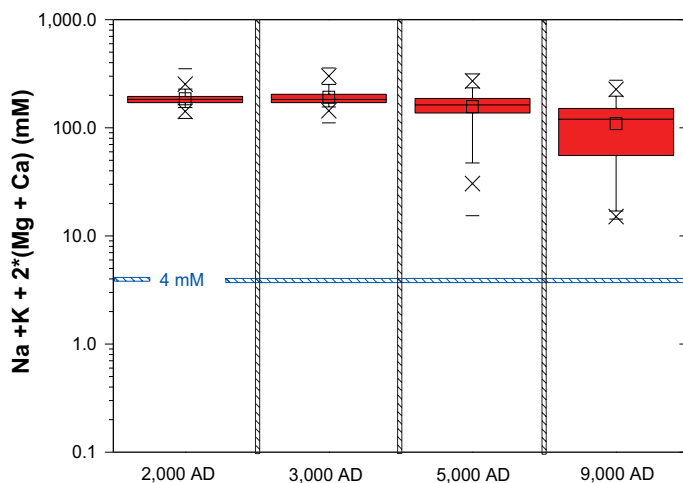
Figure 6-3. Box-and-whisker plots showing the statistical distribution of the calculated safety function factor $\sum q[M^{q+}]$ for the positions located within the candidate repository volume at Forsmark. The statistical measures are the median, the 25th and 75th percentile (box), the mean (square), the 5th and 95th percentile ("whiskers"), the 1st and 99th percentile (crosses) and the maximum and the minimum values.
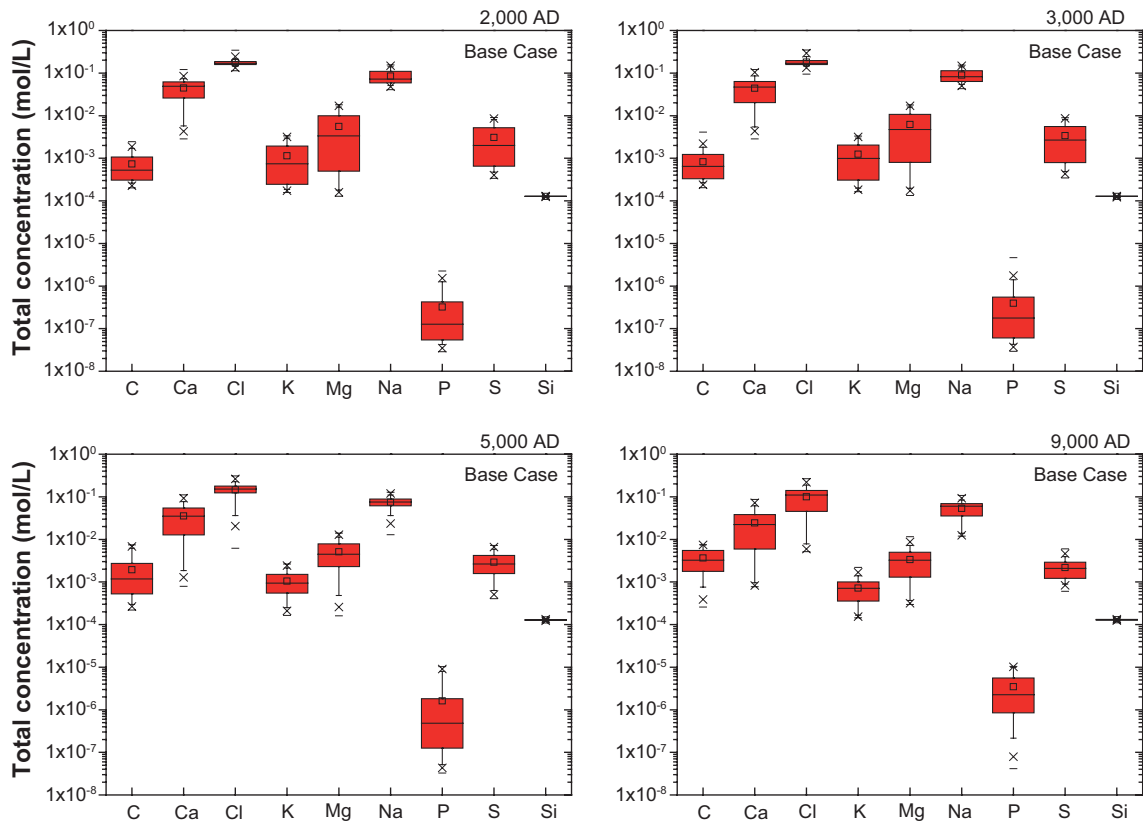
Figure 6-4. Box-and-whisker plots showing the statistical distribution of the calculated safety function factor $\sum q[M^{q+}]$ for the positions located within the candidate repository volume at Forsmark. The statistical measures are the median, the 25th and 75th percentile (box), the mean (square), the 5th and 95th percentile ("whiskers"), the 1st and 99th percentile (crosses) and the maximum and the minimum values.
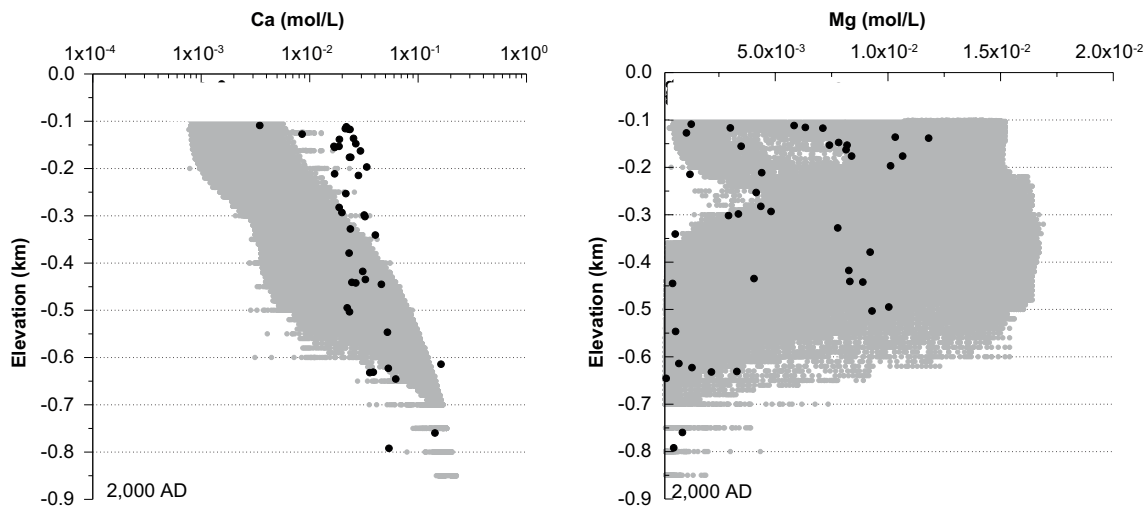
Figure 6-5. The concentration of calcium and magnesium in groundwaters sampled in boreholes at the Forsmark site (black dots) compared with values calculated using the proportions of reference waters obtained from the hydrogeological model as input for chemical mixing and reactions, including, among others, calcite dissolution and precipitation (grey dots). The groundwater data with category 3 or better /Laaksoharju et al. 2008/ has been plotted.

At Forsmark, the Deep Saline groundwaters are quite rich in calcium, and examination of the groundwaters at depths larger than $\approx$100 m shows that the calcium concentrations may be simulated by mixing of reference waters and that the relative effects of chemical reactions are minor. However, the analytical data show relative high concentrations of calcium at depths between –100 and –300 m which have not been accurately reproduced by our calculations. The other major divalent cation is magnesium, which is normally regulated in granitic groundwaters by the precipitation and dissolution of chlorite, a mineral that may have a wide range of compositions. In general, magnesium concentrations in groundwaters are much lower than those of calcium, and because of the low solubility of chlorites and the uncertainty in the composition of this mineral, the modelling of magnesium concentrations is much more uncertain than that of calcium (Figure 6-5). In general, comparing with the analytical data, our model computes higher magnesium concentrations and lower calcium concentrations for depths ranging from –100 m to –600 m. This coupled trend shows as mixing and calcite equilibrium would not be the only geochemical mechanisms controlling cation concentrations in the Forsmark groundwaters. As it has been previously commented (see Section 4.5), cation exchange reactions could play a significant role modifying the distribution of the cationic aqueous species.

Potassium concentrations are generally low in the groundwaters sampled, as observed also in other Fennoscandian sites in granitic rocks. Solubility control by sericite has been proposed as a mechanism controlling the maximum concentrations of potassium /Nordstrom et al. 1989/, but ion-exchange processes and illitic clays weathering cannot be ruled out. Even if the exact mechanism is not known all available groundwater data indicates that the increased infiltration of waters of meteoric origin will not increase the potassium concentrations found at present. The reaction modelling performed within SR-Site is not well suited to constrain potassium concentrations because, as mentioned, there is not enough information available on the possible reactions that could control this element.

The results about the hydrodynamics of the meteoric origin waters are shown in Appendix 2 which illustrates the gradual dilution of the groundwaters at repository depth due to the inflow of superficial waters of meteoric origin. The simulated ratios of the others four end-members (Deep Saline, Old Meteoric and Littorina groundwaters, and glacial origin waters) are also described in Appendix 2.

At 2,000 AD, in the central areas of the repository volume, the simulated groundwater composition is mainly a consequence of the mixing between the Old Meteoric groundwaters and the glacial origin groundwaters. On the other hand, to the eastern and the southern areas, groundwater composition is remarkably controlled by the high ratios of Littorina waters (and, additionally, Old Meteoric groundwaters). During the period 2,000–3,000 AD, the simulated cation concentrations remain practically constant (Figure 6-6). After then, the solute concentrations clearly evolves according to the dilution by the meteoric waters. Two aspects are important in the evolution of the calculated cation concentrations within the repository volume:

(1) the minimum values of calcium concentration computed at 9,000 AD are in the order of the calcium concentration of the meteoric waters ($7.70 \cdot 10^{-4}$ mol/L, Figure 6-6, and $4.70 \cdot 10^{-4}$ mol/L respectively), and

(2) in the period 3,000–5,000 AD, the range of magnesium and potassium concentrations signiphicantly decrease (Figure 6-6), as a consequence of the practically total dilution of the Littorina waters, and the Old Meteoric groundwaters, during this period. The mixing calculations give maximum values of potassium concentrations below 0.004 mol/L at any time.

Chloride, sulphate, silica and phosphate

Although chloride and sulphate are not listed in the safety function indicator criteria, chloride is used when selecting radionuclide transport properties (sorption coefficients) and sulphate is important when determining the solubility limits for radium. These two components behave almost conservatively, i.e. they participate in chemical reactions only to a very limited extent, and they have been modelled by mixing calculations in SR-Site.

The computed evolution of sulphate concentrations (Figure 6-7) is similar to that previously described for the Littorina end-member (see Appendix 2). These waters show the highest concentrations of the five end-members ($9 \cdot 10^{-3}$ mol/L, approximately), one order of magnitude higher than the sulphate concentrations of the Old Meteoric groundwaters and the Deep Saline and the Altered Meteoric concentrations.
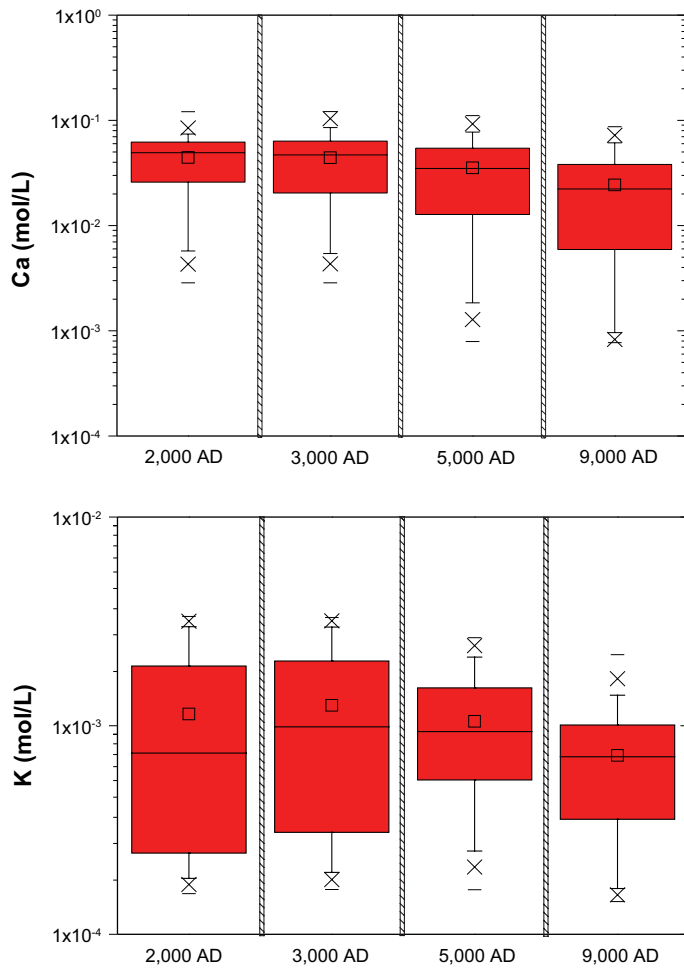
Figure 6-6. *Box-and-whisker plots showing the statistical distribution of the calculated Ca and potassium concentrations for the positions located within the candidate repository volume at Forsmark. The statistical measures are the median, the 25th and 75th percentile (box), the mean (square), the 5th and 95th percentile ("whiskers"), the 1st and 99th percentile (crosses) and the maximum and the minimum values.*
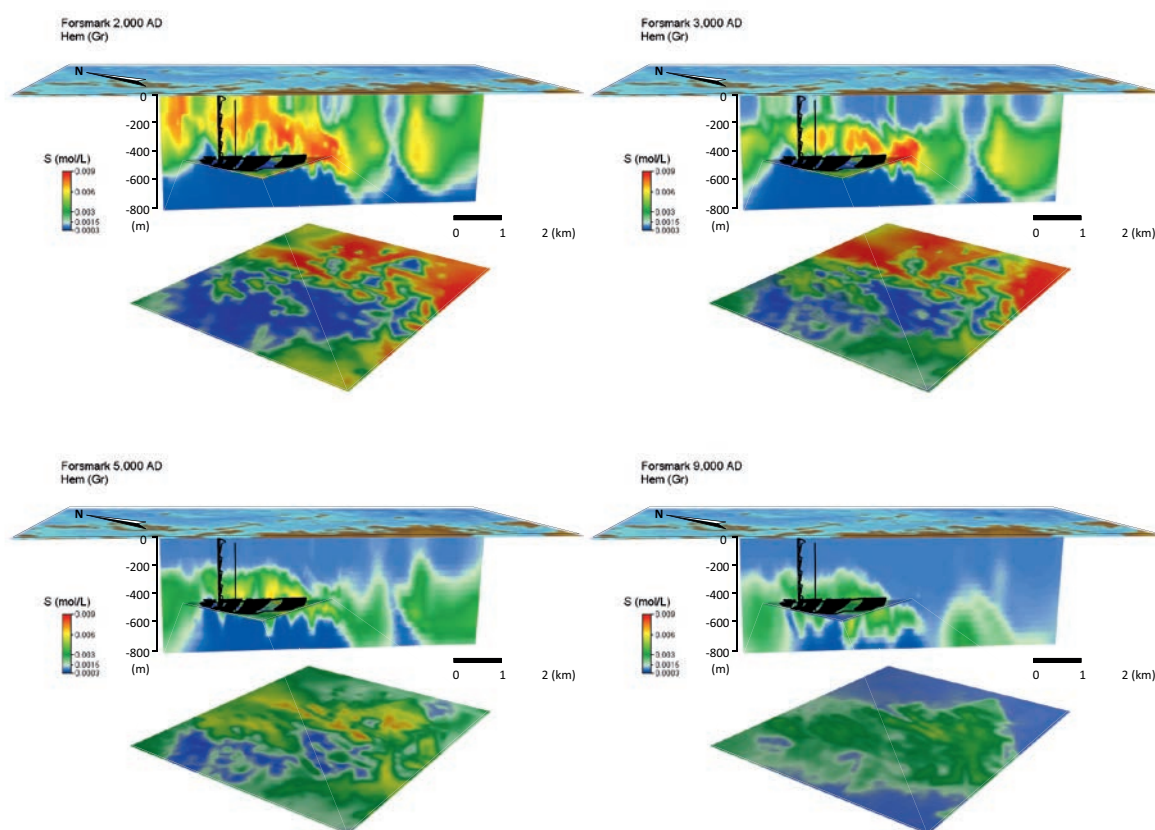
Figure 6-7. *Distribution of the computed concentrations of total sulphur aqueous species (mainly S(VI)), for Forsmark in vertical slices at times equal to 2,000 AD, 3,000 AD, 5,000 AD and 9,000 AD.*

Figure 6-8 shows that the groundwater concentrations of chloride and sulphate at repository level tend to decrease with time as waters of meteoric origin become increasingly dominant.

The concentration of the dissolved silica is basically controlled by quartz equilibrium in the computed groundwater compositions. During the simulated period, it practically does not change ($1.28–1.30 \cdot 10^{-4}$ mol/L), because the quartz solubility is not very sensitive with respect to the groundwater composition, in the range of temperatures considered in the present work.

The concentration of phosphate is obtained assuming thermodynamic equilibrium with respect to hydroxyapatite at all points in space and time (Figure 6-9). Within the candidate repository volume, the average values are progressively increasing during the simulated period (from $6.29 \cdot 10^{-8}$ to $1.12 \cdot 10^{-6}$ mol/L at 2,000 and 9,000 AD, respectively; Figure 6-4), when the model calculations show that waters of meteoric origin infiltrate into the repository volume.

The groundwater data collected during the site investigation show that the equilibrium assumption with respect to hydroxyapatite, see Section 4.5.1 (Figure 4-4), results in high phosphate concentrations at depths above −600 m (Figure 6-9). Although the phosphate numerical results do not show the same trend as the groundwater analytical data, the numerical results are considered conservative when assessing radionuclide solubilitites and migration.

pH values and total inorganic carbon concentrations

The pH values samples in the boreholes of the Forsmark site are, in general, ranged between 7.0 and 8.5 showing a large variability (Figure 6-10).

The simulated pH values are not sensitive with respect to the Fe-bearing mineral chosen to be in equilibrium in the groundwaters, Fe(III) oxyhydroxides or amorphous Fe(II) sulphides. The computed evolution of the pH (Figure 6-11) shows a progressive decrease above –400 m, from values around
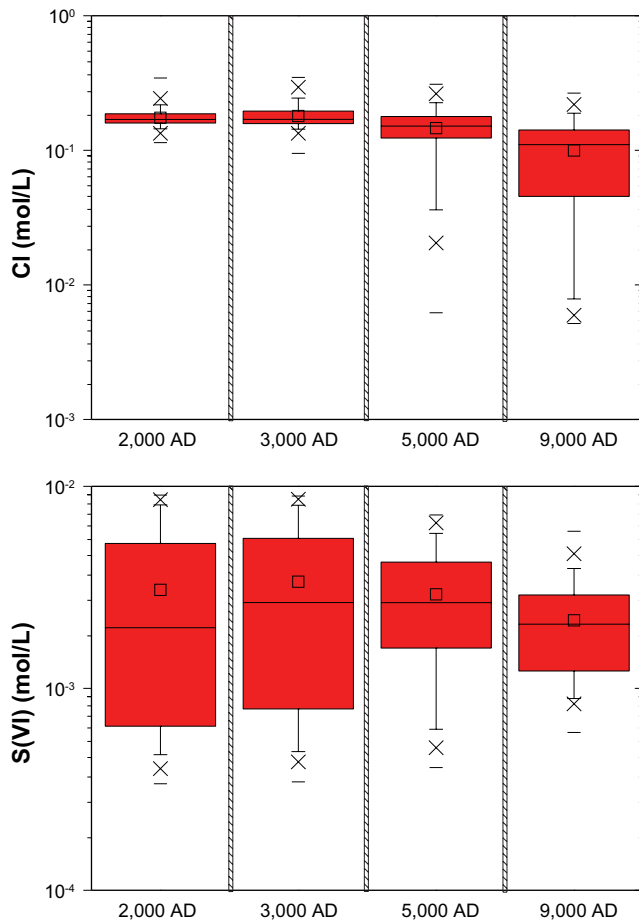
Figure 6-8. *Box-and- whisker plots showing the distribution of chloride concentrations (top) and of sulphate concentrations (bottom) for the positions located within the candidate repository volume at Forsmark. The statistical measures are the median, the 25th and 75th percentile (box), the mean (square), the 5th and 95th percentile ("whiskers"), the 1st and 99th percentile (crosses) and the maximum and the minimum values.*
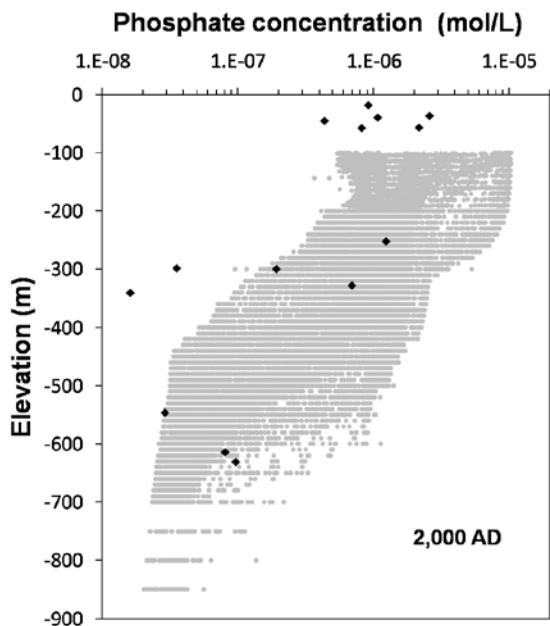
Figure 6-9. *Phosphate concentrations in groundwaters sampled in boreholes at the Forsmark site (field measurements, black dots) compared with values calculated using the proportions of reference waters obtained from the hydrogeological model as input for chemical mixing and reactions, including, among others, hydroxyapatite dissolution and precipitation (grey dots).*
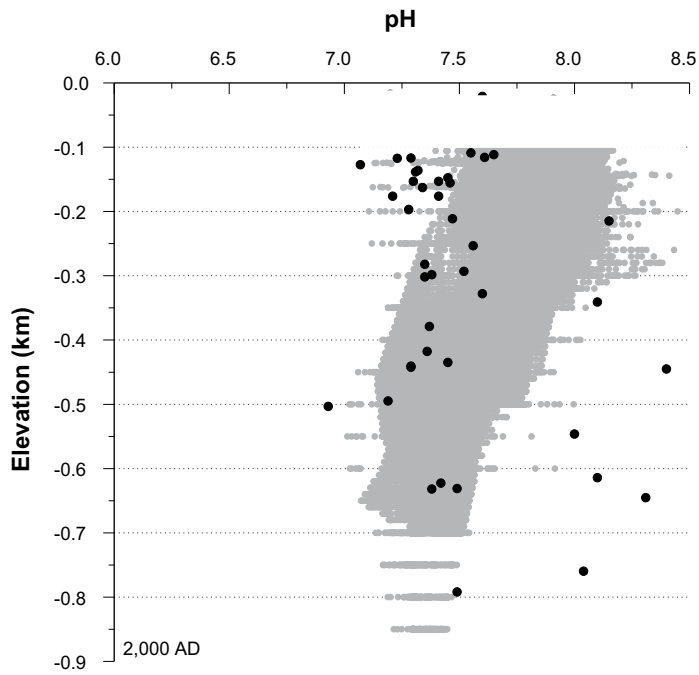
Figure 6-10. *pH values in groundwaters sampled in boreholes at the Forsmark site (measured in field, black dots)compared with values calculated using the proportions of reference waters obtained from the hydrogeological model as input for chemical mixing and reactions, including, among others, calcite dissolution and precipitation (grey dots). The groundwater data with category 3 or better /Laaksoharju et al. 2008/ has been plotted.*
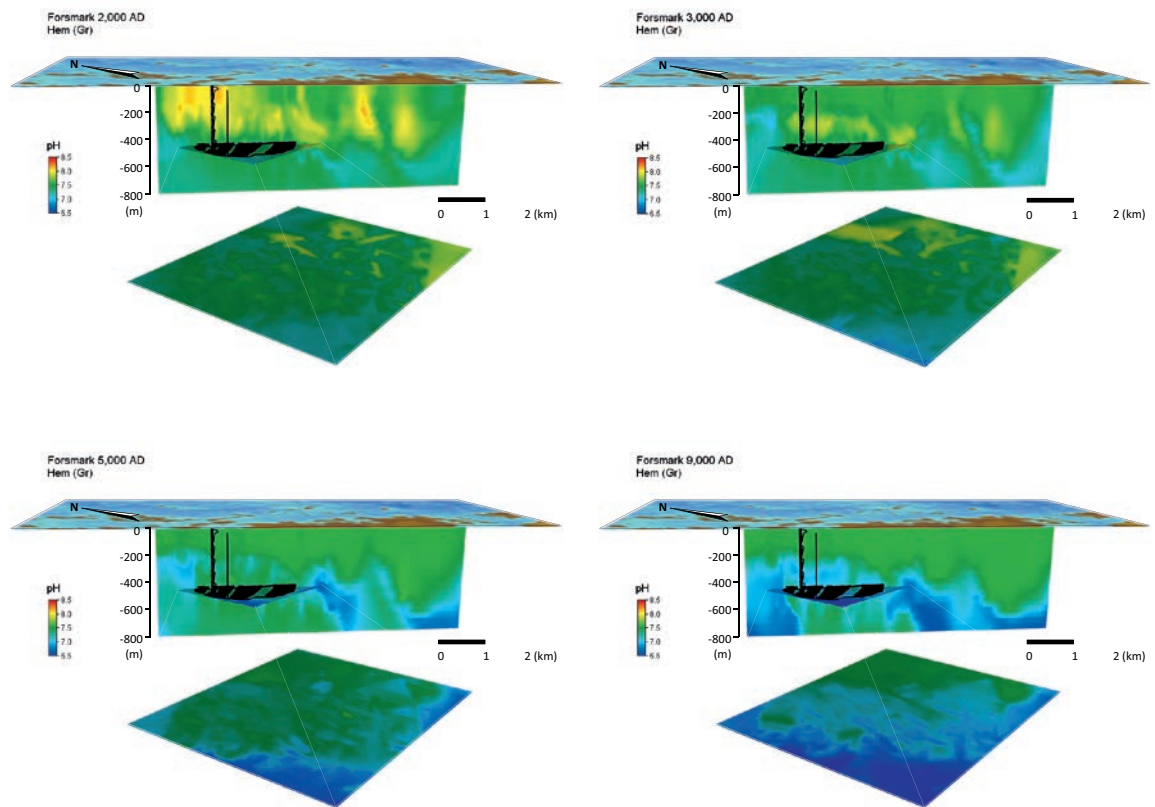
Figure 6-11. *Distribution of the computed pH values, for Forsmark in vertical slices at times equal to 2,000 AD, 3,000 AD, 5,000 AD and 9,000 AD.*

8.0–8.5 at 2,000 AD, to values around 7.5 at 9,000 AD. This evolution is a consequence of the infiltration of the meteoric origin waters and the equilibrium with respect to calcite of the resulting mixture.

At the repository depth, within the repository volume, the average values of pH are around 7.4 during 2,000 and 3,000 AD, decreasing to 7.33 and 7.07 at 5,000 AD and 9,000 AD, respectively (Figure 6-12). A significant decrease of the pH values has been computed between 3,000 and 5,000 AD (Figure 6-12). From 5,000 AD, the pH drops to values around 7.0, which is less than the minor value considered for the five end-members (7.3 for the altered meteoric waters). At 9,000 AD, the computed pH values are lesser than 7.0 at depths below 400–500 m (7.0–6.5). However, below the repository volume, the computed pH values remain around 7.5, because significant proportions of Deep Saline groundwaters are also preserved (see Appendix 2).

As it has been previously commented, the general decrease of the pH values within the repository volume is a consequence of (1) the enrichment of the meteoric waters in the mixing, and (2) calcite precipitation. The evolution of the concentrations of the total inorganic carbon also reflects these processes (Figure 6-13). The calculated partial pressures of dissolved carbon dioxide increase with time, as it is assumed in the modelling that the infiltrating meteoric waters have a higher CO_2 content than the other waters in the system.

In this way, as the time progresses, the aqueous carbonate concentrations also increase in groundwater, as a consequence of the infiltration of the meteoric waters. As a consequence of the mixing between these meteoric solutions and groundwaters more concentrated in calcium (Littorina waters and the Old Meteoric groundwaters), calcite becomes supersaturated. To maintain calcite equilibrium with the solute concentrations resulting from the mixing processes, the computed values of pH drop below the pH implemented for the meteoric waters (Figure 6-14).

As a conclusion, for pH and total inorganic carbon, the mixing and reaction calculations are dominated by the precipitation and/or dissolution of calcite. The numerical results show that the pH values remain approximately in the range 6.5 to 8, and that bicarbonate values increase gradually with time up to about 0.0075 mol/L. The conclusion is that the criterion for the safety function indicator R1e (pH < 11) is fulfilled during the whole temperate period following repository closure.
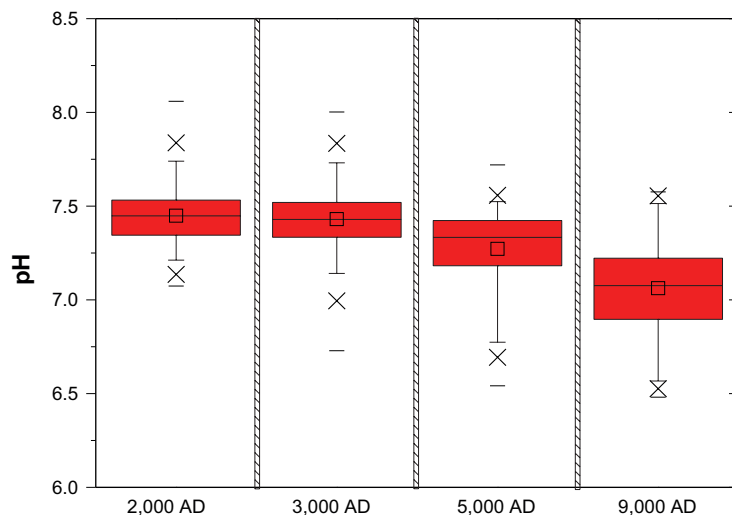
Figure 6-12. *Box-and-whisker plots showing the statistical distribution of the calculated pH. The statistical measures have been obtained for the positions located within the candidate repository volume at Forsmark and they are the median, the 25th and 75th percentile (box), the mean (square), the 5th and 95th percentile ("whiskers"), the 1st and 99th percentile (crosses) and the maximum and the minimum values.*
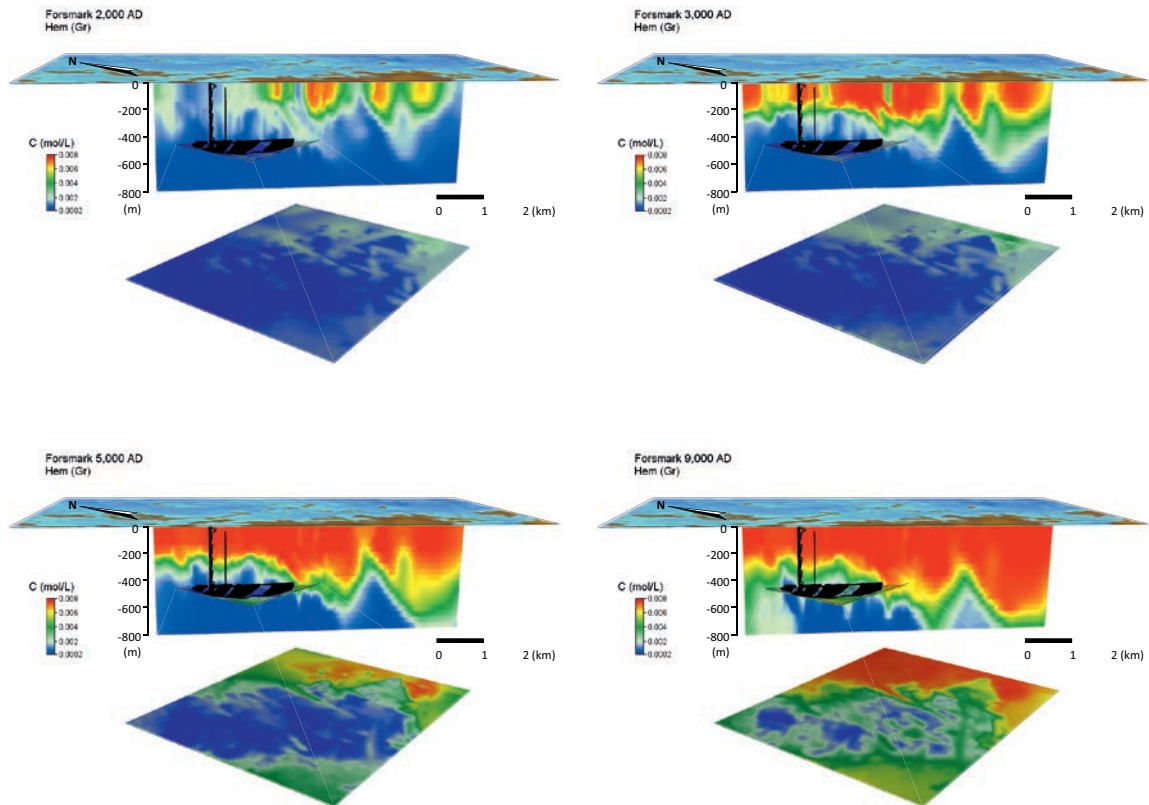
Figure 6-13. *Distribution of the computed concentrations of total inorganic carbon, for Forsmark in vertical slices at times equal to 2,000 AD, 3,000 AD, 5,000 AD and 9,000 AD.*
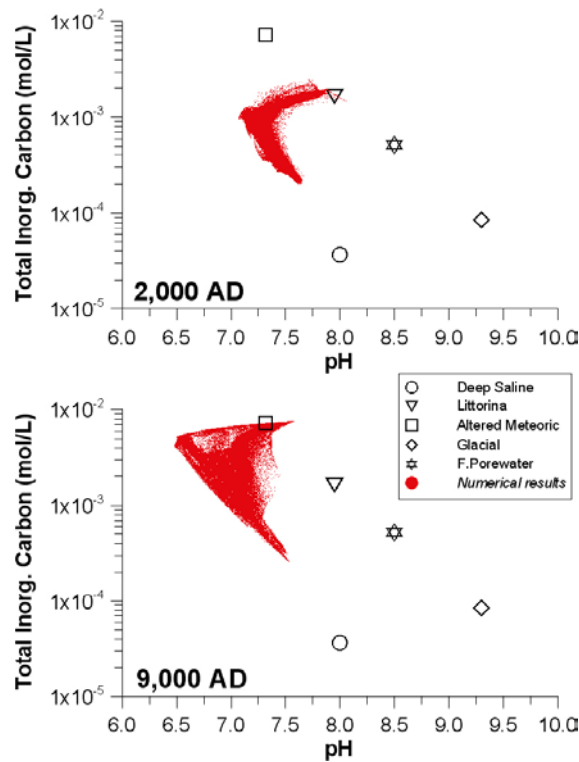
Figure 6-14. *Correlation and evolution of the calculated pH values and the concentrations of the total inorganic carbon for the positions located within the candidate repository volume at Forsmark corresponding to 2,000 AD (top) and 9,000 AD (bottom).*

Sulphide and iron concentrations

The content of sulphide in groundwaters is controlled by a steady state between microbial sulphate reduction and processes that remove sulphide: oxidation and precipitation with metals. Under oxidising conditions, for example in superficial waters, sulphide is quickly oxidised to sulphate. Under reducing conditions, dissolved Fe(II) is normally present and the maximum sulphide concentrations are regulated by the precipitation of Fe(II) sulphide.

Sulphide concentrations have been analysed during the site characterisation process and during the following groundwater monitoring. The data are often below the detection limit of the analysis procedure, but in some borehole sections sulphate reduction has taken place during the monitoring period and relatively high sulphide concentrations have been observed (Figure 6-15).

In the reaction modelling performed within SR-Site, apart from the "marine" and "Deep-Saline" components, the reference waters used in the mixing calculation were assumed to contain no sulphide. The marine waters infiltrating the rock may be relatively rich in organic matter, and observations at Äspö have show that some sulphate reduction takes place in these groundwaters.

The results of mixing of the marine component with the other reference waters are shown in Figure 6-16, illustrating the decrease in sulphide values as meteoric waters become increasingly dominant with time. The average values in the repository volume are practically constant (around $2 \cdot 10^{-6}$ mol/L; Figure 6-16). However, the minimum values are strongly decreasing with time, resulting, at 9,000 AD, concentrations lesser than 10^{-11} mol/L. These values are obtained under the assumption of the Fe(III) oxyhydroxides equilibrium, which corresponds with a relatively high oxidizing environment. In reality the concentrations of sulphide are not expected to decrease to the same degree as the figure shows, because the calculations only reflect the effect of dilution with meteoric waters and does not include the possibility of pyrite dissolution.

From the sulphide data in Figure 6-15 it may be concluded that sulphide concentrations averaged over the temperate period will be at the levels found at present at the sites or lower, that is, lower than 10^{-5} mol/L. For any given deposition hole oscillations in sulphide levels will take place, but the time-averaged concentrations are expected to be lower than 10^{-5} M. However, there is a probability that for some deposition holes the surrounding groundwaters have sulphide concentrations as high as $10^{-3.9}$ M, as shown in Figure 6-15.
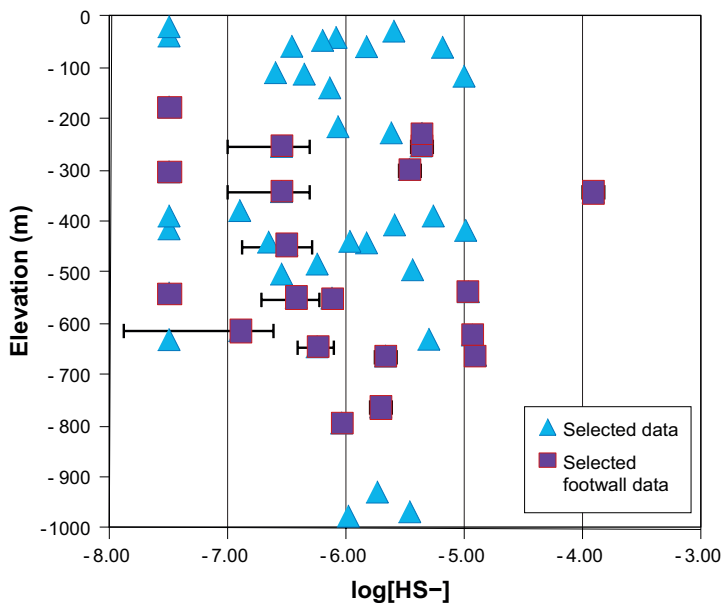
Figure 6-15. *Selected set of sulphide concentrations in contemporary groundwaters of the Forsmark area. In general only one value has been selected for any given depth Section of each borehole for cases where several analyses have been performed. Data below the detection limit of the analyses, which is between 0.03 and 0.002 mg/L, are shown in this diagram at $10^{-7.5}$ M, i.e. at 0.001 mg/L.*
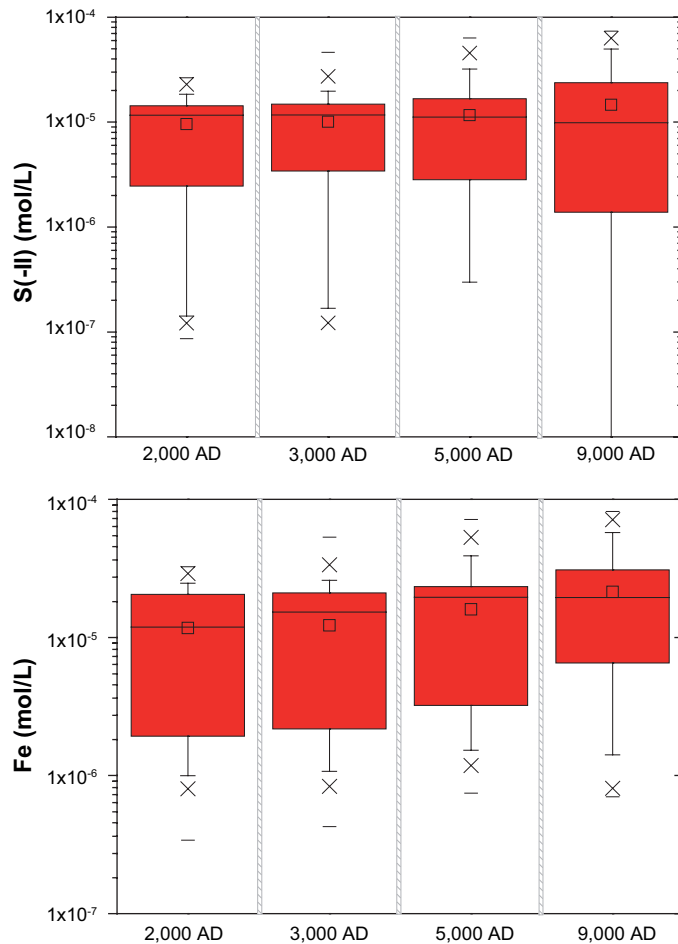
Figure 6-16. *Box-and-whisker plots showing the statistical distribution of the calculated sulphide (top) and iron (bottom) concentrations for the positions located within the candidate repository volume at Forsmark as a function of time. The statistical measures are the median, the 25th and 75th percentile (box), the mean (square), the 5th and 95th percentile ("whiskers"), the 1st and 99th percentile (crosses) and the maximum and the minimum values.*

The concentration of Fe(II) is regulated by a complicated set of reactions including the slow dissolution of Fe(II) silicates, such as chlorite and biotite, the precipitation of Fe(II) sulphides and redox reactions. The concentrations of Fe(III) are, in general, negligible in granitic groundwaters, as the Fe(III) oxyhydroxides are quite insoluble and they quickly precipitate. For the reaction modelling in SR-Site, it has been assumed that either Fe(III) oxyhydroxide or amorphous Fe(II) sulphide are in equilibrium, and the calculated results using both assumptions are included in the statistics displayed in Figure 6-16, which shows that the calculated Fe concentrations of groundwaters at repository level are expected to increase with time as waters of meteoric origin become increasingly dominant.

The distribution of Fe aqueous species is not in accordance with the distribution of one of the five end-members considered in our models. Only the distribution of Littorina waters seems to be a slight influence on the computed Fe concentrations in especific areas (it presents the highest Fe concentration of the five end-members: $8.262 \cdot 10^{-6}$ mol/L).

Using this methodology, we can observe as the most probable Fe concentration within the repository domain slightly increases during the simulated period (around 10^{-5} mol/L). The differences between the maximum and the minimum values are around two orders of magnitude. In spite of this, Fe concentrations less than 10^{-7} mol/L and higher than $8 \cdot 10^{-5}$ mol/L have not been computed in the repository volume.

6.1.3 The redox evolution of the system

Evidence from the Äspö laboratory, and other Swedish sites, shows how anoxic conditions prevail in the host rock even at a short distance from tunnel walls or from the ground surface. Air will be entrapped in the buffer and backfill, but anoxic conditions are expected to be established soon after the tunnels become re-saturated. Even if the buffer or backfill do not become fully saturated during this period, oxygen consumption processes will take place in the partially saturated materials, as shown from the data obtained at the Febex and Prototype experiments /Jockwer and Wieczorek 2003/.

The hydrogeological modelling shows that the proportion of waters of meteoric origin will increase with time (see Appendix 2). This evolution is not expected to change the reducing characteristics of the groundwater, as infiltrating meteoric waters become depleted of oxygen by microbial processes in the soil layers of the site, if there are any, or after some tens of metres along fractures in the bedrock, as shown by the data collected within the Rex experiment /Puigdomenech et al. 2001/ and from groundwaters sampled at 40 to 70 m depth during the "Redox Zone" experiment at Äspö /Banwart 1999, Banwart et al. 1999/.

The calculations for Forsmark including equilibrium with either an Fe(III) oxyhydroxide and with Fe(II) sulphide are presented in Figure 6-17 and in Figure 6-18 which show that the redox potentials increase slightly with time but remain well below –50 mV at the end of the simulation period.

At 2,000 A.D. the most probable values of Eh are included in the range between –250 and –200 mV. Figure 6-17 shows as the minimum and the maximum values progressively increase to more oxidizer values. In this way, at 9,000 AD, the most probable values will be included in the range of –225 and –125 mV, with a maximum value around –60 mV. At the regional scale, the maximum computed Eh values occurs towards the southern and the western area of the repository domain to the final simulation time (9,000 AD; Figure 6-19), under the assumptions of Fe(III) oxyhydroxides equilibrium.

Calculations include two geochemical variant cases: considering equilibrium with either Fe(III) oxyhydroxide and with amorphous Fe(II) sulphide. The results are slightly dependent on the solid phase chosen. However, there are no geochemical arguments that can be used to postulate what mineral regulates the measured redox potentials of groundwaters, and therefore the calculated redox potentials from both options are given the same weight in SR-Site, which is the same strategy adopted for iron above.

It may, therefore, be concluded that for both sites the anoxic groundwater conditions now prevailing at repository depth will continue for the whole temperate period following the closure of the repository, in spite of the increasing proportion of meteoric waters with time.
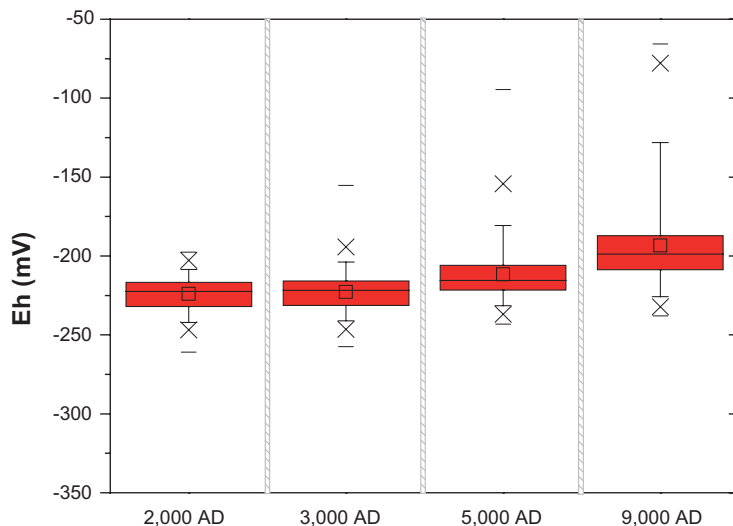
Figure 6-17. *Box-and-whisker plots showing the statistical distribution of the calculated Eh (redox potential) taking into account results using either equilibrium with Fe(III) oxyhydroxide or amorphous Fe(II) sulphide. The statistical measures have been obtained for the positions located within the candidate repository volume at Forsmark and they are the median, the 25th and 75th percentile (box), the mean (square), the 5th and 95th percentile ("whiskers"), the 1st and 99th percentile (crosses) and the maximum and the minimum values.*
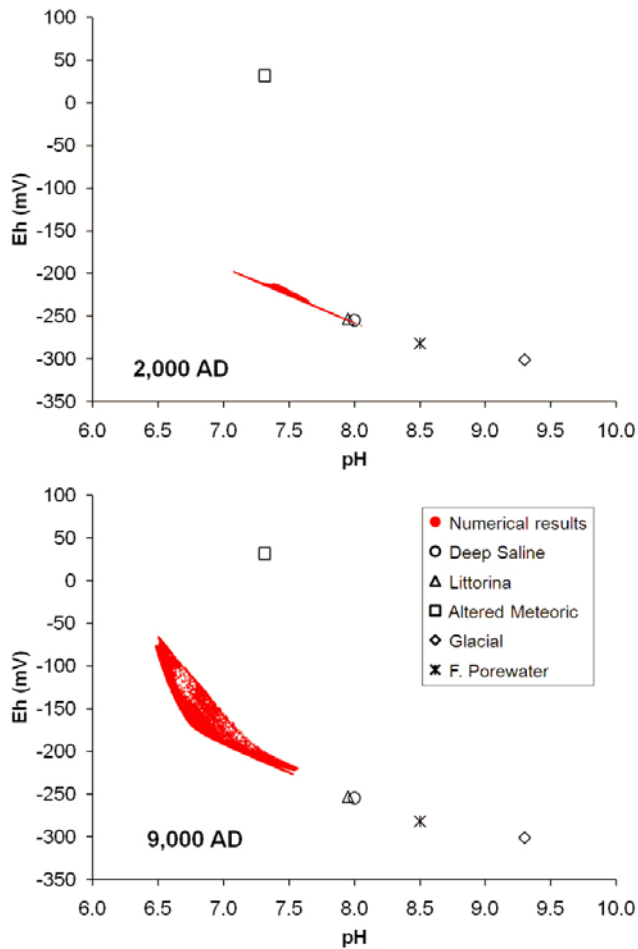
Figure 6-18. *Correlation and evolution of the calculated values of pH and of Eh (redox potential) for the positions located within the candidate repository volume at Forsmark corresponding to 2,000 AD (top) and 9,000 AD (bottom).This calculations only include the results obtained considering on equilibrium with respect to Fe(III) oxyhydroxides.*

6.1.4 Evaluation of a global warming evolution

A climatic evolution of global warming has been also evaluated /Joyce et al. 2010/. This variant case describes a future climate development influenced by both natural climate variability, and climate change induced by anthropogenic emissions of greenhouse gases, with the latter resulting in weak to moderate global warming. There are two main reasons for analysing cases of global warming:

1. modelling studies of climate reponse to increases greenhouse gas emissions, mainly CO_2, indicate that global temperatures will increase in the future under such condition /IPCC 2007/ and /Kjellström et al. 2009/ and,

2. natural long-term climate cycles are believed be driven mainly by changes in solar insolation /Berger 1978/ and /Berger and Loutre 2002/.

For the global warming variant, atmospheric CO_2 levels increase, temporarily up to 1,000 ppm /IPCC 2001/, corresponding to about four times the pre-industrial values. The consequences of the increased acidity of the superficial waters on a granitic aquifer were analysed in /Wersin et al. 1994/, where it was concluded that several tens of thousands of years would be necessary to exhaust the calcite present in fracture-filling minerals. In addition, silicate weathering and ion-exchange processes also contribute to neutralise the increased inflow of carbonic acid in infiltrating waters. It may thus be concluded that the groundwater conditions will be similar to those of the reference evolution, with the difference that a longer period of exposure to groundwaters of meteoric origin is expected to have some influence at repository depth. The composition of the waters is, however, not expected to vary substantially during the temperate period /Wersin et al. 1994/.
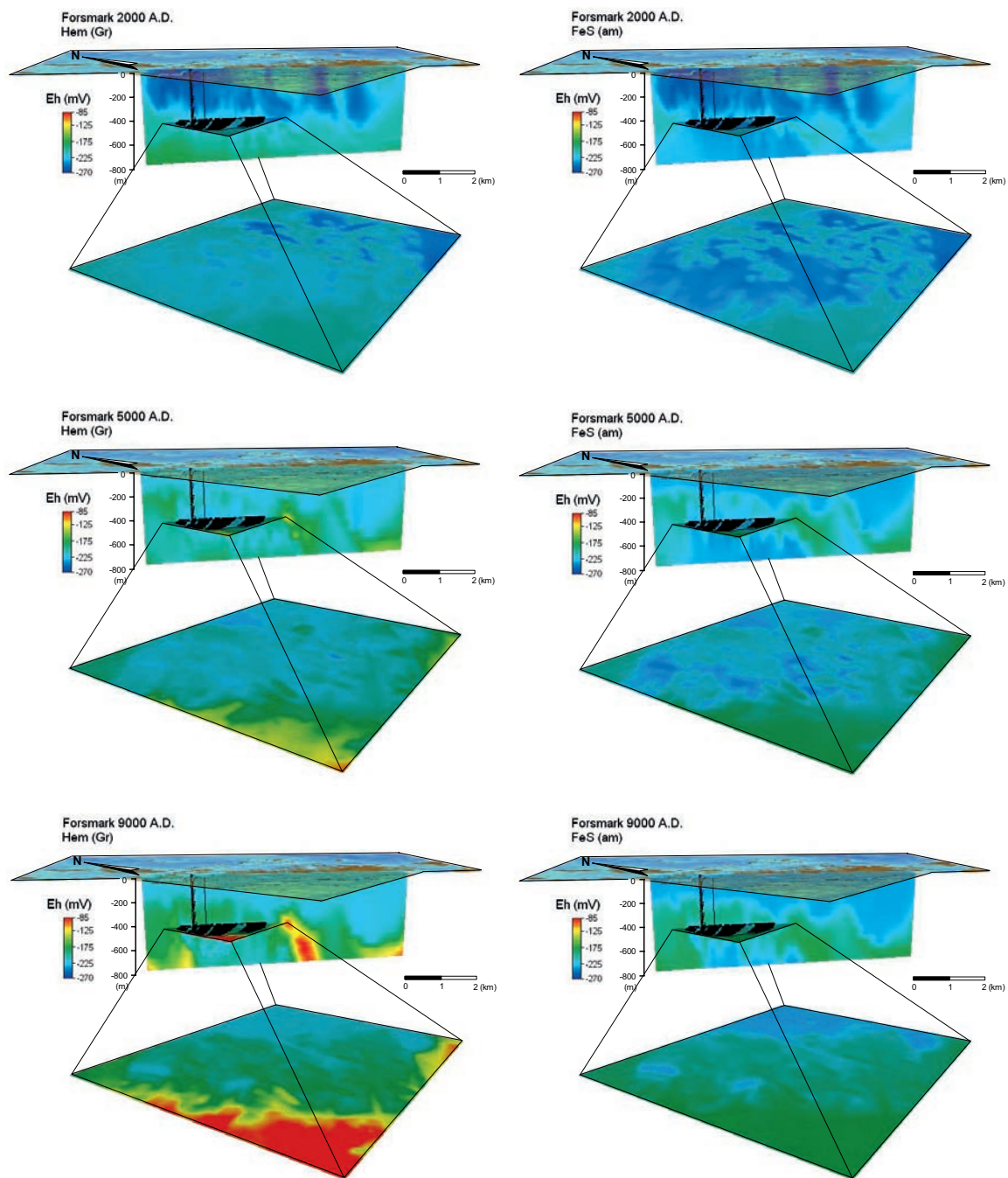
Figure 6-19. *Distribution of the computed Eh values under the assumptions of Fe(III) oxyhydroxides equilibrium (left), and amorphous Fe(II) sulphides equilibrium (right), for Forsmark in vertical slices at times equal to (from top to bottom) 2,000 AD, 5,000 AD and 9,000 AD.*

6.2 Sensitivity analyses of the obtained Eh values and the concentrations of iron and sulphide in different geochemical assumptions

As it has been previously specified, in the statistical post-processing of the numerical results, a "Base Case" has been defined. It assumes that groundwaters are in thermodynamic equilibrium with Fe(III) oxyhydroxides and, in the case of the Eh values and the iron concentrations, equilibrium with respect to amorphous Fe(II) sulphides is also implemented. In this section, the statistical distribution of both parameters will be analysed considering that groundwaters are in equilibrium with one of the two mineral phases previously mentioned (Fe(III) oxyhydroxides or amorphous Fe(II) sulphides).

In spite of sulphide concentrations have been calculated with the model which considers equilibrium with respect to Fe(III) oxyhydroxides, they have been also analysed considering the equilibrium with respect to amorphous Fe(II) sulphides.

Additionally, a case that considers no equilibrium between the redox pairs S(-II)/S(VI) and C(IV)/C(-IV) has been evaluated.

The pH values and the concentrations of the major components in solutions are not sensitive with respect these geochemical variant cases. Consequently, they have not been included in this discussion.

6.2.1 Iron concentrations and redox potential in equilibrium with Fe(III) oxyhydroxides or amorphous Fe(II) sulphides

As it has been previously commented (Figure 4-5 and Section 4.5), the computed iron concentrations and the redox potential obtained within the candidate repository volume have been statistically evaluated through a new case called "Base Case", that considers together equilibrium with respect to amorphous Fe(II) sulphides and Fe(III) oxyhydroxides (Figure 6-20).

As it was expected, the maximum iron concentrations have been computed when amorphous Fe(II) sulphide is considered to be in equilibrium in all points (Figure 6-20). These concentrations are initially within the range $8 \cdot 10^{-6}$ and $3 \cdot 10^{-5}$ mol/L and progressively increase in successive time steps. In this way, they are between $7 \cdot 10^{-5}$ and 10^{-5} mol/L to the final computed time (9,000 AD). On the other hand, when Fe(III) oxyhydroxides is exclusively considered to be in equilibrium, the simulated iron concentrations are significantly lower (between 10^{-6} and $3 \cdot 10^{-6}$ mol/L, during the initial stage of the temperate period, increasing to values around $3-9 \cdot 10^{-6}$ to the final stage of the temperate period).

The Eh values obtained considering equilibrium with respect to amorphous Fe(II) sulphides and those obtained considering Fe(III) oxyhydroxides are similar and mainly limited between –250 and –175 mV (Figure 6-21).
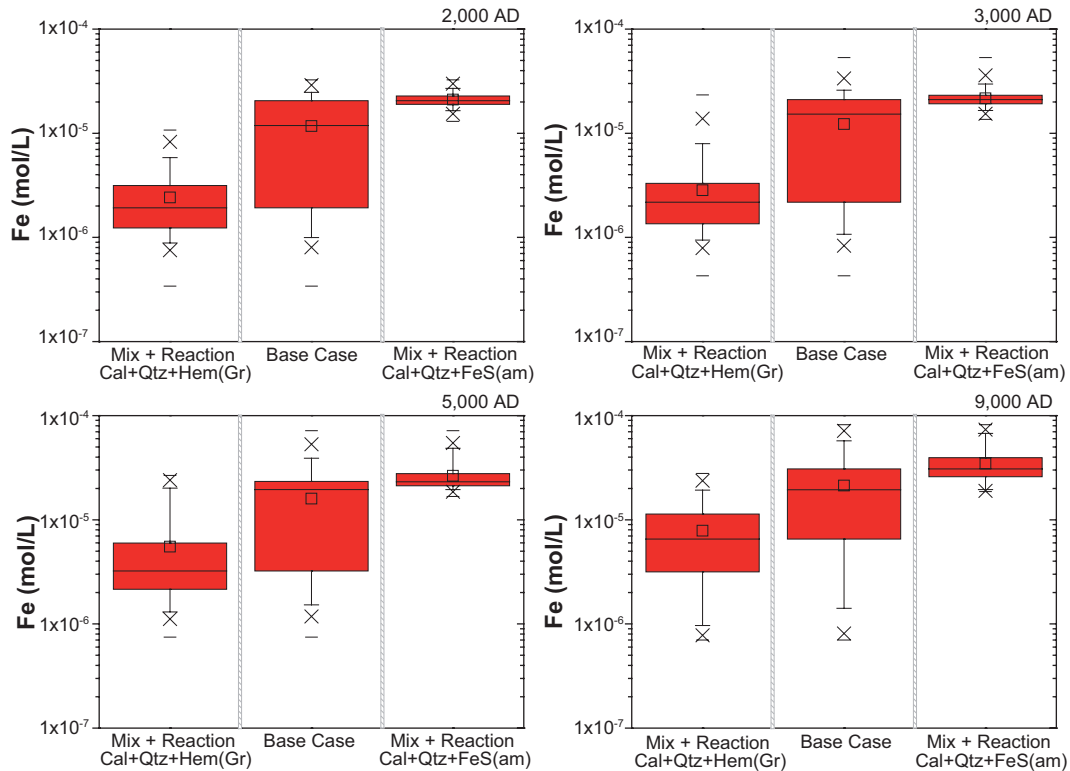
Figure 6-20. *Box-and-whisker plots showing the statistical distribution of the Fe concentration for the geochemical variant cases. The statistical measures are the median, the 25th and 75th percentile (box), the mean (square), the 5th and 95th percentile ("whiskers"), the 1st and 99th percentile (crosses) and the maximum and the minimum values.*
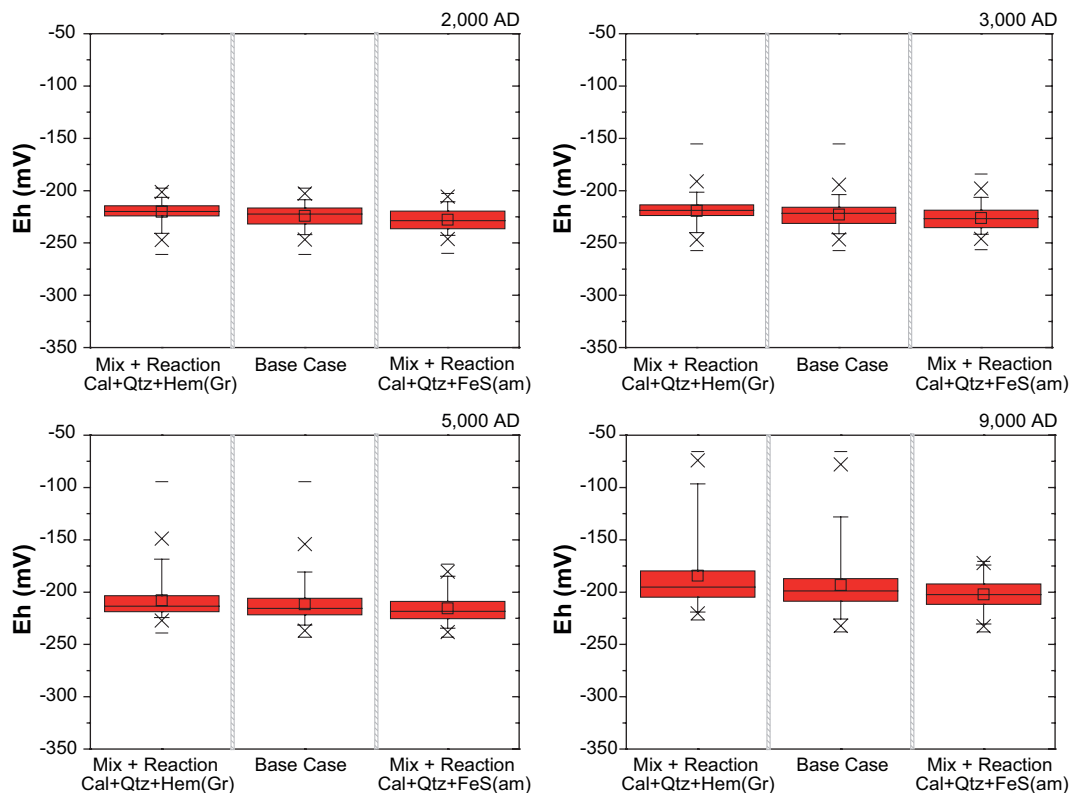
Figure 6-21. *Box-and-whisker plots showing the statistical distribution of the Eh for the geochemical variant cases. The statistical measures are the median, the 25th and 75th percentile (box), the mean (square), the 5th and 95th percentile ("whiskers"), the 1st and 99th percentile (crosses) and the maximum and the minimum values.*

In general, the computed Eh values increase with time. In the case of equilibrium with respect to amorphous Fe(II) sulphides, the redox potential remains practically constant around –225 mV during the period 2,000–5,000 AD, increasing to –200 mV to the final stage of the simulations (9,000 AD; Figure 6-21). In the case of the Fe(III) oxyhydroxides equilibrium, the average of the computed Eh values is around –215 mV or –200 mV, during the period 2,000–5,000 AD. It increases to a range between –200 mV and –175 mV to the year 9,000 AD. However, the maximum Eh computed within the candidate repository volume clearly increases from –190 mV (2,000 AD) to –60 mV (9,000 AD).

6.2.2 Sulphide concentrations in equilibrium with amorphous Fe(II) sulphides

In contrast to the redox potential and the iron concentrations, in the statistical treatment of the calculated sulphide concentrations, the previously called "Base Case" only considers equilibrium with respect to Fe(III) oxyhydroxides. In this way, it is relevant to compare these results with those obtained considering amorphous Fe(II) equilibrium (Figure 6-22).

The range of sulphide concentrations calculated considering the redox potential obtained by the Fe(III) oxyhydroxides equilibrium is limited by 10^{-7} and $5 \cdot 10^{-6}$ mol/L, for the 75% of the points within the repository domain. The maximum values are always lower than 10^{-5} mol/L, and the minimum are progressively decreasing, reaching concentrations lower than 10^{-11} mol/L for more than 5% of the simulated points, in the year 9,000 AD.

However, under the assumption of equilibrium with respect to amorphous Fe(II) sulphides, the computed sulphide concentrations are always higher than 10^{-5} mol/L, in all points within the candidate repository volume. This is not consistent with the analytical data collected in the boreholes of the Forsmark site. In this way, this hypothesis about the equilibrium model has not been included in the analysis of the results.
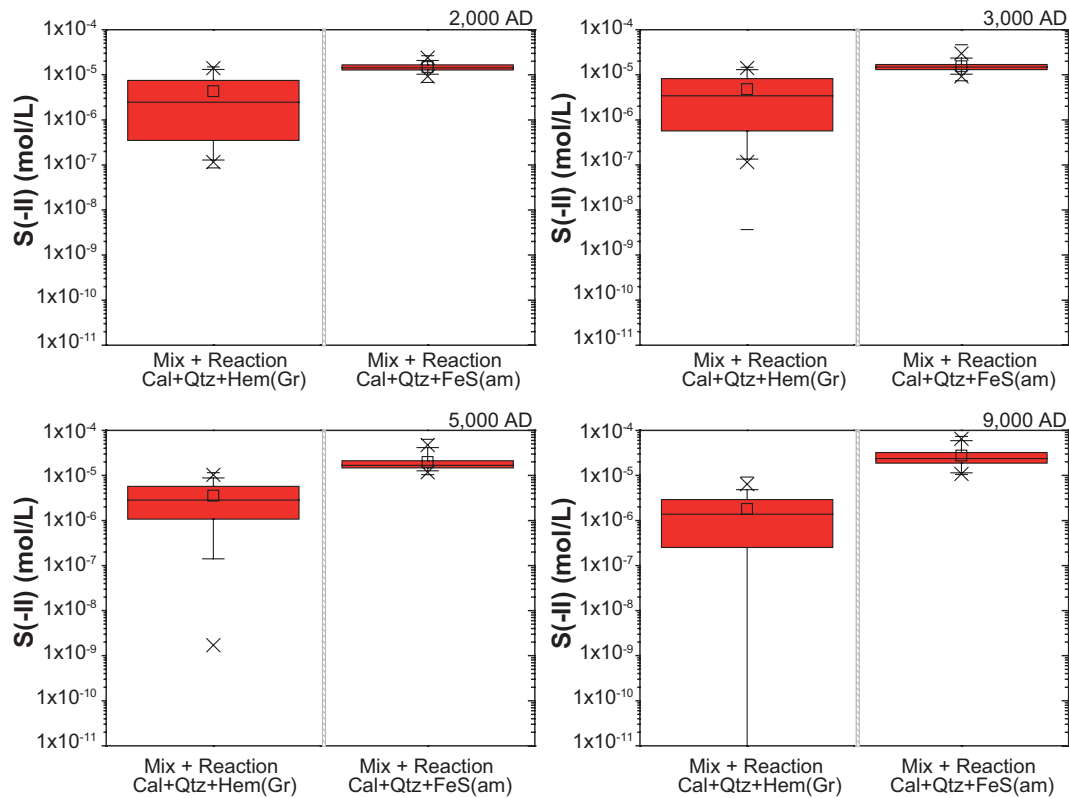
Figure 6-22. *Box-and-whisker plots showing the statistical distribution of the S(-II) concentration for the geochemical variant cases. The statistical measures are the median, the 25th and 75th percentile (box), the mean (square), the 5th and 95th percentile ("whiskers"), the 1st and 99th percentile (crosses) and the maximum and the minimum values.*

6.2.3 Non-equilibrium between the redox pairs S(-II)/S(VI) and C(IV)/C(-IV)

A series of calculations has been performed in order to evaluate the influence of the kinetic processes of the redox reactions between the pairs S(-II)/S(VI) and C(IV)/C(-IV). The reference database (see Section 4.3) which includes equilibrium between sulphide and sulphate as well as between carbonate and methane, has been adapted, uncoupling the equilibrium reactions related to both redox pairs. Calculations have been performed considering the case of Fe(III) oxyhydroxides equilibrium.

As it was expected, no differences have been computed with regard to the pH values and the concentrations of most of the aqueous species. However, differences in the computed Eh values, and in the iron and sulphide concentrations, have been identified (Figure 6-23).

During the initial stages of the temperate period (2,000 AD and 3,000 AD), the pH values obtained with the uncoupled database are lower than those obtained with the coupled database. When meteoric origin waters are predominant within the candidate repository volume (from 5,000 AD), the Eh values obtained with the uncoupled database are clearly higher (Figure 6-23). In general, the variability of the numerical results is wider with the uncoupled version of the database. Using both databases, the maximum values obtained are practically identical, and the minimum values are remarkably lower with the uncoupled database.

Using the coupled and the uncoupled database, the statistical distribution of the sulphide concentrations are comparable. However, the variability range of the numerical results is wider with the coupled database, whereas the minimum values are orders of magnitude lower (Figure 6-23). The maximum values computed under the two mentioned geochemical assumptions are limited between $5 \cdot 10^{-6}$ and 10^{-5} mol/L, being lower than those obtained with the uncoupled database.

Significant differences have been computed in reference to the iron concentrations (Figure 6-23). The variability range is wider when calculations have been performed with the coupled database.
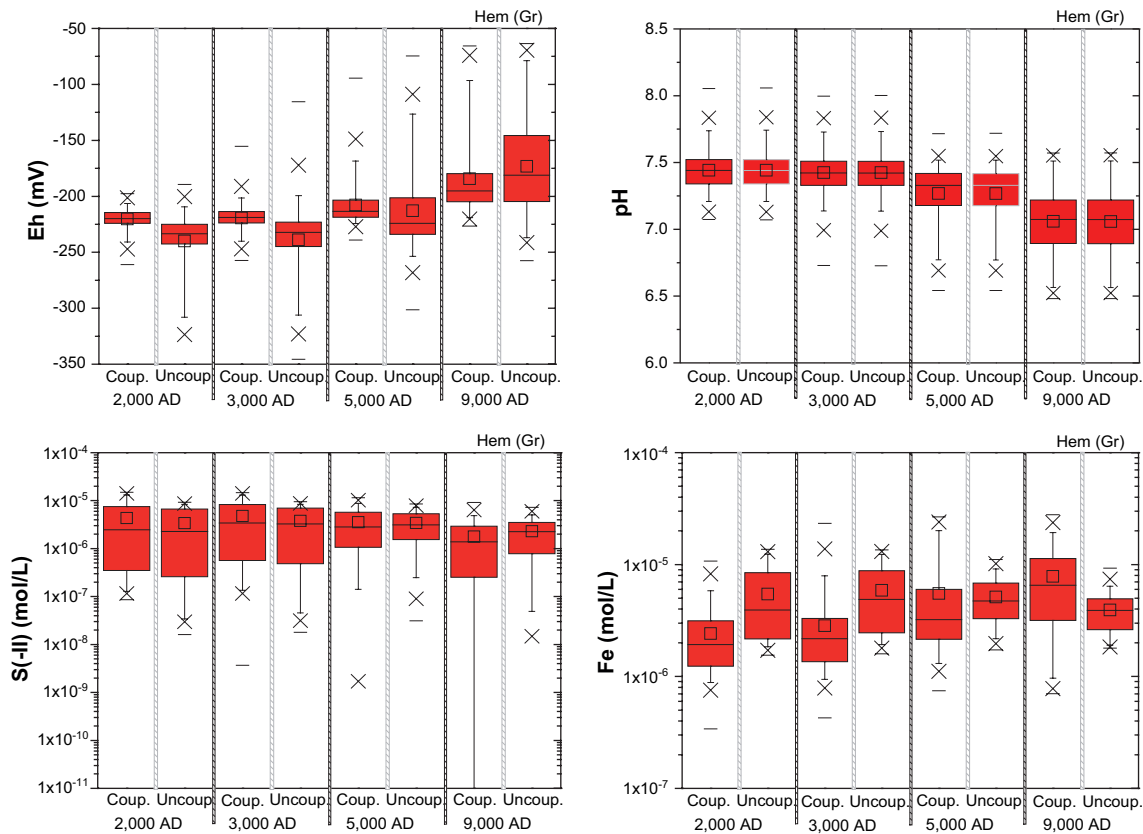
Figure 6-23. *Box-and-whisker plots showing the statistical distribution of the Eh, pH, and Fe and S(-II) concentrations for the geochemical variant case which considers (1) equilibrium with respect to Fe(III) oxyhydroxides, and (2) non thermodynamic equilibrium between the S(VI) and S(-II) species (TDB uncoupled). The statistical measures are the median, the 25th and 75th percentile (box), the mean (square), the 5th and 95th percentile ("whiskers"), the 1st and 99th percentile (crosses) and the maximum and the minimum values.*

On the other hand, the average concentration is lower during the first stages of the temperate period (2,000 AD and 3,000 AD), but it is progressively increasing up to attain values clearly higher to the end of the modelled period (9,000 AD; $3 \cdot 10^{-6}$ mol/L with the uncoupled database, and $7 \cdot 10^{-6}$ mol/L with the coupled one).

No changes in the total C(IV) concentrations, and the associated parameters, have been detected by using the coupled or the uncoupled database. As mentioned in Section 4.5.2, with the coupled database PHREEQC assumes redox equilibrium between all redox pairs, and it calculates a value for the CH_4 concentration depending on the total carbon and on the Eh-pH values. On the other hand, for the uncoupled database, the equilibrium between C(IV) and C(-IV) is not considered and, as a consequence, methane generation is suppressed and the total concentration of carbonate remains unchanged. In our calculations, the redox potentials obtained with the coupled database are not low enough to generate significant amounts of C(-IV) aqueous species.

6.3   Hydrological variant cases

As it has been previously commented in the Chapter 3, it is assumed that there is some correlation between the hydraulic parameters implemented in the hydrogeological models (transmissivity, e.g.), and the physical characterization of the site (size and orientation of fractures, e.g.). In this way, a series of simulations have been performed in order to evaluate the sensitivity of the results in reference of variations of the hydraulic models.

6.3.1 Extended spatial heterogeneity

The hydrological base case uses a hydraulic rock domain model from site descriptive modelling that covers the repository site area, based on the available data. Outside this area, the rock is modelled as a continuum porous medium with homogeneous and isotopic properties for each depth zone. However, this greatly reduces the effect of outcropping sub-vertical deformation zones on particle exit points /Joyce et al. 2010/.

For the extended spatial heterogeneity case, there are fewer particles at the NE boundary and fewer at intermediate locations, although there are some extra locations at the N of the model. The enhanced effect of the deformation zones seems to have caused more particles to exit closer to the repository.

In general, the geochemical calculations don't show significant differences with respect to the results obtained with the "Base Case", described in the previous sections (Figure 6-24). Salinities practically don't vary in both hydrological assumptions, except for the year 9,000 AD, when the salinities
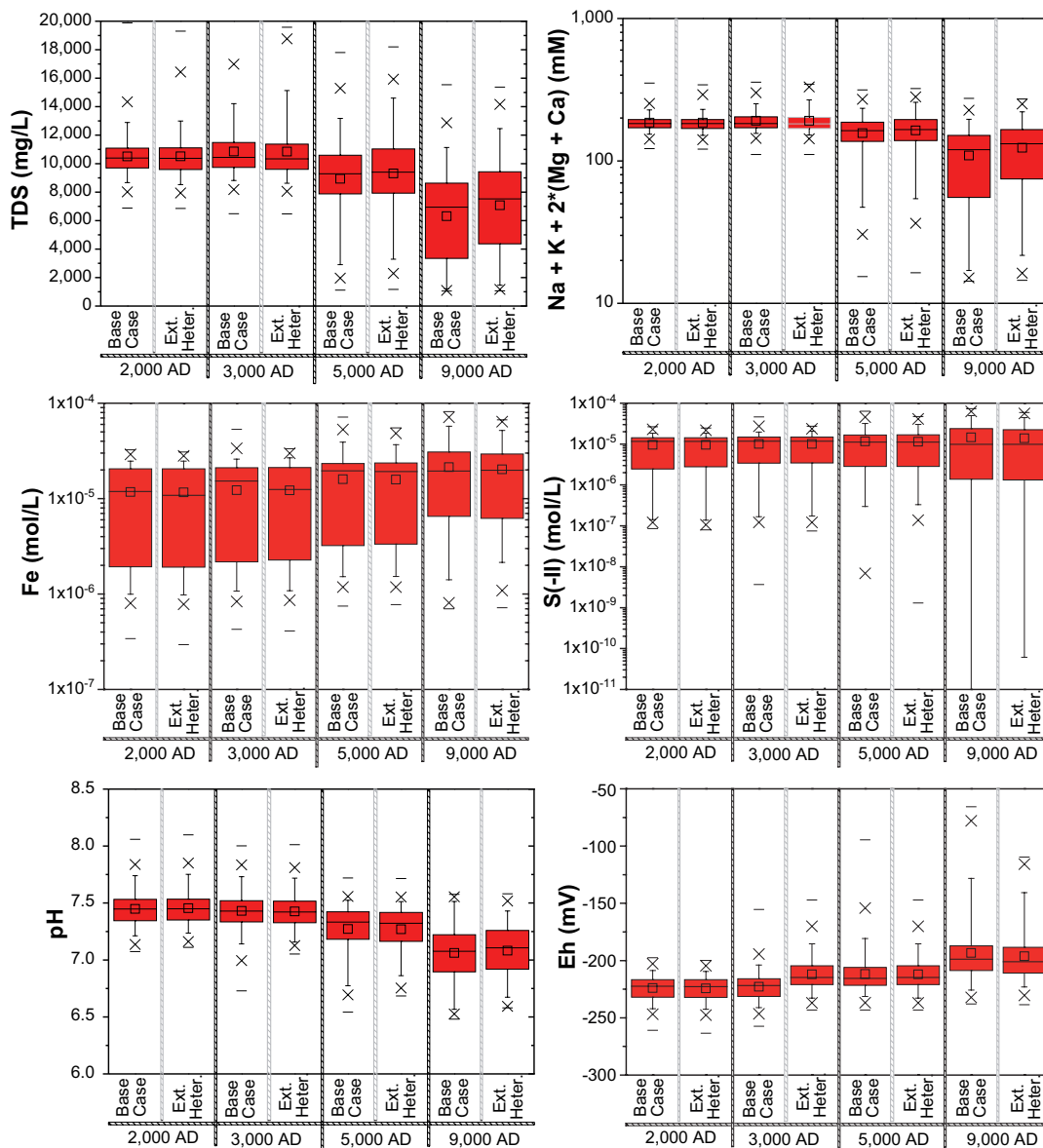
Figure 6-24. *Box-and-whisker plots showing the statistical distribution of the TDS, the safety function $\sum q[M^{q+}]$, the concentrations of iron and sulphide, and the computed Eh and pH values, comparing the hydrological base case and the extended spatial heterogeneity case. The statistical measures are the median, the 25th and 75th percentile (box), the mean (square), the 5th and 95th percentile ("whiskers"), the 1st and 99th percentile (crosses) and the maximum and the minimum values.*

within the candidate repository volume are higher for the case of the extended spatial heterogeneity (7.5 g/L in front of 6.9 g/L calculated for the standard temperate period). The same trend is shown for the concentrations of the major components and, therefore, for the safety function $\sum q[M^{q+}]$, with a lower value that is higher than 14 mM, in any case.

The distribution of the iron concentrations obtained with the hydrological base case and the heterogeneity spatial case are practically identical (Figure 6-24). During the first stages of the temperate simulations (2,000 AD and 3,000 AD), the results obtained by the extended spatial heterogeneity model are slightly lower than those obtained with the hydrological base case. However, in the last periods (5,000 and 9,000 AD), no significant differences have been computed.

The calculated sulphide concentrations, and the Eh and the pH values show the same similarities between both hydrological hypotheses (Figure 6-24). In the case of the sulphide concentrations, it is significant as the minimum concentrations calculated in the extended spatial heterogeneity case are orders of magnitude lower than those calculated with the hydrological base case. On the other hand, the pH values calculated by both hydrological models are also practically identical. It is only notably as the minimum values computed within the candidate repository volume are between 0.10 and 0.25 units of pH higher in the extended spatial heterogeneity case. Accordingly, the maximum Eh values computed for the extended spatial heterogeneity case are remarkably lower than those calculated with the hydrological base case (Figure 6-24).

6.3.2 Other hydrological variant cases

As it has been commented in Chapter 3, the hydrological "base case" relates fracture radius to transmissivity according to the relationship:

$$T = 10^{\log(ar^b) + \sigma N(0,1)}$$ (Equation 6-1)

where a and b are the factor and exponent, respectively, of the power-law relationship between r and the mean of $\log_{10}(T)$, σ is the standard deviation of $\log_{10}(T)$, and $N(0,1)$ denotes a normally distributed random deviate with a mean equal to zero and a standard deviation of 1 /Joyce et al. 2010/. The transmissivity is limited to two standard deviations either side of the mean by resampling values outside of this range. In this way, two hydrological variant cases (called "Case 5" and "Case 9") have been performed in order to establish the sensitivity of the geochemical results with respect to the variability of the parameter N. The reference case that has been selected for this sensitivity analysis is the "Base Case", performed for the year 2,000 AD of the temperate period.

The distribution of the calculated concentrations of the major aqueous components within the candidate repository volume is practically identical to the three hydrological models (Figure 6-25). Sistematically, the range of variability is slightly narrower for the two variant cases, with respect to the results obtained with the hydrological base case. In this way, it has computed the maximum concentrations. In contrast, the iron and the sulphide concentrations are remarkably lower than the hydrological base case, with maxima limited by $3 \cdot 10^{-5}$ mol/L and 10^{-5} mol/L for iron and sulphide, respectively.

The pH values obtained are also practically identical in the three cases. The range of Eh also shows no significant differences. The maximum pH values and the corresponding minimum Eh values have been computed for the hydrological variant case "Case 9". However, both parameters are limited for 99% of the simulated points within the candidate repository domain by 7.1 and 7.9, in the case of the pH values, and –250 mV and –200 mV, in the case of the redox potential (Figure 6-25).
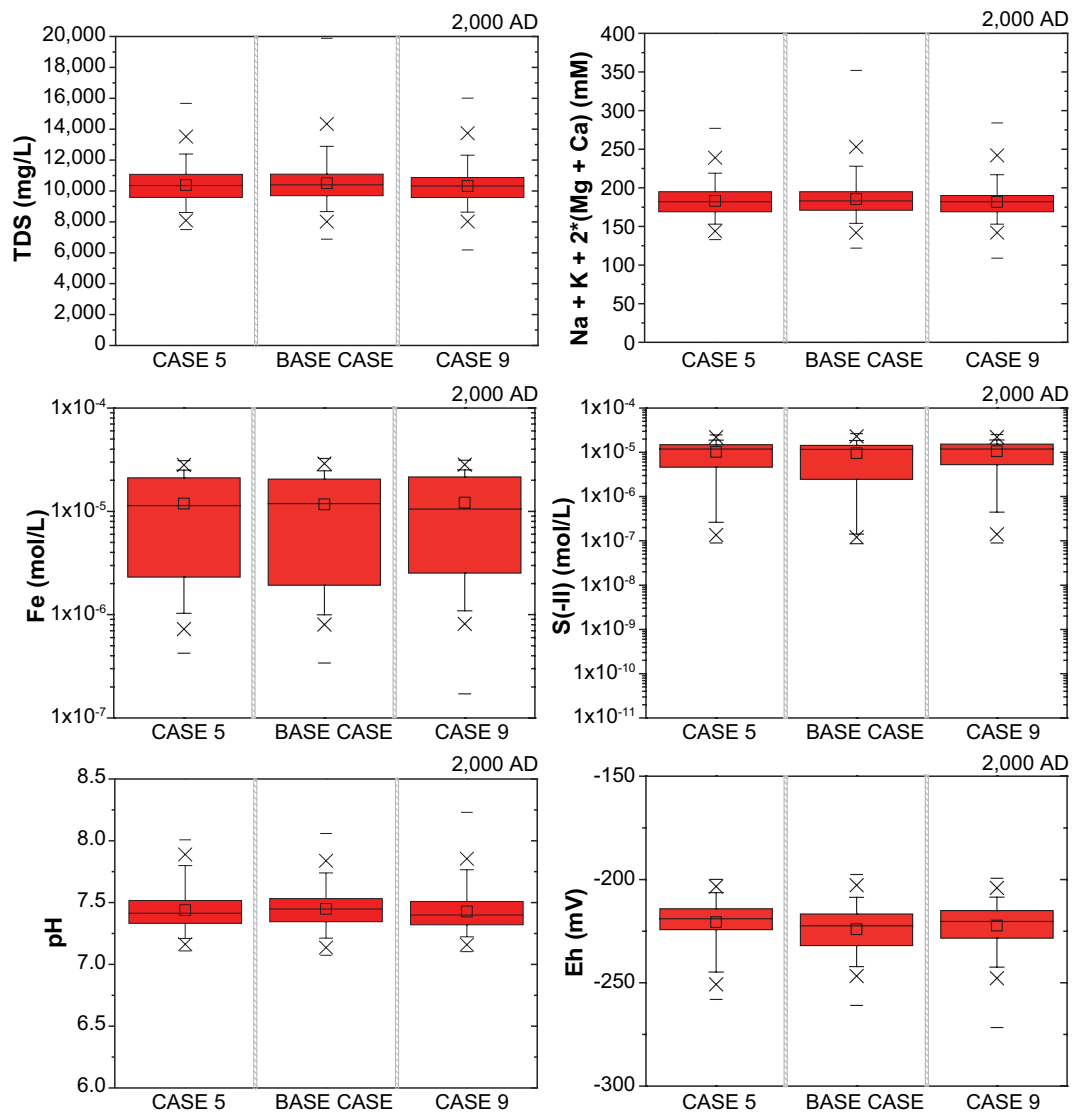
Figure 6-25. *Box-and-whisker plots showing the statistical distribution of the TDS, the safety function $\sum q[M^{q+}]$, the concentrations of iron and sulphide, and the computed pH and Eh values, comparing the hydrological base case and the hydrological variant cases 5 and 9. The statistical measures are the median, the 25th and 75th percentile (box), the mean (square), the 5th and 95th percentile ("whiskers"), the 1st and 99th percentile (crosses) and the maximum and the minimum values.*

6.4 Conclusions of the temperate period simulations

The salinity at the Forsmark site during the temperate period has been demonstrated to be below 15 g/L, corresponding to a chloride concentration around 0.5 mol/L. Upconing effects on salinity during the excavation/operation phase have also been studied and found to be negligible. On the other hand, the safety function $\sum q[M^{q+}]$ will be higher than 4 mM in all points within the repository volume, at all time.

Colloids are partly stabilised by electric repulsions between charges in their surfaces. Some of these charges arise from the dissociation of acid-base groups, and are, therefore, pH dependent. The presence of cations in the water counteracts these charge effects, and, therefore, most colloids quickly sediment in waters containing $\sum q[M^{q+}]$ lower than 0.004 mol/L. The results from the modelling calculations show that colloids will not be especially stable during this period, because the pH values, salinities and cation concentrations will be high enough to destabilise them. The conclusion is that colloid concentrations are expected to remain at the levels that have been measured during the site investigations, i.e. less than 200 µg/L //Hallbeck and Pedersen 2008a/.

The results also indicate that groundwater pH at the Forsmark site will be around 7 to 8 (lower than 11).

During the initial temperate domain following repository closure, within the candidate repository volume, the potassium concentrations are expected to remain lower than 0.004 mol/L, sulphide and phosphate concentrations are expected to be also lower than 10^{-5} mol/L and 10^{-6} mol/L, respectively, for most deposition positions averaged over the temperate period, whereas iron concentrations are expected to gradually increase up to 10^{-4} mol/L.

The analyses have lead to the conclusion that the chemical conditions will be reducing shortly after deposition in individual deposition holes and deposition tunnels and shortly after closure in the repository as a whole. This is of fundamental importance for the long-term safety of the repository and no process has been identified that challenges this conclusion during the initial temperate period after closure.

It is significant the strong sensitivity of the calculated iron concentrations with respect to the Fe-bearing mineral considered to be in equilibrium in our simulations. However, the redox potential does not show the same relative dependence. As it was expected, the computed redox potential has shown a high sensitivity with respect to the kinetic processes of the redox reactions between the pairs S(-II)/S(VI) and C(IV)/C(-IV). Consequently, the iron concentrations necessary to maintain the thermodynamic equilibrium with the Fe(III) oxyhydroxides is also linked with the variability of the calculated Eh values.

In contrast to the sensitivity analysis performed for the geochemical constraints of the model, no relevant differences have been computed with the variant hydrological models. In this way, the geochemical uncertainties seem to have more influence determining the potential variability of the results. In any case, this sentence is only applicable for the simulations performed for the temperate period. As it will be shown in the next chapter, conceptual variations of the hydrological model can have influence in a more deterministic the obtained results during the glacial cycle.

7 Simulation of geochemical evolution for the remaining part of the reference glacial cycle

The successions of temperate, periglacial and glacial climate domains will affect the flow and composition of the groundwaters around the repository. The transition between climate domains will be gradual, without a clear boundary between them. For example, during a temperate domain, temperatures may slowly decrease such that permafrost regions slowly develop within parts of the repository region.

In SR-Site, the evaluation of geochemical effects is restricted to using separate specifications for the different climatic domains. It is expected that different groundwater compositions will prevail around the repository as a result of the different types of climate domains and their corresponding hydraulic conditions. This Section discusses the groundwater chemistry for periods in which the repository is (1) below permafrost, during periglacial climatic conditions, or (2) under an ice sheet during glacial conditions. In addition this Section discusses groundwater chemistry for periods in which the repository area is submerged either under a lake of glacial melt waters, or under seawater, such as the Littorina seawater periods in the past.

For the glacial cycle of the reference evolution (about 120,000 years) the Forsmark site is covered by an ice sheet during a few periods with a total duration of about 30 thousand years. Groundwater flow during the glacial domain has been estimated using a Darcy Tools model representing a large regional scale including the Forsmark area /Vidstrand et al. 2010/. The results of that model include evaluations of the salinity distribution beneath an ice sheet, and the modelling included situations where the ice sheet advanced either over an unfrozen terrain or over an area subjected to permafrost.

7.1 Methodology

The modelling for the remaining part of the reference glacial cycle is similar to that performed for the initial temperate period described in the previous chapter. Groundwater compositions are modelled through advection, mixing and chemical reactions with fracture-filling minerals. Equilibrium with respect to calcite, quartz, hydroxyapatite and Fe(III) oxyhydroxides has been assumed. On the other hand, in the statistic post-processing, a "Base Case" has been defined assuming that the Eh values and the iron concentrations have to be evaluated considering the possibility of equilibrium with respect to amorphous Fe(II) sulphides at all points in space and time.

The groundwater flow modelling of the periglacial and glacial conditions using Darcy Tools is described in Chapter 3. One of the processes modelled is the transport of salts. Contrary to the modelling of the initial temperate period, the models for the periglacial and glacial periods have not included the fractions of selected reference waters. In the geochemical models, either for the glacial evolution without permafrost or in the glacial evolution with permafrost, the rock volume initially contains a mixture of two end-member waters: a Deep Saline groundwater and a water of meteoric origin. The proportion of these two end-members can be obtained from the salinity at any point. With the advance and retreat of the glacier, the proportion of a third mixing end-member (glacial melt water) is calculated from the decrease of salinity at any point in space.

This methodology has shown a series of disadvantages when:

(1) a decrease of salinities is computed, because it is exclusively attributed to an increase of glacial melt waters,

(2) no large changes in salinity occurs. In this case, the infiltration of glacial melt waters is not accurately reproduced.

These numerical anomalies have been modelled, i.e. in the southern area of the modelled domain. In this case, it has considered that they don't have any influence in the numerical results within the candidate repository volume.

On the other hand, this methodology implicitly considers that Deep Saline groundwaters are the exclusive suppliers of salinity. These waters are characterised by very low concentrations of aqueous sulphur (around 10^{-4} mol/L) in front of Littorina waters (around 10^{-2} mol/L). In this way, the sulphide concentrations calculated using this methodology are lower than 10^{-10} mol/L in the initial stages of the glacial cycle. This is in apparent contradiction with respect to the results obtained during the temperate period, where more of the simulated values are higher than 10^{-8} mol/L.

This strategy is used as well to describe the site submerged by a glacial melt water lake. For periods when the candidate site is submerged under seawater, the same model is used as for the initial temperate period and, therefore, the hydrogeological results include the mixing proportions of end-member waters.

A process that must be evaluated is the out-freezing of dissolved salts when ice builds up underground during periglacial periods. The Darcy Tools model includes density-driven groundwater flow and transport of salts, but the out-freezing of salts is not included. The process has instead been evaluated using a two-dimensional model set-up /Hartikainen et al. 2010/.

7.2 Temperate and periglacial periods

7.2.1 Introduction

The glacial cycle begins with an initial stage ("temperate" period) where glacial origin waters have not been considered to be present as a component of the groundwaters. In this way, within the candidate repository volume, the average of the simulated groundwater compositions is around 95% of diluted groundwaters and 5% of saline groundwaters, approximately.

The subsequent periglacial conditions are characterised by perennial freezing of groundwaters, i.e. permafrost, and the frozen areas may be continuous or discontinuous. In any case the permafrost areas will include taliks where sufficiently large lakes are encountered. There is very little information concerning the chemical characteristics of groundwaters under permafrost. This is due to practical difficulties when drilling and sampling at ambient temperatures where freezing of drilling fluids and groundwater samples occurs.

Many geochemical characteristics or groundwaters are expected to be almost unaffected by the permafrost. The study at the Lupin Mine in N. Canada /Frape et al. 2004, Ruskeeniemi et al. 2004, Stotler et al. 2009/ may be used to illustrate this: the pH values for sampled groundwaters vary between 6 and 9, and bicarbonate concentrations are found to be below $5 \cdot 10^{-3}$ mol/L. For potassium, the concentrations are higher than for the groundwaters sampled at Forsmark or Laxemar: sub-permafrost groundwaters at Lupin have concentrations lesser than $2.6 \cdot 10^{-3}$ mol/L. For iron, most of the groundwaters sampled at Lupin had concentrations lesser than $5.4 \cdot 10^{-5}$ mol/L. Thus, the concentrations and pH values found are not far from those for groundwaters sampled elsewhere.

7.2.2 Numerical results. Base case

The results obtained for the periglacial period show that the range of the calculated salinities decreases with respect to those obtained for the temperate period (Figure 7-1). Within the repository domain, the average salinity in both cases is around 3 g/L (between 1 and 10 g/L). The maximum values decrease from 10 g/L, for the temperate period, to 6.5 g/L, for the periglacial simulations.

In reference to the cation concentrations, the simulated potassium concentrations are around $1–2 \cdot 10^{-4}$ mol/L in both periods, and the safety function $\sum q[M^{q+}]$ computes values higher than 10 mM, in the case of the temperate period, and higher than 20 mM, for the periglacial calculations (Figure 7-1).

Most of the simulated pH values within the candidate repository volume are between 6.5 and 7.0 (Figure 7-2). In both periods (temperate and periglacial), the Eh values are less than –50 mV. In the periglacial simulations, the average Eh values are around –100 mV, whereas in the temperate period they are between –100 and –180 mV. The variability of the pH and the Eh values obtained for the repository depth are less in the case of the periglacial calculations.
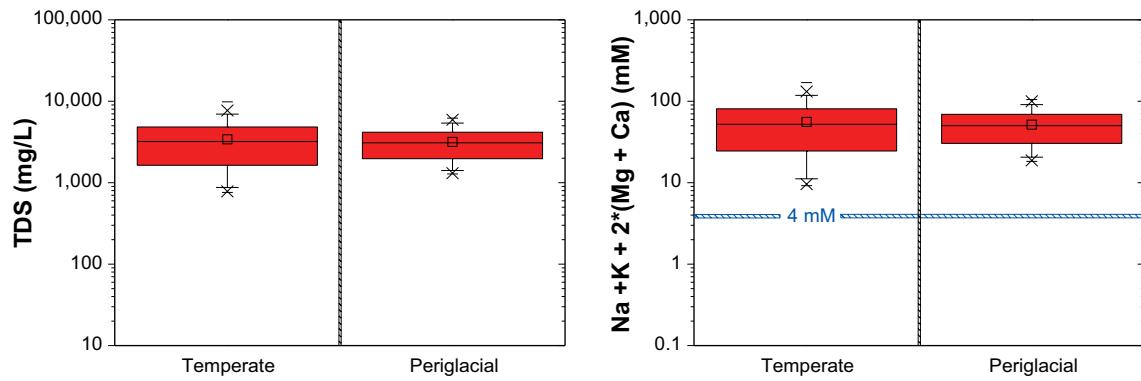
Figure 7-1. *Box-and-whisker plots showing the statistical distribution of the calculated TDS (left) and the safety function $\sum q[M^{q+}]$ (right) for the positions located within the candidate repository volume at Forsmark, and for the initial stage of the glacial cycle (temperate period) and for the periglacial simulations. The statistical measures are the median, the 25th and 75th percentile (box), the mean (square), the 5th and 95th percentile ("whiskers"), the 1st and 99th percentile (crosses) and the maximum and the minimum values.*
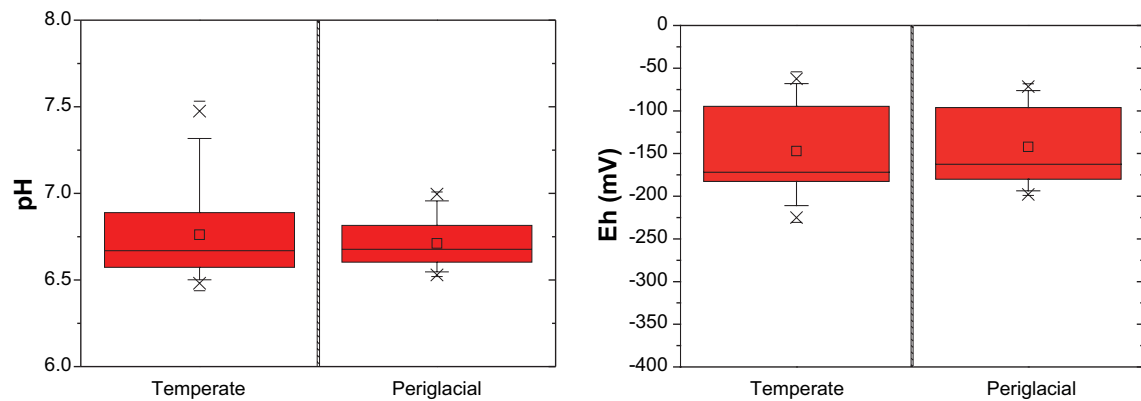
Figure 7-2. *Box-and-whisker plots showing the statistical distribution of the calculated pH (left) and the Eh values (right) for the positions located within the candidate repository volume at Forsmark, and for the initial stage of the glacial cycle (temperate period) and for the periglacial simulations. The statistical measures are the median, the 25th and 75th percentile (box), the mean (square), the 5th and 95th percentile ("whiskers"), the 1st and 99th percentile (crosses) and the maximum and the minimum values.*

As it has been previously commented, the calculated S(-II) concentrations are lower than 10^{-10} m/L in both periods (temperate and periglacial; Figure 7-3). It is in apparent contradiction with the calculated values previously described for the temperate period (2,000 AD, 3,000 AD, 5,000 AD and 9,000 AD; Figure 6-16), where most of the simulated values are higher than 10^{-8} mol/L. As previously commented, this inconsistency is a consequence of the methodology employed in the evaluation of the fractions of the selected reference waters (Deep Saline groundwaters and Altered Meteoric waters) for the initial stages of the glacial cycle. Altered meteoric waters and Deep Saline groundwaters are characterized by very low concentrations of S(VI) (around 10^{-4} mol/L), in front of the Littorina waters (around 10^{-2} mol/L). Additionally, relative high Eh values have been computed during these two periods, resulting in S(-II) concentrations lower than 10^{-10} mol/L. However, the iron concentrations obtained in both periods are in accordance with the concentrations calculated for final stages of the temperate period described in the Chapter 7 (9,000 AD; Figure 6-16). On the other hand, no significant differences have been computed with regard to the iron concentration during the temperate and the periglacial periods (between 10^{-6} and 10^{-4} mol/L).

Comparing the phosphate concentrations obtained during the final stage of the temperate period (9,000 AD; see Section 6.1.2 and Figure 6-4) and during the temperate stage previous to the glacial cycle (T_0), differences of up to one order of magnitude, approximately, are found (not shown in
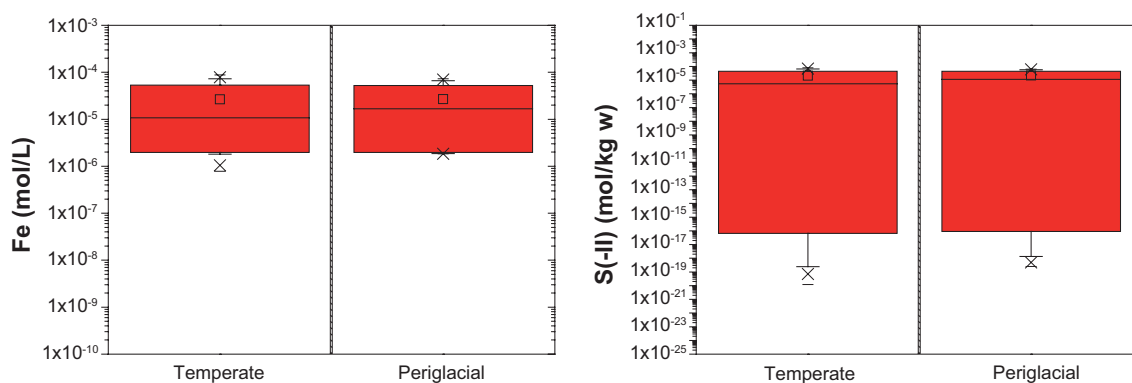
Figure 7-3. *Box-and-whisker plots showing the statistical distribution of the calculated Fe and S(-II) concentrations for the positions located within the candidate repository volume at Forsmark, and for the initial stage of the glacial cycle (temperate period) and for the periglacial simulations. The statistical measures are the median, the 25th and 75th percentile (box), the mean (square), the 5th and 95th percentile ("whiskers"), the 1st and 99th percentile (crosses) and the maximum and the minimum values.*

the figures). This is a consequence of the conceptual constraints applied in the calculations for the glacial period, see sections 4.1 and 7.1. In any case, the results provide pessimistic values for the phosphate contents in groundwaters (see Section 6.1.2 and Figure 6-9). However, the numerical results for the points included within the candidate repository volume for the stage T_0 and for the periglacial period are practically identical (around $5 \cdot 10^{-6}$ mol/L). Only significant differences have been detected with respect to the maximum values computed, $0.7 \cdot 10^{-5}$ mol/L in the case of the periglacial stage and $1 \cdot 10^{-5}$ mol/L for the temperate period.

7.2.3 Conclusions

The salinity at the Forsmark site during the initial stage of the glacial cycle and the periglacial period has been demonstrated to be below 10 g/L. On the other hand, the safety function $\Sigma q[M^{q+}]$ will be higher than 10 mM in all points within the candidate repository volume (higher than 20 mM for the periglacial simulations). The results also indicate that the pH values at the Forsmark site will be around 6.5 to 7.0 during these climatic periods, attaining maximum values of 7.5 in some locations within the candidate repository volume (less than 1% of the simulations points). In any case, the pH is lower than 11. Consequently, the results for the initial stages of the glacial cycle and for the periglacial period show that colloids will not be especially stable during these periods, because the pH values, salinities and cation concentrations will be high enough to destabilise them. As in the case of the temperate simulations, colloid concentrations are expected to remain at the levels that have been measured during the site investigations (less than 200 µg/L /Hallbeck and Pedersen 2008a/).

During the temperate and periglacial periods (previous to the initial of the glacial cycle), the potassium and the iron concentrations are expected to remain lower to 0.0003 and 0.0001 mol/L, respectively. The trend of the phosphate concentrations plots around $5 \cdot 10^{-6}$ mol/L under both climatic periods, remaining below 10^{-5} mol/L in any case. The sulphide concentrations resulting from the calculations are lower than 10^{-7} mol/L for the temperate period, and lower than 10^{-11} mol/L for the periglacial simulations. However, these results are not considered correct due to numerical uncertainties.

The redox potential calculated for the points included in the candidate repository volume shows Eh values lower than -50 mV, in both periods. During the temperate period, the calculated Eh values are in the range of -100 and -175 mV, increasing to values around -75 and -125 mV during the periglacial period.

7.3 Hydrogeochemical evolution during the stages of ice advance and retreat

7.3.1 Introduction

There is almost no information concerning the chemical characteristics of groundwaters in fractured rock under an ice sheet or even close to the margin of an ice sheet. This is partly due to practical difficulties when drilling and sampling at ambient temperatures where freezing of drilling fluids and groundwater samples occurs.

The composition of glacier melt waters was reviewed in /Brown 2002/. Although, as expected, some of these waters are extremely dilute (1 mg/L), others have gained solutes from mineral weathering reactions, reaching salinities up to 0.2 g/L. Other examples of dilute granitic waters are those sampled in Gideå (0.33 g/L) and Grimsel (0.08 g/L). Although dilute, both these waters are close to saturation with calcite. The relatively high pH values, around 9, originate from the weathering of bedrock minerals.

SKB, together with NWMO (Canada) and Posiva (Finland) have started a joint project that will attempt to drill boreholes and sample groundwaters in an area close to Kangerlussuaq in Greenland. At present, the evaluation of geochemical characteristics of groundwaters during a glacial period must rely almost exclusively on modelled results and chemical reasoning.

7.3.2 Base Case. Numerical results

A glacial period of 18,850 years has been simulated in 10 time steps, reproducing the advance and the retreat of the ice front (Figure 1-1, Table 3-1). Three hydrological stages have been considered: i) when the ice front is advancing to the repository area (2,900 years, approximately), ii) when the repository is entirely covered by a warm-based ice sheet i.e. an ice sheet with basal melting (15,000 years) and, finally, iii) when the ice sheet is retreating (1,200 years) and the area is covered by a 100 m deep melt water lake.

Two cases of an ice sheet advancing over a permafrost area have been modelled in /Vidstrand et al. 2010/. In this chapter only one of these cases will be presented: the model in which there is a remaining permafrost zone below the ice sheet, as it advances 2 km from the ice margin (Figure 7-4). In this way, a series of geochemical simulations has been performed in order to evaluate the effect of the presence of a permafrost domain on the hydrogeochemical characterization of groundwaters within the candidate repository volume.
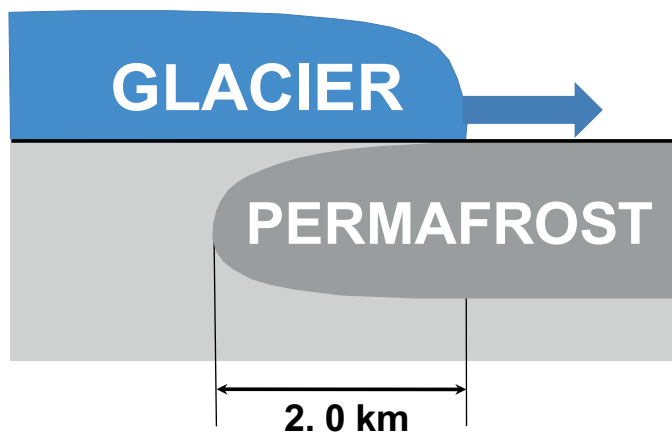
Figure 7-4. Conceptual scheme of the relative location of the permafrost with respect to the glacier front in the hydrological model considered in our calculations.

Evolution of salinity

Dilute waters of a glacial origin are expected under a warm-based ice sheet. Significant changes in groundwater composition are expected as soon as the ice front advances over the repository area. The calculated results shown in Figure 7-5 indicate that salinities in the upper part of the modelled domain usually would be lower than 2 g/L.

The model results illustrate also the upconing of Deep Saline waters under an advancing and a retreating warm-based ice sheet. The calculated salinities can reach values up to 20 g/L in locations affected by upconing. Because the advancement of the ice sheet is a relatively fast process and the retreat even more so, the high salinity conditions are predicted to last only a few centuries at most.

Figure 7-6a presents the calculated changes with time of the distribution of salinities when an ice sheet advances over unfrozen ground and retreats behind a lake of glacial melt water. The figure shows the results within the candidate repository volume at Forsmark (due to the hydrogeological
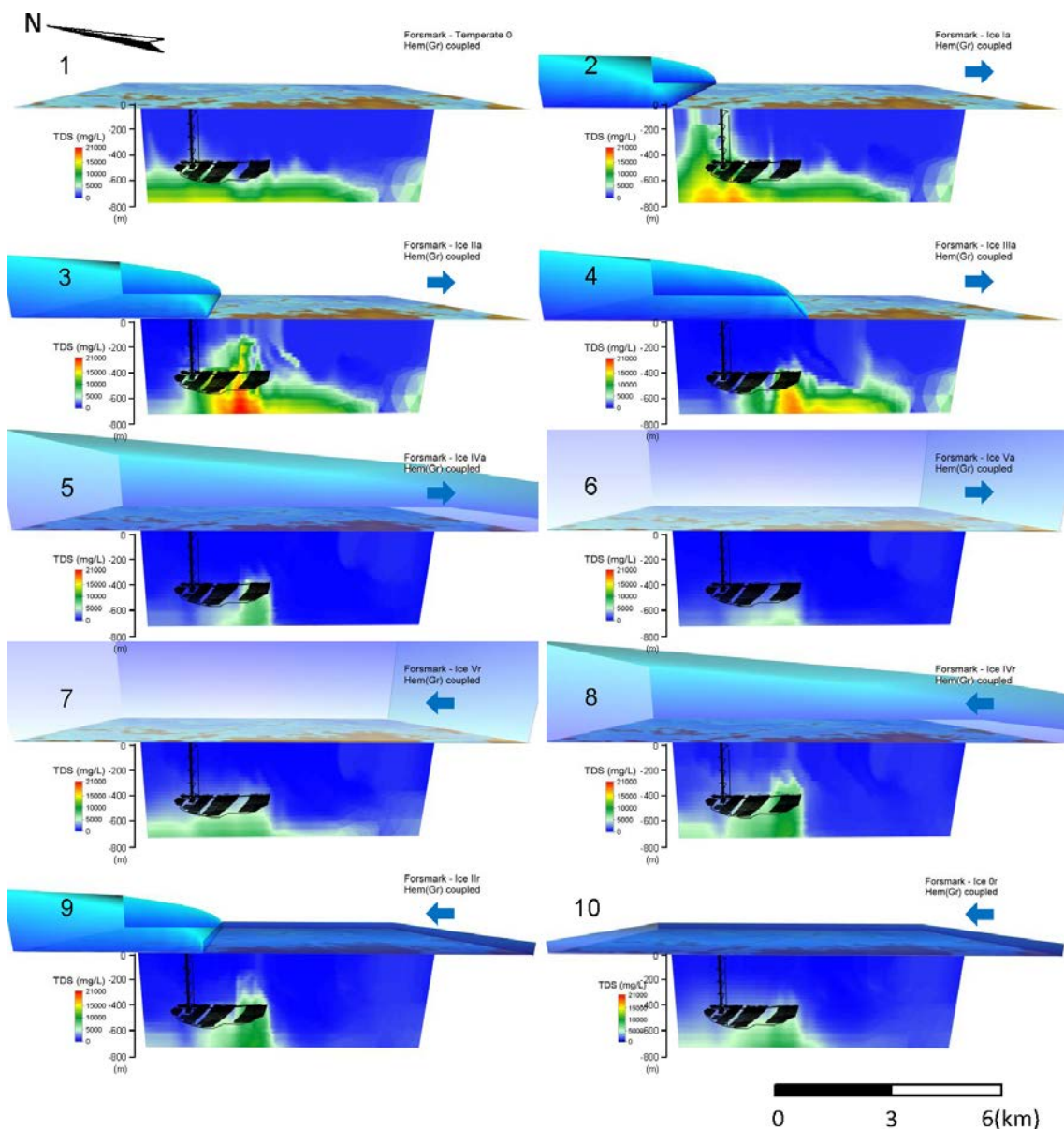
Figure 7-5. *Ice sheet advancing and retreating over unfrozen ground: Changes in the distribution of TDS (total dissolved solids, mg/L) shown in vertical slices when an ice sheet advances and retreats over the unfrozen Forsmark area. The figure shows results during the glacial sheet advance (1 to 6) and the glacial retreat (7 to 10) calculated using the model described in Chapter 3. When the ice sheet retreats the area is covered by a 100 m deep glacial melt water lake.*

grid, depths between 432 and 528 m have been included). The computed salinity is not homogeneously distributed; the calculations show groundwaters having salinities between about 0.03 g/L (during and soon after the glacial advance over the repository) and 20 g/L, as a consequence of the upconing of Deep Saline waters when the ice front margin is located on top or the repository (step IIIa). During the ice retreat, the calculated salinities within the candidate repository volume relatively are mostly around 1–4 g/L, with minimum values which can reach 0.1 g/L when the glacial retreats over the repository (step IIr).

Figure 7-6b compares the calculated salinities during the ice advance, considering that the glacier advances over frozen lithologies (permafrost). It indicates that although the calculated salinities in general show a narrower range of values, for a few of the modelled grid points there is a possibility of having higher salinities in the case of the ice sheet advancing over permafrost as compared with the ice sheet advancing over an unfrozen area. The most significant differences are computed in the step Ia, before the arrival of the ice sheet at the repository area. In this period, the average of salinities calculated within the candidate repository volume is around 5.5 g/L considering on an unfrozen soil. If the effect of the presence of permafrost is simulated, the average salinity increases to 10 g/L.
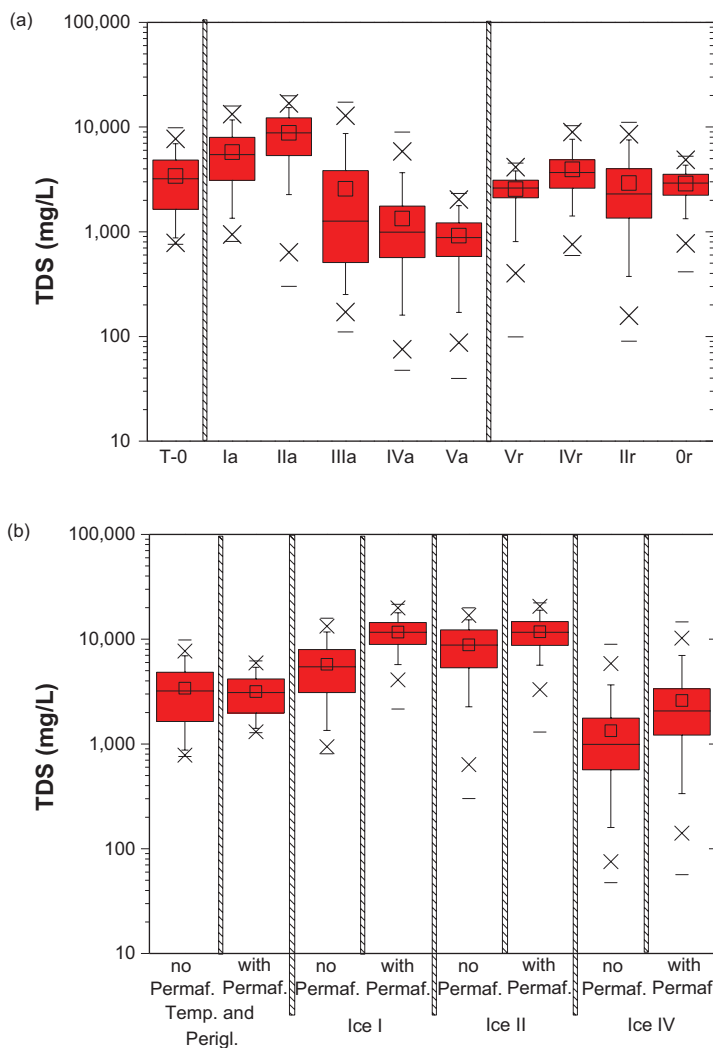
Figure 7-6. Box-and-whisker plots showing the statistical distribution of the calculated TDS (total dissolved solids) within the candidate repository volume during the glacial cycle (a). The figure illustrates the steady-state temperate model (left) and the TDS distribution at different stages of the ice sheet advancement over unfrozen ground (ice front locations Ia to Va) and ice sheet retreat (ice front locations Vr to 0r). Figure (b) illustrates the comparison between the advance of an ice sheet over unfrozen terrain with the advancement over a permafrost area for different ice front locations. The statistical measures are the median, the 25th and 75th percentile (box), the mean (square), the 5th and 95th percentile ("whiskers"), the 1st and 99th percentile (crosses) and the maximum and the minimum values.

Evolution of the concentration of natural groundwater components

Chemical components not participating extensively in chemical reactions (such as Cl, Na, sulphate, and perhaps to some extent Ca), follow the salinity patterns under the ice sheet described above. The results displayed in Figure 7-7 indicate that dilute melt waters, with $\sum q[M^{q+}]$ lesser than 4 mM, may occur within the candidate repository volume for some period of time during the advance and retreat of an ice sheet IIIa, Iva, Va, Vr and IIr), violating the criterion for the safety function indicator R1c. It should be noted that the model results indicate that after the complete retreat of the ice sheet the salinities, shown in Figure 7-6 above, and the concentration of cations, shown in Figure 7-7 below, are back, approximately, to the levels estimated before the onset of the glacial period.

Comparing these results with those obtained by the simulations that consider the presence of a frozen soil under the ice sheet (Figure 7-7a), it is notable as the development of a permafrost will affect on groundwater flow and, consequently, the end-members ratios estimated in the domain. In this way, the groundwater composition within the candidate repository volume changes, showing a significant increase of solute concentrations. However, the simulated potassium concentration doesn't remarkably differ in both periods (between 10^{-5} and $3 \cdot 10^{-4}$ mol/L).

Other components, such as bicarbonate, iron, sulphide and pH, that are controlled by relatively fast chemical reactions and reactions with minerals can also be affected by the glacial conditions to a less extent.

The calculation results shown in Figure 7-8 indicate that glacial conditions may result in a general increase of pH values, an effect which is observed for example in the Grimsel groundwaters. When
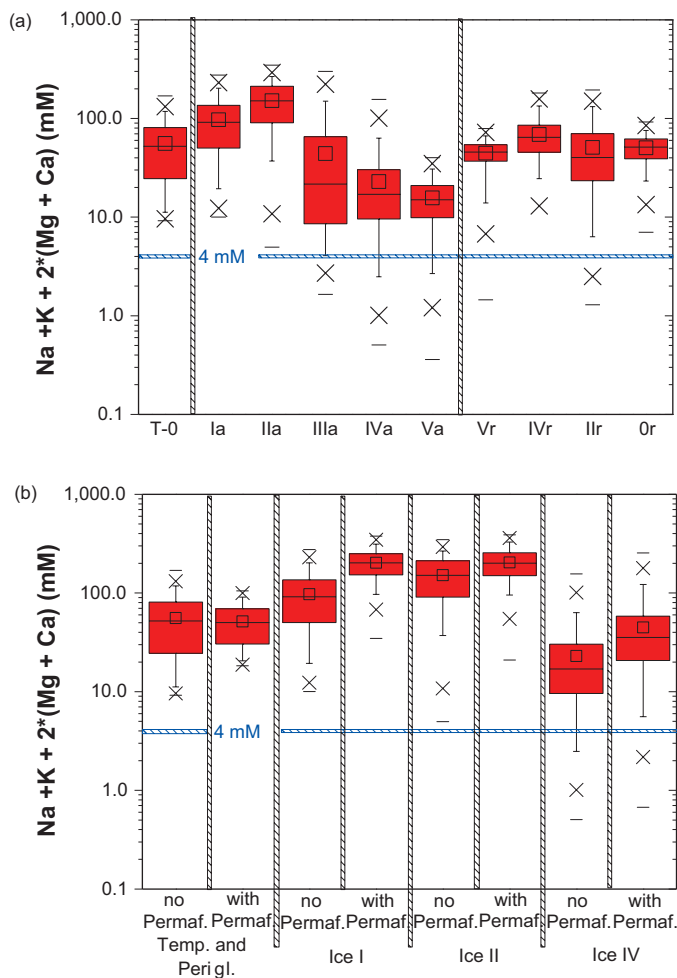
Figure 7-7. *Box-and-whisker plots showing the statistical distribution of the safety function indicator $\sum q[M^{q+}]$ for (a) the simulated glacial cycle when the ice sheet advances and retreats over unfrozen ground, and (b) considering on the existence of a frozen ground during the glacier advance. The statistical measures are the median, the 25th and 75th percentile (box), the mean (square), the 5th and 95th percentile ("whiskers"), the 1st and 99th percentile (crosses) and the maximum and the minimum values.*
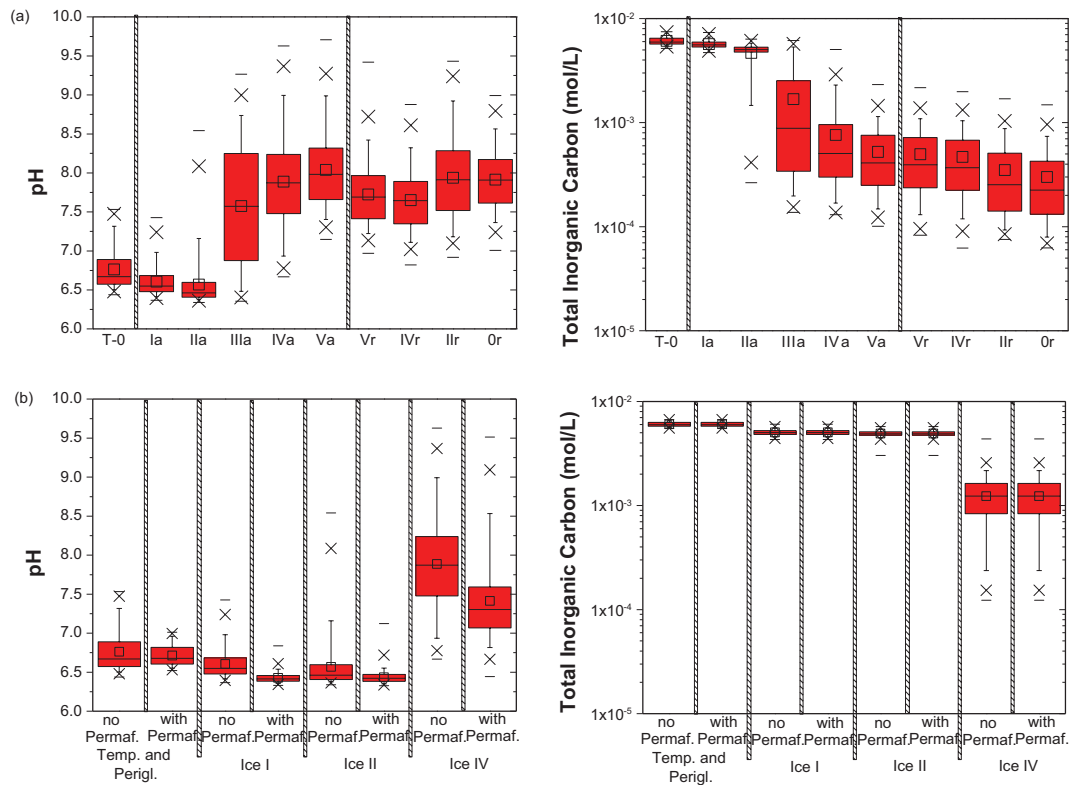
Figure 7-8. *Box-and-whisker plots showing the statistical distribution of calculated pH values and TIC concentrations for (a) the glacial cycle period considering on the ice sheet advancing and retreating over unfrozen ground, and (b) the glacier advance period considering on a frozen ground. The statistical measures are the median, the 25th and 75th percentile (box), the mean (square), the 5th and 95th percentile ("whiskers"), the 1st and 99th percentile (crosses) and the maximum and the minimum values.*

the ice sheet remains over the candidate repository volume, most of simulated groundwaters are characterized by pH values between 7.25 and 8.25, obtaining maximum values of around 9.5. In any case, the safety function criteria R1e in Figure 1-3 will be fulfilled in that pH will remain lower than 11. The presence of a frozen soil over the repository affects to the groundwater composition within the candidate repository domain decreasing the simulated pH values (Figure 7-8b).

As previously commented, the methodology employed (converting salinities in fractions of reference waters) has not supplied good results in order to reproduce the expected S(-II) concentrations, comparing with the final stages of the temperate period. The maximum amount of S(-II) obtained by this methodology is limited by concentrations around $2 \cdot 10^{-7}$ mol/L.

The evolution of the total inorganic carbon (TIC) during the glacial cycle shows a progressive decrease from values around 0.005 mol/L, before the arrival of the ice front over the repository (steps Ia and IIa), to values around 0.0004 mol/L, when the ice sheet is retreating (Figure 7-8).

In reference to the computed iron concentrations (Figure 7-9), the average values are less than 10^{-5} mol/L during most of the glacial cycle, with maximum values lesser than 10^{-4} mol/L in any case. No significant differences have been computed considering on the presence of a frozen soil over the repository.

The maximum phosphate concentrations simulated within the candidate repository volume during the glacial cycle (under the assumption of hydroxyapatite equilibrium) show an evolution from 10^{-5} mol/L, during the temperate period previous to the glacier advance, to values enclosed within the range 10^{-5} and 10^{-6} mol/L during the stage of the glacier advance. They remain below 10^{-6} mol/L during the stage of glacier retreat. In any case, and taking into account that the assumptions implemented in the calculations provide pessimistic results (see Figure 6-9), it may be assumed that phosphate concentrations during the temperate period and the glacial cycle could be lower than 10^{-6} mol/L. No large differences have been computed when considering the development of a frozen soil.
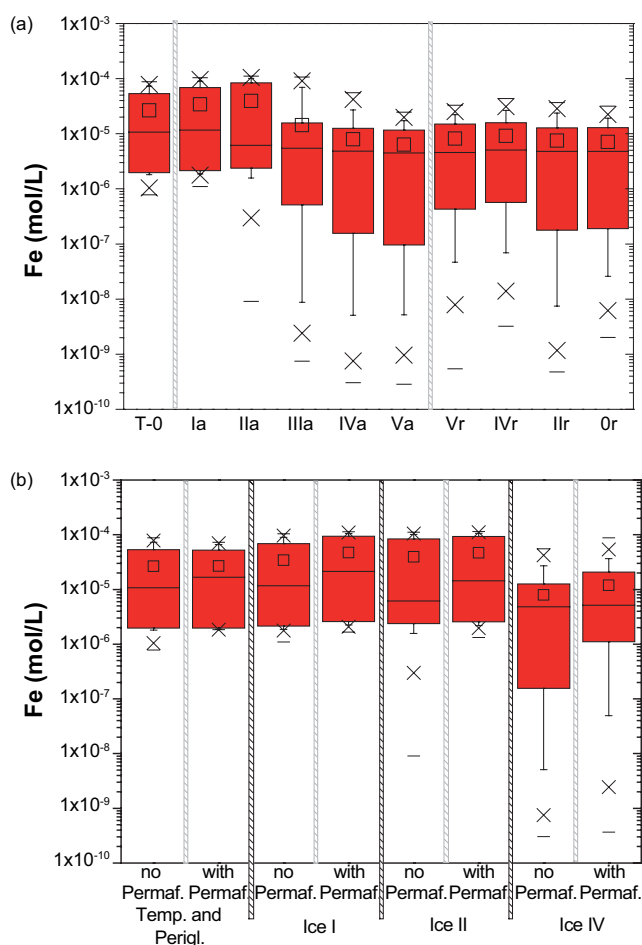
Figure 7-9. *Box-and-whisker plots showing the statistical distribution of calculated iron concentrations for (a) the glacial cycle period considering the ice sheet advancing and retreating over unfrozen ground, and (b) the glacier advance period considering on a frozen ground. The statistical measures are the median, the 25th and 75th percentile (box), the mean (square), the 5th and 95th percentile ("whiskers"), the 1st and 99th percentile (crosses) and the maximum and the minimum values.*

Redox evolution of groundwaters within the candidate repository volume

Two geochemical assumptions, namely equilibrium with respect to amorphous Fe(II) sulphide and Fe(III) oxyhydroxide, have been simulated in order to estimate the evolution of the redox potential in the area of the Forsmark site. Because the model is based on chemical equilibrium, it assumes that oxygenated waters are not present.

Under equilibrium conditions, any infiltrating oxygen with the glacial melt waters would react with the Fe(II) bearing minerals included in the model.

The results obtained when an ice sheet advances and retreats over unfrozen ground show that relative oxidizing groundwaters could reach to the Forsmark candidate repository, affecting the stability of the redox sensitivity components during the first stages of the glacier advance. Associated to the upconing of Deep Saline groundwaters, relative oxidizing groundwaters could also affect to the repository domain (Figure 7-5, Figure 7-10 and Figure 7-11).

As predictable, the most oxidizing values have been computed under the assumptions of Fe(III) oxyhydroxides equilibrium (Figure 7-10). When equilibrium with respect to amorphous Fe(II) sulphides is only simulated (Figure 7-11), the calculated Eh values drop with respect to those calculated under the Fe(III) oxyhydroxides equilibrium. As both possibilities have been considered to be probable, they have been analyzed in the statistical study of the simulated points within the candidate repository volume.
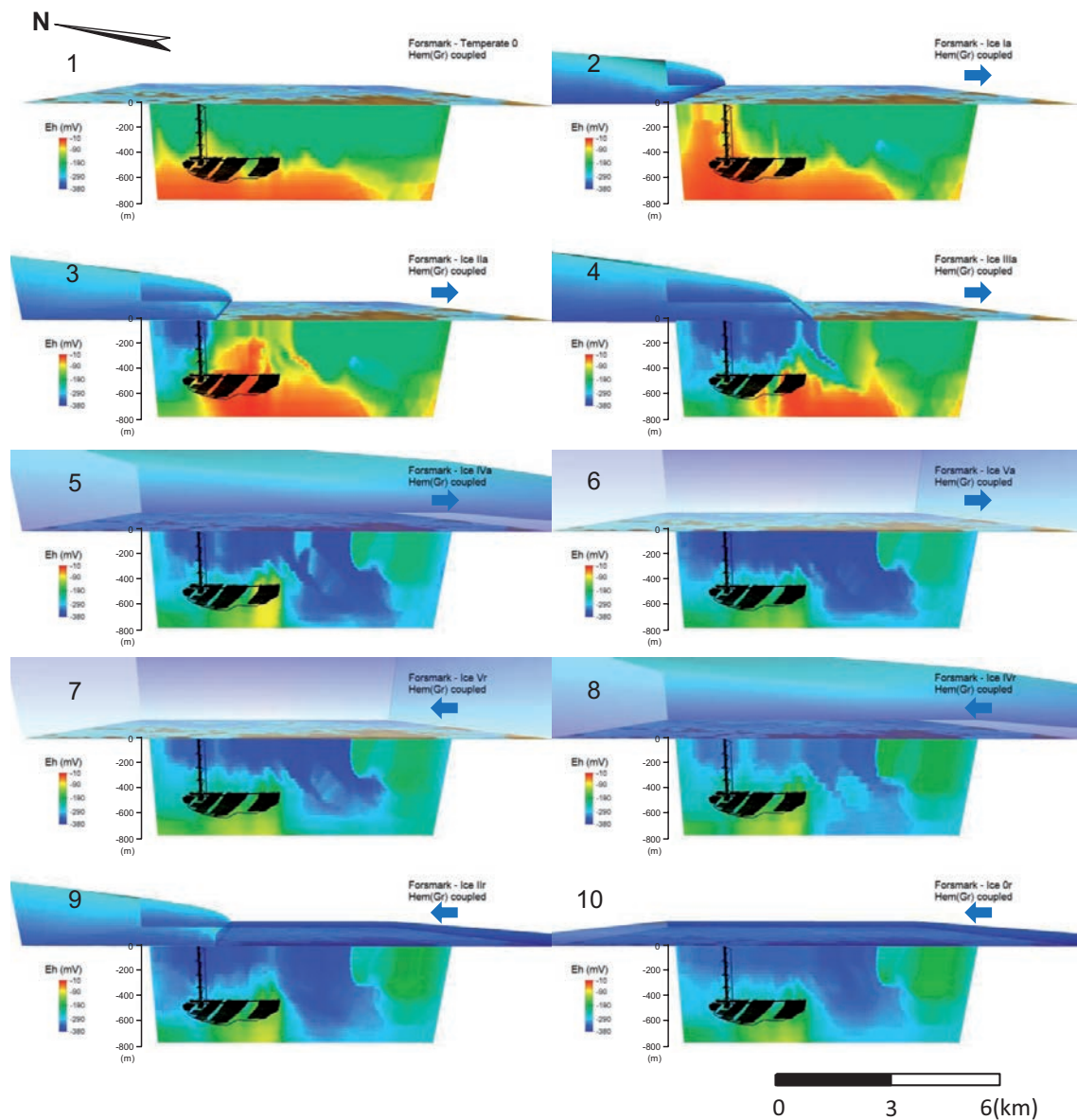
Figure 7-10. Ice sheet advancing and retreating over unfrozen ground: Changes in the distribution of Eh, computed under the assumption of Fe(III) oxyhydroxides equilibrium, and shown in vertical slices when an ice sheet advances and retreats over the unfrozen Forsmark area. The figure shows results during the glacial sheet advance (1 to 6) and the glacial retreat (7 to 10) calculated using the model described in Chapter 3. When the ice sheet retreats the area is covered by a 100 m deep glacial melt water lake.
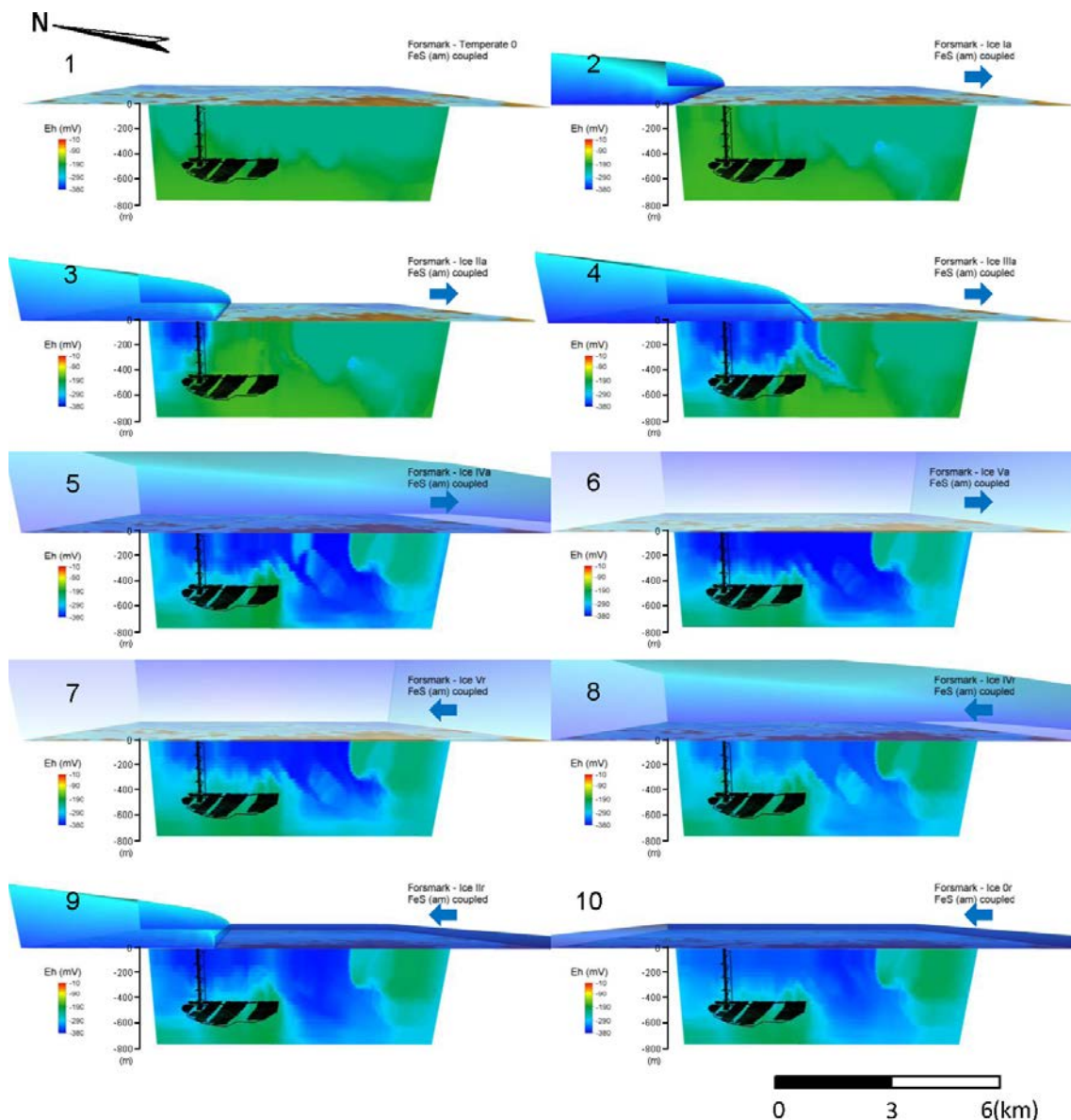
Figure 7-11. *Ice sheet advancing and retreating over unfrozen ground: Changes in the distribution of Eh, computed under the assumption of amorphous Fe(II) sulphides equilibrium, and shown in vertical slices when an ice sheet advances and retreats over the unfrozen Forsmark area. The figure shows results during the glacial sheet advance (1 to 6) and the glacial retreat (7 to 10) calculated using the model described in Chapter 3. When the ice sheet retreats the area is covered by a 100 m deep glacial melt water lake.*

The statistical distribution of calculated Eh values is shown in Figure 7-12. Due to the imposed mineral equilibrium, the general variations in the pH values, shown in Figure 7-8, are reflected in corresponding variations in the calculated Eh.

The wide variability of the computed results is significant. When the ice sheet covers the area of the candidate repository volume, the computed Eh values plot around –225 and –275 mV. Previously, when the ice front is just over the repository, the numerical results show the wider variability of the redox potential within the candidate repository volume, with maximum values higher than –50 mV, and minimum values around –350 mV. However, in the first stages of the glacial cycle, the redox potential ranges between –50 and –175 mV. Similar values of Eh are obtained from the modelling of the advancement of an ice sheet over permafrost.

In general, during the development of the glacial cycle, the redox potential of the groundwaters within the candidate repository domain is expected to be clearly reducing.
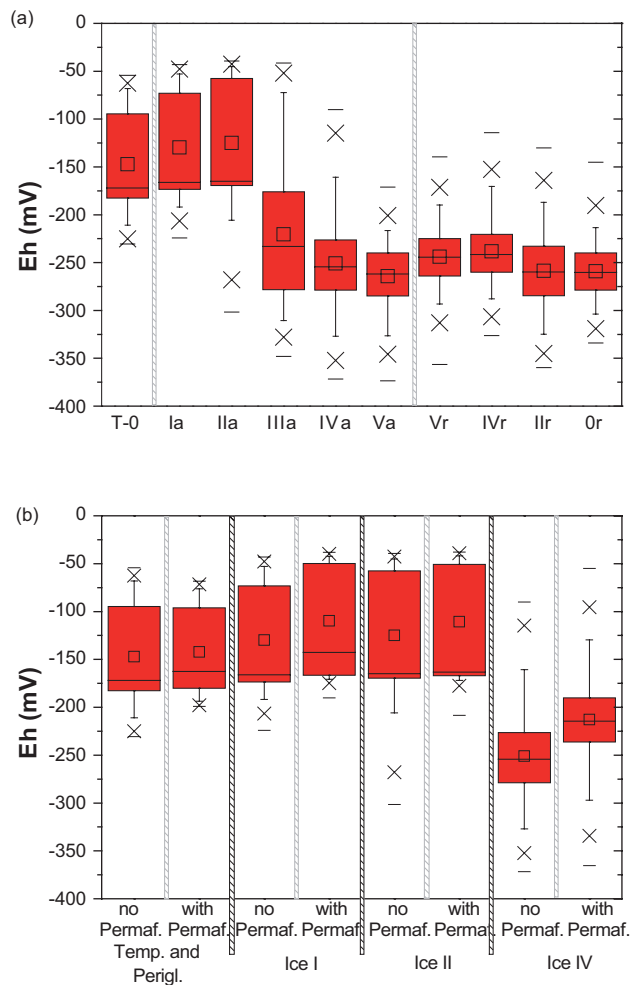
Figure 7-12. *Box-and-whisker plots showing the statistical distribution of calculated redox potential under (a) the glacial cycle period considering the ice sheet advancing and retreating over unfrozen ground, and (b) the glacier advance stages considering on a frozen ground. The statistical measures are the median, the 25th and 75th percentile (box), the mean (square), the 5th and 95th percentile ("whiskers"), the 1st and 99th percentile (crosses) and the maximum and the minimum values.*

Conclusions

During the glacial cycle, the estimated salinity is below 20 g/L within the candidate repository volume. The maximum values (higher than those calculated for the temperate and the periglacial periods) correspond with periods of upconing. However, during the stages IIIa, IVa, Va, Vr and IIr, as a consequence of infiltration of glacial melt waters, the safety function $\Sigma q[M^{q+}]$ (Figure 1-3) shows values lesser than 4 mM in more than 5% of the numerical points within the candidate repository volume. On the other hand, numerical results also show as the pH values remain lower than 11 during the glacial cycle (accordingly with the safety indicators previously mentioned). In general, salinity, cation concentrations and pH show narrower ranges of calculated values when a frozen soil is developed in the area of the glacial front. In spite of this, the lowest cation concentrations have been obtained in the case of the ice sheet advancing over a unfrozen soil. As an indirect conclusion of the distribution of these geochemical indicators, colloids would not be especially stable during a hypothetical glacial cycle.

In reference to the other safety functions (Figure 1-3), sulphide concentrations have not been accurately reproduced (as it has been commented in this chapter). In any case, the obtained concentrations are lower than 10^{-7} mol/L. On the other hand, the maximum concentrations of potassium and iron simulated during the glacial period remain limited by $3 \cdot 10^{-4}$ and 10^{-4} mol/L, respectively. The evolution of the maximum phosphate concentrations within the candidate repository volume

has been from values of around 10^{-5} mol/L, during the temperate period previous at the beginning of the glacial cycle, to values of around 10^{-6} mol/L when the ice sheet is retreating and under the submerged conditions that is expected to occurs to the end of the glacial cycle.

The simulated redox potential shows Eh values lower than –50 mV within the candidate repository volume. In more than 50% of the simulated points, the Eh values are lower than –200 mV when the glacial melt waters affect the candidate repository volume. Only during the first stages of the glacier advance, the average values of the redox potential is clearly higher than –150 mV.

7.4   Submerged conditions after the retreat of an ice sheet

As previously commented in Chapter 3, after the retreat of the ice sheet during the glacial period, isostatic depression will set the ground surface at the repository site below the Baltic Sea surface level. It is a repetition of the last glacial cycle (the Weichselian), when the Forsmark site is expected to be below lakes of glacial melt water, and sea or brackish waters during a period of time between a few thousand years up to perhaps ten thousand years. Both the site descriptive modelling of the Forsmark site since the retreat of the last ice sheet to the present-day situation and the SR-Site modelling show a relatively fast turnover of groundwaters, where glacial melt is replaced by a succession of waters penetrating from the surface: the Littorina Sea gradually evolving into the present day Baltic Sea, and finally modern meteoric waters.

7.4.1   Submerged conditions under a lake of glacial melt waters

The model results presented above indicate that concerning salinity and the concentration of cations, the conditions when the site is submerged under a lake of glacial melt water are similar to those found before the onset of the glacial cycle (see the starting steady state temperate result "T-0" and the ice front locations "0r" in Figure 7-6 and Figure 7-7). Other more reactive groundwater components such as carbonate or pH (Figure 7-8), iron concentration (Figure 7-9) or Eh (Figure 7-12) may remain affected, but all groundwater characteristics are expected to satisfy the safety function indicators and criteria R1a to R1f in Figure 1-3.

7.4.2   Submerged saline conditions

The possible infiltration for relatively short periods of time of waters of marine origin after a glacial cycle has been modelled. Within such a period, equivalent to the Littorina Sea episode that had its maximum salinity at 4,000 BC, the salinity of groundwaters at repository depth could increase due to density driven groundwater flow.

The results modelled for 3,000 BC show that the effects of the marine water intrusion at repository depth are delayed in time and that the proportion of Littorina waters in the repository volume is larger at present than it was then (Figure 7-13). The infiltration of marine waters from the surface of the model has as a consequence the decrease of the fractions of the glacial origin waters. In spite of this, the fractions of marine origin groundwaters within the candidate repository volume are lesser than those estimated for the initial stage of the temperate period (Figure 7-13; 2,000 AD).

In general, the geochemical characteristics of the groundwaters simulated within the candidate repository volume are remarkably similar to those calculated for the initial stage of the temperate period (Figure 7-14 and Figure 7-15). Most of the computed salinities plot between 7 and 12 g/L, with maximum values around 13 and 16 g/L, and minimum higher than 5 g/L. In this way, the safety function $\Sigma q[M^{q+}]$ is, in any case, higher than 75 mM. The potassium concentrations show a similar trend, with values between 10^{-4} and $4 \cdot 10^{-3}$ mol/L.

The iron and sulphide concentrations calculated in the submerged saline period are also similar to those obtained for the initial stages of the temperate period. Within the candidate repository volume, the computed iron concentrations range between $5 \cdot 10^{-7}$ and $2 \cdot 10^{-5}$ mol/L, whereas the sulphide concentrations are limited between 10^{-8} and 10^{-5} mol/L.
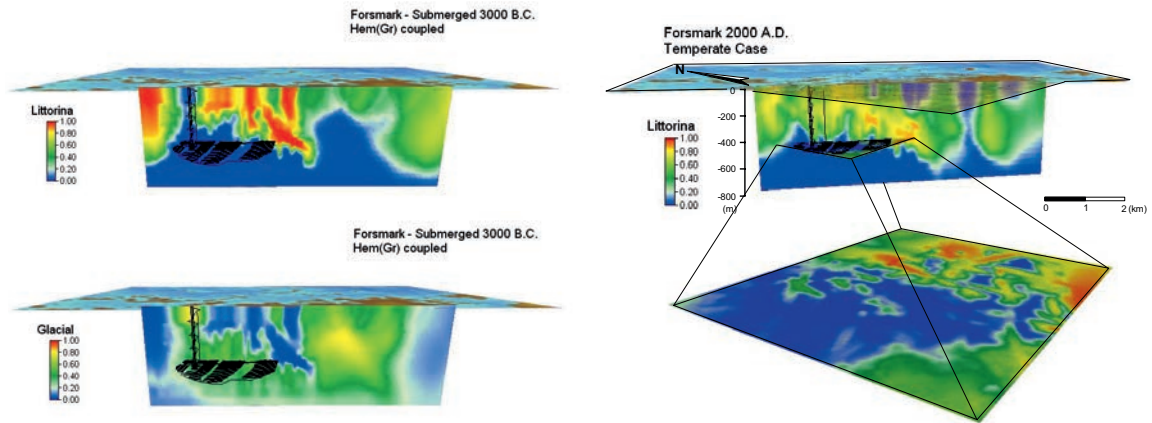
Figure 7-13. *Fractions of Littorina water and glacial origin waters for the computed submerged saline period (left), and fraction of Littorina waters in the initial stage of the temperate simulations (right; 2,000 AD). The figure shows as in spite Littorina waters are predominant in the superficial lithologies during the submerged saline period (3,000 BC), the candidate repository volume is more affected by the marine origin groundwaters at the present day.*
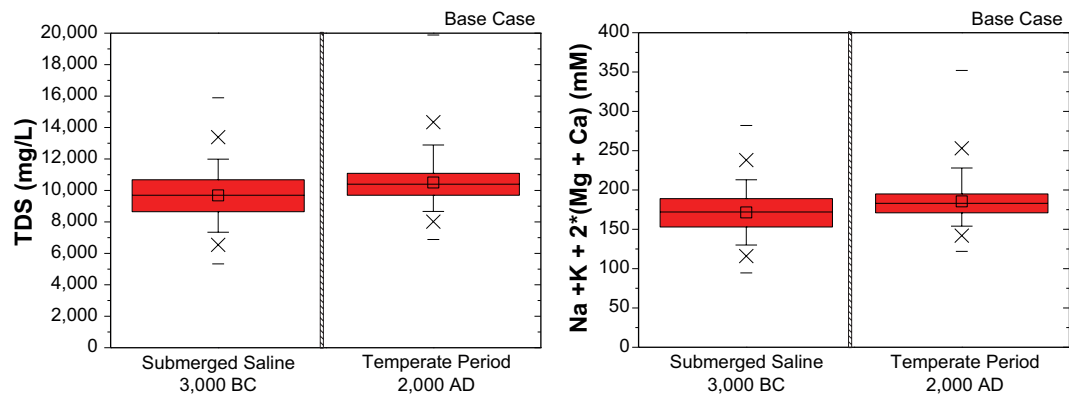
Figure 7-14. *Box-and-whisker plots showing the statistical distribution of calculated TDS and the safety function indicator $\sum q[M^{q+}]$ during the stage of submerged saline conditions (3,000 BC), compared with the results obtained for the initial stage of the temperate simulations (2,000 AD). The statistical measures are the median, the 25th and 75th percentile (box), the mean (square), the 5th and 95th percentile ("whiskers"), the 1st and 99th percentile (crosses) and the maximum and the minimum values.*
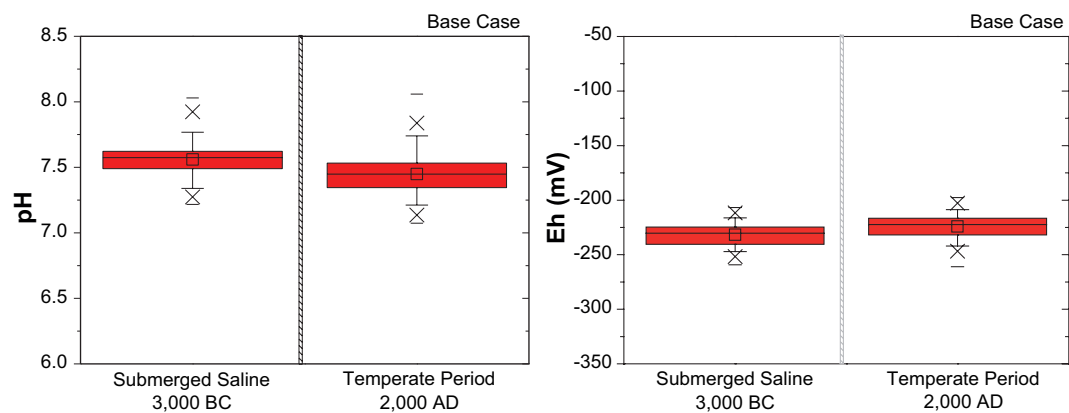
Figure 7-15. *Box-and-whisker plots showing the statistical distribution of calculated pH and Eh values during the stage of submerged saline conditions (3,000 BC), compared with the results obtained for the initial stage of the temperate simulations (2,000 AD). The statistical measures are the median, the 25th and 75th percentile (box), the mean (square), the 5th and 95th percentile ("whiskers"), the 1st and 99th percentile (crosses) and the maximum and the minimum values.*

Figure 7-15 shows as the pH values obtained in the submerged saline period (within the candidate repository volume) are around 7.5 (between 7.25 and 8.0), and more than 99% of the obtained Eh values are between –200 and –250 mV. Both, the pH and the redox potential are practically identical to those previously computed for the year 2,000 AD of the temperate simulations.

Conclusions

The calculated groundwater compositions for 3,000 BC show that the charge concentration of cations around the repository is well above 0.004 mol/L, corresponding to compliance with the safety function indicator R1c in Figure 1-3. As the salinities are not expected to increase above those of seawater during any period of time, the swelling capacity of the backfill will not be affected (see safety function indicator R1b in Figure 1-3).

During the submerged periods (under a lake of glacial melt waters and under seawater), the average of the phosphate concentrations is around 3.5 and $5.0 \cdot 10^{-8}$ mol/L within the candidate repository volume (two orders of magnitude lower than the concentrations simulated during the temperate and the glacial periods). However, during the submerged saline period, maximum concentrations of 10^{-6} mol/L have been computed.

7.5   Variant case: ice advance N-S

In the previous models, the advance of the ice sheet takes place from the continental areas to the present day shoreline. In this way, a variant case has been performed in order to evaluate the influence on the hydrogeochemistry within the repository domain of an hypothetical change in the glacier movement. Only two stages have been modelled during the glacier advance (steps IIa and IIIa), and the obtained results have been compared with those obtained considering the standard movement of the glacier.

In general, no major changes are simulated in the chemical composition of the groundwaters around the candidate repository volume (Figure 7-16). Only slight differences in salinities have been computed. Despite the fact that the average values are practically identical (Figure 7-16), the minimum values calculated are lower in the case of the ice advance N-S (around 0.1 g/L during the stage IIa and 0.05 g/L during the stage IIIa). This trend is also reproduced by the concentration of the major components of groundwaters and for the safety function $\Sigma q[M^{q+}]$, obtaining values lower than 4 mM in, approximately, 2–10% of the points within the candidate repository volume for the stages IIa and IIIa, respectively).

The pH and the Eh values obtained are remarkably similar to those obtained for the "standard" movement of the glacier (Figure 7-16). During the stage IIa, previously at the arrival of the ice front, the maximum pH obtained is around 9.0, 0.5 units of pH higher than that obtained with the simulations of the standard movement of the glacier. Similarly, the corresponding Eh values are also practically identical for both hydrological hypothesis. More significant differences have been computed in the stage IIIa, when the ice front is just over the repository volume. In this case, the average of the computed pH values drops to 7.0 (with respect to an average value around of 7.5 obtained with standard movement of the glacier), and the corresponding Eh values increase from –225 mV to –200 mV, approximately.

As a conclusion, the results obtained during the stage IIIa show significant differences with respect to those calculated with the hydrological reference model (pH and Eh values, mainly; see Section 7.3). The relationships between the preferential directions of the fracture zones and the glacier movement play an important role in the infiltration mechanisms of the glacial melt waters.
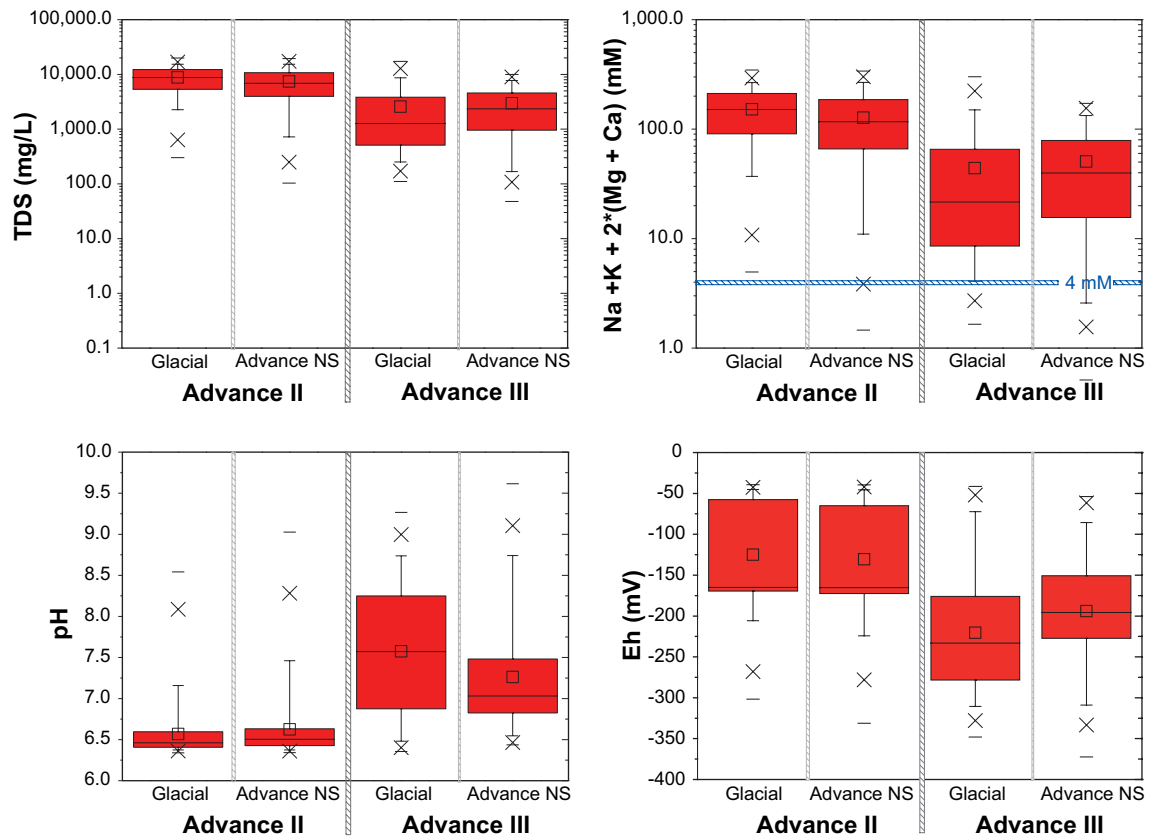
Figure 7-16. *Box-and-whisker plots showing the statistical distribution of calculated TDS, the safety func-*
tion ∑q[M^q+], and the pH and Eh values during a stage of ice advance with N-S directionality (comparing
with the standard case previously detailed) for the stages II and III. The statistical measures are the
median, the 25th and 75th percentile (box), the mean (square), the 5th and 95th percentile ("whiskers"),
the 1st and 99th percentile (crosses) and the maximum and the minimum values.

7.6 Conclusions and discussion

Temporal changes in groundwater conditions are expected throughout a complete glacial cycle. Short
periods of upconing of deep reducing groundwaters, with an increase of salinity, will be followed by
longer periods with glacial melt water intruding into the rock.

7.6.1 Salinity and concentrations of major groundwater components

As indicated previously, salinity levels are expected in general to decrease during glacial periods.
Dilute melt waters, with $\sum q[M^{q+}]$ lower than 4 mM, may occur within the candidate repository
volume for some period of time during the advance and retreat of an ice sheet, violating the criterion
for the safety function indicator R1c. Upconing of deep seated saline groundwaters during the glacial
period is not expected to affect the swelling capacity of the backfill, corresponding to the safety
function indicator R1b.

Major groundwater components, such as chloride, sodium, sulphate, and calcium, will follow the
salinity trends. Other components, such as bicarbonate, potassium, iron, sulphide and pH, which
are controlled by relatively fast chemical reactions and mineral dissolution/precipitation, are less
affected by the glacial conditions. However, all the evidence points towards dilute waters with
relatively high pH. The criteria concerning the safety function indicators R1d and R1e in Figure 1-3
will be fulfilled in that pH will remain lower to 11, and the concentrations of K, HS⁻ and Fe will
remain limited. On the other hand, we could assume that phosphate concentrations remain below
10^{-6} mol/L, in spite of maximum concentrations of around 10^{-5} mol/L have been computed during
the initial stages of the glacial cycle.

7.6.2 Expected concentrations of colloids

Colloids are known to be strongly destabilised at high ionic strengths, and at high concentrations of divalent cations (Ca^{2+}) in particular. Therefore, during periods of glaciation, with predominantly dilute groundwaters, it cannot be excluded that colloids may perhaps be generated and transported by groundwater easily. However, a high potential stability of colloids does not necessarily indicate a high colloid concentration. It has, for example, been shown that the granitic groundwaters at Grimsel, which are quite dilute and where colloids, if formed, are quite stable, have low concentrations of colloids (less than 0.1 mg/L). The reason for this is not clear: there might be some unknown mechanism that removes colloids at that site, or perhaps there is no significant generation of colloids at Grimsel. The conclusion is, therefore, that there is a potential for higher colloid concentrations in groundwaters during a glacial period, especially during the advance and retreat of an ice sheet when groundwater velocities are highest. An upper limit would be the highest colloid concentrations in montmorillonite suspensions, about 40 g/L /Birgersson et al. 2009/.

7.6.3 Sulphide concentrations

The distribution of sulphide concentrations is relevant because it is used to estimate canister corrosion rates during the glacial and submerged periods.

Although sulphide concentrations are obtained as a result of the PHREEQC modelling previously described in Chapter 4, it is believed that (1) the equilibrium solubility constraints applied, and (2) the methodology which considers that initial groundwater compositions is only a mixing between Deep Saline groundwaters and Altered Meteoric waters can not reflect the variability of sulphide concentrations that can be expected during glacial and submerged conditions. Because of this, the sulphide concentrations for the glacial and submerged conditions are assumed to be the same as the observed distribution of sulphide in groundwaters during the present temperate conditions, which is after a recent period of possible intrusion of marine sulphate-rich waters.

The intensity of microbially mediated sulphate reduction to produce sulphide will probably decrease under an ice sheet due to the lower temperatures. Compared with previous temperate and periglacial periods, sulphate concentrations might increase during the short periods of upconing waters and they will decrease substantially during the longer periods of intrusion of glacial melt waters. Therefore, sulphate reduction may only occur during periods of upconing. In any case, reducing agents are required for any sulphate reduction to take place, and under glacial conditions the inflow of organic matter from the surface will become negligible. Sulphate reduction could still be sustained by the gaseous groundwater components methane and hydrogen. If microbial sulphide production occurs during upconing periods, it will be limited by the availability of both sulphate and mainly methane. The amounts of methane will be controlled by its production and flow from the deeper parts of the bedrock. There is not enough data at present to quantify this process, but there are no indications that methane should increase in concentration during such periods, and there is no evidence to support increased sulphide production under ice sheets.

7.6.4 Discussion about the expected oxygen content of groundwaters during a theoretical glacial cycle

Arguments have been put forward that if glacial melt waters were rich in dissolved atmospheric gases, reducing conditions might no longer prevail at repository depth, infringing the safety function indicator criterion R1a in Figure 1-3 /Puigdomenech et al. 2001/.

Large changes in hydraulic conditions are expected when the ice front margin passes over the repository volume. During these periods, that are expected to be relatively limited in time, large quantities of glacial melt water may intrude into the rock, owing to the drastic change in hydraulic head gradients. In the remainder of a complete glaciation cycle, the magnitude of the hydraulic head gradient over the repository volume will be much lower, with groundwater flow rates not considerably different from temperate conditions, and probably lower.

The compaction of snow into glacier ice involves the incorporation of substantial amounts of air /Martinerie et al. 1992/. Thus, glacier melt water may initially contain dissolved carbon dioxide and oxygen at above the concentrations expected for aerated water. The oxygen concentration in pure

water in equilibrium with air is temperature dependent, approximately 8 mg/L at 20°C. For glacial melt waters, based on theoretical constraints, the maximum oxygen concentration has been estimated to be 45 mg/L /Ahonen and Vieno 1994/, and this is the concentrations observed in some samples of glacier ice thawed under laboratory conditions. However, it has been noted that much lower values are normally measured in sampled glacial melt waters in the field, in the range 0–5 mg/L /Gascoyne 1999/. It may be argued that degassing could have partly contributed to the observed decrease in the oxygen levels of these field samples. Also, photosynthetic and heterotrophic microbial activity on the surface of glaciers may partly be responsible for the low oxygen content /Hallbeck 2009/. Furthermore, glacial melt water is expected to react rapidly with sub-glacial rock minerals and debris. Solute concentrations of up to 0.2 g/L /Brown 2002, Cooper et al. 2002/ have been found, supposedly generated from acid dissolution of calcite and pyrite oxidation:

$$CaCO_3(s) + CO_2(g) + H_2O \rightarrow Ca^{2+} + 2\ HCO_3^- \qquad \text{(Equation 7-1)}$$

$$4\ FeS_2(s) + 14\ H_2O + 15\ O_2(g) \rightarrow 16\ H^+ + 8\ SO_4^{2-} + 4\ Fe(OH)_3(s) \qquad \text{(Equation 7-2)}$$
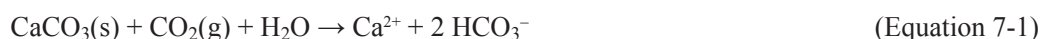
In this way, the amounts of sulphate found in glacial melt waters are sufficient to explain the low oxygen concentrations found.

During present-day temperate conditions, the top soil and the uppermost part of the rock contains relatively large amounts of organic material. Mediated by microbes the degradation of the organic substances explains the lack of oxygen below a few metres in the rock at Forsmark. During a glacial cycle, the amount of degradable organic substances is uncertain, although microbial activity is observed at the surface of most glaciers, and in glacial melt water. The main reducing capacity in the absence of organic material is comprised of ferrous minerals in the rock. Biotite inside the bulk of the rock matrix and chlorite adjacent to fractures has been shown to dominate the contribution to the reducing capacity in the absence of organic substances. The ferrous iron content in the bulk rock is approximately one percent by weight in the dominant rock types in Forsmark, accessible through diffusion in the pores of the matrix. Fracture minerals directly accessible in flowing fractures have even larger ferrous iron content.

No indications of ongoing or past intrusion of oxygen have been found in boreholes in the rock at Forsmark. In these studies no measurements were carried out at shallow depths (less than 5 m). Oxygen reduction potential (ORP) measurements in soil pipes have shown that most of the oxygen under present day conditions is depleted within the first few metres at the site. Although no general depth trend of oxygen intrusion can be found at greater depths than a few meters, this does not exclude the possibility of greater intrusion depths in transmissive domains such as deformation zones, where only scattered samples have been taken. In addition to the investigations made at the Forsmark site, redox transition zones have been investigated in many locations in Scandinavia as well as in various sites throughout the world. Although the historical hydraulic properties at many of the investigated sites are difficult to evaluate, it is generally found that traces of oxygen intrusion are seldom found below 200 metres.

Based on observations and results from conservative modelling efforts, oxygen intrusion to repository depth in highly transmissive deformation zones cannot be discarded. Model results indicate that thousands of years of the worst realistic glaciation assumption would be needed for oxygen to reach the canisters in the repository. Therefore it is concluded that reducing conditions will prevail in the repository, satisfying the safety function indicator criterion R1a in Figure 1-3.

7.6.5 Discussion about the expected minimum pH values of groundwaters during the temperate period and the remaining glacial cycle

In the calculations presented in this report, the redox potential of groundwaters is basically controlled by the equilibriums between Fe(II) aqueous species and Fe(III) oxyhydroxides or between Fe(III) species and amorphous Fe(II) sulphides. Along these equilibriums, the Eh values are fixed in each point when the pH of the mixture is defined by calcite equilibrium.

Mixing effects are not so simple as to explain them in terms of "dilution/concentration". Mixing results in non-linear effects on the thermodynamic activities of the species controlling the water-mineral reactions (e.g. through the ionic activity product). Thus, depending on the characters of the

mixed end-members both calcite oversturation and subsaturation can be obtained in a not predictable if geochemical simulations were not performed. For example, mixing between the Glacial end-member (extremely dilute waters) and the Deep Saline end-member promotes calcite oversaturation over almost all possible mixing proportions /Gimeno et al. 2009/.

To the end of the temperate period, the range of the calculated pH plots minimum values around 6.5, approximately. This is a consequence of the existence of the maximum fractions of Altered Meteoric waters within the candidate repository volume, instead of Littorina and Old Meteoric waters. However, the minimum values of pH have been calculated during the initial stages of the glacial cycle, associated to the upconing processes of the Deep Saline groundwaters. They are characterized by relatively high Ca concentrations. In this way, as a result of the equilibrium:

$$CaCO_3 + H^+ = Ca^{2+} + HCO_3^- \quad \log K_{25°C} = 1.849 \qquad \text{(Equation 7-3)}$$
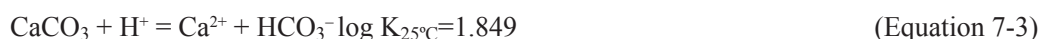
the increase of the fraction of Deep Saline groundwaters within the candidate repository volume produces a decrease of the resulting pH of the mixture. This is mainly effective during the stages Ia and IIa of the glacial cycle, with resulting pH ranges showing minimum values around 6.3. When the glacier front is located on the candidate repository (stage IIIa), higher pH values are computed as a consequence of the increase of the fractions of glacial melt waters within the repository volume. In this way, the lowest pH values has been calculated when the candidate repository volume is not affected by glacial melt waters, by the mixing between the Altered Meteoric and the Deep Saline end-members considering calcite equilibrium.

The mixing between the Altered Meteoric and the Deep Saline end-members results minimum pH values (pH = 6.3) when the fraction of the saline end-member ranges between 30% and 60% (Figure 7-17). For higher fractions, the pH values increase to 8, corresponding to 100% of the Deep Saline term.

During the stage of the glacier retreat, the upconing processes return to be functional (Vr and IVr stages, mainly), decreasing slightly the average values of the calculated pH (Figure 7-8).
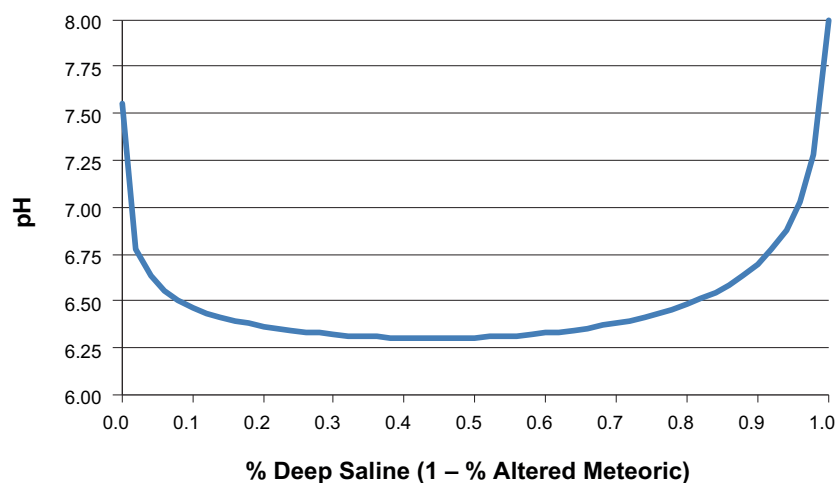
Figure 7-17. Trend of the calculated pH values in equilibrium with respect to calcite for different mixture fractions between the Deep Saline and the Altered Meteoric end-members.

8 Evaluation of other geochemical parameters

8.1 Introduction

The main aim of this Section is the assessment of the possible contents of certain components (colloids, dissolved and total organic carbon[2], nitrite, ammonia, acetate, methane and molecular hydrogen) expected over the future evolution of the Forsmark groundwaters.

The analysis of potential contents of these parameters through time is based on a large literature survey but some important sources should be highlighted here:

- The available data and interpretations for the two sites, Forsmark and Laxemar, from the Site Descriptive Modelling. The data used here can be found in the SICADA tables and a general overview can be found in the corresponding background reports /Laaksoharju et al. 2008, 2009/. A more detailed presentation of the data together with interpretations of most of these parameters are available in /Gimeno et al. 2008, 2009/ and /Hallbeck and Pedersen 2008a, b/.

- The available data in other crystalline systems like Olkiluoto (Finland; /Pitkänen et al. 2004, Pitkänen and Partamies 2007, Pedersen 2008/, Grimsel (Switzerland; /Degueldre 1994, Degueldre et al. 1996/) or the Canadian Shield (/Vilks et al. 1991, Gascoyne 2004/).

- Information on some "non-natural" boundary conditions such as those imposed by the accumulation of organic materials during the construction and operation of the repository /Hallbeck et al. 2006, Hallbeck 2010/ or by the presence of the bentonite barrier as source of colloids /Wold 2010/.

- And finally, data on acetate contents in groundwaters from crystalline systems (as acetate concentrations were not determined during the site characterization programs in Sweden or Finland). Analytical data are available from the sulphide monitoring program under progress at Laxemar and Äspö. Some additional information can be obtained from the replica experiment in REX project /Trotignon et al. 2002/ and from the MICROBE experiment at Äspö /Hallbeck and Pedersen 2008c/.

The future stages considered here cover the time span of a Quaternary glacial cycle, which is 120,000 years. Hence, they include the excavation/operation period, the initial temperate period, and the evolution during the glacial period[3] following the initial temperate period. In addition, immediately after the retreat of an ice sheet, isostatic depression will set the ground surface at the repository site below the Baltic Sea surface level. In the reference evolution, which is a repetition of the last glacial cycle, the Weichselian, the Forsmark site is expected to be below lakes of glacial melt waters (such in the Ancylus period in the past), and sea or brackish waters (such as the Littorina seawater periods in the past) during a period of time between a few thousand years up to perhaps ten thousand years. The model results presented above indicate that the conditions when the site is submerged under a glacial melt water lake are similar to those found before the onset of the glaciation. Thus, only a "marine" submerged period is discussed in this section.

In this scheme, the excavation/operation period (that includes the re-saturation phase of the repository[4]; /SKB 2010/ is treated in a "special way". During the excavation and operation phases, the chemical situation close to the repository may undergo several changes. Increased infiltration of meteoric waters, upconing of Deep Saline waters, oxygen intrusion, changes in microbial communities etc, will promote the existence of variable chemical conditions that, in turn, will affect most of the considered parameters in a very short time perspective.

After closure, during the return to "natural conditions", degradation of organic materials (e.g. microbial biofilms, plastics, cellulose, hydraulic oil, surfactants, etc.) accumulated in the repository and/or

---

[2] The contents of TOC (analysed in unfiltered samples) and DOC (analysed in filtered samples) in the Laxemar and Forsmark groundwaters are usually very similar. Only locally TOC was found to be significantly greater than DOC. Thus, only the values of dissolved organic carbon will be discussed in this section.

[3] In this section, the term "glacial period" includes the permafrost and glacial stages.

[4] It will take several hundreds of years for the repository to reach full saturation (Main Report of the SR-Site project, 2010).

corrosion affecting the metallic parts used as repository components, may affect the chemical evolution of most of the parameters of interest. The expected effects may occur during the re-saturation phase but also during the temperate period. However, in order to make the description easier, these effects will only be discussed in the Section of the excavation/operation period.

Finally, most of the parameters analysed here have fairly similar sources, sinks and conditioning factors (e.g. those related to microbial activities). Hence, in the following text the reader will find a certain degree of redundancy when reviewing the different parameters. This redundancy has been kept in order to make each description self-consistent and easier.

8.2 Dissolved organic carbon (DOC)

8.2.1 Overview/general description

The concentration of dissolved organic carbon (DOC) is of special interest for microbiological interpretations as DOC is expected to be related to microbiology: DOC can be used as a source of energy, electrons and carbon by heterotrophic microorganisms, while autotrophic microorganisms will produce DOC (e.g. acetate; see Section 8.3). DOC contents may favour reducing environments through microbial activities but also may have detrimental effects if sulphate reduction (and sulphide generation) is the favoured microbial activity. Moreover, the formation of organic complexing compounds and organic colloids might enhance the potential for radionuclide transport during later periods.

In the Forsmark area (Figure 8-1a), at the shallower and more hydraulically active levels (down to 200 m depth) DOC contents show significant variations and the highest value, up to around 35 mg/L (2.92 mM), is observed in a brackish marine groundwater. Deeper down (below 200 m depth), DOC values are between 1 and 5 mg/L (0.08–0.42 mM) except for a few exceptions with higher values (around 12 mg/L ≈ 1.0 mM)) in some brackish non marine to saline groundwaters (Figure 8-1a). A similar behaviour is found at the Laxemar and Äspo areas with the highest values, up to around 20 mg/L (1.67 mM) and 26 mg/L (2.17 mM), respectively in mixed brackish type groundwaters (Figure 8-1b).

DOC values at depth are expected to be low and the reason for these slightly increased values (also found in Laxemar) or the high values found in the brackish-marine groundwaters is not clearly known. Contamination during drilling/sampling, new routines for cleaning the equipment, natural sources such as asphaltite or autotrophic metabolisms, Littorina Sea influences, etc. have been discussed. It is hoped that additional data from the monitoring program will clarify the long term behaviour of DOC /Laaaksoharju et al. 2009/.
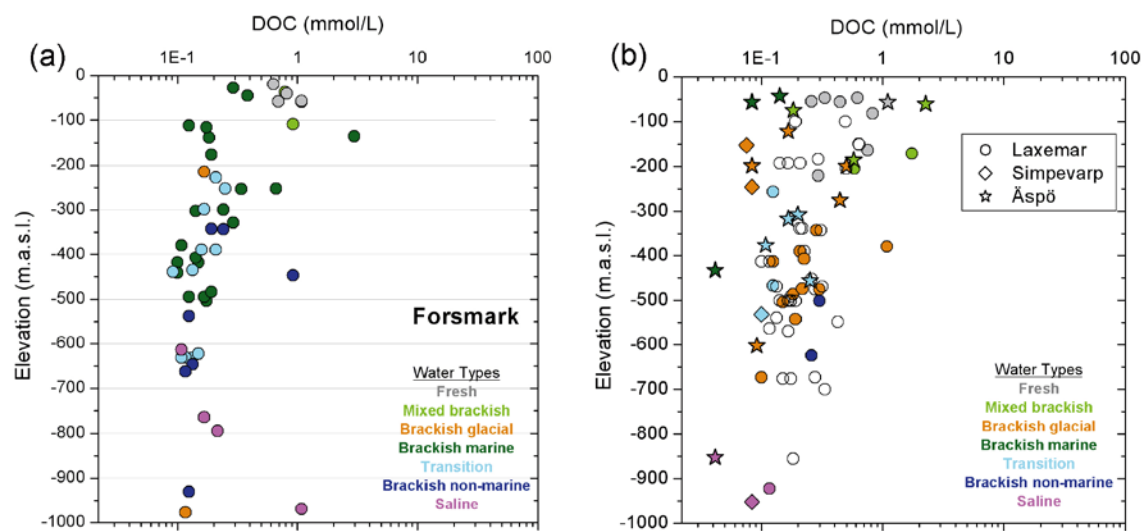
Figure 8-1. Depth distribution of dissolved organic carbon (DOC) in the Forsmak (a) and Laxemar-Simpevarp-Äspö (b) areas. Samples are coloured by water type as indicated in the legends /Laaksoharju et al. 2008, 2009/. Open symbols in the Laxemar-Simpevarp plot corresponds to samples for which a water type has not been defined.

8.2.2 Estimated values over time

The excavation and operation phases (Open repository)

Decomposition of organic materials (including microbial biofilms, tobacco, plastics, cellulose, hydraulic oil, surfactants and cement additives) may increase DOC contents promoting an increase in microbial activity. This effect could in turn enhance the reducing capacity of the repository near-field and contribute to a quick consumption of any oxygen left in the repository. However, it may also favour an increase in the activity of SRB and thus in dissolved sulphide contents after closure.

An inventory of organic materials and an assessment of their impact on microbial processes were prepared by /Hallbeck et al. 2006/ for SR-Can and more recently by /Hallbeck 2010/ for SR-Site. In this last work, three main pools of organic material in the repository have been identified. The largest pool is the organic material in bentonite although it may be questionable whether this material is available for degradation /Hallbeck 2010/; the second largest pool are the biofilms formed on rock surfaces, while the third main pool is the organic material that can be produced by microorganisms with hydrogen from anaerobic corrosion of iron in steal as energy source /Hallbeck 2010, SKB 2010/.

If all the estimated organic carbon in the deposition tunnels would dissolve in their pore space it would result in a DOC concentration as high as 0.45 M. However, if the amount of organic carbon with the bentonite is excluded (assuming that it is insoluble) the DOC concentration would be around 1.2 mM. From the calculations performed by /Hallbeck 2010/, maximum concentrations around 0.36 mM of DOC (only from hydrogen produced during the anaerobic corrosion of steel and from biofilms) can be deduced for the deposition tunnels and other areas at the repository in Forsmark. Thus, these are highly uncertain values that strongly depend on the assumptions and simplifications considered in the calculations.

Moreover, the degradation rate of organic materials, especially man-made materials, is still poorly known. Some of the problems related to degradation of man-made materials can be exemplified by the results obtained in the REX project. In the supporting laboratory experiment of that project (the replica experiment; /Trotignon et al. 2002/), waters with dissolved oxygen were injected periodically (pulses) during 1 year in a core Section extracted from the REX borehole. The return from oxic to reducing conditions was monitored between each series of pulses, including chemical (e.g. DOC, TOC, dissolved sulphide and acetate) and microbiological analysis of waters. Also, biofilm investigations were performed on solid surface samples collected at the end of the experiment, both from the core and from the experimental setup (resins, PETP – polyethylenterephthalate- cap, O-ring, etc).

An artefact, associated to an unexpected carbon source supplied by the experimental setup, was discovered. DOC and TOC concentrations in solution reached more than 40 mM during the anoxic periods. Some of the main organic contributors to the bulk DOC and TOC were identified to proceed from the PETP cap and the epoxy resin used to seal the cylindrical part of the core. Biofilm investigations confirmed this finding: fermentative anaerobes were present mostly on the sealing epoxy resin; aerobes and IRB were present at significant levels both on plastic surfaces and on the core.

Organic carbon concentration increased in solution from the first to the last pulses (from 0.1 to 46 mM) and because of this extra carbon source, "explosive" heterotrophic (iron reduction bacteria) and fermentative bacteria development was favoured in this experiment. However, the concentration of preferred bacterial substrates such as acetate remained low (below 70 μM; see Section 8.3.1) suggesting that organics released by the resin or PETP cap are slow to transform into easily assimilated molecules at the temporal scale of the experiment (one year; /Trotignon et al. 2002/.

The conditions and scale of the replica experiment are not equivalents to those of the repository after closure. However, it would indicate that high DOC contents may develop locally from degradation of some artificial materials, clearly enhancing microbiological activities although the bulk amounts of DOC were not totally bioavailable.

Thus, all the estimations on the DOC contents in this stage must be taken cautiously as important uncertainties remain in the degradation rate of organic materials but also in the biodegradability of the organic matter in the bentonite.

Temperate period

The performed simulations indicate that dilute waters will reach greater depths, mainly at the end of the temperate period and, thus, an increment in the DOC contents would also be expected. In Forsmark present fresh and shallow (< 100 m) groundwaters have DOC concentrations around 10–15 mg/L (0.83–1.25 mM; Figure 8-1a). In Laxemar, which is more active hydraulically and where fresh groundwaters reach presently higher depths, DOC contents are lower (0.25–0.83 mM; Figure 8-1b).

DOC contents are expected to decrease during infiltration due to microbial activity. Moreover, DOC at deeper levels is a less suitable substrate for microbial use because it has been exposed to microbial degradation at shallower depths /Kotelnikova 2002/ reducing the metabolic suitable part of DOC (e.g. short-chain organic molecules like acetate; see Section 8.3). Thus, neither the amounts of "superficial" DOC reaching the repository level during the temperate period nor the effect of a potential increase in DOC at this depth on microbial activity are clear. A conservative estimation may be a DOC concentration of about 10–15 mg/L (0.83–1.25 mM) from the present fresh and shallow groundwaters at Forsmark.

Glacial period

During this period the input of organic carbon with the recharging groundwater is expected to be low, because photosynthetic production of organic carbon will cease. Measured values of DOC in several glacier ice samples range from 0.06 to 46.6 ppb ($5 \cdot 10^{-6}$ to $3.9 \cdot 10^{-3}$ mM; /Barker et al. 2006/). Thus, it is not expected in this period an increase in the microbial degradation of organic matter promoted by this "external" input (microbial activity will be sustained mainly by autotrophic metabolisms). A conservative estimation may be a DOC content of 0.5 mg/L (0.042 mM) for this period.

Submerged period

In periods where seawater covers the repository site, larger amounts of organic matter (and sulphate) would be expected in the marine recharge groundwaters, enhancing microbial activity (e.g. Fe (III) reduction, sulphate reduction) at shallower levels (sediments). However, the efficiency of DOC at deeper levels would diminish because, as stated above, DOC is a less suitable substrate for microbial utilisation the further from the surface.

Presently, some of the groundwaters at the sites with a high old-marine Littorina contribution have the highest DOC concentrations (up to 2.92 mM; Figure 8-1). However, other groundwaters with similar characters have very low DOC contents. As stated above, the origin of these high values is not known and more data are needed to clarify the long term behaviour of DOC /Laaaksoharju et al. 2009/. Therefore, there are not clear limits to the amount of bulk DOC that eventually could reach the repository depth although some estimate on the amount of suitable DOC for metabolic activities (e.g. acetate) can be made (see Section 8.3.2). This estimate suggests that the input of marine waters do not provide an important source of carbon additional to the already present at repository depth.

8.3 Acetate

8.3.1 Overview/general description

Acetate, as well as molecular H_2 and other simple organic molecules, are continuously produced by fermentative bacteria from complex organic compounds during the degradation sequence of organic matter. It is also produced by autotrophic acetogens using hydrogen as electron donor (reduction of CO_2 via the acetyl-CoA pathway; e.g. /Drake et al. 2006a, Konhauser 2007/. The produced acetate serves as an important substrate for a variety of microorganisms, including sulphate reducing bacteria and, thereby, it may contribute to the amount of produced sulphide. Moreover, acetate contents may contribute, as one of the involved factors (oxidising agent), to stress corrosion cracking (SSC) of the copper canister (see Section 5.3).

Acetate is one of the components included in the bulk DOC concentration. But, unfortunately, acetate contents in the groundwaters were not determined during the site characterization programs in Sweden (or Finland) and, as far as the authors know, there are no available data on acetate contents in other crystalline systems. However, some analytical data are available from the sulphide

monitoring program under progress at Laxemar and Äspö; also, some additional information can be obtained from the replica experiment in the REX project /Trotignon et al. 2002/ and from the MICROBE experiment at Äspö /Hallbeck and Pedersen 2008c/.

As there are no published works on the behaviour of acetate in crystalline systems, the scarce available information will be analysed below in the context defined by the state of the art in other low temperature natural systems.

In natural low-temperature and reducing water systems, both biogenic H_2 (Section 8.5) and acetate are key intermediate metabolites for different dissimilatory metabolic pathways. Thus, they have rather short turnover times (minutes to hours; Konhauser, 2007) which translates in to the existence of low concentrations in waters from sediments and superficial aquifers. H_2 concentrations are measured in nmols/L (Section 8.5.1) while acetate concentrations are in the micromolar range (usually tenths of micromoles, reaching occasionally several hundreds of µmoles/L; /Wellsbury and Parkes 1995, King 1991, Hansen et al. 2001, Koizumi et al. 2004, Konhauser 2007, Jakobsen and Cold 2007, Heuer et al. 2009/.

Higher acetate concentrations may locally appear in low temperature systems where changes (e.g. seasonal) in the microbial population occur (e.g. /Hoehler et al. 1999/). They are promoted by the transient decoupling of acetate production (by fermentative bacteria) and consumption (by heterotrophic metabolisms) but these effects are of short duration (months).

In the *sulphide monitoring program* the highest values of acetate were measured in KLX06 borehole: samples KLX06-1 and KLX06-2-1 with 13.7 mg/L (232.2 µM) and 40.6 mg/L (688 µM), respectively (Figure 8-2), but they correspond to standpipe and tube samples. The representative groundwater samples have acetate concentrations below 13.7 mg/L ($\approx$ 232.2 µM). Acetate appears to be a minor constituent of bulk DOC in the studied groundwaters, usually contributing less than 10%.

Under *in situ* laboratory conditions *in the MICROBE experiment* quantitative information on acetate contents and production rate have also been obtained. A circulation system connected to a conductive fracture was installed at a depth of 447 m. In this system groundwater is pumped from the fracture through flow cells and then back to the fracture again while being maintained under *in situ* conditions. Acetate determinations were performed in a closed mode, where the connection to the aquifer was blocked but pressure was maintained and groundwater was re-circulated through the flow cells in the system.
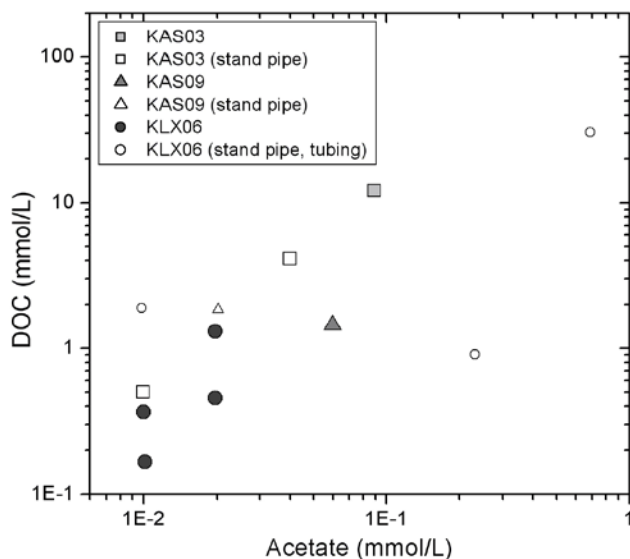
Figure 8-2. DOC versus acetate contents measured during the on going monitoring program in groundwaters from KLX06 (Laxemar) and KAS03, and 09 (Äspö) boreholes in the Laxemar and Äspö zones. Samples with open symbols correspond to standpipe and tubing samples and, therefore, they are not representative from the natural groundwaters.

The concentration of acetate (and also the dissolved sulphide) increased from 2.3 to 14.9 mg/L (39 to 252 μM) in approximately 60 days, when it ceased at the same time as the most probable numbers of both sulphate reducing bacteria and autotrophic acetogens started to decrease. The increments of sulphide and acetate would correspond to production rates of approximately 0.08 mg sulphide L^{-1} day^{-1} (2.5 μmol L^{-1} day^{-1}) and 0.14 mg acetate L^{-1} day^{-1} (2.37 μmol L^{-1} day^{-1}).

The acetate production rates found in the experiment were large relative to the concentrations of acetate found in the monitored sections from Laxemar and Äspö or to the DOC found in the analysed groundwaters from the potential repository sites (Figure 8-1). Assuming these production rates it would only take 40 days and three months to reach, respectively, the highest acetate and DOC concentrations found in the studied systems. However, the available data indicate that a very large increase of acetate in the analysed groundwaters, promoted by such production rate, is not observed. This fact would suggest that acetate is consumed by heterotrophic microorganisms at approximately the same rate as it is produced in these crystalline environments /Hallbeck and Pedersen 2008c/, in agreement with what has been observed in other natural systems.

In the supporting laboratory experiment of **the REX project** (the replica experiment; /Trotignon et al. 2002/, waters with dissolved oxygen were injected periodically (pulses) in a core Section extracted from the REX borehole. The return from oxic to reducing conditions was monitored between each series of pulses, including chemical (e.g. dissolved sulphide and acetate) and microbiological analysis.

During the anoxic periods between oxygen pulses fermentative anaerobes increased, strongly favoured by an extra carbon source supplied by the experimental setup (resins, polyethylenterephthalate, etc). This increment in the amount of fermentative bacteria could represent a source of additional acetate. However, acetate concentrations remained at low levels, always below 70 μM, during the experiment. The increase in the fermentative activity agreed with the explosive development of iron reduction bacteria (IRB) which would consume the additional acetate, lowering the concentration at the observed low levels.

All these observations indicate that acetate contents and limiting factors are common to all low temperature natural systems. The acetate pool would be controlled by a balance of acetate producing and consuming processes: acetate production by fermentation of organic matter or by autotrophic acetogens and acetate consumption by heterotrophic metabolisms (e.g. sulphate reducing bacteria or acetoclastic methanogens).

Microbiological analysis performed at Forsmark and Laxemar suggest the existence of the same sources and sinks. Acetogens, both autotrophic and fermentative-heterotrophic, were the dominant microorganisms in the studied sections (there are often one or two orders of magnitude more acetogens than the second most common organism type; /Hallbeck and Pedersen 2008a, b/. A wide variety of heterotrophic, acetate consuming metabolisms has also been detected and, therefore, acetate concentration in groundwaters is expected to remain low, in the micromolar range.

In summary, as acetate is one of the most microbially used organic molecules, increments in acetate production should be compensated by a parallel increase in its consumption by heterotrophic metabolims, especially in the low-nutrient conditions of groundwaters in crystalline systems. Acetate accumulation could arise from decreasing rates of acetate consumption but, as stated above, this situation appears to be very transient (months) in low temperature environments. Finally, the possible increments in the acetate production rate (by fermentative processes) and its reflection in an enhanced sulphate-reducing activity must be assessed in a generic way considering the present state of knowledge. The easiest way is considering the supply of complex organic components as basic constituents of the organic matter degradation chain, able to induce an increase in the fermentative activity and, subsequently, in the sulphate-reducing activity. Therefore, the analysis presented below has a clear parallelism with that performed for DOC in Section 8.2.

8.3.2   Estimated values over time

The excavation and operation phases

Important changes in the microbial communities are expected during this stage, with extensive microbial activity promoted by the large amounts of organic materials found at or near the repository and the variable environmental conditions associated with oxygen intrusion, mixing of oxidising and reducing waters, etc.

After closure, degradation of organic materials could contribute to quick consumption of oxygen left in the repository but also to higher rates of acetate production that may induce higher rates of sulphide production in the vicinity of the deposition holes. Moreover, the anaerobic corrosion of steel could contribute indirectly to the pool of organic material in the repository. The hydrogen produced in the corrosion process may act as an energy source for various microbial processes, including acetogens. These microorganisms would increase the amounts of acetate that, in turns, would increase SRB activity.

In the inventory of organic materials prepared by /Hallbeck et al. 2006/ for SR-Can, net acetate concentrations of 32–36 μM from fermentation of carbohydrates and biofilms were obtained for deposition tunnels and other cavities in the repository. From the mass balance calculations presented by /Hallbeck 2010/ for SR-Site, concentrations of around 200 μM of acetate (contributed by biofilms and in a less extend by hydrogen produced in the anaerobic corrosion of steel) can be deduced.

Acetate may be used by SRB, increasing the amounts of dissolved sulphides. The reaction involving acetate and dissolved sulphide is equimolar with respect to both components (see reaction 6); thus, from the above estimations of 0.2 mM for acetate, similar amounts of sulphide should be produced (around 6.5 mg/L or 0.2 mM of dissolved sulphide; /Hallbeck 2010/.

Some of the sulphide could diffuse to the canister where corrosion would take place. But, it must be taken into account that these values are overall and non time-average values expressed in a per litre basis that must be relaxed during the evolution of the Excavation/Operation period and, probably, during the temperate period as well. Moreover, not all the acetate will be used by SRB as other, more energetically favoured metabolisms will have used part of this organic carbon previously. Furthermore, most of the sulphide produced will either react with Fe(II) in the groundwater or with the corrosion products, or will diffuse away from the canister and, therefore, this sulphide would have a negligible impact on the copper casing of the canisters.

However, the acetate and sulphide values are largely uncertain /Hallbeck 2010/ and, also, they are based only in a part of the bulk organic pool in the repository (i.e. excluding the organic matter in bentonite; see Section 8.2.2).

In any case, the maximum concentrations of acetate allowed by the balance between microbial producing and consuming processes at any time would be in in the micromolar range. Immediately after repository closure, microbial activity will continue at a high rate due to the high temperature and, therefore, some transient increments in the acetate concentrations would be expected (e.g. in the millimolar range). However, once the repository has cooled down, microbial processes rates will go down and a decrease of the acetate concentrations at "normal" levels in low temperature systems (micromolar range) is expected.

Temperate Period

The performed simulations (Section 6.1) indicate that dilute waters will reach greater depths than today (mainly at the end of the temperate period) and thus an increment in bulk DOC contents would be expected. Present fresh and shallow (< 100 m) groundwaters in Forsmark have concentrations of about 10–15 mg/L (0.83–1.25 mM; Figure 8-1a). In Laxemar, more hydraulically active and with fresh groundwaters reaching greater depths, DOC contents are lower (0.25–0.83 mM; Figure 8-1b).

DOC contents are expected to decrease during infiltration due to microbiological activity. Moreover, this activity will decrease the proportions of the adequate substrates (simple organic molecules like acetate) included in the bulk DOC (as observed in the present analysed groundwaters; Figure 8-2) and therefore, the DOC reaching deeper levels will be a less suitable substrate for microbial use.

The amount of acetate reaching the repository level during the temperate period is not known but it is expected to be in the micromolar range (as most of the low temperature aquatic systems) which will not represent an important additional source for heterotrophic metabolisms such as sulphate reduction.

Glacial Period

During this period, due to the suspension of photosynthetic production of organic carbon, the input of organic carbon and acetate with recharging groundwater is expected to be low. Therefore, an increment in the microbial degradation of organic matter promoted by this "external" input over the Glacial period

is not anticipated, and microbial activity will be mainly sustained by autotrophic metabolisms. Thus, micromolar concentrations of acetate would be also expected from the relationship between acetate production (by fermentative or autotrophic metabolisms) and consumption (by heterotrophic metabolisms).

Submerged Period

It is expected that the infiltrating recharge waters through marine sediments will follow the known degradation sequence of organic matter controlled by microbiological processes and, thus, with acetate concentrations in the micromolar range.

8.4   Methane

8.4.1   Overview/general description

Methane may be generated both by organic processes (methanogenic microorganisms) and inorganic processes at depth in crystalline systems /Pitkänen and Partamies 2007, Hallbeck and Pedersen 2008a, b/ and references therein. Inorganic methane may come from this deep source and move slowly by diffusion towards the surface, mixing with methane from biogenic origin if present. This possible dual origin makes the prediction of methane contents in a specific period very difficult.

Methane is a chemically active gas that may participate or control the redox state of the groundwater system at different depths, under different conditions and with variable rates or intensities depending on its origin. Also, the oxidation of methane may contribute to oxygen reduction in oxygen intrusion evolutions /Puigdomenech 2001/ and it is a substrate for different metabolic activities. It may be used, for example, by methanotrophs under oxic conditions but it can participate as well in a special type of microbial sulphate reduction coupled to CH_4 oxidation in anaerobic conditions /Kotelnikova, 2002, Pitkänen et al. 2004/, increasing dissolved sulphide contents.

Methane contents are very low in the Forsmark area. They are always below $5.5 \cdot 10^{-3}$ mM except in the case of KFM01D borehole at 445 m depth where a value as high as 4.2 ml/L (0.2 mM) was measured (Figure 8-3a), without any evident correlation with depth or with the presence of methanogens (barely present in this area, usually below 10 cell/mL; /Hallbeck and Pedersen 2008a/. A similar situation can be observed for methane in the Laxemar-Simpevarp area (Figure 8-3b; /Hallbeck and Pedersen 2008b/) with the highest value of methane below $4 \cdot 10^{-2}$ mM.

These observations contrast with those from other systems like Olkiluoto where methane contents (and also the total amount of dissolved gases) are much higher. This is especially clear for most saline and deepest Olkiluoto groundwaters, where methane is the most abundant gas /Pitkänen and Partamies 2007/ and its concentrations clearly increase with depth from around 0.1 ml/L ($4.5 \cdot 10^{-3}$ mM) in the near-surface groundwaters to around 1,000 ml/L ($44.6 \cdot 10^{-3}$ mM) at 750 m depth (Figure 3c). However, the amounts of methanogens in the Olkiluoto groundwaters were usually at or below the detection limits due to unclear causes (see the discussion by /Pedersen 2008/, pp 102–103).

The available data for the Forsmark area indicate that methane originates mostly from an inorganic source. The sample with the highest proportion of biogenic methane corresponds to KFM01D borehole at 445 m depth, in the Section with the highest volume of methane measured in that area (Figure 8-3a; /Hallbeck and Pedersen 2008a/). Also, a dominant inorganic source has been proposed for Laxemar /Hallbeck and Pedersen 2008b/. In Olkiluoto, isotopic data have allowed a more precise determination on the origin and distribution of methane. This gas seems to have two primary sources: a thermal origin from inorganic hydrocarbons, predominant in the deepest groundwaters, and a bacterial origin, steadily increasing in importance towards the shallowest and CH_4-poor parts of the system /Pitkänen and Partamies 2007/.

Therefore, methane from biogenic and abiogenic sources is present and "mixed" in the Forsmark, Laxemar and Olkiluoto groundwaters. However, the sparseness of data for the examined rock volume in Forsmark and Laxemar prevent from observing any clear trend. All these circumstances highlight the need for more data in order to clarify its origin and distribution in the studied systems and to fill these important gaps in the overall understanding of the redox processes. On top of that, methodological improvements in the sampling procedures are also badly needed /Hallbeck and Pedersen 2008a, b/.
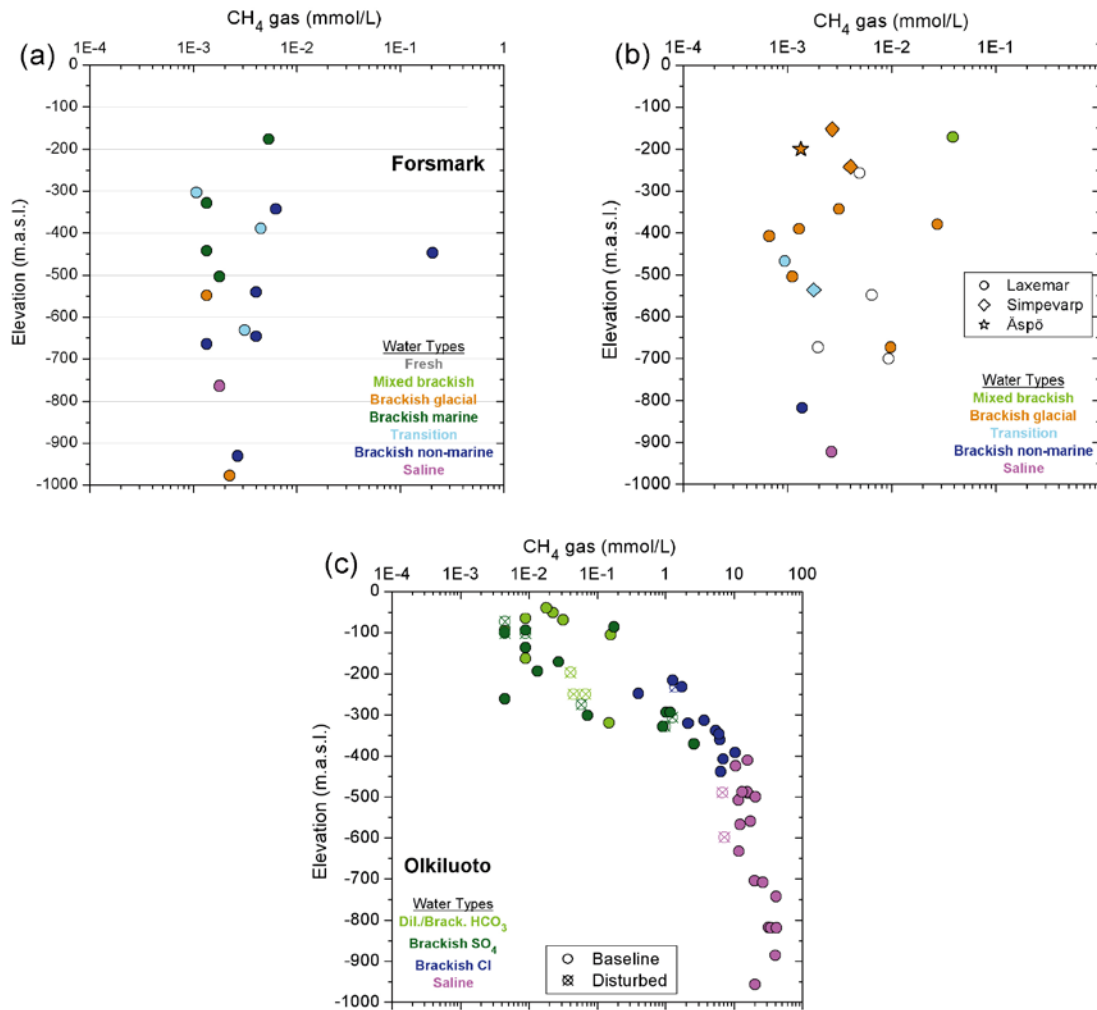
Figure 8-3. *Depth distributions of methane in Forsmark (a), Laxemar(b) and Olkiluoto(c) groundwaters.*

8.4.2 Estimated values over time

Excavation and operational phases

Decomposition of organic materials accumulated in the repository will increase microbial activity. Methanogenesis is usually the last metabolic step in the degradation sequence of organic matter and could probably be an effective process during this period. Acetoclastic methanogens disproportionate acetate to form methane and CO_2:

$$CH_3COOH \rightarrow CH_4 + CO_2 \hspace{2cm} \text{(Equation 8-1)}$$

Also, autotrophic (hydrogenotrophic) methanogens may use H_2 and CO_2:

$$CO_2 + 4H_2 \rightarrow CH_4 + 2H_2O \hspace{2cm} \text{(Equation 8-2)}$$

The intensity of these processes and the amounts of methane generated are unclear. Some rough estimations can be made from the net amount of acetate (see Section 8.3.2) or hydrogen (from corrosion; see Section 8.5.2) produced in the repository. Thus, through Equation 8-1, a concentration of methane of around 200 μM can be obtained; and through Equation 8-2, the calculated concentration of methane is 27 μM.

The concentration of methane is of importance as a nutrient source for microbially mediated sulphate reduction to sulphide:

$$SO_4^{2-} + CH_4 \rightarrow HS^- + HCO_3^- + H_2O \hspace{2cm} \text{(Equation 8-3)}$$

and from the above estimations, a net value of around 7.0 mg/L (0.21 mM) of dissolved sulphide can be obtained. This estimation may be extremely conservative because not all the acetate or hydrogen will be used by the SRB as other more energetically favoured metabolisms will have used part of these components previously. Moreover, most of the sulphide produced will either react with Fe(II) in the groundwater or in the corrosion products, or diffuse away from the canister, drastically diminishing its impact on the copper casing of the canisters. However, these values are derived from mass balance results largely uncertain /Hallbeck 2010/ based on the inventory of organic materials in the repository (see Section 8.2.2 and Section 8.3.2)

Temperate Period

The performed simulations (Section 6.1) indicate that dilute waters will reach deeper depths than today, mainly at the end of the temperate period. Unfortunately, there are no data on CH_4 contents of fresh groundwaters in the Swedish sites that could serve as reference for this dilution evolution. At Olkiluoto, the maximum CH_4 content in dilute, shallow groundwaters is around 0.2 mM (Figure 8-3c).

Assuming that the concentration of dissolved natural gases remains substantially the same as those before repository construction /SKB 2010/, a mean value of $1.55 \cdot 10^{-2}$ mM can be obtained from the present groundwaters (Table 2) with a maximum value (in the sample with high biogenic contribution in KFM01D; see above) of 0.2 mM, very similar to the values from Olkiluoto. This maximum value can be used tentatively as a reference value for this period.

If the maximum contents of methane in the Forsmark groundwaters were quantitatively used by microbes in sulphate reduction (assuming that CH_4 contents are not replenished), the sulphide concentration would increase at up to 0.2 mM (6.4 mg/L) according to Equation 8-3.

Glacial Period

During permafrost, the perennial freezing of rock volumes will effectively shut down the hydraulic circulation in the bedrock, at least locally. In this way, microbial populations could be isolated from the surface, with negligible inflow of organic matter; also, methane gas can be trapped as clathrate hydrates. Under these conditions, the intensity of sulphide production due to microbially mediated SO_4^{2-} reduction will probably decrease. However, sulphide production could be sustained by methane and hydrogen (e.g. through Equation 8-3 and Equation 8-4) depending on the balance between 1) the production and flow of CH_4 and H_2 from the deep bedrock and from biogenic origin, 2) the impervious frozen layers at the top of the site, and 3) the incorporation of CH_4 in the ice as clathrates. If clathrate formation occurs, the dissociation of these compounds to release methane during permafrost decay would add to the nutrient sources for microbial populations in the bedrock at the end of the Glacial period (see, for example, the discussion in /SKB 2006b, 2010/). Taking into account all these processes and feedbacks, any estimation of the concentration of methane is difficult, if not impossible.

Under glacial conditions, the presence of significant amounts of CH_4 and H_2 may have a positive effect on the chemical stability of the groundwaters by contributing to the consumption of the oxygen potentially capable of reaching the repository. It may be envisaged that methane and hydrogen dissolved in deep groundwaters (or the up-welling of methane and hydrogen from deep crustal layers) can be used by microbes to consume the oxygen infiltrated from the surface. During the Matrix experiments at Äspö, it was observed that the rock matrix contains methane and other dissolved gases in concentrations similar to those found in groundwater. Consequently, if methane is consumed or flushed out from the fractures of an aquifer, it will diffuse from the rock matrix into the fractures and the process can continue. As the volume of water in the rock matrix porosity is larger than the volume of groundwater in the fractures, this process could continue throughout a glaciation cycle. This aspect merits further studies as CH_4 and H_2 can also have a negative effect, enhancing sulphate reduction.

In conclusion, there are not enough data at present to quantify the concentration of CH_4 and H_2 during this period. Not having better options, the maximum concentrations of hydrogen and methane detected presently in the Forsmark groundwaters could be used tentatively as recommended values for this glacial period.

Submerged Period

During the submerged period marine waters will recharge the aquifer system infiltrating through the sediments and at the same time advancing in the redox sequence, including methanogenesis. In other words, the infiltration of marine water would incorporate exclusively biogenic methane into the system. However this conclusion cannot be confirmed by the analysis of groundwaters with a Littorina signature (as it was performed for ammonium in Section 8.6.2) as they do not have higher methane contents. This can be due to the fact that not all the methane produced in the marine sediments diffuses downwards: some of it can go upwards decreasing the level in the infiltrating groundwaters. Additionally, methane can also disappear (e.g. consumed) during infiltration of marine waters in the bedrock. In any case, the maximum value of methane in the groundwaters at present (0.2 mM) can be used as a reference value for this period.

8.5 Molecular Hydrogen

8.5.1 Overview/general description

Molecular hydrogen, like methane, can be generated by biological and inorganic processes at depth in crystalline systems. In the degradation sequence of organic matter, biogenic molecular H_2 and simple organic molecules (e.g. acetate, Section 8.3) are continuously produced by fermentative bacteria and heterotrophic acetogens from complex organic compounds. In turn, the produced H_2 (or acetate) is quickly metabolised by other microorganisms (e.g. turnover times from minutes to hours; /Konhauser 2007/ using different terminal electron acceptors (TEAs) and lowering hydrogen concentrations to values below 50 nM /Lovley and Goodwin 1988, Hoehler et al. 1998, Christensen et al. 2000, Lin et al. 2005/ or to values below 150 nM if acetogenesis is involved /Hoehler et al. 1998, Heimann et al. 2010/.

This behaviour is the consequence of the strong coupling of hydrogen to a very broad spectrum of interrelated microbial activities. Hydrogen is an excellent electron donor for a large number of microbial metabolisms, including methanogenesis, acetogenesis, sulphate reduction, iron reduction, and manganese reduction, among others /Postma and Jakobsen 1996, Hoehler et al. 1998, Christensen et al. 2000, Appelo and Postma 2005/. However, the existence of an additional, inorganic source for H_2 (at least, six different inorganic processes may produce abiogenic H_2; e.g. /Hallbeck and Pedersen 2008a, b/ makes this analysis considerably more difficult. It may increase the intensity and diversity of the aforementioned heterotrophic metabolisms and it may be metabolised by autotrophic methanogens and, especially, acetogens, to create a background level of suitable organic carbon, such as acetate, in crystalline groundwater systems /Pedersen 2001, Lin et al. 2005/. Since the produced acetate can be used by different heterotrophic organisms, it could increase the overall metabolic intensity, including sulphate reduction.

High hydrogen concentrations may favour high metabolic intensities and, even, diversities (indirectly, through acetate production by acetogens or, directly, as electron donor for a wide number of metabolic activities). The net effects of all these linked processes will depend, in the last term, on the inflow and consumption rate of hydrogen (for example, radiolysis can produce millimolar concentrations of H_2 for every million years of subsurface isolation if there is no H_2 consumption; /Lin et al. 2005/.

Thus, abiogenic and biogenic sources of hydrogen in the studied systems are of major concern because hydrogen concentrations may be determined by (and may determine) most of the proposed microbiological metabolic activities in the groundwaters. Hydrogen may not only couple oxidative and reductive processes, but also regulate the flow of carbon and electrons in virtually every step in the breakdown of organic matter /Hoehler et al. 1998/ and of the overall food chain emanated from the "Deep Biosphere" concept /Pedersen 1993, 1997a, b/. For further discussion, see /Gimeno et al. 2009/.

The available data on hydrogen contents in the Forsmark area are very scarce. From the sixteen analysed samples only six have values above the detection limit, in the range 0.24–19.2 μM, with maximum values between 300 and 500 m depth (Figure 8-4a). These maximum values are slightly higher than those found in the Laxemar area (Figure 8-4b). At Olkiluoto, the latest data presented by /Pedersen 2008/ show a rough increase of hydrogen with depth, reaching maximum values of around 3.5 μM at the maximum sampled depth (742 m). Much higher contents were found at higher depths by /Pitkänen and Partamies 2007/, with concentrations from 300 to 1,000 μM in 800–1,000 m depth interval (Figure 8-4c).
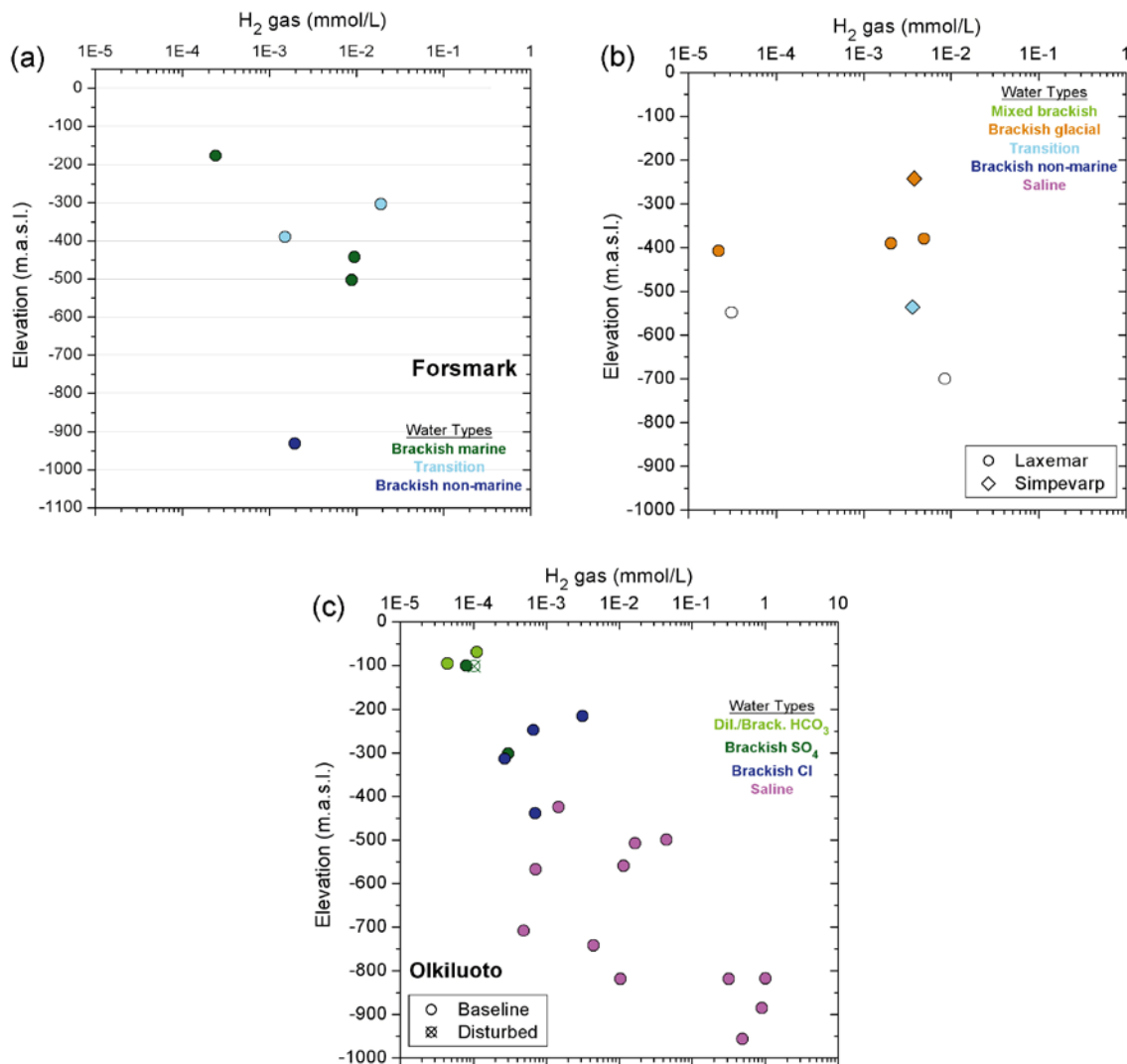
Figure 8-4. *Depth distributions of hydrogen in Forsmark (a), Laxemar (b) and Olkiluoto(c) groundwaters.*

Overall, the maximum detected amounts of hydrogen in the Forsmark area (and also in Laxemar) are lower than at Olkiluoto (in the milimolar range, similar to other groundwaters in crystalline systems; /Lin et al. 2005, Sherwood Lollar et al. 2007/ but they are several orders of magnitude higher than the maximum values (from biogenic origin) found in marine sediments, soils or shallow aquifers (with maximum values around 50–150 nM; /Lovley and Goodwin 1988, Hoehler et al. 1998, Christensen et al. 2000, Lin et al. 2005/. The heterogeneity and variability in the distribution of hydrogen contents in the compared systems is still not well understood.

8.5.2 Estimated values over time

The excavation and operation phases

During excavation and operation, a large pool of organic material will be introduced as structural and stray material promoting an overall increase in the microbial activity. Fermentative metabolisms would increase the amounts of hydrogen and other simple organic molecules that, in turn, would enhance other types of metabolisms, including sulphate reduction. The interplay between sources and sinks would probably maintain low hydrogen contents (below 150 nM) though an increment in sulphate reduction activity and thus in the amount of dissolved sulphide is also possible. However, it is considered that fermentative processes cannot produce high concentrations of hydrogen /SKB 2010/.

In addition, corrosion processes may also represent an additional source of hydrogen that may increase SRB activity, either directly through the reaction

$$SO_4^{2-} + 4H_2 + H^+ \rightarrow HS^- + 4H_2O \hspace{4cm} \text{(Equation 8-4)}$$

or indirectly through the acetate produced by autotrophic acetogens using hydrogen as electron donor:

$$4H_2 + 2CO_2 \rightarrow CH_3COO^- + H^+ + 2H_2O \hspace{3cm} \text{(Equation 8-5)}$$

followed by

$$CH_3COO^- + SO_4^{2-} \rightarrow HS^- + 2HCO_3^- \hspace{3.5cm} \text{(Equation 8-6)}$$

From the calculations performed by /Hallbeck 2010/, this source of hydrogen could rise net values to $1.6 \cdot 10^{-2}$ and $2.7 \cdot 10^{-2}$ mM in the deposition tunnels from Forsmark and Laxemar, respectively, assuming 100% of iron corrosion.

The estimated amounts of hydrogen-mediated dissolved sulphide in the repository (via reactions 9-4 to 9-6) are very low, between 0.13 and 0.22 mg/L ($4.06 \cdot 10^{-3}$ and $6.9 \cdot 10^{-3}$ mM), compared to those previously estimated from other organic sources like organic material in biofilms (around 6.4 mg/L $\approx$ 0.2 mM of dissolve sulphide; see Section 8.2.2).

For acetate, these values are "cumulated" and non time-average values expressed in a per litre basis that must be relaxed during the evolution of the Excavation/Operation period. The maximum concentrations of hydrogen allowed by the balance between microbial producing and consuming processes at any time would be in the nanomolar range.

Temperate Period

For this period, concentrations of dissolved natural gases (including hydrogen) are expected to remain the same as before repository construction /SKB 2010/. Thus, from present Forsmark groundwater data, mean and maximum values of $3.37 \cdot 10^{-3}$ mM. and $1.92 \cdot 10^{-2}$ mM can be given for hydrogen.

As Equations 8-4 to 8-6 suggest, hydrogen is an important source of nutrients for the microbially-mediated reduction of sulphate to sulphide. If the maximum values of hydrogen were quantitatively used by microbes in sulphate reduction, the amount of sulphide would increase at most by $10^{-5.6}$ M (0.08 mg/L of dissolved sulphide assuming that H_2 is not replenished). If the maximum hydrogen concentrations found in Olkiluoto are considered in the predictive calculations, the amount of dissolved sulphide would be higher, $10^{-3.6}$ M (8 mg/L). However, such a high hydrogen content has not been found at repository levels in any of the studied systems.

Glacial Period

Methane and hydrogen have been treated together in Section 8.4.2 (Glacial period of methane) and their behaviour can be considered parallel, except for clathrates.

Submerged Period

It is expected that infiltrating recharge waters through marine sediments follows the known degradation sequence of organic matter controlled by microbiological processes and, thus, with hydrogen concentrations below 150 nM (see above). In that case, the concetration of hydrogen at repository depth during this period would depend on abiotic sources, still poorly known. Not having better options, the maximum concentration of hydrogen detected presently in the Forsmark groundwaters ($1.92 \cdot 10^{-2}$ mM) could be used tentatively as recommended values.

8.6 Nitrite and Ammonia

8.6.1 Overview/general description

As it has been stated in the Introduction, nitrite and ammonia may contribute, as oxidising agents, to stress corrosion cracking (SSC) of the copper canister. Whereas nitrite is often found in natural aquatic systems at trace levels, ammonia (NH_3) is only stable in alkaline (pH>9) and very reducing conditions (close to the stability boundary for water; /Kehew 2001, Appelo and Postma 2005/). Thus, it is not expected to find significant amounts of ammonia during the evolution of the sites. In this Section the possible evolution of nitrate, nitrite and ammonium is evaluated.

In natural waters nitrogen occurs in various oxidation states from N(+V) to N(-III) and the transformation between them is almost exclusively facilitated by microorganisms /Kehew 2001/. Organic nitrogen is converted to ammonium (ammonification) and, under oxidizing conditions, ammonium is oxidised to nitrite (NO_2^-) or further oxidised to nitrate (NO_3^-) by specialised nitrifying bacteria (two-step nitrification).

Under anaerobic conditions, nitrate is the most thermodynamically favoured electron acceptor for the oxidation of organic substrates and it is used by nitrate reducing bacteria (NRB) for respirative energy production. This nitrate reduction process (denitrification) occurs in different steps, each of which is catalyzed by specific NRB, producing nitrite, nitrous oxide, ammonium or nitrogen gas /Hallberg and Keeney 1993, Chapelle 2001/. The nitrification-denitrification cycle can be broken into aerobic and anaerobic conditions. Under aerobic conditions nitrification may lead to nitrate accumulation and under anaerobic conditions nitrate is depleted by denitrification processes. This usually results in an overall depletion of nitrogen species in anaerobic groundwater systems /Chapelle 2001/.

Therefore, it could be said that the behaviour of nitrogen species in groundwater systems is strongly affected by the existence of aerobic or anaerobic conditions and the observed evolution in the Forsmark groundwaters shows the general depletion of nitrogen usually observed in anaerobic groundwater systems as residence time and/or depth increase.

In general, near-surface groundwaters in crystalline systems /Gimeno et al. 2009/ have the widest variability and highest concentrations of nitrogen species. In Forsmark maximum measured values are 0.032 mM for NO_3^-, 0.003mM for NO_2^- and 0.55 mM for NH_4^+. In Laxemar the highest contents reach 0.18 mM for nitrate (though most of them are below ≈ 0.02mM), 0.02 mM for nitrite (the rest are clearly below $\approx 5.5 \cdot 10^{-4}$ mM) and 16.6 to 33.2 mM for NH_4^+ (although most of the available data are below ≈ 0.22 mM).

The range of variation and maximum contents of nitrogen species decrease with depth in crystalline systems /Gascoyne 2004, Pitkänen et al. 2004, Gimeno et al. 2009/. With respect to NO_3^- and NO_2^-, their contents in Forsmark are very low and in many cases below detection limit; the highest analysed contents are $4 \cdot 10^{-4}$ mM and 10^{-4} mM, respectively (Figure 8-5a for nitrite). In Laxemar the maximum contents of dissolved NO_3^- and NO_2^- are around 10^{-4} mM (Figure 8-5c for nitrite). This situation is in agreement with nitrate instability in the reducing conditions generally found in these groundwaters and with the aforementioned depletion of nitrogen species in anaerobic groundwater systems.

With respect to NH_4^+, its content in deep groundwaters is also restricted in range compared with the shallow groundwaters. High NH_4^+ values (from 0.055 to 0.19 mM) down to 500 m depth (Figure 8-5b) are systematically associated with brackish marine groundwaters with the highest Littorina contributions /Gimeno et al. 2009/. In Laxemar-Simpevarp groundwaters, the largest variability is found also in the first 500 m with contents up to 1.1 mg/L (0.061 mM; Figure 8-5d) in the brackish marine groundwaters located at Äspö. This association also occurs in the Olkiluoto area where groundwaters with a high Littorina contribution have variable and high NH_4^+ concentrations (with maximum values near 0.9 mg/L ≈ 0.05 mM; /Pitkänen et al. 2004/. These observations indicate that high NH_4^+ concentrations could represent an inherited character from an old marine origin /Gimeno et al. 2009/.

In summary, the main sustainable source of nitrate to groundwater should be from surface ecosystems (currently also from soil fertilisers). Oxygen is rapidly removed by microbial respiration in shallow, infiltrating groundwater. When oxygen is used up, nitrate will be reduced. Most deep groundwater systems are, consequently, depleted not only in oxygen but also in nitrite (as seen in Forsmark, Laxemar and other crystalline systems when residence time and/or depth increase), a metastable intermediate product in the denitrification process, with very low concentration in most natural waters /Appelo and Postma 2005/.
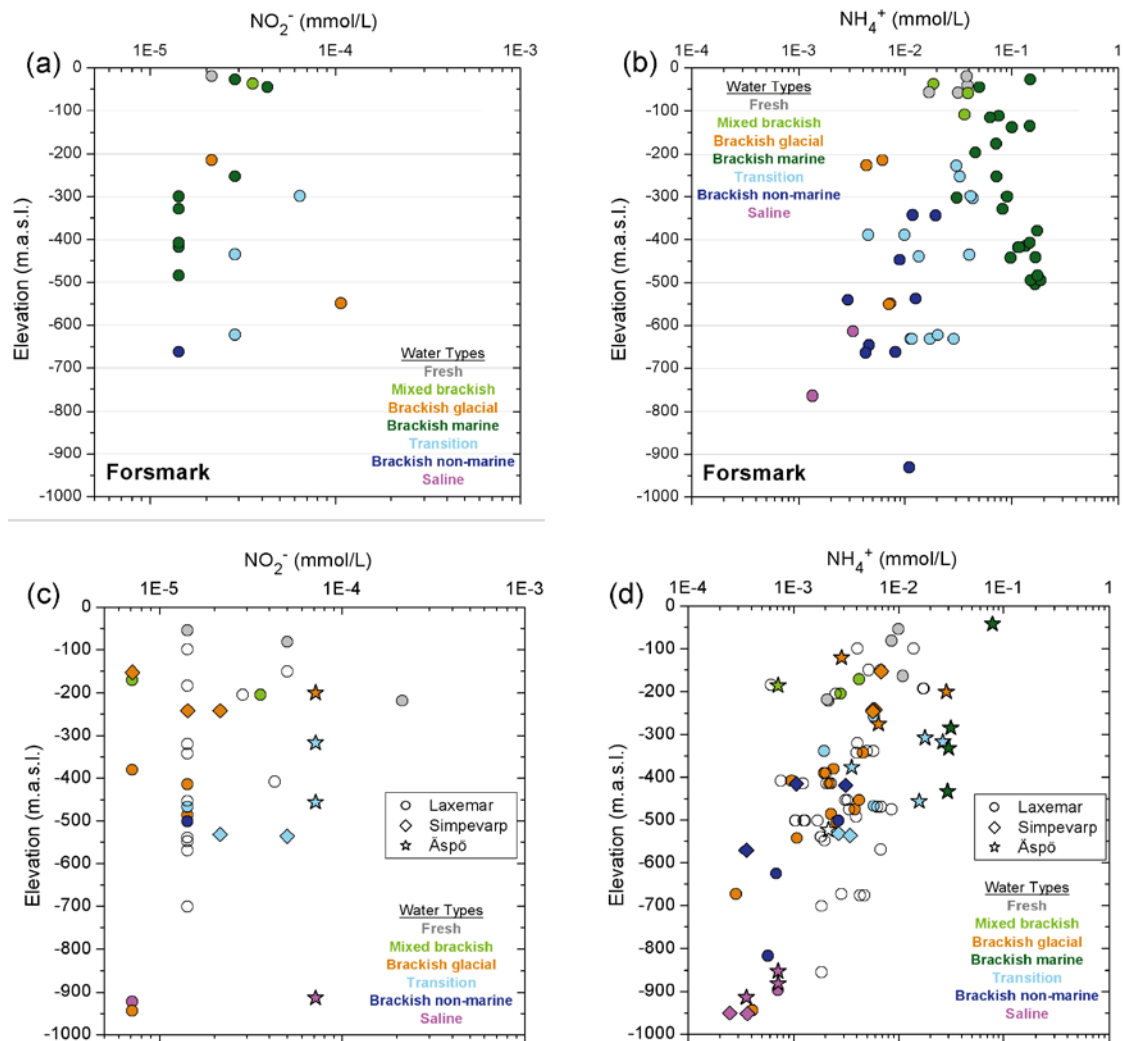
Figure 8-5. *Depth distribution of nitrite (a) and ammonium (b) in the Forsmark and Laxemar (c and d) groundwaters.*

8.6.2 Estimated values over time

The excavation and operation phases

If large amounts of organic structural stray material occur in the repository, decomposition of organic materials may increase the microbial activity during this stage. After the consumption of oxygen, bacterial nitrate reduction is by far the most favoured heterotrophic respirative pathway, even independent of fermentative bacteria /Appelo and Postma 2005, Konhauser 2007/. If dissolved nitrate is present in the repository at this stage, activity of nitrate reduction bacteria will quickly consume it /Hallbeck et al. 2006, Hallbeck 2010/. This effect would enhance the reducing capacity of the repository near-field but it may also increase the amounts of dissolved nitrite and ammonium.

Nitrate derived from agricultural uses or blasting residues are the main potential sources of this component at the repository at this stage. From the present concentrations in the near surface groundwaters at Forsmark or Laxemar, it is expected that intruding superficial waters do not represent a meaningful source of nitrates. Remnants of blasting, however, may be an important source of nitrate for groundwaters at the repository level. As far as the authors know, there are not available estimations on this source for the Excavation and Operation phases as it would depend on the method used for construction, blasting or rock-drilling machines /Hallbeck et al. 2006, Hallbeck 2010/.

The effects of blasting relative to nitrate have been studied in some works at the Whiteshell Underground Research Laboratory site (Canada). Increases in NO_3^- concentrations were observed in fractures adjacent to blast sites /Gascoyne and Thomas 1997/ and, also, it was estimated that this nitrate "pollution" could

increase groundwater bacterial populations by several orders of magnitude /Stroes-Gascoyne and Gascoyne 1998/. These observations were confirmed in the Blast Damage Assessment Project developed at that URL where it was concluded that blasting residues (nitrates) can enhance microbial growth one to four orders of magnitude with respect to nutrient-poor groundwaters /Martino et al. 2004/.

Another source of information comes from the effect of blasting in mine-related groundwaters, which appears to be variable. From the nearly fifty Canadian and Fennoscandian Shield sites reviewed by /Stotler et al. 2009/ samples from only three mines have recorded nitrate concentrations higher than 100 mg/L (1.61 mM). But in the Lupin Mine (Canada), exceptionally high nitrate concentrations (423–2,630 mg/L or 6.82–42.4 mM), attributed to remnants of blasting, have been recorded in the permafrost groundwaters between 200 and 600 m depth /Stotler et al. 2009/. The persistence of such amounts of nitrate was due to oxic to suboxic conditions identified at these depths and to the absence of a significant denitrification process (by nitrate reducing bacteria).

Finally, around the SFR facility (final repository for short-lived radioactive waste, excavated and constructed some twenty years ago), nitrate levels at present are only locally higher (and not especially higher) than those observed in pristine conditions at Forsmark or Laxemar. This suggests that nitrate from blasting residues are not accumulated in high proportions or are quickly removed under the mildly reducing conditions observed in the groundwaters of that site.

In any case, if blasting is used in the repository construction, the residual amounts of nitrate and the processes that may mitigate its accumulation should be evaluated. The presence of nitrate is relevant if, as expected, meaningful amounts of organic structural stray material occur in the repository. Under these conditions, the production of nitrites, ammonium or even nitrogen (the stable endpoint of the denitrification chain) can be large, at least locally /SKB 2010/.

A dramatically time-substained increase in nitrite concentrations would be not expected as it is a metastable intermediate product in the overall denitrification processes and it is often found at trace levels in most aqueous systems /Appelo and Postma 2005, Rivett et al. 2008/. However, ammonium may be stable under reducing conditions and, with the available data, it is not possible to estimate the amount of this component.

Temperate Period

The performed simulations (Section 6.1) indicate that dilute waters will reach deeper depths than today, mainly at the end of the temperate period. Present fresh and shallow (< 100 m) groundwaters in Forsmark have very low concentrations of NO_2^- and NH_4^+ (below $2 \cdot 10^{-5}$ mM and $4 \cdot 10^{-2}$ mM, respectively; Figure 8-5) as is the case in Laxemar and Olkiluoto /Gimeno et al. 2009, Pitkänen et al. 2004/.

Assuming that concentrations of dissolved NO_2^- and NH_4^+ will remain substantially the same as before repository construction, mean values of $3.08 \cdot 10^{-5}$ mM for NO_2^- and $5.42 \cdot 10^{-2}$ mM for NH_4^+ as measured in present groundwaters (Table 2) can be expected. Maximum values of $1.07 \cdot 10^{-4}$ mM and $0.186 \cdot$ mM for NO_2^- and NH_4^+, respectively, would represent a conservative estimate, specially for NH_4^+ as maximum values of this component are associated with groundwaters with marked Littorina characters and therefore, with important marine contribution (see submerged period below) Thus, a value of $4 \cdot 10^{-2}$ mM for NH_4^+ (the maximum value excluding the groundwaters with Littorina contribution) could be proposed.

Glacial period

During the infiltration of glacial melt waters nitrate is expected to decrease due to the decrease of superficial biological activity under such conditions. Nitrate content in present glacier ice and snow is very low (e.g. $4.5 \cdot 10^{-3}$ to $6.8 \cdot 10^{-3}$ mM); /Hallbeck 2009/. Considering that nitrite and ammonia can only be produced by bacterial activity on nitrate, the expected concentrations of these two nitrogen species are also low, below the expected contents for the temperate period.

Submerged period

In marine sediments with organic matter, bacterial activity promotes the transformation of organic nitrogen compounds and the formation of NH_4^+. Therefore, during the submerged period (under marine waters), the high biological activity in the marine sediments will lead to a noticeable increase, at least in the ammonium contents in the recharging marine waters infiltrating through them. This is observed at present: seawater has very low NH_4^+ concentrations (usually well below 0.05 mg/L or $2.8 \cdot 10^{-3}$ mM in the available samples from the present Baltic Sea) but increasing ammonium concentrations with depth in the interstitial waters from marine sediments is a common observation. It also occurs in the present sediments of the Baltic Sea, where NH_4^+ concentrations from 0.22 to 0.89 mM are frequent /Carman and Rahm 1997/. However, ammonium is not a conservative component and reactions (e.g. exchange reactions) can reduce NH_4^+ concentrations during circulation of these marine waters through the fractured bedrock.

This stage would be comparable to the Littorina period and, as indicated above, NH_4^+ contents in groundwaters with a clear Littorina signature range from 0.055 to almost 0.19 mM /Gimeno et al. 2009/. These values, considerably higher than the contents found in the rest of the Forsmark groundwaters, are slightly lower than the ones found in Baltic Sea sediments, probably due to the decreasing effect of cation exchange. However, cation exchange has not been able to completely mask the marine signature in Forsmark, Laxemar-Simpevarp and Olkiluoto groundwaters, probably favoured by the stability of dissolved ammonium in reducing environments. A value for NH_4^+ of 0.19 mM could be proposed for this period.

8.7 Colloids

8.7.1 Overview/general description

The concentration of natural colloids should be low to avoid colloid-mediated transport of radionuclides. The stability of the colloidal fraction in groundwaters is mainly linked to the neutralising electric repulsions between charges in their surfaces. In turn, these charges depend on pH, ionic strength and counterions. Overall, colloid stability is largely decreased at high ionic strengths and/or if the concentration of divalent cations exceeds 1 mM.

In Forsmark groundwaters most of the measured colloid concentrations are below 60 µg/L. Three samples exceeded that amount with maximum contents of 164 µg/L (Figure 8-6a) /Hallbeck and Pedersen 2008a/. In Laxemar the concentrations are below 40 µg/L except in two samples with values around 90 µg/L (Figure 8-6b) /Hallbeck and Pedersen 2008b/. These values are in agreement with those found in other crystalline rock groundwaters like in Switzerland (30 ± 10 and 10 ± 5 µg/L; /Degueldre 1994/) or in Canada (300 ± 300 µg/L; /Vilks et al. 1991/).

Plotting colloid concentration versus elevation (Figure 8-6) shows that the greatest colloid concentrations are found in waters with a clear brackish marine signature, mainly at the shallowest depth (KFM01A, 112 m), but also at 442 m and 328 m depth in boreholes KFM03A and KFM10A, respectively. The lowest concentration in the Forsmark area is found in saline groundwaters (KFM06A, 645 m; high ionic strength increases colloidal aggregation and sedimentation; e.g. /Degueldre et al. 1996, 2000/).

Inorganic and organic colloids exist at Forsmark and Laxemar and some colloids have been identified as microbes and even viruses. Clay colloids seem to be the dominant fraction, whereas organic colloids (humic and fulvic acids), bacteria and viruses appear to represent only a minor part /Nilsson and Degueldre 2007, Hedqvist and Degueldre 2008, Wold 2010/. However, contribution of microorganisms to the colloidal fraction may be higher than thought /Hallbeck and Pedersen 2008a, b/ and additional investigations are needed to assess the importance of these type of biogenic colloids.
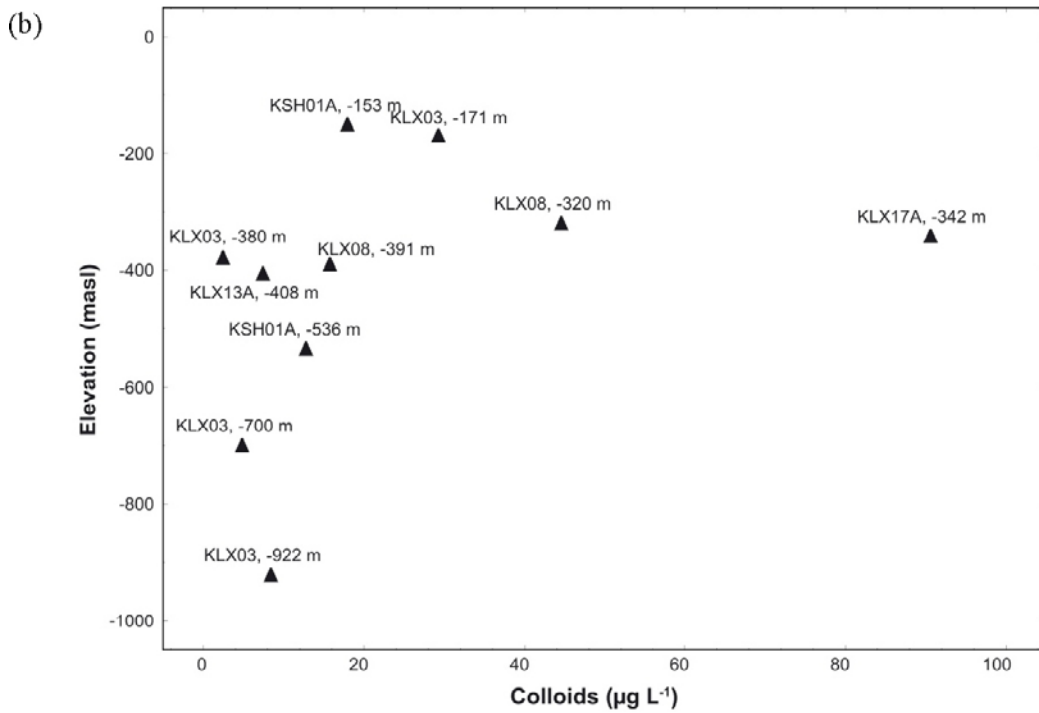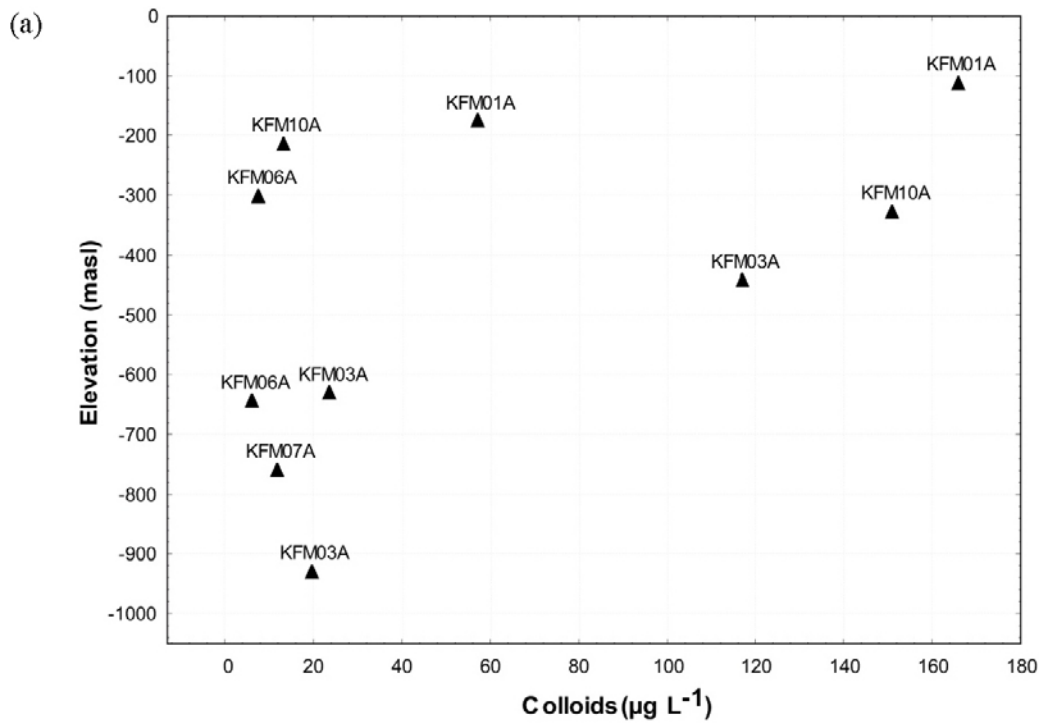
Figure 8-6. *Colloid concentration (µg/L) plotted against elevation in the Forsmark (a) and Laxemar (b) areas. In the Forsmark area silica data for KFM01A (112 m) and KFM08D are omitted due to sampling artefacts. In the Laxemar area data from KLX15A (467 m) are also excluded due to sampling artefacts. Data taken from /Hallbeck and Pedersen 2008a/ and /Hallbeck and Pedersen 2008b/.*

8.7.2 Estimated values over time

The excavation and operation phases

During the excavation and operation phases, substantial amounts of colloids may be formed by microbial activity, bentonite erosion by diluted meteoric waters, precipitation of amorphous Fe (III) hydroxides, etc. These colloids are expected to be short-lived, mainly because colloids will aggregate and sediment in moderately saline waters /Degueldre et al. 1996/. Other processes contributing to the elimination of colloids are microbial decomposition of organics, and the re-crystallization and deposition of amorphous materials. In conclusion, an increased formation of colloids during the excavation and operational phases is not expected to affect the performance of the repository in the long-term, because colloid concentrations will quickly decrease and resume the natural values.

In any case, a maximum pessimistic value of 0.5 mg/L for the concentration of colloids has been proposed for this period in the Geosphere Process Report /SKB 2010/ from /Laaksoharju et al. 1995/.

Temperate period

As stated above, colloid stability is controlled by pH, salinity and cation concentrations. In ground-waters containing more than either 1 mM of Ca^{2+} or 100 mM Na^+, colloids are not stable and colloid concentration must be low (e.g. below 100 μg/L; /Degueldre et al. 1996/. Results coming from modelling indicate that pH, salinity and calcium concentration in the groundwaters at that period will be high enough to destabilise colloids, for which their concentrations are expected to remain at the levels measured at present during the site investigation program, i.e. less than 180 μg/L.

Glacial Period

Under glacial conditions the inflow of organic matter from the surface will be negligible and the input of organic colloids (e.g. fulvic or humic acids) to the groundwaters must decline. However, the generation of inorganic colloids is favoured at low ionic strengths and low concentrations of cations. As during the glacial stage the expected groundwater composition will be predominantly dilute, the possible generation and transport of colloids by these groundwaters cannot be excluded.

Hence, there is a potential for higher colloid concentrations in groundwaters during a glacial period, especially during the advance and retreat of the ice sheet, when groundwater velocities are higher. A reasonable upper limit would be in the mg/L range from the highest measured colloid concentrations in groundwaters from crystalline environments at repository depths (from the reviews by /Degueldre et al. 2000/ or /Wold 2010/).

In addition, as the buffer swells into fractures, the bentonite barrier can release montmorillonite colloids in contact with dilute groundwaters increasing colloids concentration in the vicinity of the bentonite barrier. Under this assumptions, experimental results reviewed by /Wold 2010/ suggest that a maximum of about 10–20 mg/L of montmorillonite colloids can be expected in a Grimsel-type groundwater (with Na and Ca concentrations of 0.001 and 0.0001 M respectively) in contact with the bentonite barrier. These values can be considered a conservative estimation as colloid contents drastically decrease with distance from the barrier /Wold 2010/.

Submerged period

Promoted by the density-driven intrusion of marine water, an increase in the salinity (and cation concentration) of the groundwaters is expected to occur in this period and, therefore, geochemical conditions would not be favourable for colloid stability. The available data for present groundwaters with an important Littorina contribution at Forsmark (KFM01A, 112 m; KFM10A, 328 m; KFM03A, 442 m; KFM01A, 176 m) indicate that some of them have the highest colloid concentration in the site (Figure 8-6a). The reason for these values is not clear although, in any case, they are in the normal range of other groundwaters in crystalline systems. The conclusion is that colloid concentrations are expected to decrease or, in the worst case, remain at the levels that have been measured at present during the site investigations, i.e. less than 180 μg/L.

Table 8-1. Recommended values of DOC, acetate, CH_4, H_2, NO_2^-, NH_4^+ and colloids for the different periods during the evolution of the Forsmark site. Concentration units are expressed in mol/L, except when indicated. Grey cells indicate values deduced from the mass balance calculations performed by /Hallbeck 2010/.

Evolutive Periods	DOC	Acetate	CH_4	H_2	NO_2^-	NH_4^+	Colloids (µg/L)
Excavation/Operation	$1.2 \cdot 10^{-3}$	$2 \cdot 10^{-4}$	$2 \cdot 10^{-4}$	$2.7 \cdot 10^{-5}$ [1]	$< 2 \cdot 10^{-5}$	$< 3 \cdot 10^{-2}$	500
		µM range		$1.5 \cdot 10^{-7}$			
Temperate	$1.25 \cdot 10^{-3}$	µM range	$2 \cdot 10^{-4}$	$1.92 \cdot 10^{-5}$	$\underline{1.07 \cdot 10^{-7}}$	$4.0 \cdot 10^{-5}$	< 180
Glacial	$4.2 \cdot 10^{-5}$		$2 \cdot 10^{-4}$	$1.92 \cdot 10^{-5}$	$\underline{\leq 1.07 \cdot 10^{-7}}$	$< 4.0 \cdot 10^{-5}$	20,000
Submerged (marine)	$2.9 \cdot 10^{-3}$		$2 \cdot 10^{-4}$	$1.92 \cdot 10^{-5}$	$1.07 \cdot 10^{-7}$	$1.9 \cdot 10^{-4}$	< 180

[1] Value estimated from iron corrosion.

Table 8-2. Main statistics for the values of the analysed parameters measured in the present groundwaters at Forsmark.

	TOC (mg/L)	DOC (mg/L)	NO_2^- (mol/L)	NH_4^+ (mol/L)	CH_4 g (mol/L)	H_2 g (mol/L)
N total	56	62	16	60	16	12
Minimum	bdl	bdl	1.43E–08	0	1.07E–06	bdl
Median	2.55	1.95	2.50E–08	3.22E–05	2.46E–06	6.03E–08
Mean	4.85	3.5	3.08E–08	5.42E–05	1.55E–05	3.37E–06
Standard Deviation	6.21	5.51	2.44E–08	5.62E–05	5.07E–05	6.09E–06
Maximum	40.3	35.7	1.07E–07	1.86E–04	2.05E–04	1.92E–05
P0.1	bdl	bdl	1.43E–08	0	1.07E–06	bdl
P5	bdl	bdl	1.43E–08	2.13E–06	1.07E–06	bdl
P95	13	13	1.07E–07	1.70E–04	2.05E–04	1.92E–05
P99.5	40.3	35.7	1.07E–07	1.86E–04	2.05E–04	1.92E–05

Table 8-3. Main statistics for the values of acetate and DOC measured during the monitoring program on going at Laxemar and Äspö.

	Acetate (M)	DOC (M)
N total	16	20
Mean	7.55E–5	2.92E–3
Standard Deviation	1.73E–4	7.04E–3
Sum	1.21E–3	5.84E–2
Minimum	0	1.66E–4
Median	1.49E–5	4.79E–4
Maximum	6.87E–4	3.06E–2
P0.1	0	1.66E–4
P5	0	1.83E–4
P95	6.87E–4	0.02136
P99.9	6.87E–4	0.03056

8.8   Compilation of values

The proposed concentration values for the parameters analysed in this section (DOC, acetate, CH_4, H_2, NO_2^-, NH_4^+ and colloids) in the different stages are summarised in Table 8-1. One of the main information sources for the compilation has been measured data in the present groundwaters at the two Swedish sites (Forsmark and Laxemar-Simpevarp). Therefore, the main statistics for the values of the parameters measured in the groundwaters from Forsmark are shown in Table 8-2, while acetate and DOC values measured during the on-going monitoring program in the Laxemar area are presented in Table 8-3.

Values and ranges included in Table 8-1 come from different sources and these are summarized next. For the Excavation/Operation period two types of values have been proposed for acetate, CH_4 and H_2 (Table 8-1). Values shaded in blue are deduced from the inventory of organic materials in the repository and mass balance calculations performed by /Hallbeck 2010/. They represent "cumulated" and non time-average values expressed in a per litre basis that must be relaxed during the evolution of the Excavation/Operation period and, probably, during the temperate period as well. Values in white cells represent the maximum amounts of acetate and hydrogen allowed by the balance between microbial producing and consuming processes in low temperature systems. They represent the expected time-averaged concentrations during this period (H_2 concentrations in the nanomolar range and acetate in the micromolar range) and, in the case of acetate, also during the other examined periods (for hydrogen, this microbiological balance may be broken by the existence of different inorganic sources for this component). The cumulated values and their possible consequences must be used with caution. The data used in the mass balance estimations are largely uncertain /Hallbeck 2010/ and different assumptions must be verified.

Most of the values proposed for the temperate period are extrapolated from contents in present groundwaters and assume that they would remain substantially the same after repository construction. Thus, the maximum measured concentrations in present groundwaters have been selected as recommended values.

Except for CH_4 and H_2, the selected values for the Glacial period are based in measurements performed in different glacier ice samples (DOC), in comparative deductions from contents in present-day groundwaters (NO_2^- and NH_4^+) and in experimental results on the interaction between bentonite and glacial waters.

As for the Temperate period, most of the values selected for the Submerged (marine) period are based on the maximum concentrations measured in present-day groundwaters. Taking into account the time span until the starting of this period, the assumption of constant concentration values is weaker than in the case of the temperate period.

All proposed values have considerable uncertainties but, in some cases, they are especially large. This is the case of DOC, NO_2^- and NH_4^+ for the Excavation/Operation period, of CH_4 and H_2 for the Glacial period and of DOC for the submerged period:

* The value proposed for DOC for the Excavation/Operation period is derived from the inventory of organic materials in the repository /Hallbeck 2010/, excluding the amounts of organic carbon with the bentonite However, this value is highly uncertain as the degradation rates of organic materials, especially man-made materials, and biodegradability of the organic matter in the bentonite are still poorly known.

* NO_2^- and NH_4^+ contents for the Excavation/Operation period have been impossible to fix or bracket due to the lack of estimations of nitrate contents, the principal source of NO_2^- and NH_4^+ through denitrification. Thus, the proposed values are the highest values found during the Site Characterization Program in some soil pipes from Laxemar (SSM000241 and SSM000242) and associated with an especially intense microbial degradation of organic matter /Gimeno et al. 2009/. However, nitrite is often found in natural aquatic systems at trace levels and ammonia (NH_3, the involved component in stress corrosion cracking, SSC, of the copper canister), is only stable in alkaline (pH>9) and very reducing conditions (close to the water stability boundary; /Kehew 2001, Appelo and Postma 2005/). Thus, the existence of meaningful amounts of ammonia during this stage would be not expected, although more detailed analysis is needed.

* The values proposed for CH_4 and H_2 during the Glacial period are extrapolated from the highest contents in present groundwaters. The estimation of CH_4 and H_2 concentrations in this period is

complicated by the existence of additional processes and different boundary conditions to those present and/or expected in the other periods. The concentration of these gases will be controlled by their production and flow from the deep bedrock and by the active microbial metabolisms (acting as sources and sinks) but also by the impervious frozen layers at the top of the site and by the formation/dissociation of clathrates during permafrost advance and decay.

- As for DOC values during the submerged period, they have been extrapolated from the highest DOC values in present-day Forsmark groundwaters with an important marine contribution (up to 2.92 mM). However, they are still subjected to different uncertainties (e.g. contamination during drilling/sampling) and, therefore, they remain uncertain.

9 Summary and conclusions

The hydrochemical evolution of the Forsmark site has been evaluated through fluid flow and solute transport, simulating groundwaters mixing and chemical reactions with fracture-filling minerals. Different climatic and hydrodynamic periods of interest in the SR Site assessment have been simulated by a methodology which integrates hydrological calculations (provided by Serco and TerraSolve using ConnectFlow), and the geochemical simulations, performed with PHREEQC. In the case of the temperate and the submerged periods, this methodology is relatively simple because the Serco team provides the fractions of the five end-members groundwaters considered to be present in the Forsmark site. However, for the glacial calculations, the TerraSolve team only provides salinities. In this case, salinities must be transformed in fractions of the reference groundwaters. In this way, a series of assumptions have been applied: (1) saline groundwaters are exclusively represented by the Deep Saline groundwaters and, (2) dilute waters are initially represented by the Altered Meteoric waters. This methodology assumes that decreasing salinities are exclusively associated with increasing fractions of the glacial melt waters. This assumption does not consider alternative evolutions (e.g. meteoric waters infiltration when the Forsmark site is not completely covered by the ice sheet).

In the transition between the temperate and the glacial periods, hydrogeochemical continuity has not been completely simulated in terms of the groundwater composition in each point. It is due to (1) conceptual differences between both hydrological models (and the kind of results provided by the modeling teams, Serco and TerraSolve), and (2) the assumptions applied in order to convert salinities in fractions of the reference waters. In this way, no coincidence has been observed between some results obtained to the end of the temperate period and the initial stage of the glacial cycle. The differences in the case of the computed Eh and pH values (Figure 9-1) are notably. However, the trend of other parameters, such as salinity or the cationic species concentrations, show a good coincidence in the transition between both climatic periods. This constraint must be taken into account when discussing about the assessment of the safety functions. In this way, It had been advisable that (1) the hydrological modelling teams (Serco and TerraSolve) had provided fractions of the reference groundwaters as a result of their models and, (2) the final stage of the temperate period was coinciding with the initial stage of the glacial cycle.

Despite the usual constraints associated with predictive numerical models, the main objective of the present work has been achieved (the assessment of the safety functions shown in Figure 1-3 within the candidate repository volume; Table 9-1). In the following sections, the main results for the different climatic and hydrological periods have been discussed. As described in each section, the results obtained for the "Base Cases" are slightly variable when simulating hydrogeological and geochemical sensitivity cases, and considering or not the permafrost development (in the case of the glacial period). On the other hand, the results obtained for the submerged saline period are similar to those obtained for the initial stage of the temperate period. More details in reference to the statistical results of the main geochemical parameters have been included in Appendix 4.

9.1 Excavation/operation phase

No calculations have been performed in order to evaluate the hydrochemical environment during the excavation/operation phase. The hydrogeochemical evolution is mainly conditioned by the disturbance of the natural conditions caused by the construction of the repository. In general, the effects on salinity from groundwater upconing and draw-down, are assessed to be negligible. On the other hand, a short alkaline pulse in the groundwater from low-pH cement, shotcrete and concrete is likely to form, but its effects will be negligible.

An increased precipitation of calcite and Fe(III) oxyhydroxides will occur at the tunnel wall during operations, but this process is evaluated as being of no consequence for the performance of the repository. On the other hand, oxygen left in the repository will be consumed by either chemical or microbial processes; most of the oxygen in the backfill, which has the largest pore volume in the deposition tunnels, will react and thus will not diffuse into the buffer and will not reach the surface of the canister.

As a conclusion, canister corrosion depths are evaluated to be tens of micrometres at most, and will thus have a negligible impact on the minimum copper coverage of the canisters.
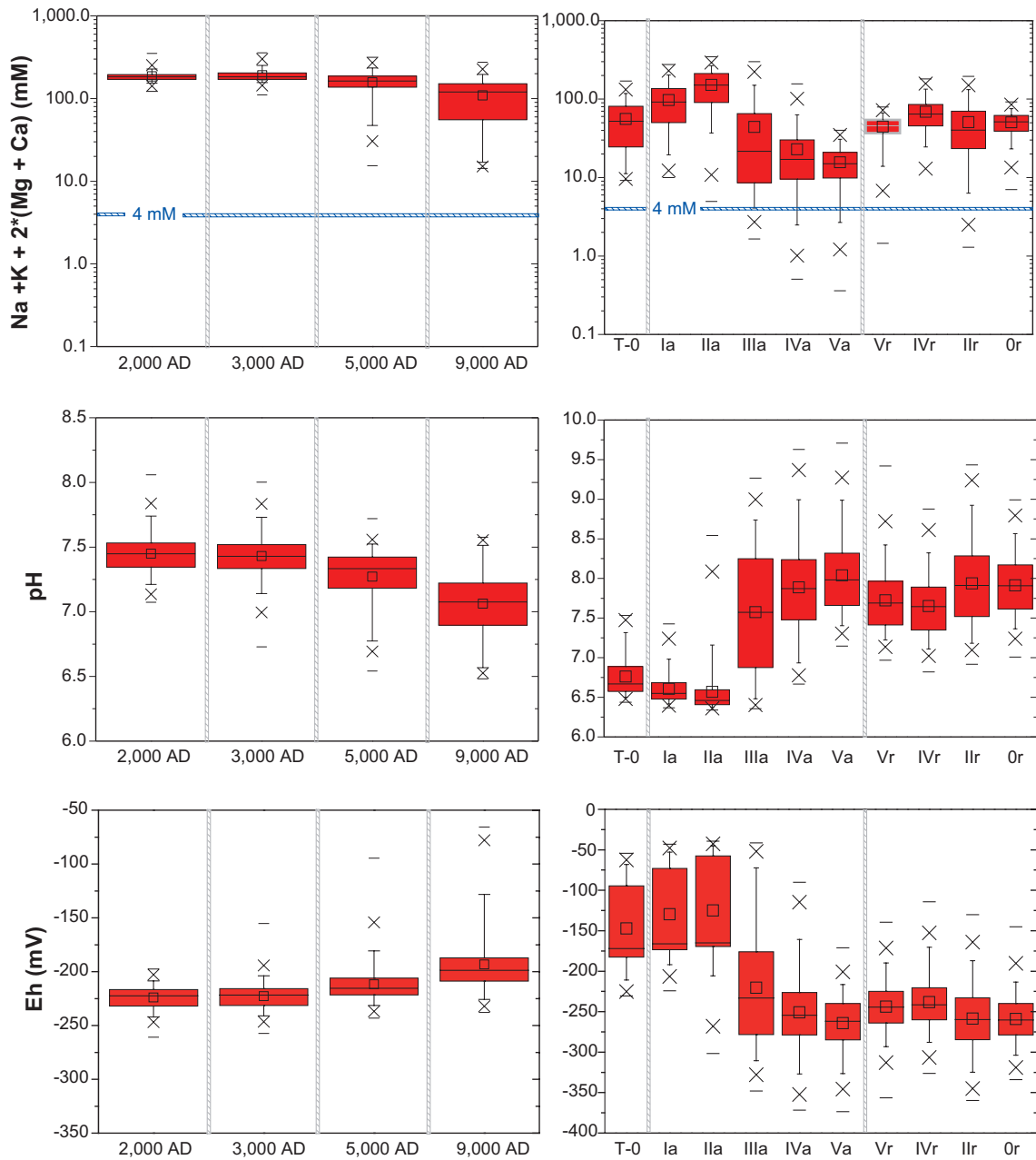
Figure 9-1. *Box-and-whisker plots showing the safety function factor $\sum q[M^{q+}]$, pH and Eh for the "Base Cases" of the temperate period and during the glacial cycle. The statistical measures are the median, the 25th and 75th percentile (box), the mean (square), the 5th and 95th percentile ("whiskers"), the 1st and 99th percentile (crosses) and the maximum and the minimum values.*

Table 9-1. Synthesis of some geochemical parameters (requested by SKB) calculated during the different climatic periods within the candidate repository volume.

	Max Cl (kmol/m³)	Max Ca/Na	Max Ca (kmol/m³)	Max Na (kmol/m³)	Min Ca/Na	Min Ca (kmol/m³)	Min Na (kmol/m³)
Temperate (2000 AD)	3.449E-01	1.219E+00	1.210E-01	1.560E-01	2.406E-02	2.860E-03	4.090E-02
Temperate (9000 AD)	2.661E-01	1.127E+00	8.700E-02	1.080E-01	4.960E-02	7.720E-04	1.200E-02
Glacial (stage IIa)	3.420E-01	1.228E+00	1.229E-01	1.001E-01	6.000E-01	1.730E-03	1.470E-03
Glacial (stage Vr)	7.834E-02	1.548E+00	2.840E-02	2.240E-02	1.023E+00	5.420E-04	3.500E-04
Permafrost (before onset of glaciation)	9.940E-02	1.036E+00	3.520E-02	3.400E-02	3.980E-01	3.890E-04	9.732E-03
Submerged glacial lake	9.130E-02	1.320E+00	3.310E-02	2.590E-02	1.200E+00	2.540E-03	1.930E-03
Submerged seawater	2.759E-01	1.230E+00	9.910E-02	1.590E-01	2.410E-02	3.040E-03	3.370E-02

	Max pH	Min pH	Max C (kmol/m³)	Min C (kmol/m³)	Max Ionic Strength (mol/L)
Temperate (2000 AD)	8.05	7.07	2.460E-03	2.020E-04	0.473
Temperate (9000 AD)	7.57	6.48	7.520E-03	2.580E-04	0.362
Glacial (stage IIa)	8.54	6.34	6.331E-03	2.650E-04	0.471
Glacial (stage Vr)	9.42	6.97	2.171E-03	8.280E-05	0.108
Permafrost (before onset of glaciation)	7.01	6.52	6.706E-03	5.518E-03	0.140
Submerged glacial lake	8.99	7.01	1.484E-03	6.253E-05	0.126
Submerged seawater	8.03	7.22	1.790E-03	1.900E-04	0.380

9.2   Temperate period

During the initial temperate period after closure, the infiltration of meteoric waters, the displacement of the Baltic shore line and the changes in annual precipitation will influence the hydrology of the site. These phenomena will induce changes in the geochemical composition of groundwater around the repository.

During the temperate period, the initial proportions of the Littorina and the Old Meteoric groundwater within the candidate repository volume progressively disappear. Only significant fractions remain in the central areas. By the end of the modelled time (9,000 AD), in the peripheral areas, the meteoric waters will completely displace and dilute the groundwaters previously placed into the Forsmark fractures.

Within the candidate repository volume, the simulated salinity has been demonstrated to be below 15 g/L during the temperate period. On the other hand, the safety function $\Sigma q[M^{q+}]$ will be higher than 4 mM in all points over the time. In conclusion, the salinities during the first temperate period following repository closure will remain limited both at Forsmark, ensuring that the swelling properties of the buffer and backfill are not negatively affected. In this context, colloids will not be especially stable during the temperate period, because the calculated pH values (in the range 6.5 and 8.0), salinities and cation concentrations will be high enough to destabilise them.

The other key parameters in the geochemical safety assessment of the candidate repository show the following trends during the temperate period simulations: potassium concentrations are expected to remain lower than 0.004 mol/L, sulphide concentrations are expected to be also lower than 10^{-5} mol/L, iron concentrations are expected to gradually increase up to 10^{-4} mol/L, and Eh remains under –175 mV for most deposition positions. On the other hand, the phosphate content in groundwaters has been estimated to be limited by concentrations of around 10^{-6} mol/L.

This analyses has lead to the conclusion that the chemical conditions will be reducing shortly after deposition in individual deposition holes, tunnels and, finally, shortly after closure of the repository as a whole. This is of fundamental importance for the long-term safety of the repository and no process has been identified that challenges this conclusion during the initial temperate period after closure. It may, therefore, be concluded that the anoxic groundwater conditions now prevailing at repository depth will continue for the whole temperate period following the closure of the repository, despite the increasing proportion of meteoric waters with time.

A series of sensitivity analysis has been performed in order to evaluate the influence on some hydrological and geochemical parameters. As it is expected, the iron concentrations are strongly dependent

of the iron-bearing mineral chosen to be in thermodynamic equilibrium with groundwaters; Fe(III) oxyhydroxides or amorphous Fe(II) sulphides. In addition, for the temperate period, the simulated redox potential does not show the same trend. In contrast to the sensitivity analysis performed with respect to the geochemical constraints of the model, no relevant differences have been computed when considering the different hydrological models implemented as input data of the geochemical calculations. In this way, the geochemical uncertainties seem to have more influence determining the potential variability of the results during the temperate period.

9.3 Remaining part of the reference glacial cycle

The geochemical calculations simulating the glacial cycle are based on the salinities provided by the TerraSolve models. During the glacial cycle, salinities are basically controlled by (1) the infiltration of glacial melt waters, and (2) the transport of salts from the deepest areas by upconing processes. Another key factor for the salts distribution is the existence of a frozen soil. Finally, when seawater covers the Forsmark area during the final stage of the glacial cycle, the infiltration of marine waters could affect the amount of solutes within the candidate repository domain.

9.3.1 Initial temperate and periglacial periods

Although groundwaters will become progressively dilute during the temperate period following the closure of the repository, permafrost can move salts to repository depth from the upper parts of the site. All evidences indicate that groundwaters under the permafrost will not become more diluted than under temperate conditions. Rather, saline waters may move downwards within conductive fracture zones. Thus, cation concentrations are expected to increase during permafrost periods and satisfy the criteria concerning the safety function indicator $\sum q[M^{q^+}] > 0.004$ mol/L. The concentration of salts at repository level due to out-freezing will not become as high as to decrease the swelling pressure of the buffer and the backfill, due, among other reasons, to the downward gravity-driven flow of saline waters. This situation will not be changed during permafrost decay as a transition to a temperate period occurs.

For major groundwater components, such as chloride, sodium, calcium, magnesium, and sulphate, the conclusion is that they will follow the trends of salinity. Other components, such as bicarbonate, potassium, iron phosphate and sulphide, as well as pH that are controlled by relatively fast chemical reactions, are expected to remain mostly unaffected by permafrost.

Therefore, the criteria concerning the safety function indicators are expected to be fulfilled, in that pH will remain lower than 11, and the concentrations of potassium, sulphide and iron will remain limited. Consequently, the results for the initial stages of the glacial cycle and for the periglacial period show that colloids will not be especially stable during these periods, because the pH values, salinities and cation concentrations will be high enough to destabilise them.

The redox potential calculated for the points included in the candidate repository volume shows Eh values lower than –50 mV. During the temperate period previous to the glacial cycle, the calculated Eh values are in the range of –100 and –175 mV, increasing to values around –75 and –125 mV during the periglacial period.

9.3.2 Advance and retreat of a glacier over the candidate repository volume

For the glacial cycle of the reference evolution (about 120,000 years) the Forsmark site is covered by an ice sheet during a few periods with a total duration of about 30,000 years.

An ice sheet advancing over both unfrozen and permafrost ground have been modelled. For the case of advancement over unfrozen ground, a glacial period of 18,850 years has been simulated in 10 time steps, reproducing the advance and retreat of the ice front. Three hydrological stages have been considered: i) when the ice front is advancing to the repository area (2,900 years, approximately), ii) when the repository is entirely covered by a warm-based ice sheet i.e. an ice sheet with basal melting (15,000 years) and, finally, iii) when the ice sheet is retreating (1,200 years) and the area is covered by a 100 m deep melt water lake.

Dilute waters of a glacial origin are expected under a warm-based ice sheet. Significant changes in groundwater composition are expected as soon as the ice front advances over the repository area. Salinities in the upper part of the modelled domain usually will be lower than 2 g/L. The model results illustrate also the upconing of Deep Saline waters under an advancing and a retreating warm-based ice sheet. The calculated salinities can reach values up to 20 g/L in locations affected by upconing. Because the advancement of the ice sheet is a relatively fast process and the retreat even more so, the high salinity conditions are predicted to last only a few centuries at most.

The trend of the chemical components not participating extensively in chemical reactions (such as chloride, sodium, sulphate, and calcium) follows the salinity patterns under the ice sheet described above. The results indicate that dilute melt waters, with $\sum q[M^{q+}]$ lower than 4 mM, may occur within the candidate repository volume for some period of time during the advance and retreat of an ice sheet, violating the criterion for the safety function indicator R1c. It should be noted that the model results indicate that after the complete retreat of the ice sheet the salinities and the concentration of cations are back, approximately, to the levels estimated before the onset of the glacial period.

Other components, such as bicarbonate, phosphate, iron, sulphide and pH that are controlled by relatively fast chemical reactions and reactions with minerals can also be affected by the glacial conditions to a lower extent. The results show that glacial conditions may result in a general increase of pH values, an effect which is observed for example in the Grimsel groundwaters. The results also indicate that the pH values at the Forsmark site will be around 6.5 to 7.0 during the initial stages of the glacial cycle, increasing to values around 8.0 during the last stages of the ice advance and during the glacier retreat. In any case (and for all the simulated points), the pH remains lower than 11. In this way, as the previous climatic periods, results indirectly indicate that colloids will not be especially stable during a hypothetical glacial cycle.

The maximum concentrations of potassium and iron simulated in the glacial period will remain limited by values of 0.0003 and 0.0001 mol/L, respectively. However, the groundwater concentrations of sulphide have not been accurately calculated, because the simplifications made to obtain mixing proportions during this period, condition very much the end-members considered and, therefore, the sulphide contents to be mixed. In any case, sulphide concentrations resulting of the calculations are lower than 10^{-7} mol/L. The phosphate concentrations remain below 10^{-6} mol/L, in spite of maximum concentrations of around 10^{-5} mol/L have been computed during the initial stages of the glacial cycle.

The redox potential calculated in the candidate repository volume shows Eh values lower than –50 mV. However, the characteristic values (more than 50% of the simulated points) are lower than –200 mV when the glacial melt waters affect the candidate repository volume. Only during the first stages of the glacier advance, the average redox potential is clearly higher than –150 mV.

A relevant conclusion of the simulations indicate that although the calculated chemical characteristics of the groundwaters in general show a narrower range of values in the case of the ice sheet advancing over permafrost when compared with the ice sheet advancing over an unfrozen area, for a few of the modelled grid points extreme values may occur. For example, there is a possibility of having lower cation concentrations in the case of the ice sheet advancing over permafrost. Immediately after the retreat of an ice sheet, isostatic depression will set the ground surface at the repository site below the Baltic Sea surface level for a period of time. In the reference evolution, which is a repetition of the last glacial cycle, the Forsmark site is expected to be below lakes of glacial melt waters, and sea or brackish waters during a period of time between a few thousand years up to perhaps ten thousand years.

The site descriptive modelling of the Forsmark site since the retreat of the last ice sheet to the present-day situation and the SR-Site modelling show a relatively fast turnover of groundwaters, where glacial melt is replaced by a succession of waters penetrating from the surface: the Littorina Sea gradually evolving into the present day Baltic Sea, and finally modern meteoric waters.

The results presented above indicate that concerning salinity and the concentration of cations, the conditions when the site is submerged under a lake of glacial melt water are similar to those found before the onset of the glaciation. Other more reactive groundwater components such as carbonate or pH may remain affected, but all groundwater characteristics are expected to satisfy the safety function indicators.

The possible infiltration of marine waters has been modelled for short periods of time after the glaciation. Within such a period, equivalent to the Littorina Sea episode that had its maximum

salinity at 4,000 BC, the salinity of groundwaters at repository depth could increase due to density driven groundwater flow. The results modelled for 3,000 BC show that the effects of the marine water intrusion at repository depth are delayed in time and that the proportion of Littorina waters in the repository volume is larger at present than it was then. The calculated groundwater compositions for 3,000 BC show that the charge concentration of cations around the repository is well above 0.004 mol/L, corresponding to compliance with the safety function indicator R1c. As the salinities are not expected to increase above those of seawater during any period of time, the swelling capacity of the backfill will not be affected.

9.4 Evaluation of the geochemical parameters not included in the geochemical calculations

The concentrations of some components not included in the calculations, but with relative importance as safety indicators (DOC, acetate, CH_4, H_2, NO_2^-, NH_4^+ and colloids), have been analytically estimated. For the temperate and submerged periods and the open repository stage, most of these values have been extrapolated from the content of the analytical samples, and the maximum concentrations have been selected as recommended values. For the Glacial period, the selection of the reference values has been based on measurements performed in different glacier ice samples (DOC), on experimental results, and analysing the evolution of the components from the present-day groundwaters (NO_2^- and NH_4^+). The recommended values are presented in Table 8-1.

9.5 Uncertainties

Four main sources of uncertainties can be identified in the predictive geochemical simulations performed for SR-Site:

- the number and composition of the end-members used to transform the hydrological data in water compositions for the whole rock volume through mixing calculations;

- the heterogeneous reactions considered to participate in the control of the composition of the mixed waters through equilibrium situations;

- the thermodynamic data used for this equilibrium reactions;

- some additional uncertainties arising from the coupling between hydrological and geochemical data.

There are other types of uncertainties related to the evaluation of some key-parameters (colloids, dissolved and total organic carbon, nitrite, ammonia, acetate, methane and molecular hydrogen) that cannot be modelled in the same way and with the same tools as the rest of the geochemical parameters assessed in the SR-Site. These other uncertainties are also described next.

9.5.1 Number and composition of the end-members

Estimation of the number of end-member waters involved in the paleohydrological evolution of the sites and their chemical compositions are key parameters in the performed simulations. The effects of the associated uncertainties have been widely discussed in the context of the Swedish and Finnish Site Characterisation programs (e.g. /Gómez et al. 2009, Gimeno et al. 2008, 2009/ and references therein).

In particular, for the SR-Site the original compositions of the end-member waters used in the geo-chemical simulations have been carefully reviewed in the SDM works /Gimeno et al. 2008, 2009/. Some of these waters are represented by real samples from the natural systems and some others (for the old end-members) are estimated from diverse geological sources. Thus, compositional uncertain-ties in these old end-members are greater. Moreover, in some cases, there are some unknown fundamental geochemical parameters, such as pH, Eh, and dissolved Fe(II) and S(-II) concentrations, that have been obtained assuming a series of mineral equilibrium reactions thought to be controlling these variables (e.g. equilibrium with calcite, quartz, Fe(III) oxyhydroxides and amorphous Fe(II) monosulphides). Thus, although the selected compositons for the end-members are able to simulate the overall geochemical characters of the present groundwaters, some degree of uncertainty remains.

The number of end-members used in simulations depends on the knowledge of the natural system under study. Thus, it has changed as more information and knowledge is available from the sites. In the SR-Site exercise a fifth end member ("Old meteoric end member"), not used in SR-Can calculations, has been included based on the works by /Smellie et al. 2008/ and /Laaksoharju et al. 2009/. It would be valuable to compare the results from the previous SR-Can simulations with the presently available results from SR-Site to analyse the effects of this change in the number of end-members. But, in any case, this type of uncertainty can be included in the usual refinement of the models.

9.5.2   Heterogeneous reactions and equilibrium assumptions

The mineral reactions chosen to be in equilibrium with the groundwater mixtures are reasonable as they include those with a fast kinetic compared to the simulated time intervals (like calcite) or those identified in apparent equilibrium situations in the present groundwaters (like quartz). In fact, they effectively represent the chemical effects observed in the reactive components discussed in this work. However, they represent only a limited subset of those present in the fractures and, thus, other minerals (e.g. chlorite, illite or K-feldspar, frequently found in the fracture fillings) could participate through dissolution-precipitation reactions. Other solid phases, such as aluminosilicates, could be stipulated as equilibrium constarints, but their selection would be difficult to justify because their solubility data show considerable uncertainties (as they depend on the particular mineral composition, order/disorder degree, etc.). Moreover, previous scoping calculations performed for the SR-Can /Auqué et al. 2006/ showed that including chlorite and illite equilibrium in the calculations had a negligible effect on the concentrations of magnesium and potassium.

Other processes diferent from dissolution-precipitation reactions, like cation exchange, could partcipate in the hydrochemical evolution of the groundwaters. Cation exchange reactions are kinetically fast and can exert an important control on the major cationic composition of the groundwaters /Appelo and Postma 2005/. These reactions may be specially activated during the mixing processes as the salinity of the groundwaters exerts a major control on the intensity and selectivity of the exchangers for the different cations.

Despite their potential importance, cation exchange proceses have not been included in the present simulations due to two main reasons: a) the available cation exchange capacites (CEC) values for fracture filling minerals, a basic parameter to include cation-exchange processes in the predictive simulations, are very scarce and uncertain /Selnert et al. 2008/; and b) the thermodynamic database selected by SKB don't have the possibility to deal with cation exchange processes (see below).

Finally, whereas most equilibrium assumptions are generalized in the present groundwaters over the whole studied rock volume, it is not the case of the heterogeneous redox equilibria. The work done for the SDM in Laxemar indicates that in some localised zones of the system, equilibrium with hematite is observed whereas in others waters seem to be in equilibrium with FeS(am). The approach used for the geochemical calculations simplifies the behaviour of the system imposing, alternatively, the equilibrium conditions in the whole volume of rock. This uncertainty has been dealt combining in the Base Case for the redox processes the results obtained from both equilibrium assumptions giving a wider range of variation for these parameters but being able to explain the two possible situations present in the real system.

The uncertainties related with redox desequilibrium situations have also been taken into account. A modified version of the thermodynamic database was implemented in the framework of this study in order to account for the groundwater Eh values controlled by the iron system and the $Fe(OH)_3/Fe^{2+}$ redox pair. The only way to do this is un-coupling the equilibrium between the HCO_3^-/CH_4, SO_4^{2-}/HS^- and $Fe(OH)_3(s)/Fe^{2+}$ redox pairs. This modified database has been named the "un-coupled" database and essentially prevents the redox pairs SO_4^{2-}/HS^- and HCO_3^-/CH_4 to participate in the homogeneous redox equilibrium during the chemical mixing and reaction simulations. The resulting Eh values are similar to the ones measured in some of the Swedish groundwaters believed to be controlled by the electro-active $Fe(OH)_3/Fe^{2+}$ redox pair /Grenthe et al. 1992/. With the original "coupled" database the resulting Eh values correspond to homogeneous redox equilibrium, consistent with the agreement between Eh values for the $Fe(OH)_3/Fe^{2+}$, SO_4^{2-}/HS^- and HCO_3^-/CH_4 couples which has been observed in some groundwater samples at Laxemar /Gimeno et al. 2009/.

Therefore, the use of these two databases and the combination of the results obtained in equilibrium with hematite and those obtained in equilibrium with amorphous Fe(II) sulphides cover the measured and calculated Eh values in SKB's site characterisation studies and although some problems in the treatment and interpretation of redox potential still persists, this methodology gives a reasonable range of Eh values in SR-Site simulations.

9.5.3 Thermodynamic data and thermodynamic database

The thermodynamic data for the mineral phases included in the simulations have been reviewed in /Auqué et al. 2006/ and /Gimeno et al. 2009/. Moreover, these data have been applied, verified and refined in the WATEQ4F database during the study of the present groundwaters in the site characterization programs both in Laxemar and Forsmark.

Consistency between this model exercise and other SR-Site geochemical models using thermodynamic data is an important issue. This is the reason why, instead of using the same WATEQ4F database as in previous geochemical calculations for SR-Can /Auqué et al. 2006/ and for Site Descriptive Modeling /Gimeno et al. 2008, 2009/, SKB decided to use a new thermodynamic database (available from SKB's Trac system) known as "TDB_SKB-2009_Amphos21.dat". This database was developed by /Hummel et al. 2002/ and was partially modified by /Duro et al. 2006/, in reference to the radionuclides thermodynamic data, and in reference to specific aqueous species of iron and sulphur.

The use of this database has limited the capacity of simulating processes such as cation exchange because this database cannot deal with them without including the necessary data into it (which would have needed a complete verification exercise as an indispensable QA requirement). The same problem has been encountered with some specific solubility data (already included and verified in the WATEQ4F database /Auqué et al. 2006, Gimeno et al. 2009/) for some important phases in the groundwater systems under study /Gimeno et al. 2009/.

The first problem has precluded the inclusion of cation exchange processes (known to be effective in the groundwater evolution from the works in the SDM; e.g. /Gimeno et al. 2008, 2009/) in the geochemical calculations. Knowing the importance of cation exchange, the University of Zaragoza group has developed the methodology and software needed to deal with cation exchange from the results provided by the hydrogeologists (mixing proportions). Some scoping calculations have been performed suggesting that these processes would not introduce drastical changes in the results. However, they also evidence that cation exchange processes must be included, at least, as variant cases in future assessments. When more precise data on CEC become available and the SKB thermodynamic data base is upgraded and verified for the simulation of this type of processes, their inclusion in the PA calculation would be straightforward as the methodology is ready.

The second problem has been solved including the necessary solubility data for the mineral phases of interest. However, the consitency of this inclusion has not been extensively verified as it was done with the previous database used in SR-Can.

9.5.4 Coupling between hydrological and geochemical data

Hydrogeological model results have been provided by the hydrogeological team of SKB through the standard QA procedures specified for SR-Site. However two types of hydrological model results have been provided: the mixing proportions of the considered end-members for the Temperate and Submerged under marine water periods and the salinities for the Glacial, Permafrost and submerged under fresh water periods.

Transformation of salinities (without any other data available) in mixing proportions has different uncertainties and, as it has been described in sections 4.1.2 and 5.1(Chapter 4 and 5), several simplified assumptions have been made. With the applied approach, the groundwater composition at the end of the temperate period (calculated from the mixing proportions provided by the SERCO model) does not overly deviate from the initial water of the glacial period (estimated from the salinities given by the TERRASOLVE model) in the bedrock. That is, there is a certain degree of coherence in the link between the two different hydrogeological models used.

However, for future performance assessment, it would be advisable that the hydrological models used for the complete Glacial Cycle would provide homogeneous results (fractions of the reference groundwaters as a result of their models).

9.5.5 Uncertainties associated to some key parameters

The possible contents of certain components (colloids, dissolved and total organic carbon, nitrite, ammonia, acetate, methane and molecular hydrogen) expected over the future evolution of the Laxemar groundwaters have been also assessed in this work. This group of parameters include components for which either the available information is insufficient for a precise quantitative evaluation of their future evolution or cannot be modelled in the same way and with the same tools as the rest of the geochemical parameters in this work.

Most of these parameters are intimately related to the microbial activity conditioning or being conditioned by different redox processes. This fact makes their evaluation a difficult task due to the complexity and the present knowledge of microbial processes in the groundwaters of crystalline systems. Thus, all proposed values have uncertainties and, in some cases, they are especially large. This is the case of DOC, acetate, CH_4, H_2 NO_2^- and NH_4^+ for the Excavation/Operation period, of CH_4 and H_2 for the Glacial period and of DOC for the submerged period.

The value proposed for DOC for the Excavation/Operation period is derived from the inventory of organic materials in the repository /Hallbeck 2010/, excluding the amounts of organic carbon with the bentonite. However, this value is highly uncertain as the degradation rates of organic materials, especially man-made materials, and biodegradability of the organic matter in the bentonite are still poorly known. This uncetainty also propagates to the net amounts of acetate, CH_4 and H_2 derived from organic materials in the repository as they are related through microbiological activities. Also, the NO_2^- and NH_4^+ contents for this period have been impossible to fix or bracket due to the lack of estimations of nitrate contents, the principal source of NO_2^- and NH_4^+ through denitrification. Moreover, the effects of blasting residues (as source of NO_3^-) have to be evaluated.

The values proposed for CH_4 and H_2 during the Glacial period are extrapolated from the highest contents in present groundwaters. The estimation of CH_4 and H_2 concentrations in this period is complicated by the existence of additional processes and different boundary conditions to those present and/or expected in the other periods. The concentration of these gases will be controlled by their production and flow from the deep bedrock and by the active microbial metabolisms (acting as sources and sinks) but also by the impervious frozen layers at the top of the site and by the formation/dissociation of clathrates during permafrost advance and decay. From the preliminary estimations on the fluxes and maximum productions of methane and hydrogen for the Forsmark and Laxemar sites, low contents of these components are expected (e.g. it is not expected an increased sulphide production under ice sheets). However, more data and studies are necessary and, also, the microbiological CH_4 production and consumption rates must be assessed.

DOC values during the submerged period have been extrapolated from the highest DOC values in present-day Forsmark groundwaters with an important marine contribution. The use of present-day groundwaters with a clear Littorina contribution as an expected analogue situation for this period would be reasonable. However, the measured DOC values (up to 2.92 mM) are still subjected to different uncertainties (e.g. contamination during drilling/sampling) and, therefore, they remain uncertain.

10 References

SKB's (Svensk Kärnbränslehantering AB) publications can be found at www.skb.se/publications.

Acero P, Auqué L F, Gimeno M J, Gómez J B, 2010. Evaluation of mineral precipitation potential in a spent nuclear fuel repository. Environmental Earth Sciences, 59, pp 1613–1628.

Ahonen L, Vieno T, 1994. Effects of glacial meltwater on corrosion of copper canisters. Report YJT-94-13, Nuclear Waste Commission of Finnish Power Companies.

Appelo C A J, Postma D, 2005. Geochemistry, groundwater and pollution. 2nd ed. Leiden: Balkema.

Arilahti E, Bojinov M, Mäkelä K, Laitinen T, Saario T, 2000. Stress corrosion cracking investigation of copper in groundwater with ammonium ions. Posiva Working Report 2000-46, Posiva Oy, Finland.

Auqué L F, Gimeno M J, Gómez J B, Puigdomenech I, Smellie J, Tullborg E-L, 2006. Groundwater chemistry around a repository for spent nuclear fuel over a glacial cycle. Evaluation for SR-Can. SKB TR-06-31, Svensk Kärnbränslehantering AB.

Banwart S A, 1999. Reduction of iron(III) minerals by natural organic matter in groundwater. Geochimica et Cosmochimica Acta, 63, pp 2919–2928.

Banwart S A, Gustafsson E, Laaksoharju M, 1999. Hydrological and reactive processes during rapid recharge to fracture zones: the Äspö large scale redox experiment. Applied Geochemistry, 14, pp 873–892.

Barker J D, Sharp M J, Fitzsimons S J, Turner R J, 2006. Abundance and dynamics of dissolved organic carbon in glacier systems. Arctic, Antarctic, and Alpine Research, 38, pp 163–172.

Bath A, 2005. Geochemical investigations of groundwater stability. SKI Report 2006:12, Statens kärnkraftinspekton (Swedish Nuclear Power Inspectorate).

Berger A L, 1978. Long-term variations of daily insolation and Quaternary climatic changes. Journal of the Atmospheric Sciences, 35, pp 2362–2367.

Berger A, Loutre M F, 2002. An exceptionally long interglacial ahead? Science, 297, pp 1287–1288.

Betova I G, Bojinov M S, Heinonen J, Kinnunen P, Lilja C, Saario T, 2005. Development of a rapid screening test for SCC susceptibility of copper in disposal vault conditions. In: Van Iseghem P (ed). Scientific basis for nuclear waste management XXIX: symposium held in Ghent, Belgium, 12–16 September 2005. Warrendale, PA: Materials Research Society. (Materials Research Society Symposium Proceedings 932), pp 821–828.

Birgersson M, Börgesson L, Hedström M, Karnland O, Nilsson U, 2009. Bentonite erosion. Final report. SKB TR-09-34, Svensk Kärnbränslehantering AB.

Brown G H, 2002. Glacier melt water hydrochemistry. Applied Geochemistry, 17, pp 855–883.

Brown G H, Sharp M, Tranter M, 1996. Subglacial chemical erosion: seasonal variations in solute provenance, Haut Glacier d'Arolla, Switzerland. Annals of Glaciology, 22, pp 25–31.

Carman R, Rahm L, 1997. Early diagenesis and chemical characteristics of interstitial water and sediments in the deep deposition bottoms of the Baltic proper. Journal of Sea Research, 37, pp 25–47.

Chapelle F H, 2001. Ground-water microbiology and geochemistry. 2nd ed. New York: John Wiley & Sons.

Choppin G R, Wong P J, 1998. The chemistry of actinide behavior in marine systems. Aquatic Geochemistry, 4, pp 77–101.

Christensen T H, Bjerg P L, Banwart S A, Jakobsen R, Heron G, Albrechtsen H-J, 2000. Characterization of redox conditions in groundwater contaminant plumes. Journal of Contaminant Hydrology, 45, pp 165–241.

Cooper R J, Wadham J L, Tranter M, Hodgkins R, Peters N E, 2002. Groundwater hydrochemistry in the active layer of the proglacial zone, Finsterwalderbreen, Svalbard. Journal of Hydrology, 269, pp 208–223.

Degueldre C, 1994. Colloid properties in groundwaters from crystalline formations. Nagra NTB 92-05, National Cooperative for the Disposal of Nuclear Waste, Switzerland.

Degueldre C, Pfeiffer H-R, Alexander W, Wernli B, Bruestch R, 1996. Colloid properties in granitic groundwater systems. I: Sampling and characterization. Applied Geochemistry, 11, pp 677–695.

Degueldre C, Triay I, Kim J, Vilks P, Laaksoharju M, Miekeley R, 2000. Groundwater colloid properties: a global approach. Applied Geochemistry, 15, pp 1043–1051.

Domènech C, Arcos D, Duro L, Grandia F, 2006. Effect of the mineral precipitation-dissolution at tunnel walls during the operational and post-operational phases. SKB R-06-108, Svensk Kärnbränslehantering AB.

Drake H, Tullborg E-L, 2009. Fracture mineralogy Laxemar. Site descriptive modelling, SDM-Site Laxemar. SKB R-08-99, Svensk Kärnbränslehantering AB.

Drake H, Küsel K, Matthies C, 2006a. Acetogenic prokaryotes. In: Dworkin M, Falkow S, Rosenberg E, Schleifer K-H, Stackebrandt E (eds). The prokaryotes: an evolving electronic resource for the microbiological community. 3rd ed. New York: Springer-Verlag, pp 354–420.

Drake H, Sandström B, Tullborg E-L, 2006b. Mineralogy and geochemistry of rocks and fracture fillings from Forsmark and Oskarshamn: Compilation of data for SR-Can. SKB R-06-109, Svensk Kärnbränslehantering AB.

Drew M C, 1983. Plant injury and adaptation to oxygen de ficiency in the root environment: a review. Plant and Soil, 75, pp 179–199.

Duro L, Grivé M, Cera E, Domènech C, Bruno J, 2006. Update of a thermodynamic database for radionuclides to assist solubility limits calculation for performance assessment. SKB TR-06-17, Svensk Kärnbränslehantering AB.

Follin S, Johansson P-O, Hartley L, Jackson P, Roberts D, Marsic N, 2007a. Hydrogeological conceptual model development and numerical modelling using CONNECTFLOW, Forsmark modelling stage 2.2. SKB R-07-49, Svensk Kärnbränslehantering AB.

Follin S, Levén J, Hartley L, Jackson P, Joyce S, Roberts D, Swift B, 2007b. Hydrogeological characterisation and modelling of deformation zones and fracture domains, Forsmark modelling stage 2.2. SKB R-07-48, Svensk Kärnbränslehantering AB.

Follin S, Hartley L, Jackson P, Roberts D, Marsic N, 2008. Hydrogeological conceptual model development and numerical modelling using CONNECTFLOW, Forsmark modelling stage 2.3. SKB R-08-23, Svensk Kärnbränslehantering AB.

Frape S K, Stotler R L, Ruskeeniemi T, Ahonen L, Paananen M, Hobbs M Y, 2004. Hydrogeochemistry of groundwaters at and below the base of the permafrost at Lupin: Report of phase II. Technical report 06819-REP-01300-10047-R00, Ontario Power Generation, Nuclear Waste Management Division, Canada.

Gabriel U, Gaudet J-P, Spadini L, Charlet L, 1998. Reactive transport of uranyl in a goethite column: an experimental and modeling study. Chemical Geology, 151, pp 107–128.

Gascoyne M, 1999. Long-term maintenanceof reducing conditions in a spent nuclear fuel repository. A re-examination of critical factors. SKB R-99-41, Svensk Kärnbränslehantering AB.

Gascoyne M, 2004. Hydrogeochemistry, groundwater ages and sources of salts in a granitic batholith on the Canadian Shield, southeastern Manitoba. Applied Geochemistry, 19, pp 519–560.

Gascoyne M, Thomas D A, 1997. Impact of blasting on groundwater composition in a fracture in Canada's Underground Research Laboratory. Journal of Geophysical Research, 102 (B1), 573–584.

Geipel G, Brachmann A, Brendler V, Bernhard G, Nitsche H, 1996. Uranium(VI) sulfate complexation studied by time-resolved laser-induced fluorescence spectroscopy (TRLFS). Radiochimica Acta, 75, pp 199–204.

Gimeno M J, Auqué L F, Gómez J, Acero P, 2008. Water-rock interaction modelling and uncertainties of mixing modelling. SDM-Site Forsmark. SKB R-08-86, Svensk Kärnbränslehantering AB.

Gimeno M J, Auqué L F, Gómez J, Acero P, 2009. Water-rock interaction modelling and uncertainties of mixing modelling. Site descriptive modelling, SDM-Site Laxemar. SKB R-08-110, Svensk Kärnbränslehantering AB.

Gimeno M J, Auqué L, Gómez J, Salas J, Molinero J, 2010. Hydrochemical evolution of the Laxemar site. SKB R-10-60, Svensk Kärnbränslehantering AB.

Gómez J B, Laaksoharju M, Skårman E, Gurban I, 2009. M3 version 3.0: Verification and validation. SKB TR-09-05, Svensk Kärnbränslehantering AB.

Grandia F, Domènech C, Arcos D, Duro L, 2006. Assessment of the oxygen consumption in the back fill. Geochemical modelling in a saturated backfill. SKB R-06-106, Svensk Kärnbränslehantering AB.

Grenthe I, Stumm W, Laaksoharju M, Nilsson A C, Wikberg P, 1992. Redox potentials and redox reactions in deep groundwaters systems. Chemical Geology, 98, pp 131–150.

Grivé M, Domènech C, Motoya V, García D, Duro L, 2010. Determination and assessment of the concentration limits to be used in SR-Can. Supplement to TR-06-32. SKB R-10-50, Svensk Kärnbränslehantering AB.

Hallbeck L, 2009. Microbial processes in glaciers and permafrost. A literature study on microbiology affecting groundwater at ice sheet melting. SKB R-09-37, Svensk Kärnbränslehantering AB.

Hallbeck L, 2010. Principal organic materials in a repository for spent nuclear fuel. SKB TR-10-19, Svensk Kärnbränslehantering AB.

Hallbeck L, Pedersen K, 2008a. Explorative analyses of microbes, colloids and gases. SKB R-08-85, Svensk Kärnbränslehantering AB.

Hallbeck L, Pedersen K, 2008b. Explorative analysis of microbes, colloids and gases together with microbial modelling. Site description model. SDM-Site Laxemar. SKB R-08-109, Svensk Kärnbränslehantering AB.

Hallbeck L, Pedersen K, 2008c. Characterization of microbial processes in deep aquifers of the Fennoscandian Shield. Applied Geochemistry, 23, pp 1796–1819.

Hallbeck L, Grivé M, Gaona X, Duro L, Bruno J, 2006. Main organic materials in a repository for high level radioactive waste. SKB R-06-104, 64 pp, Svensk Kärnbränslehantering AB.

Hallberg G R, Keeney D R, 1993. Nitrate. In: Alley W M (ed). Regional ground-water quality. New York: Van Nostrand Reinhold, pp 297–322.

Hansen L K, Jakobsen R, Postma D, 2001. Methanogenesis in a shallow sandy aquifer, Rømø, Denmark. Geochimica et Cosmochimica Acta, 65, pp 2925–2935.

Hartikainen J, Kouhia R, Wallroth T, 2010. Permafrost simulations at Forsmark using a numerical 2D thermo-hydro-chemical model. SKB TR-09-17, Svensk Kärnbränslehantering AB.

Hedqvist I, Degueldre C, 2008. Oskarshamn site investigation. Granitic groundwater colloids sampling and characterisation. Colloids analysis from KLX17A (416.0 to 437.5 m) and KLX15A (623.0 to 634.5 m). SKB P-08-101, Svensk Kärnbränslehantering AB.

Heimann A, Jakobsen R, Blodau C, 2010. Energetic constraints on H_2-dependent terminal electron accepting processes in anoxic environments: a review of observations and model approaches. Environmental Science & Technology, 44, pp 24–33.

Heuer V B, Pohlman J W, Torres M E, Elvert M, Hinrichs K-W, 2009. The stable carbon isotope biogeochemistry of acetate and other dissolved carbon species in deep subseafloor sediments at the northern Cascadia Margin. Geochimica et Cosmochimica Acta, 73, pp 3323–3336.

Hoehler T M, Alperin M J, Albert D B, Martens C S, 1998. Thermodynamic control on hydrogen concentrations in anoxic sediments. Geochimica et Cosmochimica Acta, 62, pp 1745–1756.

Hoehler T M, Albert D B, Alperin M J, Martens C S, 1999. Acetogenesis from CO_2 in an anoxic marine sediment. Limnology and Oceanography, 44, pp 662–667.

Hummel W, Berner U, Curti E, Pearson F J, Thoenen T, 2002. Nagra/PSI Chemical thermodynamic data base 01/01. Boca Raton: Universal Publishers.

Ikeda B M, Litke C D, 2000. The effect of oxidant flux, nitrite concentration and chloride concentration on the stress corrosion cracking behaviour of non-welded and electronbeam welded copper. Report 06819-REP-01200-10049-R00, Ontario Power Generation, Nuclear Waste Management Division, Canada.

Ikeda B M, Litke C D, 2004. Status report for 2003 on stress corrosion cracking of OFP copper in ammonia. Report 06819-REP-01300-10078-R00, Ontario Power Generation, Nuclear Waste Management Division, Canada.

Ikeda B M, Litke C D, 2007. Stress corrosion cracking of copper in nitrite/chloride mixtures at elevated temperatures. NWMO TR-2007-04, Nuclear Waste Management Organization, Canada.

IPCC, 2001. Climate Change 2001: synthesis report. Contribution of Working Groups I, II, and III to the Third Assessment Report of the Intergovernmental Panel on Climate Change. Watson R T, the Core Writing Team (eds). Cambridge: Cambridge University Press.

IPCC, 2007. Climate Change 2007: the physical science basis. Contribution of Working Group I to the Fourth Assessment Report of the Intergovernmental Panel of Climate Change, 2007. Solomon S, Qin D, Manning M, Chen Z, Marquis M, Averyt K B, Tignor M, Miller H L (eds). Cambridge: Cambridge University Press.

Jakobsen R, Cold L, 2007. Geochemistry at the sulfate reduction–methanogenesis transition zone in an anoxic aquifer – A partial equilibrium interpretation using 2D reactive transport modeling. Geochimica et Cosmochimica Acta, 71, pp 1949–1966.

Jockwer N, Wieczorek K, 2003. Gas generation measurements in the FEBETX project. (Abstract). In: Clays in natural and engineered barriers for radioactive waste confinement: proceedings from the international meeting held in Reims, 9-12 December 2002. Châtenay-Malabry: Agence nationale pour la gestion des déchets radioactifs (ANDRA), pp 108–117.

Joyce S, Simpson T, Hartley L, Applegate A, Hoek J, Jackson P, Swan D, Marsic M, Follin S, 2010. Groundwater flow modelling of periods with temperate climate conditions – Forsmark. SKB R-09-20, Svensk Kärnbränslehantering AB.

Kehew A E, 2001. Applied chemical hydrogeology. Upper saddle River, NJ: Prentice Hall.

King F, 2007. Status of the understanding of used fuel container corrosion processes. Summary of current knowledge and gap analysis. NWMO TR-2007-09, Nuclear Waste Management Organization, Canada.

King F, Ahonen L, Taxén C, Vuorinen U, Werme L, 2001. Copper corrosion under expected conditions in a deep geologic repository. SKB TR-01-23, Svensk Kärnbränslehantering AB.

King G M, 1991. Measurement of acetate concentrations in marine pore waters by using an enzymatic approach. Applied and Environmental Microbiology, 57, pp 3476–3481.

King-Clayton L, Chapman N, Ericsson L O, Kautsky F (eds), 1997. Glaciation and hydrogeology. Proceedings of the workshop on the impact of climate change & glaciations on rock stresses, groundwater flow and hydrochemistry: past, present and future. Hässelby, Sweden, 17–19 April 1996. SKI Report 97:13, Statens kärnkraftinspektion (Swedish Nuclear Power Inspectorate).

Kinnunen P, 2006. Stress corrosion cracking investigation of copper in groundwater with acetate ions. Posiva Working Report 2006-18, Posiva Oy, Finland.

Kjellström E, Strandberg G, Brandefelt J, Näslund J-O, Smith B, Wohlfarth B, 2009. Climate conditions in Sweden in a 100,000 year time perspective. SKB TR-09-04, Svensk Kärnbränslehantering AB.

Koizumi Y, Kojima H, Oguri K, Kitazato H, Fukui M, 2004. Vertical and temporal shifts in microbial communities in the water column and sediment of saline meromictic Lake Kaiike (Japan), as determined by a 16S rDNA-based analysis, and related to physicochemical gradients. Environmental Microbiology, 6, pp 622–637.

Konhauser K, 2007. Introduction to geomicrobiology. Oxford: Blackwell.

Kotelnikova S, 2002. Microbial production and oxidation of methane in deep subsurface. Earth-Science reviews, 58, pp 367–395.

Laaksoharju M, Wallin B, 1997. Evolution of the groundwater chemistry at the Äspö Hard Rock Laboratory. Proceedings of the second Äspö International Geochemistry Workshop, Äspö, Sweden, 6–7 June 1995. SKB HRL International Cooperation Report ICR 97-04, Svensk Kärnbränslehantering AB.

Laaksoharju M, Degueldre C, Skårman C, 1995. Studies of colloids and their importance for repository performance assessment. SKB TR 95-24, Svensk Kärnbränslehantering AB.

Laaksoharju M, Smellie J, Tullborg E-L, Gimeno M, Hallbeck L, Molinero J, Waber N, 2008. Bedrock hydrogeochemistry Forsmark. Site descriptive modelling, SDM-Site Forsmark. SKB R-08-47, Svensk Kärnbränslehantering AB.

Laaksoharju M, Smellie J, Tullborg E-L, Wallin B, Drake H, Gascoyne M, Gimeno M, Gurban I, Hallbeck L, Molinero J, Nilsson A-C, Waber N, 2009. Bedrock hydrogeochemistry Laxemar. Site descriptive model. SDM-Site Laxemar. SKB R-08-93, Svensk Kärnbränslehantering AB.

Lin L-H, Slater G F, Sherwood Lollar B, Lacrampe-Couloume G, Onstott T C, 2005. The yield and isotopic composition of radiolytic H2, a potential source for deep subsurface biosphere. Geochimica et Cosmochimica Acta, 69, pp 893–903.

Litke C D, Ikeda B M, 2006. The effect of acetate concentration, chloride concentration, and applied current on stress corrosion cracking of OFP copper. Report 06819-REP-01300-10005-R00, Ontario Power Generation, Nuclear Waste Management Division, Canada.

Lovley D R, Goodwin S, 1988. Hydrogen concentrations as an indicator of the predominant terminal electron-accepting reactions in aquatic sediments. Geochimica et Cosmochimica Acta, 52, pp 2993–3003.

Luna M, Arcos D, Duro L, 2006. Effects of grouting, shotcreting and concrete leachates on backfill geochemistry. SKB R-06-107, Svensk Kärnbränslehantering AB.

Martinerie P, Raynaud D, Etheridge D M, Barnola J-M, Mazaudier D, 1992. Physical and climatic parameters which influence the air content in polar ice. Earth and Planetary Science Letters, 112, pp 1–13.

Martino J B, Kozak E, Woodcock D, Stroes-Gascoyne S, 2004. The blast damage assessment project at the URL. Ontario Power Generation, Nuclear Waste Management Division Report 06819-REP-01200-10123-R00. Toronto, Canada.

McCarthy J F, Czerwinski K R, Sanford W E, Jardine P M, Marsh J D, 1998. Mobilization of transuranic radionuclides from disposal trenches by natural organic matter. Journal of Contaminant Hydrology, 30, pp 49–77.

Mitchell A C, Brown G H, 2007. Diurnal hydrological – physicochemical controls and sampling methods for minor and trace elements in an Alpine glacial hydrological system. Journal of Hydrology, 332, pp 123–143.

Molinero-Huguet J, Samper-Calvete F J, Zhang G, Yang C, 2004. Biogeochemical reactive transport model of the Redox Zone experiment of the Äspö Hard Rock Laboratory in Sweden. Nuclear Technology, 148, pp 151–165.

Nilsson A-C, Degueldre C, 2007. Forsmark site investigation. Granitic groundwater colloids sampling and characterisation. SKB P-07-169, Svensk Kärnbränslehantering AB.

Nordstrom D K, Ball J W, Donahoe R J, Whittemore D, 1989. Groundwater chemistry and water-rock interactions at Stripa. Geochimica et Cosmochimica Acta, 53, pp 1727–1740.

Parkhurst D L, Appelo C A J, 1999. User's guide to PHREEQC (version 2): a computer program for speciation, batch-reaction, one-dimensional transport and inverse geochemical calculations. Denver, Co: U.S. Geological Survey. (Water resources investigations report 99-4259)

Pastina B, Hellä P, 2006. Expected evolution of a spent nuclear fuel repository at Olkiluoto. Posiva 2006-05, Posiva Oy, Finland.

Pedersen K, 1993. The deep subterranean biosphere. Earth-Science Reviews, 34, pp 243–260.

Pedersen K, 1997a. Microbial life in deep granitic rock. FEMS Microbiology Reviews, 20, pp 399–414.

Pedersen K, 1997b. Investigations of subterranean microorganisms and their importance for performance assessment of radioactive waste disposal. Results and conclusions achieved during the period 1995 to 1997. SKB TR 97-22, Svensk Kärnbränslehantering AB.

Pedersen K, 2001. Diversity and activity of microorganisms in deep igneous rock aquifers of the Fennoscandian Shield. In: Fredrickson J K, Fletcher M (eds). Subsurface microbiology and biogeochemistry. Chichester: Wiley, pp. 97–139.

Pedersen K, 2006. Microbiology of transitional groundwater of the porous overburden and underlying fractured bedrock aquifers in Olkiluoto, Finland. Posiva Working Report 2006-09, Posiva Oy, Finland.

Pedersen K, 2008. Microbiology of Olkiluoto groundwater, 2004–2006. Posiva 2008-02, Posiva Oy, Finland.

Pedersen K, Kennedy C, Nederfeldt K-G, Bergelin A, 2004. Äspö Hard Rock Laboratory. Prototype repository. Chemical measurements in buffer and backfill; sampling and analyses of gases. SKB IPR-04-26, Svensk Kärnbränslehantering AB.

Pitkänen P, Partamies S, 2007. Origin and implications of dissolved gases in groundwater at Olkiluoto. Posiva 2007-04, Posiva Oy, Finland.

Pitkänen P, Luukkonen A, Ruotsalainen P, Leino-Forsman H, Vuorinen U, 1999. Geochemical modelling of groundwater evolution and residence time at the Olkiluoto site. Posiva 98-10, Posiva Oy, Finland.

Pitkänen P, Partamies S, Luukkonen A, 2004. Hydrogeochemical interpretation of baseline groundwater conditions at the Olkiluoto site. Posiva 2003-07, Posiva Oy, Finland.

Postma D, Jakobsen R, 1996. Redox zonation: Equilibrium constraints on the Fe(III)/SO4-reduction interface. Geochimica et Cosmochimica Acta, 60, pp 3169–3175.

Puigdomenech I (ed), 2001. Hydrochemical stability of groundwaters surrounding a spent nuclear fuel repository in a 100,000 year perspective. SKB TR-01-28, Svensk Kärnbränslehantering AB.

Rhén I, Follin S, Hermanson J, 2003. Hydrological Site Descriptive Model – a strategy for its development during Site Investigations. SKB R-03-08, Svensk Kärnbränslehantering AB.

Rivett M O, Buss S R, Morgan P, Smith J W N, Bemmen C D, 2008. Nitrate attenuation in groundwater: A review of biogeochemical controlling processes. Water Research, 42, pp 4215-4232.

Ruskeeniemi T, Ahonen L, Paananen M, Frape S, Stotler R, Hobbs M, Kaija J, Degnan P, Blomqvist R, Jensen M, Lehto K, Moren L, Puigdomenech I, Snellman M, 2004. Permafrost at Lupin: report of Phase II. Report YST-119, Geological Survey of Finland, Nuclear Waste Disposal Research.

Sanding A, Bruno J, 1992. The solubility of (UO2)3(PO4)2•4H2O and the formation of U(VI) phosphate complexes: their influence in uranium speciation in natural waters. Geochimica et Cosmochimica Acta , 56, pp 4135–4145.

Sandström B, Tullborg E-L, 2006. Mineralogy, geochemistry, porosity and redox capacity of altered rock adjacent to fractures. Forsmark site investigation. SKB P-06-209, Svensk Kärnbränslehantering AB.

Sandström B, Tullborg E-L, Smellie J, McKenzie A, Suksi J, 2008. Fracture mineralogy of the Forsmark site SDM-Site Forsmark. SKB R-08-102, Svensk Kärnbränslehantering AB.

Selnert E, Byegård J, Widestrand H, 2008. Forsmark site investigation. Laboratory measurements within the site investigation programme for the transport properties of the rock. Final report. SKB P-07-139, Svensk Kärnbränslehantering AB.

Selroos J-O, Follin S, 2010. SR-Site groundwater flow modelling methodology, setup and results. SKB R-09-22, Svensk Kärnbränslehantering AB.

Sherwood Lollar B, Voglesonger K, Lin L-H, Lacrampe-Couloume C, Telling J, Abrajano T A, Onstott T C, Pratt L M, 2007. Hydrogeologic controls on episodic H2 release from precambrian fractured rocks – energy for deep subsurface life on Earth and Mars. Astrobiology, 7, pp 971–986.

Silver W L, Lugo A E, Keller M, 1999. Soil oxygen availability and biogeochemistry along rainfall and topographic gradients in upland wet tropical forest soils. Biogeochemistry, 44, pp 301–328.

SKB, 2005a. Hydrogeochemical evaluation. Preliminary site description. Forsmark area – version 1.2. SKB R-05-17, Svensk Kärnbränslehantering AB.

SKB, 2005b. Preliminary site description. Forsmark area – version 1.2. SKB R-05-18, Svensk Kärnbränslehantering AB.

SKB, 2006a. Long-term safety for KBS-3 repositories at Forsmark and Laxemar – a first evaluation. Main report of the SR-Can project. SKB TR-06-09, Svensk Kärnbränslehantering AB.

SKB, 2006b. Fuel and canister process report for the safety assessment SR-Can. SKB TR-06-22, Svensk Kärnbränslehantering AB.

SKB, 2006c. Site descriptive modelling Forsmark stage 2.1. Feedback for completion of the site investigation including input from safety assessment and repository engineering. SKB R-06-38, Svensk Kärnbränslehantering AB.

SKB, 2006d. Geosphere process report for the safety assessment SR-Can. SKB TR-06-19, Svensk Kärnbränslehantering AB.

SKB, 2010. Geosphere process report for the safety assessment SR-Site. SKB TR-10-48, Svensk Kärnbränslehantering AB.

Smellie J, Tullborg E-L, Nilsson A-C, Sandström B, Waber N, Gimeno M, Gascoyne M, 2008. Explorative analysis of major components and isotopes. SDM-Site Forsmark. SKB R-08-84, Svensk Kärnbränslehantering AB.

Stotler R L, Frape S K, Ruskeeniemi T, Ahonen L, Onstott T, Hobbs M Y, 2009. Hydrogeochemistry of groundwaters in and below the base of thick permafrost at Lupin, Nunavut, Canada. Journal of Hydrology, 373, pp 80–95.

Stroes-Gascoyne S, Gascoyne M, 1998. The introduction of microbial nutrients into a nuclear waste disposal vault during excavation and operation. Environmental Science and Technology, 32, pp 317–325.

Svensson U, Follin S, 2010. Groundwater flow modelling of the excavation and operation periods – Forsmark. SKB R-09-19, Svensk Kärnbränslehantering AB.

Tranter M, Sharp M J, Lamb H R, Brown G H, Hubbard B P, Willis I C, 2002. Geochemical weathering at the bed of Haut Glacier d'Arolla, Switzerland: a new model. Hydrological Processes, 16, pp 959–993.

Trotignon L, Michaud V, Lartigue J-E, Ambrosi J-P, Eisenlohr L, Griffault L, de Combarieu M, Daumas S, 2002. Laboratory simulation of an oxidizing perturbation in a deep granite environment. Geochimica et Cosmochimica Acta, 66, pp 2583–2601.

Tullborg E-L, 1997. How do we recognize remants of glacial water in bedrock?. In: King-Clayton L, Chapman N, Ericsson L O, Kautsky F (eds). Glaciation and hydrogeology. Proceedings of the workshop on the impact of climate change & glaciations on rock stresses, groundwater flow and hydrochemistry: past, present and future, Hässelby, Sweden, 17–19 April 1996. SKI Report 97:13, Statens kärnkraftinspektion (Swedish Nuclear Power Inspectorate).

Tullborg E-L, Drake H, Sandström B, 2008. Palaeohydrogeology: a methodology based on fracture mineral studies. Applied Geochemistry, 23, pp 1881–1897.

Tullborg E-L, Smellie J, Nilsson A C, Gimeno M J, Auqué L F, Brüchert V, Molinero J, 2010. SR-Site – sulphide content in the groundwater at Forsmark. SKB TR-10-39, Svensk Kärnbränslehantering AB.

Vidstrand P, Svensson U, Follin S, 2006. Simulation of hydrodynamic effects of salt rejection due to permafrost. Hydrogeological numerical model of density-driven mixing, at a regional scale, due to a high salinity pulse. SKB R-06-101, Svensk Kärnbränslehantering AB.

Vidstrand P, Follin S, Zugec N, 2010. Groundwater flow modelling of periods with periglacial and glacial climate conditions – Forsmark. SKB R-09-21, Svensk Kärnbränslehantering AB.

Vilks P, Miller H, Doern D C, 1991. Natural colloids and suspended particles in the Whiteshell Research area, Manitoba, Canada, and their potential effect on radiocolloid formation. Applied Geochemistry, 8, pp 565–574.

Wallin B, 1995. Paleohydrological implications in the Baltic area and its relation to the groundwater at Äspö, south-eastern Sweden. A literature study. SKB TR 95-06, Svensk Kärnbränslehantering AB.

Wellsbury P, Parkes R J, 1995. Acetate bioavailability and turnover in a estuarine sediment. FEMS Microbiology Ecology, 17, pp 85–94.

Wersin P, Bruno J, Laaksoharju M, 1994. The implications of soil acidification on a future HLW repository. Part II: Influence on deep granitic groundwater. The Klipperas study site as test case. SKB TR 94-31, Svensk Kärnbränslehantering AB.

Wold S, 2010. Sorption of prioritized elements on montmorillonite colloids and their potential to transport radionuclides. SKB TR-10-20, Svensk Kärnbränslehantering AB.

Öhman J, Follin S, 2010. Site investigation SFR. Hydrogeological modelling of SFR. Model version 0.2. SKB R-10-03, Svensk Kärnbränslehantering AB.

Example of the calculation procedure

In this section, the methodology used in the process of calculation has been synthesized. This methodology (and the associated programs) has been mainly developed by the University of Zaragoza (UNIZAR), and consists in:

1) slice selection from the hydrological data, using the program "Select data v4.exe",

2) creation of the input files for PHREEQC with the selected data (mixing and mineral equilibrium),

3) running PHREEQC,

4) creation of the tabulated output, selecting key parameters, and

5) statistical analysis and postprocessing.

A1.1   List of the hydrological files that have been used for the geochemical calculations

A1.1.1   Temperate period

Base case

SRS_HCD2h100A2b_HRD5r1_phi7F_HSD5d_IC4Mat_MD2_MOW_RMD1000_exp_save_chemistry_2000.val

SRS_HCD2h100A2b_HRD5r1_phi7F_HSD5d_IC4Mat_MD2_MOW_RMD1000_exp_save_chemistry_3000.val

SRS_HCD2h100A2b_HRD5r1_phi7F_HSD5d_IC4Mat_MD2_MOW_RMD1000_exp_save_chemistry_5000.val

SRS_HCD2h100A2b_HRD5r1_phi7F_HSD5d_IC4Mat_MD2_MOW_RMD1000_exp_save_chemistry_9000.val

Hydrological variant cases. Cases 5 and 9

SRS_HCD2hr5_HRD5r5_phi7F_HSD5d_IC4Mat_MD2_MOW_RMD1000_exp_savechemistry_2000.val

SRS_HCD2hr9_HRD5r9_phi7F_HSD5d_IC4Mat_MD2_MOW_RMD1000_exp_savechemistry_2000.val

Hydrological variant cases. Extended heterogeneity

100223_SRS_HCD2h100A2b_HRD5r1-ext_het_ph7F_HSD5d_IC4Mat_MD2_MD2_MOW_RMD1000_exp_save_chemistry_2000.val

100223_SRS_HCD2h100A2b_HRD5r1-ext_het_ph7F_HSD5d_IC4Mat_MD2_MD2_MOW_RMD1000_exp_save_chemistry_3000.val

100223_SRS_HCD2h100A2b_HRD5r1-ext_het_ph7F_HSD5d_IC4Mat_MD2_MD2_MOW_RMD1000_exp_save_chemistry_5000.val

100223_SRS_HCD2h100A2b_HRD5r1-ext_het_ph7F_HSD5d_IC4Mat_MD2_MD2_MOW_RMD1000_exp_save_chemistry_9000.val

A1.1.2 Glacial cycle. Unfrozen soil

Initial temperate

Chem_Forsmark_0.txt

Glacier advance

Chem_Forsmark_I.txt
Chem_Forsmark_II.txt
Chem_Forsmark_III.txt
Chem_Forsmark_IV.txt
Chem_Forsmark_Va.txt

Glacier retreat

Chem_Forsmark_Vr.txt
Chem_Forsmark_IVr.txt
Chem_Forsmark_IIr.txt

Final temperate. Submerged under a lake of glacial melt waters

Chem_Forsmark_0r.txt

Hydrological variant case. Advance N-S

Chem_Forsmark_vNS_IIa.txt
For_vNS_SDM_covered(iceIVa)_xyzpss.txt

A1.1.3 Glacial cycle. Permafrost

Periglacial conditions

xyzpss_IP_permIFL0.txt

Glacier advance

xyzpss_IP_permI.txt
xyzpss_IP2_permII.txt
xyzpss_IP4_permIV.txt

A1.1.4 Submerged saline period

SRS_HCD2h100A2b_HRD5r1_phi7F_HSD5d_IC4Mat_MD2_MOW_RMD1000_exp_save_
chemistry_3000BC.val

A1.2 Slice extraction using the program "Select data v4.exe"

This program selects subsets of data points from the hydrogeological files. These subsets can be planes perpendicular to the X, Y or Z co-ordinate, vertical planes (Z-planes) with any orientation, or sets of points defined by a horizontal polygonal boundary. In each case, different options for their selection are available.

First, one of the input hydro files (corresponding to one site and one year) is selected. Then, the format of the hydro file (x y z + data, Serco-2009, Serco-2006, Serco-2004, Colenco, TerraSolve) is specified. Finally, the subset of data to extract ("Action to take", Figure A1-1) is chosen.

Option "run" starts the program and creates a new file with the word "cut" added to the original name, containing the extracted subset of data points in a comma-separated format.

The files with the extracted data subsets are named as indicated above: L or F for the site, then the year, and then de type of section.

Once the files with the extracted subsets have been created, and before using them in the pqi creator interface program, they must be edited to modify the column headings by removing the explanations and leaving each title separated by a space from the next one.

These files are the input files for all the geochemical calculations performed with PHREEQC.

The options for the slices (subsets of data points to be extracted) are described in the next sections.

A1.2.1 "Selection based on a X, Y or Z plane"

It creates slices based on coordinates N-S, E-W and depth. We will use this option to extract the horizontal plane (Z-plane) at the repository depth. Figure A1-1 shows how to select a set of points in a specific interval (± 60 m) at the repository depth (–470 in the case of Forsmark).
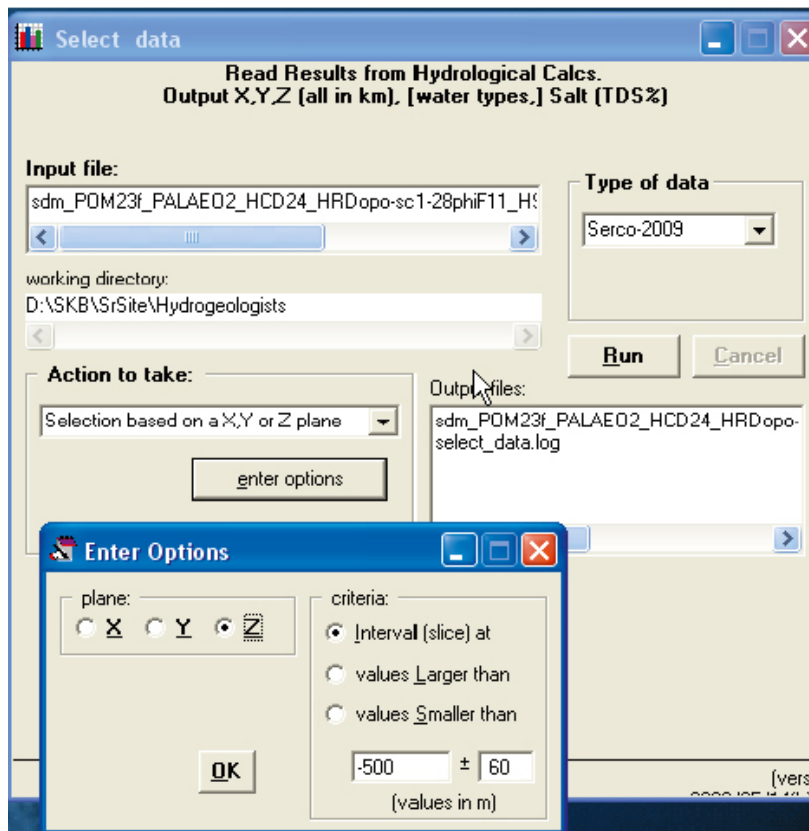
Figure A1-1. *Example of the first window when running Select_data_v4.exe for the selection of different types of subsets.*

A1.2.2 "Use an X-Y boundary"

This option extracts all data points inside a specified closed horizontal boundary. It is very useful when the user wants to limit the set of points to those inside the repository volume. In this particular case (the one used for most of the calculations in the SR-Site base case) the procedure consists of two steps: (a) extraction of the slice at the desired depth (–470 m for Forsmark); and (b) the slice just created is selected as the new input file (F_2000.470.val in the example shown in Figure A1-2; the file name indicates that data are from Forsmark for the year 2,000), using "x y z + data" as Type of data and indicating the number of columns after the coordinates; then the option X-Y boundary is selected and the program asks for a file with the x-y coordinates of the boundary (Figure A1-2).

The boundary files for the repository volumes of Forsmark are

* 1,630.62, 6,701.17, –0.47,
* 1,633.37, 6,701.17, –0.47,
* 1,633.37, 6,698.90, –0.47,
* 1,630.62, 6,698.90, –0.47.

All points with a depth between –490 and –450 m were selected.

A1.2.3 "Select a vertical plane based on a line"

This option creates a vertical cross section at any user-defined orientation. We have used this option to create vertical sections through the repository volume and parallel or perpendicular to the coast. Apart from asking for the coordinates of the plane, the program also asks for an error range (in meters) and if the user wants to have the data projected onto the extraction plane (to which you must say yes). The vertical planes used in SR-Site for Forsmark are the followings (Figure A1-3):

* NW: 1,628,519 m / 6702421,
* SE: 1,636,272 m / 6694615.

When this option is used, apart from the data already contained in the hydrogeological file, the program adds an additional column with the distance along the line. This distance is used to plot the points instead of the X and Y coordinates.
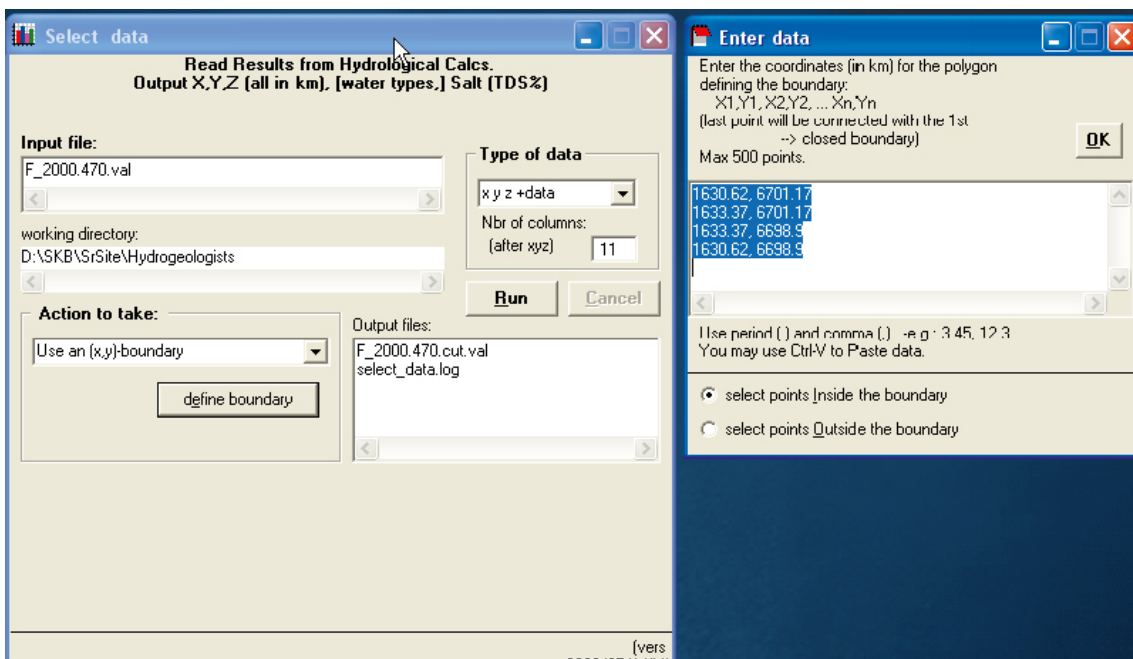
Figure A1-2. *Another example of the Select data program when the choice is an area inside an area. When clicking on "define boundary" the program opens the window on the right, and the coordinates of the vertices must be indicated there.*
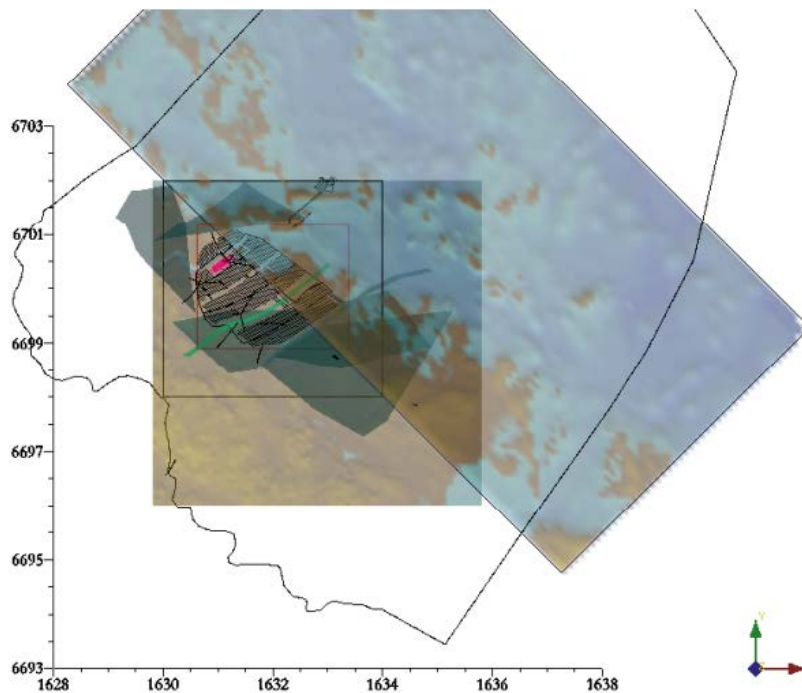
Figure A1-3. *Example of the area selected for Forsmark and the location of the vertical plane.*

An additional question that should be taken into account when selecting vertical planes is that the hydrogeological results for the whole volume include points down to 2,500 m depth and we will only use data down to 1,000 m, in the case of Forsmark. The rows corresponding to points below those depths can be removed later inside the specific plotting software (e.g. Origin).

A1.3   Salinity transformation into mixing proportions ("Salinity2Mixprop.exe") in the case of the glacial cycle

In the case of the TerraSolve models (glacial cycle), they are expressed chemical compositions as salinities values for each data point. They must be transformed in files with mixing proportions for each point. It is the only way to couple these results with the geochemical model PHREEQC using the software generated for the SR-Can. They will be used (as for the temperate period) to create input files for PHREEQC, in order to obtain the detailed chemical composition at each point. So, the main difference with respect to the temperate period calculations is the transformation of salinities into mixing proportions.

The specific procedure is explained below. Run the program "Salinity2Mixprop.exe":

1. The program first asks whether the file to be transformed corresponds to the first time slice or not:
    First time slice (y/n)?

If the answer is YES (y) the program will calculate the mixing proportions based only on the salinity values at that time (t=0).

2. Then it asks for the name of the file with the slice extracted from the hydro files:
    Hydro-data file name (< 40 characters)?
    Eg: .....V0F_sal_0_vert.txt

3. Next it asks for the number of columns with coordinates. This number is 3 for horizontal slices and 4 for vertical slices (with the distance along the projection line added as a new column, see above).
    Number of columns with co-ordinates
    Enter the number 3 or 4 (4 in the example as it is a vertical plane)

4. The program then echoes a message with the number of samples read from the hydro file:

E.g. 20672 samples read

and produces an output file with the mixing proportions in the points of the selected slice.

Eg: ..... V0F_sal_0_vert.txt.res

If the answer to the first question is **NO** (n), the program understands that the slice under calculation corresponds to a state (I, II, III, etc.) different from the initial state (0), and then it proceeds to compare the salinity in the new state with the salinity in the previous time. Therefore, the program asks for the name of the file under calculation (time t):

Hydro-data file for time t (< 40 characters)?

Eg: ..... V1F_sal_I_vert.txt

And then, it asks for the name of the file with the mixing proportions obtained in the previous time period (time t-1):

Mixprop file for time t-1 (< 40 characters)?

Eg: ..... V0F_sal_0_vert.txt.res

The program then echoes a message with the number of samples read from both files (it must be the same; otherwise the programs ends with an error message):

E.g. 20672 samples read

and produces an output file with the mixing proportions in the points of the selected slice.

Eg: ..... V1F_sal_I_vert.txt.res

Now these output files have the same structure as the files provided by the hydrogeologists with the CONNECTFLOW for the temperate period. Therefore, they can be used to create the input files for PHREEQC (pqi_mp.exe). The procedure to perform the PHREEQC calculations and select the output is the same already explained for the temperate case.

A1.4   Creation of the input file for PHREEQC

As explained above, from the original hydrogeological data file, two data subsets are extracted:

a) the subset with the data points in the repository volume (at repository depth –470 m at Forsmark), and

b) a vertical slice approximately parallel to the general coast trend.

These subsets, with the mixing proportions for each data point, are then used to create input files for PHREEQC in order to obtain the detailed chemical composition at each point. The specific procedure is explained below. The following methodology will be used once we know the end-member ratios for each point. This information is obtained directly from the hydrological calculations (for the Temperate and Submerged periods, SERCO), or applying the methodology described in the Section 4.1 from the TerraSolve hydrological models (Glacial period).

Two different types of simulations with PHREEQC can be considered:

(1) mixing (including aqueous reactions), and

(2) mixing and reaction (including equilibrium with minerals).

In our case, only the second option will be applied. This type of simulation is a better approximation to what is actually happening in the system as it considers the re-equilibration of groundwaters with specific minerals, as it has been found in the geochemical modelling of the SDM.

Figure A1-4. *Running pqi_mp.exe.*

The program to create the corresponding PHREEQC input pqi file is "pqi_mp.exe" (Figure A1-4):

1. The program requests the type of simulation (only mixing or mixing and reaction):

   Mixing (M) or mixing+reaction (R)?

   Enter "R" in this case

2. Then it asks for the name of the file containing the extracted slice from the hydro file:

   Hydro-data file name (< 40 characters)?

   e.g. "2000.dat"

3. Next it asks for the number of columns with coordinates. This number is 3 for horizontal slices and 4 for vertical slices (with the distance along the projection line added as a new column, see above)

   Number of columns with co-ordinates

   Enter the number 3 or 4

4. The program then echoes a message with the number of samples read from the hydro file:

   E.g. 65237 samples read

5. The next question requests the user to define the maximum number of samples to be put onto each output file (preventing this way memory problems with too long PHREEQC output files).

   Maximum number of samples per output file

   The suitable number of samples depends also on the type of simulation to be done, as the more complex a simulation is (mixing + reaction + exchange) the bigger (in size) is the file created by PHREEQC.

   E.g., 70000.

6. The program then echoes the number of pqi files that will be created. For example, in the case shown here, the hydro file has 65,237 samples, so we select 70,000 as the maximum number of samples per file to get only one output file.

   Maximum number of samples per output file

   70000

   Warning: 1 output files will be created

7. The above message is important as it gives the number of files corresponding to each simulation. Let call this number *k*.

8. Then, the program asks for the name of the file containing the chemical composition of the end members (see section A1.7.1).

End-member file name (< 40 characters)?

At this point, one must be aware of the type of simulation that is being performed (coupled or uncoupled data base) and the site being analysed (Laxemar or Forsmark) because, as indicated above, there are four different end-member files.

9. Finally, the program asks for the format file in which, apart from the number and name of the end members in the same order as they appear in the hydro file, it contains the number and name of the phases to be considered when performing equilibrium reactions (which will be zero for only mixing) and the number of exchangers (zero in all these simulations). There are different format files depending on the simulation case.

Format file name (< 40 characters)?

For mixing and reaction simulations, there are two different files: one with hematite "Fases_FeOH3.dat", and the other with the FeS(am) "Fases_FeSppt.dat" (see section A1.7.2).

After running, the program creates k output files with the initial part of the name identical to the hydro file and ending in "_01.pqi", "02_pqi", etc

E.g. F_2000_Rep.dat_01.pqi.

This name must be changed for another one more informative about what it contains, indicating the simulation case. F_year_Cut_mr_Hemcoup.pqi (for example for the case of the use of the coupled data base and the hematite as redox controlling phase).

These files are then used as input to the batch version of PHREEQC (phreeqc_batch.exe).

As indicated above, if the mineral phases to be used as equilibrium phases are not included in the thermodynamic data base or they have a different thermodynamic value from the one considered suitable for the system under study (e.g., hematite or FeS(am)), these phases must be addedd by hand to the pqi files already created, For that purpose, the following lines should be added at the beginning of every input file:

PHASES
Fe(OH)3(hematite_grenthe)
    Fe(OH)3 + 3 H+ = Fe+3 + 3 H2O
    log_k –1.1
FeS(ppt) 119
    FeS + H+ = Fe+2 + HS–
    log_k –3.00
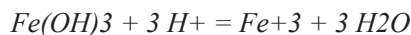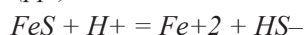
"PHASES" is the keyword used by PHREEQC to do this.

There is an additional problem to be taken into account. When the uncoupled database is used the definition of the sulphide species is different and thus the definition of the thermodynamic data for FeS(ppt) must be different too. It will be as follows:
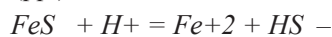
FeS(ppt) 119
    FeS_ + H+ = Fe+2 + HS_–
    log_k –3.00

In other words, the expression of the set of minerals added with this option will be different when using the coupled or the uncoupled thermodynamic database.
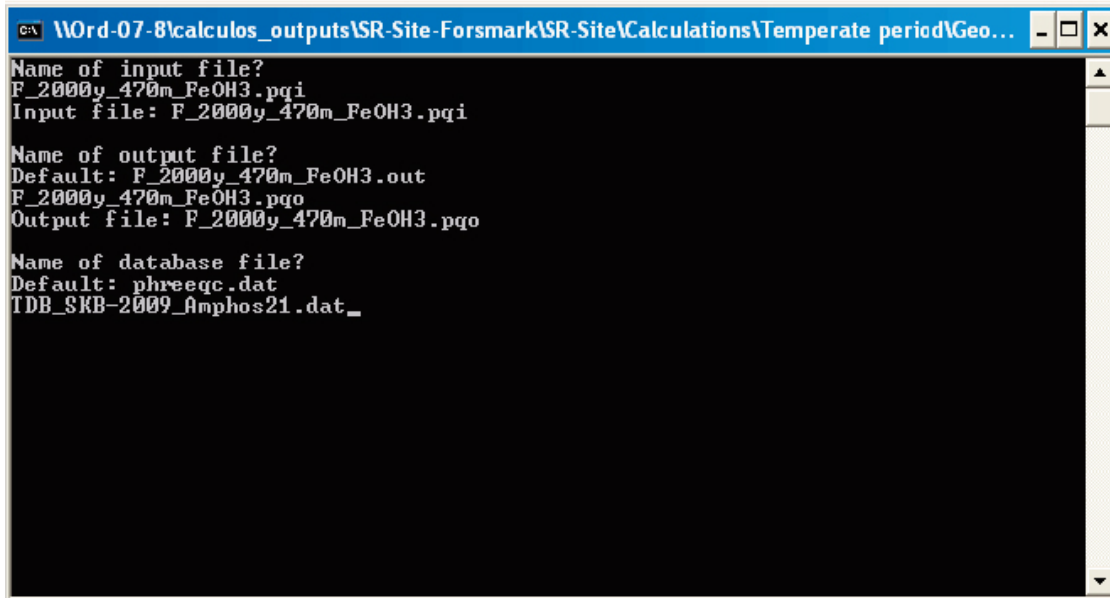
A1.5 Running PHREEQC

As the version used here is a batch version and all the needed information is included in the pqi file, running PHREEQC is exactly the same for all the simulated cases. PHREEQC asks for the names of the input file, the output file, and the thermodynamic database file (Figure A1-5):

1. First it asks for the input file, which will be the one created with the pqi creator interface program ("pqi_mp.exe").

2. Then it asks for the name of the output file (usually the same name with the extension ".pqo").

3. Finally, it asks for the thermodynamic data base to be used for the calculations (see Section 4.3):

    TDB_SKB-2009_Amphos 21.dat

4. Once the output file has been obtained, it will be passed through the selected output interface program to extract the desired information in a tabular form.

The mixing and chemical reaction simulations (*Equilibrium_Phases* option in PHREEQC*)* are used to equilibrate each water with an specific set of mineral phases. In this case the output file includes the detailed chemical composition of the groundwaters at each grid point *and* the amount of mass transfer for the equilibrated minerals.

The "TDB_SKB-2009_Amphos21.dat" database (and the equivalent uncoupled "TDB_SKB-2009_ Amphos21_no_S-redox.dat") has been used to carry out the chemical mixing and reaction simulations. As some of the mineral phases of interest are not included in the database, new phases (solubility for Fe-III oxyhydroxides, iron monosulphides and some aluminosilicates (kaolinite, albite and K-feldspar) were added to the pqi files as PHASES to be considered in the calculations. The detailed description of these phases and the reason for their selection can be found in /Auqué et al. 2006/.

Figure A1-5. *Running phreeqc_batch.exe.*

A1.6   Creation of the tabulated output

The procedure is the same for *all* simulations but the interface program to be used and the format files (and obviously the problem files) are different. The dialogue with the interface program ("SelectedOutput.exe") in all the cases is the following (Figure A1-6):

1. The user can chose whether to include or not the sample coordinates in the final table:
    Add coordinates to output file (y/n)?

2. And to include or not the mixing proportions:
    Add mixing proportions to output file (y/n)?

3. Then the program asks for the name of the PHREEQC output file ("F_year_cut_m.pqo").
    PHREEQC .pqo file name (< 20 characters)?

4. Next, it asks for the name of the format file with the information the user wants to extract from the complete pqo file (which will be different for each simulation):
    Input data file name (< 20 characters)?

    Each of the four simulation cases has a different format file indicating the different minerals in the equilibrium set and the use of the coupled or uncoupled thermodynamic database (see section A1.7.3):

*   "format_FeOH3_coup.dat",
*   "format_FeS_coup.dat",
*   "format_FeOH3_uncoup" and
*   "format_FeS_uncoup.dat".

5. Files generated with the Selected Output interface program are in the form of tables with the extracted information in columns and the grid points in rows. They have the same name as the PHREEQC pqo file but ended in ".res". In the three simulation cases (mixing, mixing+reaction, mixing+reaction+exchange) these file contain information on the composition of the waters at each grid point. The columns in these files are:

    *   X, Y, Z coordinates (the distance along the line calculated for the vertical plane is not stored here as it is not included in the PHREEQC output; therefore if the user wants to plot spatial distributions, this value must be calculated again using the equation $Distance = \sqrt{X^2 + Y^2}$

    *   Mixing proportions of the end-member waters for each point: Deep Saline, Littorina, Altered Meteoric, Glacial, PoreWater.

    *   Mass transfers for the equilibrated minerals (only if equilibrium reactions are imposed).

    *   TDS

    *   Molality of the elements included in the selected output's format file: result of mixing, or mixing and reaction or mixing, reaction and exchange (depending on the simulation).

    *   pH, pe, ionic strength total alkalinity, charge balance.

    *   Activity and molality of the selected species.

    *   Saturation indexes of the waters with respect to the selected mineral phases.

        When a simulation case has been divided into several files (_01, _02, etc), the user must run the selected output interface program on each of them and then combine manually the output into a single file with the whole set of samples (for graphical purposes).

6. All these files have a tabular format and can be easily imported into other software packages for graphical purposes.
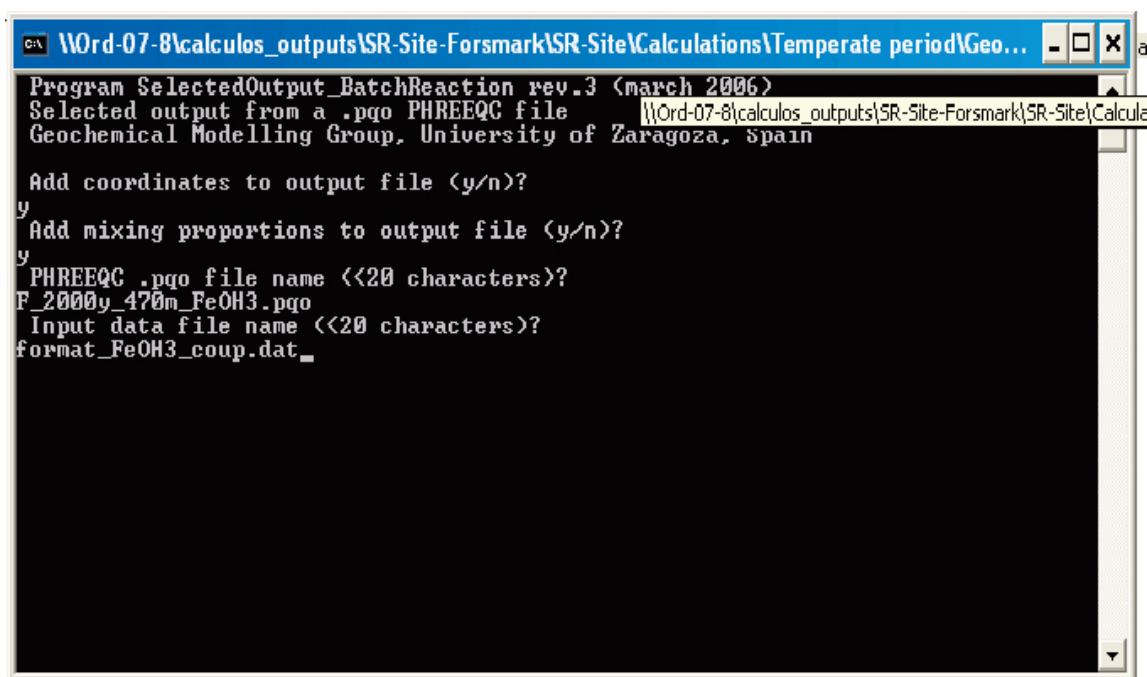
Figure A1-6. *Running "SelectedOutput.exe".*

A1.7 Postprocessing

The selected results have been post-processed by a three dimensional visualization using VOXLER, as requested by SKB.

In the case of the calculations for the points within the candidate repository volume, the selected results have been enclosed in a excel file, and treated with specific statistical analysis. In these cases, the post-processing will be performed by "Box-and-whisker plots", using ORIGIN, showing the statistical distribution of the chosen parameters. The statistical measures included are the median, the 25th and 75th percentile, the mean, the 5th and 95th percentile, the 1st and 99th percentile, and the maximum and the minimum values.

Excel files have been generated for each time or stage corresponding to each simulated period (and for each hydrological variant case). They consist in three sheets which contain:

- Sheet 3, "F_470_temperate_2000y_BaseCase", e.g.: 37 columns and 130,475 rows (or 35 columns and 48, 849 rows, in the case of the glacial cycle) with the selected output results (see previous section) and other derived functions. Rows from 2 to 65,238 (or to 24,425 in the case of the glacial cycle) are representative of the results obtained considering equilibrium with respect to Fe(III) oxyhydroxides, and rows from 65,239 to 130,475 (or from 24,425 to 48,849, in the case of the glacial cycle) are representative of the results obtained considering equilibrium with respect to amorphous Fe(II) sulphides.

- Sheet 2, "Statistics 2000", e.g.: Statistics calculations of the selected results for pH, Eh, TDS (in g/L), ionic strength, alkalinity, total concentrations of Na, K, Ca, Mg, Fe, C, Cl, S(VI), S(-II), Si and P, and the functions [Na+Ca] and [Na+K+2·(Ca+Mg)].

- Sheet 1, "SR-Site_List_2000", e.g.: A summarizing table with the values of the parameters analyzed in the previous sheet and corresponding to the points where the highest and the lowest values of [Na/Ca], [Na+Ca], pH, Eh, and the total concentrations of Ca, Na, Cl, S(VI) HCO3, total Fe and P, K have been calculated.

The output files are named as follow:

A1.7.1   Temperate period
Base case

F470_temperate_2000 AD_BaseCase.xlsx

F470_temperate_3000 AD_BaseCase.xlsx

F470_temperate_5000 AD_BaseCase.xlsx

F470_temperate_9000 AD_BaseCase.xlsx

Hydrological variant cases. Cases 5 and 9

F470_temperate_2000 AD_vc5_BaseCase.xlsx

F470_temperate_2000 AD_vc9_BaseCase.xlsx

Hydrological variant cases. Extended heterogeneity

F470_temperate_exhet_2000 AD_BaseCase.xlsx

F470_temperate_exhet_3000 AD_BaseCase.xlsx

F470_temperate_exhet_5000 AD_BaseCase.xlsx

F470_temperate_exhet_9000 AD_BaseCase.xlsx

A1.7.2   Glacial cycle. Unfrozen soil
Initial temperate

F470_Gla0_BaseCase.xlsx

Glacier advance

F470_GlaIa_BaseCase.xlsx

F470_GlaIIa_BaseCase.xlsx

F470_GlaIIIa_BaseCase.xlsx

F470_GlaIVa_BaseCase.xlsx

F470_GlaVa_BaseCase.xlsx

Glacier retreat

F470_GlaVr_BaseCase.xlsx

F470_GlaIVr_BaseCase.xlsx

F470_GlaIIr_BaseCase.xlsx

Final temperate. Submerged under a lake of glacial melt waters

F470_Gla0r_BaseCase.xlsx

Hydrological variant case. Advance N-S

F470_Gla0_BaseCase.xlsx

F470_GlaNSIVa(IIIa)_BaseCase.xlsx

A1.7.3   Glacial cycle. Permafrost

Periglacial conditions

F470_perm0_BaseCase.xlsx

Glacier advance

F470_permI_BaseCase.xlsx

F470_permII_BaseCase.xlsx

F470_permIV_BaseCase.xlsx

A1.7.4   Submerged saline stage

F470_3000BC_submerged_BaseCase.xlsx

A1.8   Format files and chemical composition of the end-members

A1.8.1   End-member files. Chemical composition of the selected "end-members"

Coupled database. "F_endmembers_SrSite_coup.dat"

SOLUTION 1 "DeepSalineForsmark". Albite, K-feldspar, hydroxyapatite, calcite, hematite_grenthe, quartz (Rimdstidt), Fix pH=8.0

    temp 15
    pH 8
    pe –4.449
    redox pe
    units mol/kgw
    density 1
    Al 7.371e-009
    Br 0.004156
    C 3.678e-005
    Ca 0.494
    Cl 1.366
    F 8.644e-005
    Fe 2.525e-007
    K 0.0008222
    Li 0.0006861
    Mg 8.952e-005
    Mn 2.615e-006
    Na 0.3801
    S 0.0001
    Si 8.808e-005
    Sr 0.003947
    -water 1 # kg

SOLUTION 2 "Littorina". Calcite, hydroxyapatite, quartz (Rimdstidt), FeS(am), kaolinite

    temp 15
    pH 7.951
    pe –4.422
    redox pe
    units mol/kgw
    density 1
    Al 3.247e-007
    Br 0.0002812
    C 0.001627
    Ca 0.003865
    Cl 0.1856
    F 2.61e-005
    Fe 8.262e-006
    K 0.003469
    Li 1.021e-005
    Mg 0.01865
    Na 0.1617
    S 0.009385
    Si 0.0001282
    Sr 3.096e-005
    -water 1 # kg

SOLUTION 3 "Altered Meteoric" Forsmark(#8335). Calcite (SI=–0.5), hydroxyapatite, kaolin-
ite, quartz (Rimdstidt), Fe(OH)3(mic)

    temp 15
    pH 7.314
    pe 0.554
    redox pe
    units mol/kgw
    density 1
    Al 7.719e-008
    Br 7.166e-006
    C 0.00723
    Ca 0.0004702
    Cl 0.005111
    F 8.431e-005
    Fe 1.793e-006
    K 0.0001434
    Li 2.019e-006
    Mg 0.0003089
    Na 0.01193
    S 0.0008858
    Si 0.0001342
    Sr 4.341e-006
    -water 1 # kg

SOLUTION 4 "Glacial". Calcite (SI=–1), hydroxyapatite, quartz (Rimdstidt), kaolinite, Fe(OH)3(mic)

    temp 15
    pH 9.3
    pe –5.26
    redox pe
    units mol/kgw
    density 1
    Al 5.205e-006
    C 8.515e-005
    Ca 7.18e-005
    Cl 1.41e-005
    Fe 8.002e-007
    K 1.023e-005
    Mg 4.114e-006
    Na 7.395e-006
    S 5.305e-006
    Si 0.0001665
    -water 1 # kg

SOLUTION 5 "Porewater Forsmark" (WAT5, Serco). Calcite, hydroxyapatite, hematite_grenthe, kaolinite, quartz (Rimdstidt), logpCO2=–4.1

    temp 15
    pH 8.5
    pe –4.925
    redox pe
    units mol/kgw
    density 1
    Al 9.141e-007
    Br 7.163e-006
    C 0.0005222
    Ca 0.001184
    Cl 0.005109
    F 8.427e-005
    Fe 8.744e-009
    K 0.0001433
    Li 2.018e-006
    Mg 0.0003088
    Na 0.01193
    S 0.0008854
    Si 0.0001396
    Sr 4.34e-006
    -water 1 # kg

Uncoupled database. "F_endmembers_SrSite_uncoup.dat"

SOLUTION 1 "DeepSalineForsmark". Albite, K-feldspar, calcite, hematite_grenthe, quartz (Rimdstidt), Fix pH=8.0

    temp 15
    pH 8
    pe −5.909
    redox pe
    units mol/kgw
    density 1
    Al 7.371e-009
    Br 0.004156
    C 3.679e-005
    Ca 0.494
    Cl 1.366
    F 8.644e-005
    Fe 7.28e-006
    K 0.0008222
    Li 0.0006861
    Mg 8.952e-005
    Mn 2.615e-006
    Na 0.38
    S 0.0001
    S_ 1.026e-015
    Si 8.808e-005
    Sr 0.003947
    -water 1 # kg

SOLUTION 2 "Littorina". Calcite, quartz (Rimdstidt), FeS(am), kaolinite

    temp 15
    pH 7.951
    pe −3.91
    redox pe
    units mol/kgw
    density 1
    Al 3.247e-007
    Br 0.0002812
    C 0.001627
    Ca 0.003865
    Cl 0.1856
    F 2.61e-005
    Fe 8.282e-006
    K 0.003469
    Li 1.021e-005
    Mg 0.01865
    Na 0.1617
    S 0.009377
    S_ 8.245e-006
    Si 0.0001282
    Sr 3.096e-005
    -water 1 # kg

SOLUTION 3 "Altered Meteoric" Forsmark(#8335). Calcite (SI=–0.5), kaolinite, quartz (Rimdstidt), Fe(OH)3(mic)

    temp 15
    pH 7.314
    pe 0.554
    redox pe
    units mol/kgw
    density 1
    Al 7.719e-008
    Br 7.166e-006
    C 0.00723
    Ca 0.0004702
    Cl 0.005111
    F 8.431e-005
    Fe 1.793e-006
    K 0.0001434
    Li 2.019e-006
    Mg 0.0003089
    Na 0.01193
    S 0.0008858
    S_ 1.001e-015
    Si 0.0001342
    Sr 4.341e-006
    -water 1 # kg

SOLUTION 4 "Glacial". Calcite (SI=–1), quartz (Rimdstidt), kaolinite, Fe(OH)3(mic)

    temp 15
    pH 9.29
    pe –2.622
    redox pe
    units mol/kgw
    density 1
    Al 5.087e-006
    C 8.613e-005
    Ca 7.229e-005
    Cl 1.41e-005
    Fe 2.107e-009
    K 1.023e-005
    Mg 4.114e-006
    Na 7.395e-006
    S 5.205e-006
    S_ 1e-007
    Si 0.0001657
    -water 1 # kg

SOLUTION 5 "Porewater Forsmark" (WAT5, Serco). Calcite, hematite_grenthe, kaolinite, quartz (Rimdstidt), logpCO2=–4.1

    temp 15

    pH 8.5

    pe –6.888

    redox pe

    units mol/kgw

    density 1

    Al 9.143e-007

    Br 7.163e-006

    C 0.0005225

    Ca 0.001184

    Cl 0.005109

    F 8.427e-005

    Fe 8.031e-007

    K 0.0001433

    Li 2.018e-006

    Mg 0.0003088

    Na 0.01193

    S 0.0008854

    S_ 1.001e-015

    Si 0.0001396

    Sr 4.34e-006

    -water 1 # kg

A1.8.2   The format files for the "pqi_mp.exe"

Equilibrium with Fe(III) oxyhydroxides. " Fases_FeOH3.dat"

    5 !Number of end members, followed by their names

    "Brine" "Littorina" "Meteoric" "Glacial" "PoreWater"

    3 !Number of phases for equilibrium calculations

    "Calcite" 0 10

    "Quartz" 0 10

    "Hydroxyapatite" 0 10

    "Fe(OH)3(hematite_grenthe)" 0 10

    0 !Number of exchangers (for cation exchange)

Equilibrium with amorphous Fe(II) sulphides. "Fases_FeSppt.dat"

    5 !Number of end members, followed by their names

    "Brine" "Littorina" "Meteoric" "Glacial" "PoreWater"

    3 !Number of phases for equilibrium calculations

    "Calcite" 0 10

    "Quartz" 0 10

    "Hydroxyapatite" 0 10

    "FeS(ppt)" 0 10

    0 !Number of exchangers (for cation exchange)

A1.8.3 The format files for the "output_batchreaction.exe"

Equilibrium with Fe(III) oxyhydroxides or amorphous Fe(II) sulphides, and coupled DTB

5 !Number of end-members (ONLY if used in the pqo file)

Brine

Littorina

DGW

Glacial

PoreWater

1 !Compute TDS (Total Dissolved Solids)?

10 !Number of elements, followed by each element (as written in section "Solution composition", in alphabetical order!)

C

Ca

Cl

Fe

K

Mg

Na

P

S

Si

0 !Number of phases, followed by each phase (as written in section "Phase assemblage",in alphabetical order!)

!Write 1 for each paramater to be output (section "Description of solution")

1 !pH

1 !pe

0 !Activity of water

1 !Ionic strength

0 !Mass of water

1 !Total alkalinity

0 !Total CO2

0 !Temperature

0 !Electrical balance

0 !Percent error

0 !Iterations

0 !Total H

0 !Total O

3 !Number of species, followed by each species (as written in section "Distribution of species")

H2S

HCO3–

HS–

1 !Number of SI, followed by each phase (as written in section "Saturation indices")

CO2(g)

Equilibrium with Fe(III) oxyhydroxides or amorphous Fe(II) sulphides, and uncoupled DTB

5 !Number of end-members (ONLY if used in the pqo file)

Brine

Littorina

DGW

Glacial

PoreWater

1 !Compute TDS (Total Dissolved Solids)?

11 !Number of elements, followed by each element (as written in section "Solution composition", in alphabetical order!)

C

Ca

Cl

Fe

K

Mg

Na

P

S

S_

Si

0 !Number of phases, followed by each phase (as written in section "Phase assemblage",in alphabetical order!)

!Write 1 for each paramater to be output (section "Description of solution")

1 !pH

1 !pe

0 !Activity of water

1 !Ionic strength

0 !Mass of water

1 !Total alkalinity

0 !Total CO2

0 !Temperature

0 !Electrical balance

0 !Percent error

0 !Iterations

0 !Total H

0 !Total O

3 !Number of species, followed by each species (as written in section "Distribution of species")

H2S_

HCO3–

HS_-

1 !Number of SI, followed by each phase (as written in section "Saturation indices")

CO2(g)

A1.9 Input files for the generation of the compositions of the five end-members groundwaters

A1.9.1 For the "coupled" DTB

```
#For AMPHOS or NAGRA TDB
SOLUTION 1 Deep Saline
   temp 15
   pH 8.00
   pe -2.0
   redox pe
   units mg/l
   density 1.051
   Cl 47200
   K 45.5
   Mg 2.12
   Ca 19300
   Na 8500
   S(6) 10
   S(-2) 1.0e-15 Mol/l
   Alkalinity 14.1 gfw 61.0171
   Si 2.9 gfw 28.086
   Fe 0.4
   Sr 337
   Br 323.6
   F 1.6
   Li 4.64
   Mn 0.14
   -water 1 # kg
SAVE solution 1
END

SOLUTION 2 Littorina
   temp 15.0
   pH 7.6
   pe -2
   redox pe
   units mg/l
   density 1
   Cl 6500
   K 134.
   Mg 448.0
   Ca 151.0
   Na 3674.0
   S(6) 890.0
   S(-2) 1e-15 Mol/l
   Alkalinity 92.5 gfw 61.0171
   Si 1.84
   Fe 0.002
   Sr 2.68
   Br 22.2
   F 0.49
   Li 0.07
   Mn 0.0
   -water 1 # kg
SAVE solution 2
END
```

```
SOLUTION 3 Glacial
  temp 15
  pH 5.8
  pe -2
  redox pe
  units ppm
  density 1
  Cl 0.5
  K 0.4
  Mg 0.1
  Ca 0.18
  Na 0.17
  S(6) 0.5
  S(-2) 1.0e-7 Mol/kgs
  Alkalinity 0.12 gfw 61.0171
  Si 0.01
  Fe 0.0
  Sr 0
  Br 0
  F 0
  Li 0
  -water 1 # kg
SAVE solution 3
END

SOLUTION 6. Porewater/Old meteoric end member. Forsmark. WAT5 #8335
  temp 15
  pH 7.91
  pe -2
  redox pe
  units ppm
  density 1
  Cl 181
  K 5.6
  Mg 7.5
  Ca 41.1
  Na 274.0
  S(6) 85
  S(-2) 1e-15 Mol/kgs
  Alkalinity 14.1 gfw 61.0171
  Si 6.68 gfw 28.086
  Fe 0.1
  Sr 0.380
  Br 0.572
  F 1.6
  Li 0.014
  -water 1 # kg
SAVE SOLUTION 6
END
```

```
SOLUTION 7. Altered Meteoric end member Forsmark. #8335
   temp 15
   pH 7.91
   pe -2
   redox pe
   units ppm
   density 1
   Cl 181
   K 5.6
   Mg 7.5
   Ca 41.1
   Na 274.0
   S(6) 85
   S(-2) 1e-15 Mol/kgs
   Alkalinity 466 gfw 61.0171
   Si 6.68 gfw 28.086
   Fe 0.1
   Sr 0.380
   Br 0.572
   F 1.6
   Li 0.014
   -water 1 # kg
SAVE SOLUTION 7
END

USE SOLUTION 1
TITLE Brine
PHASES
Fix_H+
   H+ = H+
   log_k 0.0
Albita
   NaAlSi3O8 + 8H2O = Al(OH)4- + 3Si(OH)4 + Na+
   log_k -19.98
   -analytic -5429.59545 -0.81939 293813.48663 1966.59164
   -17577933.12184
Feldespato_K
   KAlSi3O8 + 8H2O = Al(OH)4- + 3Si(OH)4 + K+
   log_k -22.62
   -analytic -5701.00975 -0.87173 304836.7864 2069.03705
   -18119139.36096
Fe(OH)3(hematite_grenthe)
   Fe(OH)3 + 3 H+ = Fe+3 + 3 H2O
   log_k -1.1
EQUILIBRIUM_PHASES 1
   Albita 0 0.01
   Calcite 0 0.01
   Quartz 0 0.01
   Fe(OH)3(hematite_grenthe) 0 10
   Feldespato_K 0 10
   Fix_H+ -8 NaOH 40
END
```

```
USE SOLUTION 2
TITLE Litorina
PHASES 2
FeS(ppt) 119
   FeS + H+ = Fe+2 + HS-
# log_k -3.915
   log_k -3.00
Caolinita_Grimaud
   Al2Si2O5(OH)4 + 7H2O = 2Al(OH)4- + 2H+ + 2Si(OH)4
   log_k -37.3
EQUILIBRIUM_PHASES 2
   Calcite 0 0.01
   Caolinita_Grimaud 0 0.01
   Quartz 0 0.01
   FeS(ppt) 0 10
END
USE SOLUTION 3
TITLE Glacial
PHASES 3
Caolinita_Grimaud
   Al2Si2O5(OH)4 + 7H2O = 2Al(OH)4- + 2H+ + 2Si(OH)4
   log_k -37.3
EQUILIBRIUM_PHASES 3
   Calcite -1 0.01
   Caolinita_Grimaud 0 0.01
   Quartz 0 0.01
   Fe(OH)3(mic) 0 10
END
USE SOLUTION 6
TITLE Porewater/Old Meteoric end-member. Forsmark. WAT5 #8335
PHASES 6
Caolinita_Grimaud
   Al2Si2O5(OH)4 + 7H2O = 2Al(OH)4- + 2H+ + 2Si(OH)4
   log_k -37.3
Fe(OH)3(hematite_grenthe)
   Fe(OH)3 + 3 H+ = Fe+3 + 3 H2O
   log_k -1.1
EQUILIBRIUM_PHASES 6
   Calcite 0 0.01
   Caolinita_Grimaud 0 0.01
   Fe(OH)3(hematite_grenthe) 0 10
   Quartz 0 0.01
   CO2(g) -4.1 10
END
USE SOLUTION 7
TITLE Altered Meteoric end-member. Forsmark. #8335
PHASES 7
Caolinita_Grimaud
   Al2Si2O5(OH)4 + 7H2O = 2Al(OH)4- + 2H+ + 2Si(OH)4
   log_k -37.3
EQUILIBRIUM_PHASES 5
   Quartz 0 0.01
   Calcite -0.5 0.01
   Caolinita_Grimaud 0 0.01
   Fe(OH)3(mic) 0 10
END
```

A1.9.2 For the "uncoupled" DTB

```
#For AMPHOS TDB uncoupled
SOLUTION 1 Deep Saline end-member
  temp 15
  pH 8.0
  pe -2
  redox pe
  units mg/l
  density 1.051
  Cl 47200
  K 45.5
  Mg 2.12
  Ca 19300
  Na 8500
  S(6) 10
  S_ 1.0e-15 Mol/l
  Alkalinity 14.1 gfw 61.0171
  Si 2.9 gfw 28.086
  Fe 0.4
  Sr 337
  Br 323.6
  F 1.6
  Li 4.64
  Mn 0.14
  -water 1 # kg
SAVE solution 1
END

SOLUTION 2 Littorina
  temp 15.0
  pH 7.6
  pe -2
  redox pe
  units ppm
  density 1
  Cl 6500
  K 134.
  Mg 448.0
  Ca 151.0
  Na 3674.0
  S(6) 890.0
  S_ 1e-15 Mol/kgs
  Alkalinity 92.5 gfw 61.0171
  Si 1.84
  Fe 0.002
  Sr 2.68
  Br 22.2
  F 0.49
  Li 0.07
  Mn 0.0
  -water 1 # kg
SAVE solution 2
END
```

```
SOLUTION 3 Glacial
  temp 15
  pH 5.8
  pe -2
  redox pe
  units ppm
  density 1
  Cl 0.5
  K 0.4
  Mg 0.1
  Ca 0.18
  Na 0.17
  S(6) 0.5
  S_ 1.0e-7 Mol/kgs
  Alkalinity 0.12 gfw 61.0171
  Si 0.01
  Fe 0.0
  Sr 0
  Br 0
  F 0
  Li 0
  -water 1 # kg
SAVE solution 3
END

SOLUTION 6. Porewater/Old meteoric end member. Forsmark. WAT5 #8335
  temp 15
  pH 7.91
  pe -2
  redox pe
  units ppm
  density 1
  Cl 181
  K 5.6
  Mg 7.5
  Ca 41.1
  Na 274.0
  S(6) 85
  S_ 1e-15 Mol/kgs
  Alkalinity 14.1 gfw 61.0171
  Si 6.68 gfw 28.086
  Fe 0.1
  Sr 0.380
  Br 0.572
  F 1.6
  Li 0.014
  -water 1 # kg
SAVE SOLUTION 6
END
```

```
SOLUTION 7. Altered meteoric end-member. Forsmark. #8335
  temp 15
  pH 7.91
  pe -2
  redox pe
  units ppm
  density 1
  Cl 181
  K 5.6
  Mg 7.5
  Ca 41.1
  Na 274.0
  S(6) 85
  S_ 1e-15 Mol/kgs
  Alkalinity 466 gfw 61.0171
  Si 6.68 gfw 28.086
  Fe 0.1
  Sr 0.380
  Br 0.572
  F 1.6
  Li 0.014
  -water 1 # kg
SAVE SOLUTION 7
END

USE SOLUTION 1
TITLE Deep Saline end member
PHASES
Fix_H+
  H+ = H+
  log_k 0.0
Albita
  NaAlSi3O8 + 8H2O = Al(OH)4- + 3Si(OH)4 + Na+
  log_k -19.98
  -analytic -5429.59545 -0.81939 293813.48663 1966.59164
  -17577933.12184
Feldespato_K
  KAlSi3O8 + 8H2O = Al(OH)4- + 3Si(OH)4 + K+
  log_k -22.62
  -analytic -5701.00975 -0.87173 304836.7864 2069.03705
  -18119139.36096
Fe(OH)3(hematite_grenthe)
  Fe(OH)3 + 3 H+ = Fe+3 + 3 H2O
  log_k -1.1
EQUILIBRIUM_PHASES 1
  Albita 0 0.01
  Calcite 0 0.01
  Quartz 0 0.01
  Fe(OH)3(hematite_grenthe) 0 10
  Feldespato_K 0 10
  Fix_H+ -8 NaOH 40
END
```

```
USE SOLUTION 2
TITLE Litorina
PHASES 2
FeS(ppt) 119
   FeS_ + H+ = Fe+2 + HS_-
# log_k -3.915
   log_k -3.00
Caolinita_Grimaud
   Al2Si2O5(OH)4 + 7H2O = 2Al(OH)4- + 2H+ + 2Si(OH)4
   log_k -37.3
EQUILIBRIUM_PHASES 2
   Calcite 0 0.01
   Caolinita_Grimaud 0 0.01
   Quartz 0 0.01
   FeS(ppt) 0 10
END
USE SOLUTION 3
TITLE Glacial
PHASES 3
Caolinita_Grimaud
   Al2Si2O5(OH)4 + 7H2O = 2Al(OH)4- + 2H+ + 2Si(OH)4
   log_k -37.3
EQUILIBRIUM_PHASES 3
   Calcite -1 0.01
   Caolinita_Grimaud 0 0.01
   Quartz 0 0.01
   Fe(OH)3(mic) 0 10
END
USE SOLUTION 6
TITLE Porewater/Old meteoric end member. Forsmark. WAT5 #8335
PHASES 6
Caolinita_Grimaud
   Al2Si2O5(OH)4 + 7H2O = 2Al(OH)4- + 2H+ + 2Si(OH)4
   log_k -37.3
Fe(OH)3(hematite_grenthe)
   Fe(OH)3 + 3 H+ = Fe+3 + 3 H2O
   log_k -1.1
EQUILIBRIUM_PHASES 6
   Calcite 0 0.01
   Caolinita_Grimaud 0 0.01
   Fe(OH)3(hematite_grenthe) 0 10
   Quartz 0 0.01
   CO2(g) -4.1 10
END
USE SOLUTION 7
TITLE Altered meteoric end-member. Forsmark. #8335
PHASES 7
Caolinita_Grimaud
   Al2Si2O5(OH)4 + 7H2O = 2Al(OH)4- + 2H+ + 2Si(OH)4
   log_k -37.3
EQUILIBRIUM_PHASES 5
   Quartz 0 0.01
   Calcite -0.5 0.01
   Caolinita_Grimaud 0 0.01
   Fe(OH)3(mic) 0 10
END
```

Mechanisms of the hydrological evolution of the reference waters (temperate and submerged periods) or salinities (glacial period)

The input data for the geochemical calculations provided by the hydrological models have been synthesized in the Appendix 2. For the temperate period, and for the submerged (under sea water) period, the Serco team has provided the mixture fractions of the five end-members groundwaters (Deep Saline, Old Meteoric, Glacial, Littorina and Altered Meteoric). On the other hand, for the glacial period (with and without permafrost), the TerraSolve team has provided salinities.

These data have been represented in vertical cross sections, cutting the candidate repository volume, and on a horizontal plane located at the repository depth (–470 m).

A2.1 Distribution of the reference waters during the temperate period

The hydrodynamics evolution of the five reference waters has been reproduced for 2,000 AD, 3,000 AD, 5,000 AD and 9,000 AD,

A2.1.1 Deep Saline groundwaters

At the year 2,000 AD, around of 40% of the groundwater compositions below –700 m of depth correspond to the Deep Saline groundwaters (Figure A2-1). These average fractions decrease with time as a consequence of the convective flow of less saline solutions from the shallowest areas of the domain. In this way, to the year 9,000 AD, the fractions of the Deep Saline groundwaters are only representative (20–30%) in restrictive areas below the central zone of the repository domain.
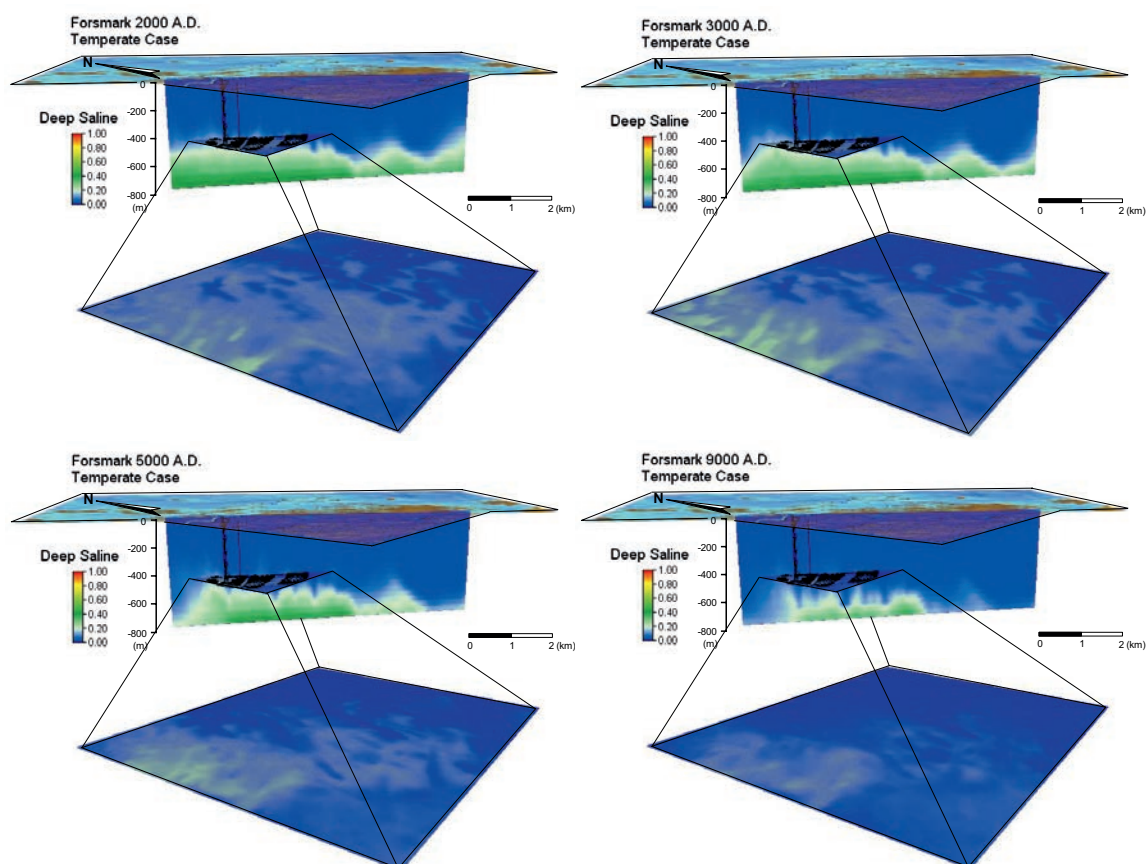
Figure A2-1. *Sequence of the evolution of the fraction of the Deep Saline waters in the groundwater of the Forsmark site (2,000 AD, 3,000 AD, 5,000 AD and 9,000 AD).*

At the repository depth (around –470 m), the highest fraction of Deep Saline groundwaters (around 25%) has been computed in the NW zone of the candidate repository volume for the year 3,000 A.D (Figure A2-1). This hydrochemical re-distribution of the Deep Saline solutions at the repository depth is a consequence of the ascending flow, along the most conductive fractures, imposed by the superficial infiltration of the Altered Meteoric waters. After then, these fractions decrease and, to the end of the temperate period (9,000 AD), the maximum fractions of the Deep Saline groundwaters are lesser than 10–15% within the candidate repository volume.

A2.1.2 Old Meteoric groundwaters

The initial fractions of the Old Meteoric groundwaters are around 40–70% in the Forsmark area, mainly focused between –400 and –800 m of depth. They are significant to the NW area of the candidate repository volume (Figure A2-2).

Within the candidate repository volume, During the period 2,000–3,000 AD, the average fraction of the Old Meteoric waters decreases into the eastern area during the period 2,000–3,000 AD, as a consequence on the convection of the Littorina groundwaters in this area. Since then, only negligible fractions of the Old Meteoric groundwaters remain along this boundary. In the other areas, the proportion of the Old Meteoric groundwaters is progressively diluted and / or displaced by the infiltration of the Altered Meteoric groundwaters. To the final stage of this period, only in the NW area of the candidate repository volume, a significant fraction of the Old Meteoric groundwaters remains as a component of groundwaters.
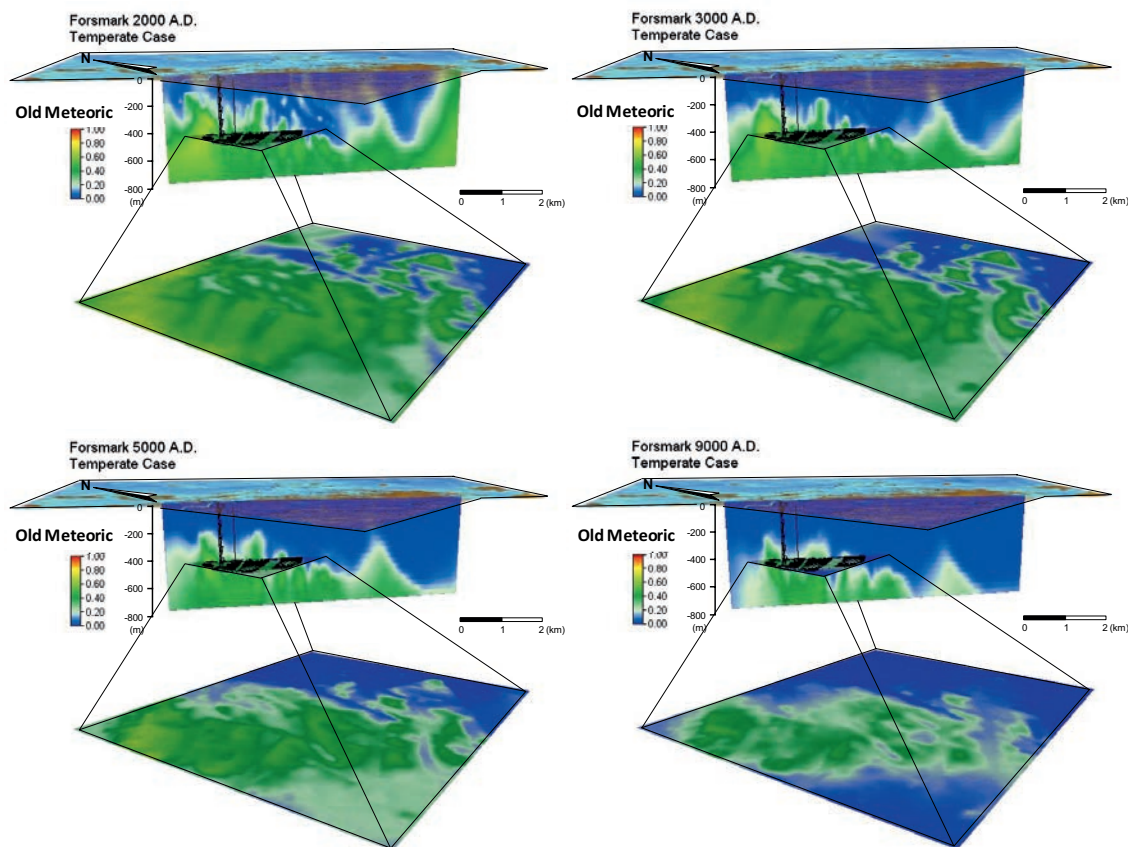
Figure A2-2. *Sequence of the evolution of the fraction of the Old Meteoric groundwaters in the Forsmark site (2,000 AD, 3,000 AD, 5,000 AD and 9,000 AD).*

A2.1.3 Glacial origin groundwaters

During the temperate period, the fractions of Glacial origin groundwaters, located in the fractures of the Forsmark area, are progressively diluted and / or displaced by the Altered Meteoric groundwaters. In the first stage of this period (2,000 AD), the fraction of the Glacial waters is only significant in the central area of the candidate repository volume (Figure A2-3). At depths between –300 and –650 m, the proportion of these groundwaters is higher than 30%, showing a wide range of variability (reaching values around 70% along the hydraulically conductive fractures).

To the year 9,000 AD, only small fractions of Glacial waters remain between –400 and –750 m of depth (Figure A2-3), mainly focused on the central areas of the candidate repository volume.

A2.1.4 Littorina groundwaters

In the Forsmark area, during the initial stage of the temperate period (2,000 AD), the fraction of the Littorina water is higher than 50% between the surface and –500 m of depth, approximately (Figure A2-4). Only along the most hydraulically conductive zones, Littorina waters have been diluted by meteoric waters.

For later times, the Littorina fraction is progressively diluted and/or displaced as a consequence of the infiltration of the Altered Meteoric groundwaters.

Within the candidate repository volume, the fractions of the Littorina waters are higher than 70% in the eastern area (Figure A2-4), reaching values close to 90–100% during the first stages of the temperate period (2,000 AD and 3,000 AD). However, in the western area, the fractions of the Littorina waters are practically negligible. At the year 5,000 AD, the Littorina waters have been completely diluted above –200 m of depth. In the central area of the candidate repository volume, fractions around 70% of Littorina water are still preserved (Figure A2-4). However, to the final of the modelled period (9,000 AD), the fractions of the remaining Littorina waters in the central areas of the repository volume are less than 40%.
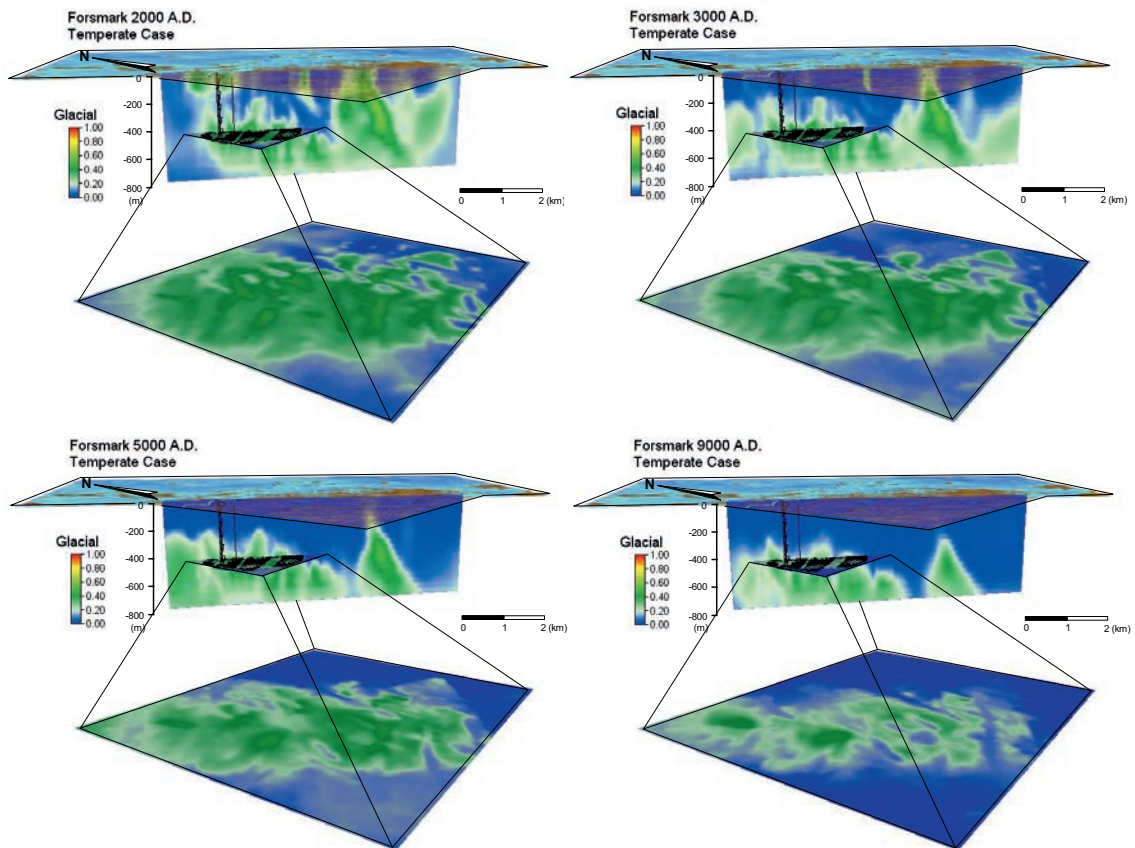
Figure A2-3. *Sequence of the evolution of the fraction of the Glacial origin waters in the groundwater of the Forsmark site (2,000 AD, 3,000 AD, 5,000 AD and 9,000 AD).*
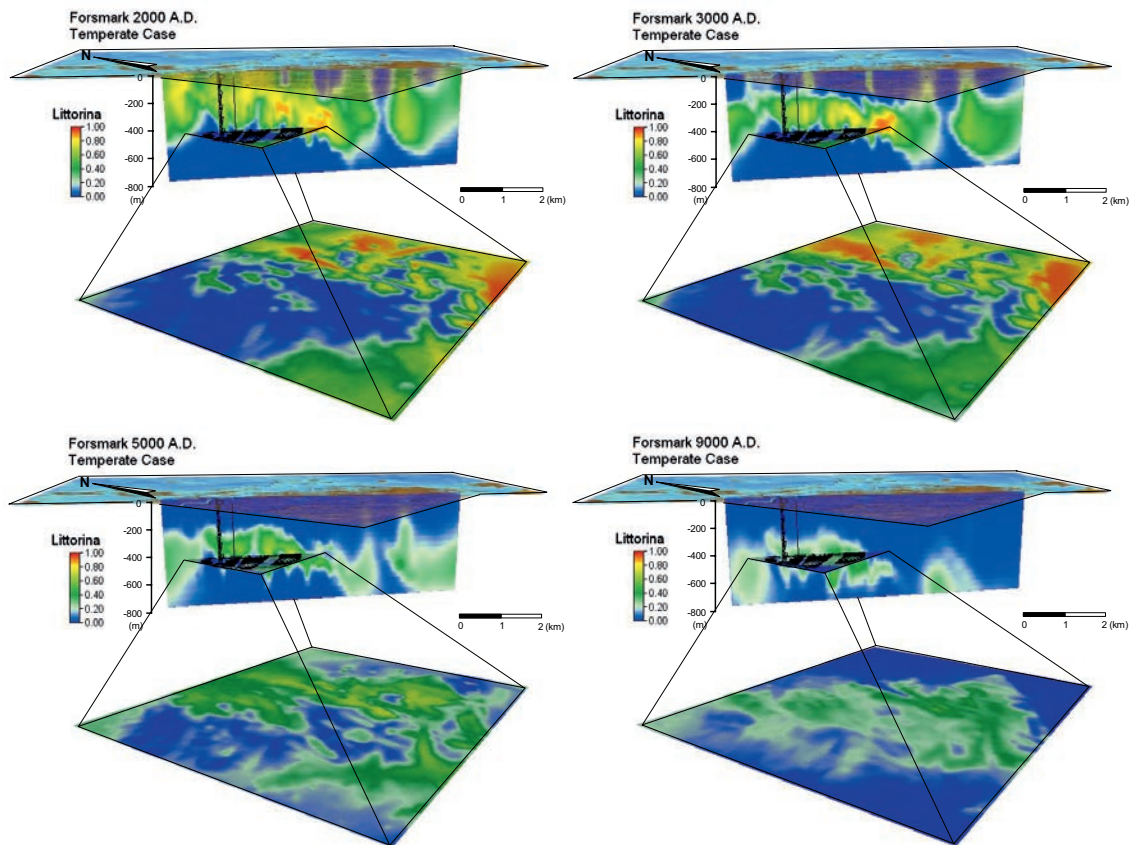
Figure A2-4. *Sequence of the evolution of the fraction of the Littorina waters in the groundwater of the Forsmark site (2,000 AD, 3,000 AD, 5,000 AD and 9,000 AD).*

A2.1.5 Altered Meteoric groundwaters

During the first stage of the temperate period (2,000 AD), the fractions of Altered Meteoric waters are negligible within the candidate repository volume. However, above –200 m of depth, towards the southern and the eastern areas of the repository domain, they are around 100% (Figure A2-5).

The infiltration of these waters continues during the temperate period. Around 3,000 AD, the fractions of the Altered Meteoric waters are practically 100% above –200 m. Only in the least hydraulically conductive zones (Figure A2-5), significant fractions of Glacial and Littorina waters remain as component of groundwaters. The front of the Altered Meteoric waters advances, reaching –200 and –400 m of depth, about the year 5,000 AD. Within the candidate repository volume, the fractions of the Altered Meteoric waters are higher than 70% along the eastern boundary, being negligible in the central areas.

To the final time of the temperate period (9,000 AD), the Altered Meteoric waters practically represent 100% of the groundwaters in the southern area of the model above –750 m of depth. However, the front of meteoric waters only reaches –300 m above the central area of the repository volume (Figure A2-5). In this way, within the candidate repository volume, the range of variability of the fractions of the Altered Meteoric waters is significant (from 0% to 30% in the central areas, and around 100% along the eastern boundary).
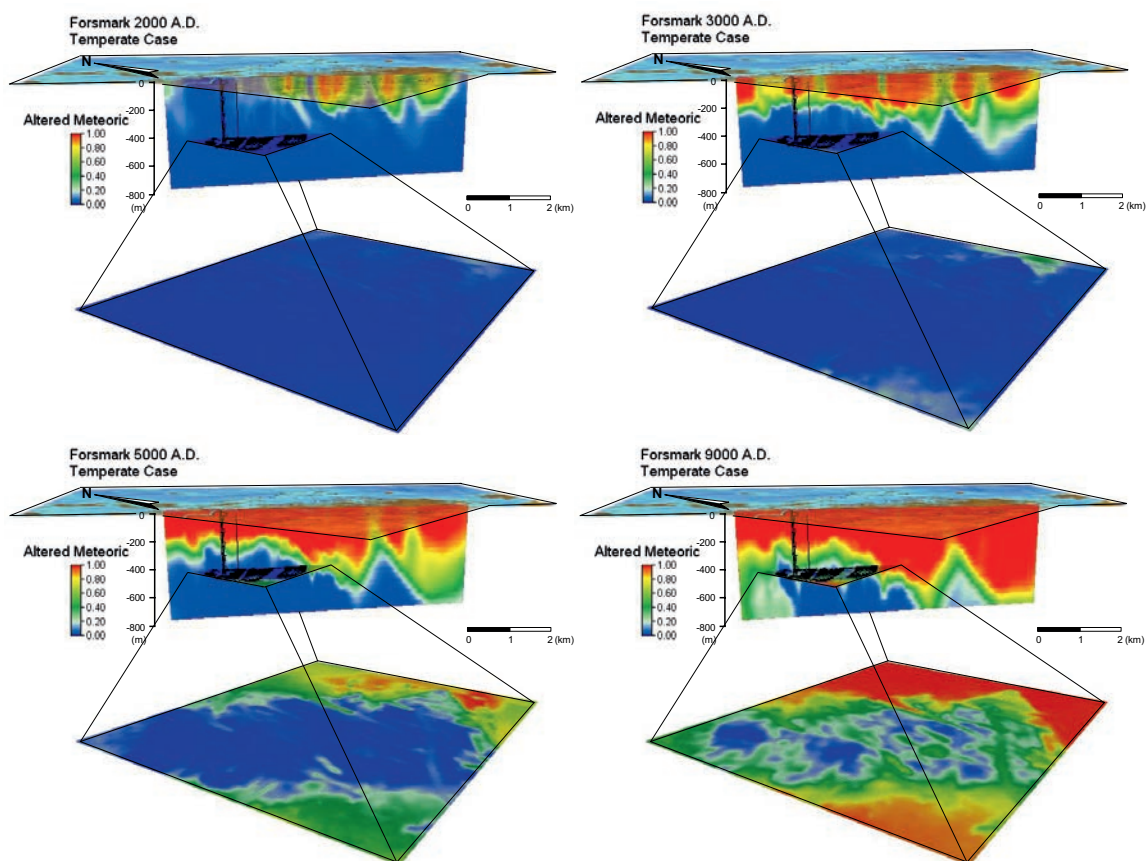
Figure A2-5. *Sequence of the evolution of the fraction of the Altered Meteoric waters in the groundwater of the Forsmark site (2,000 AD, 3,000 AD, 5,000 AD and 9,000 AD).*

A2.2 Salinity evolution during the glacial and the periglacial periods

A2.2.1 Initial temperate, glacial and submerged (under a lake of glacial melt waters) periods

As it has been previously commented, the hydrological model performed by TerraSolve (reproducing the remaining glacial cycle) supply salinities. Using the methodology described in the Section 4.1, they have been converted to proportions of the three end-members chosen to be applied in the geochemical calculations (Deep Saline, Altered Meteoric and Glacial origin waters).

During the temperate period (stage 1 in Figure A2-6), under –600 m of depth, salinities higher than 10 g/L have been calculated. When the glacier advances over the candidate repository area (stages 2, 3 and 4, Figure A2-6), salinities around 20 g/L have been computed at the repository depths, as a consequence of upconing mechanisms of the Deep Saline groundwaters. Once the ice sheet totally covers the area of the Forsmark site (stages 5 and 6; Figure A2-6), salinities decrease as a consequence of the infiltration of glacial melt waters. In this way, the highest values computed (8 g/L) only remain in a narrow area below the candidate repository volume.

After 15,000 years, the glacier begins to retreat (stages 7, 8 and 9, Figure A2-6), and the upconing mechanisms newly transport saline groundwaters towards the candidate repository volume, reaching salinities higher than 10 g/L. Towards the end of the glacial cycle, a lake of glacial melt waters covers the Forsmark region. In this period, salinities around 5 and 8 g/L can affect the candidate repository volume. It is predicted that they will decrease with time.
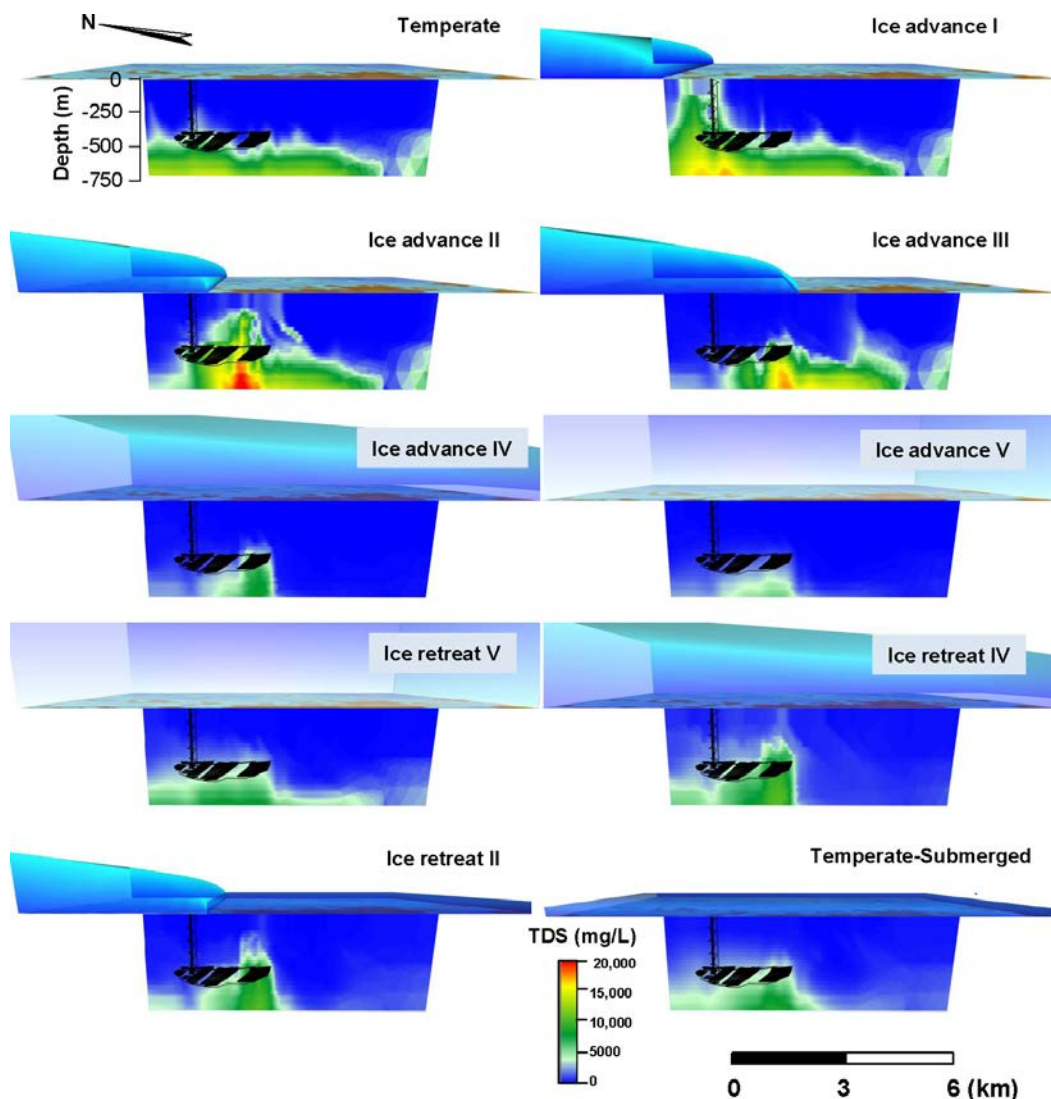
Figure A2-6. *Vertical cross sections of the evolution of the salinity (as TDS, mg/L) estimated by the hydrological calculations, when an ice sheet advances and retreats over the unfrozen ground of the Forsmark area. The figure shows salinities during the glacial sheet advance (1 to 6) and the glacial retreat (7 to 10). When the ice sheet retreats the area is covered by a 100 m deep glacial melt water lake.*

A2.2.2 Periglacial and glacial cycle with permafrost

The periglacial period has been initially simulated (stage 1, Figure A2-7). During this period, salinities around 8–10 g/L are homogeneously distributed on the bottom boundary of the hydrological model. These salinities are relatively lower than those obtained for the temperate period at the beginning of the glacial cycle. As soon as the glacier advances over the frozen ground located over the candidate repository area (stages 2 and 3, Figure A2-7), salinities increase to values higher than 20 g/L at the repository depth as a consequence of the upconing processes. These salinities are significantly higher than those calculated considering an unfrozen soil under the ice sheet.

Consequently, the presence of a permafrost system is one of the key factors controlling the increase of salinities in groundwaters during the glacial and the periglacial periods. It also seems to enhance the effect of salts transport during the stages of upconing. On the other hand, the infiltration rate of the glacial melt waters also changes with respect to the case of the ice advance over an unfrozen soil.

When the glacial front is over the candidate repository domain, the dilution by the infiltration of glacial melt waters is obvious (Figure A2-7). In this way, the expected salinities within the candidate repository volume are lower than those estimated in the same stage where the ice advance is effective over an unfrozen soil (without permafrost).
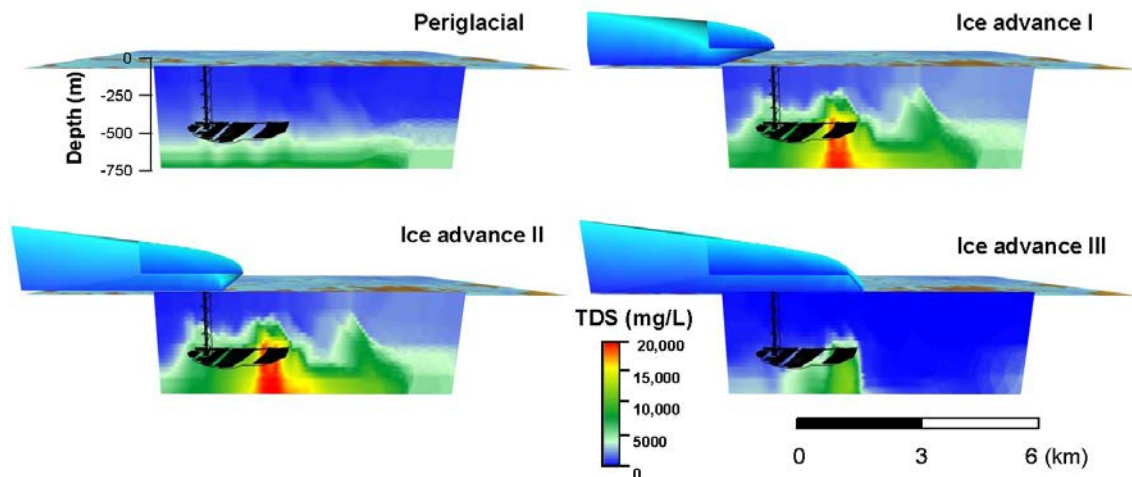
Figure A2-7. *Vertical cross sections of the salinity evolution (TDS, mg/L) calculated by the hydrological calculations, when a permafrost is developed during the glacial cycle in the Forsmark area. The figure shows the periglacial stage (1), and three stages during the advance of the glacial sheet (2 to 4).*

A2.3 Distribution of the reference waters during the submerged marine period

Immediately after the retreat of an ice sheet, isostatic depression will set the ground surface at the repository site below the Baltic Sea level. In the reference evolution, which is a repetition of the last glacial cycle (the Weichselian), the Forsmark site is expected to be below lakes of glacial melt water, and sea or brackish waters, during a period of time between a few thousand years up to perhaps ten thousand years. The hydrological models have reproduced this climatic and hydrological period, representative of the environmental conditions at the year 3,000 BC.

No significant fractions of Altered Meteoric waters have been computed in groundwaters during this period. On the other hand, it is notable as the fraction of marine waters (Littorina) is practically 100% in the aquifer system above the candidate repository volume (Figure A2-8). This distribution is affected by the location of the hydraulically conductive fractures above –400 m. However, no significant fractions of marine waters are calculated within the candidate repository volume for this time. At the repository depths, the Old Meteoric and Glacial groundwaters are the most representative reference waters (Figure A2-8).

A2.4 Conclusions

During the temperate period, the main hydrological process controlling the hydrogeochemical evolution in the Forsmark area is the infiltration of the Altered Meteoric groundwaters. The groundwater convection is strongly controlled by the existence of high conductive areas associated to the fracture zones. Within the candidate repository volume, the initial fractions of the Littorina and Glacial waters, and the Old Meteoric groundwaters, are progressively diluted by the infiltration of the Altered Meteoric groundwaters, remaining only significant fractions in the central areas. However, in the peripheral areas, the Altered Meteoric waters completely displace and dilute the groundwaters previously placed into the Forsmark fractures.

During the remaining glacial cycle, salinities are basically controlled by (1) the infiltration of glacial melt waters and (2) the transport of salts by upconing mechanisms from the deepest zones. Another key factor for the salts distribution is the existence of a frozen soil. The development of permafrost increases groundwater salinities within the candidate repository volume during the first stage of the glacier advance. On the other hand, when seawater covers the Forsmark area during the final stage of the glacial cycle, the infiltration of marine waters will affect distribution of salinities and compositions of groundwaters in the shallowest areas of the fractured aquifer.
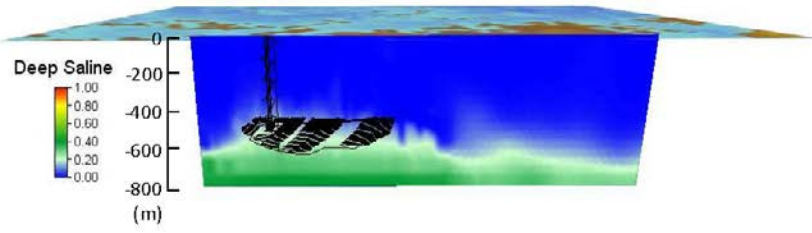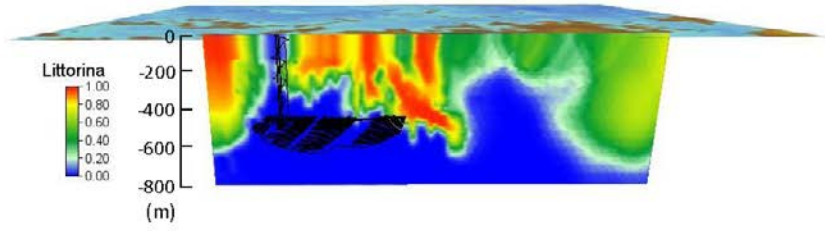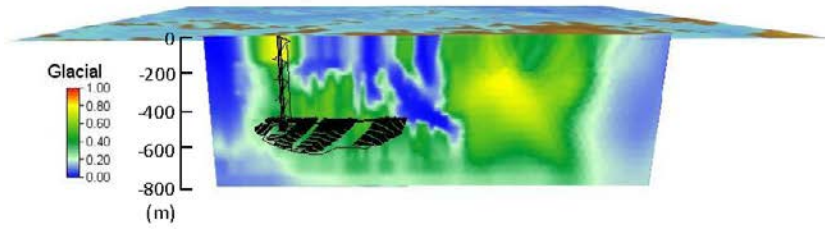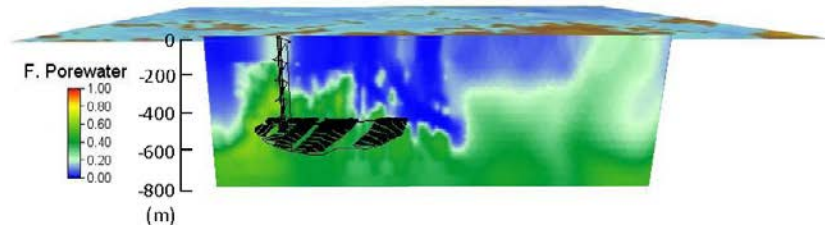
Figure A2-8. *Vertical cross sections of the fractions of the reference waters in the Forsmark site, at times equal to 3,000 BC. The fraction of the Altered Meteoric waters is negligible.*

Estimation of glacial derived groundwater compositions

The composition adopted for the Glacial end-member (used for mass balance and M3 calculations) in the site investigation programmes (Table A3-1) corresponds to present melt waters from one of the largest glaciers in Europe, the Josterdalsbreen in Norway, located on a crystalline granitic bedrock /Laaksoharju and Wallin 1997/. The major element composition of these waters is similar to the one estimated by /Pitkänen et al. 1999, 2004/ in a model study of Olkiluoto (Finland). These glacial melt waters represent the chemical composition of surface melt waters prior to the water-rock interaction processes undergone during their infiltration into the bedrock. They have a very low content of dissolved solids, even lower than present-day meteoric waters, a pH value of 5.8, and an isotopically light signature (Table A3-1).

To obtain the possible compositional characters of these waters after water-rock interaction processes (even in the first 100 m depth), groundwater samples having clear glacial signatures cannot be used because in the Forsmark and Laxemar areas the composition of groundwaters having glacial signatures has been drastically modified by mixing with waters of other origins (e.g. sample 1,569 at Äspö, Table A3-1). Therefore, there are no "undisturbed" glacial melt water remnants that could be considered a a pure glacial component modified only by water-rock interaction processes.

Nevertheless, the effect and extent of the expected water-rock interaction processes during the infiltration of glacial melt waters may be inferred from the study of waters in other zones not affected by mixing. The review performed by /Gimeno et al. 2008, 2009/ on the available data from the SKB site characteri-sation program has identified groundwaters of glacial or meteoric origin (but with high residence times) and corresponding to climates colder than at present (Table A3-2). Despite the fact that many of the sites studied in the Swedish program lack representative hydrochemical data (e.g. because of contamination with drilling water and/or other groundwaters), some indications of ancient glacial melt water are apparent. For example, groundwaters below 500 m depth in Fjällveden seem to be residual melt waters or alternatively meteoric waters from a colder climate /Wallin 1995, Tullborg 1997/. A glacial origin for these groundwaters is suggested in the work of /Bath 2005/ where "apparent" ^{14}C ages of around 12,000 to 14,000 years (i.e. late-glacial) are reported. At Gideå, there seems to be an indication of mixing between meteoric and post-glacial melt waters /Wallin 1995/. Finally, groundwaters in Lansjärv also show the isotopically light signature ($\delta^2H = -109.3‰$ and $\delta^{18}O = -13.8‰$) typical of glacial or old meteoric waters from colder climates.

Compared with the original composition of glacial melt waters (compare values in Table A3-1 and Table A3-2), all the Swedish waters have a more alkaline pH (≥ 9) and higher TDS values as a conse-quence of water-rock interaction. The differences are of orders of magnitude, especially for chloride, sodium and alkalinity. However, the final salt contents are still very low in absolute terms, even taking into account potential contamination. This means that, as expected, water-rock interaction modifies the overall compositional characteristics in a quite limited scale but pH values are clearly increased.

Table A3-1. Chemical composition of the glacial end-members used in the Swedish /Laaksoharju and Wallin 1997/ and Finnish /Pitkänen et al. 1999, 2004/ site characterization programs. The composition of a present meteoric water with very low residence time together with one of the real samples with a clear glacial signature (Äspö groundwater, sample 1569), are also shown. Concentrations in mg/L.

	Glacial end-member (Sweden)	Glacial end-member (Finland)	Meteoric water (HBH02, #1931)	Äspö (KAS03, #1569 at 129–134m depth)
T(°C)		1.0	16	10.2
pH	5.8	5.8	6.8	8.0
Eh (mV)	----	----	----	−280
Alkalinity	0.12	0.16	63.0	61
Cl	0.5	0.7	5.0	1,220.0
SO_4^{2-}	0.5	0.05	13.2	31.1
Ca	0.18	0.13	15.4	162
Mg	0.1	0.1	1.9	21.0
Na	0.17	0.15	11.5	613.0
K	0.4	0.15	2.3	2.4
Si	----	0.005	3.4	4.9
δ^2H (‰)	−158.0	−166.0	−77.1	−124.8
$\delta^{18}O$ (‰)	−21.0	−22.0	−10.2	−15.8

Similar conclusions have been obtained when analysing other cold meteoric and glacial waters in crystalline basements. For example, groundwaters from a recent meteoric origin at 450 m depth in the crystalline rocks of the Grimsel Test Site (Switzerland) are also alkaline, with pH = 9.6, and very diluted /Degueldre et al. 1996/ similar to the ones observed in the Swedish groundwaters (Table A3-2).

The required time to reach these alkaline characters might not be so long as suggested by the residence time of the examined groundwaters. The presence of geochemically-reactive minerals like calcite, even at the trace amounts found in many crystalline systems exert an important control in the compositional evolution of glacial melt waters /Brown 2002, Mitchell and Brown 2007/. This control is dominant in environments out of contact with the atmospheric CO_2 and where other sources of acidity (e.g. pyrite dissolution) are limited (calcite is one of the most abundant minerals at all depths in the fracture fillings of Forsmark and Laxemar, whereas pyrite is much more scarce and evenly distributed; /Drake et al. 2006b/), as it occurs during the infiltration of melt waters in the bedrock.

For example, if the Swedish Glacial end-member presented in Table A3-1 dissolves 2.2 mg/L of calcite it would reach a saturation index value of –2.0 (a high undersaturated state) but the pH would be of 9.0. If the amount of calcite dissolved is 4.6 mg/L, the S.I. would be of –1.0 (still a clearly undersaturated situation) but the pH would reach a value of 9.61. The participation of other feasible minerals considered in this evolution (e.g. equilibrium respect to kaolinite and microcrystalline iron oxyhidroxides; see /Auqué et al. 2006/ does not change significantly the obtained results. For instance, the Swedish Glacial end-member equilibrated with kaolinite, microcrystalline iron oxyhidroxide and with calcite at a S.I. value of –2.0 would reach a pH value of 8.81 (dissolving 3 mg/L of calcite); and if the calculation is performed considering a S.I. value for calcite of –1.0, the final pH value would be of 9.3 (dissolving 6.7 mg/L of calcite). This last situation corresponds to the Glacial end-member composition used in the simulations performed in SR-Can /Auqué et al. 2006/ and SR-Site.Minor amounts of calcite dissolution (even far from equilibrium conditions) could promote clearly alkaline conditions and, thus, this situation can be reached soon during the infiltration of glacial waters in the bedrock. Studies performed at present on the subglacial waters at the ice-bedrock interface in the Haut Glacier d'Arolla in Switherland (developed on crystalline rocks with disseminated calcite; /Brown et al. 1996, Brown 2002, Tranter et al. 2002/ indicate that despite the existence of an atmospheric CO_2 contribution to the acidity of these waters or the presence of reactive sulphides, the measured pH values range from 7 to 9.1. These values support the ability of the calcite interaction to promote the alkaline conditions in the glacial melt water quite soon during its infiltration.

Thus, a range of pH values between 9.0 and 9.3 can be proposed for the infiltrated glacial melt waters in the bedrock from analytical data of glacial groundwater samples (Table A3-2) and geochemical modelling reasoning.

Table A3-2. Compositional data for different groundwaters from a glacial infiltration or simply cold waters in different zones in Sweden and Switzerland. pH and Eh data in the Swedish sites have been obtained from the continuous logging with Chemmac (only pH data in bold and italics correspond to values determined in laboratory). Chemical contents in mg/L. Taken from /Gimeno et al. 2008/.

	Fjällveden[1] KFJ02 (#267)	KFJ07 (#372)	Gidea[2] KGI04 (#194)	Lansjärv KLJ01 (#1410)	Svartboberget KSV04 (#116)	KSV04 (#122)	Switzerland GTS[3]
Depth (m)	605–607	542–544	404–406	237–500	430–436	630 –633	450
T (ºC)	-----	-----	-----	-----	----	-----	12
pH	8.9	9.2	9.3	9.2	9.1	9.1	9.6
Eh (mV)	----	–200	–200	---	–75	–150	–171
Alk.	83.0	150.0	18	44.0	130.0	126.0	17.1
Cl	170.0	3.0	178	0.8	8.0	7.0	4.96
SO_4^{2-}	0.2	bdl.	0.1	4.4	1.2	0.8	5.8
Ca	12.0	10.0	21.0	7.7	17.0	17.0	6.61
Mg	0.8	2.0	1.1	1.2	2.0	1.9	0.05
Na	130.0	46	105.0	11.3	35.0	35.0	16.1
K	1.0	3.6	1.9	1.52	0.9	0.7	0.14
Si	4.3	n.a.	4.7	3.7	4.3	6.8	5.6
Fe	0.34	0.51	0.07	0.01	0.25	0.27	0.06
δ^2H (‰)	–102.9	----	–99.4	–109.6	–95.0	–95.4	----
$\delta^{18}O$ (‰)	–14.11	----	–13.63	–13.80	–13.0	–13.1	----

(1) Wallin (1995), Tullborg (1997), Bath (2005); (2) Wallin (1995); (3) Grimsel Test Site (Switzerland; Degueldre, 1994).

Appendix 4

Tables of the statistical results

A4.1 Temperate period: Base Case and Submerged period. All concentrations and the ionic strength are in mol/L, and the Eh is reported in mV.

Temperate period — 2000 AD

	pH	Eh	TDS (g/L)	Ionic Str	Na	K	Ca	Mg	Fe	Alk	C	Cl	S(VI)	S(-II)	Si	P	£qM*°
Min=	7.08	-261	6.88	0.1507	4.08E-02	1.57E-04	2.86E-03	1.29E-04	3.41E-07	2.15E-04	2.02E-04	1.14E-01	3.38E-04	8.62E-08	1.19E-04	2.89E-08	121.85
0.1%	7.09	-251	7.39	0.1637	4.45E-02	1.65E-04	3.69E-03	1.40E-04	6.93E-07	2.18E-04	2.06E-04	1.23E-01	3.50E-04	9.53E-08	1.21E-04	2.98E-08	130.86
5%	7.21	-242	8.66	0.1897	5.14E-02	1.85E-04	5.73E-03	1.80E-04	9.97E-07	2.67E-04	2.60E-04	1.44E-01	4.70E-04	1.29E-07	1.25E-04	4.23E-08	153.66
Median=	7.44	-222	10.39	0.2248	7.20E-02	7.39E-04	4.92E-02	3.34E-03	1.19E-05	5.10E-04	5.25E-04	1.69E-01	2.00E-03	2.46E-06	1.28E-04	1.28E-07	183.14
95%	7.74	-209	12.89	0.2944	1.42E-01	2.98E-03	7.41E-02	1.60E-02	2.47E-05	1.70E-03	1.71E-03	2.18E-01	8.10E-03	1.32E-05	1.29E-04	1.26E-06	227.75
99.9%	7.89	-199	17.65	0.4179	1.52E-01	3.25E-03	1.06E-01	1.75E-02	3.13E-05	2.15E-03	2.16E-03	3.05E-01	8.82E-03	1.45E-05	1.30E-04	1.83E-06	312.59
Max=	8.05	-198	19.87	0.4726	1.56E-01	3.34E-03	1.21E-01	1.79E-02	3.25E-05	2.44E-03	2.46E-03	3.45E-01	9.06E-03	1.49E-05	1.31E-04	2.25E-06	351.64

Temperate period — 3000 AD

	pH	Eh	TDS (g/L)	Ionic Str	Na	K	Ca	Mg	Fe	Alk	C	Cl	S(VI)	S(-II)	Si	P	£qM*°
Min=	6.73	-257	6.49	0.1220	4.29E-02	1.64E-04	2.86E-03	1.34E-04	4.27E-07	2.16E-04	2.04E-04	9.49E-02	3.45E-04	3.67E-09	1.19E-04	2.93E-08	111.20
0.1%	6.91	-250	7.51	0.1548	4.68E-02	1.73E-04	3.49E-03	1.54E-04	7.37E-07	2.23E-04	2.11E-04	1.21E-01	3.69E-04	8.40E-08	1.20E-04	3.08E-08	132.71
5%	7.14	-241	8.81	0.1863	5.41E-02	1.98E-04	5.42E-03	1.96E-04	1.07E-06	2.71E-04	2.66E-04	1.44E-01	4.87E-04	1.35E-07	1.24E-04	4.30E-08	155.52
Median=	7.42	-222	10.43	0.2233	8.26E-02	9.87E-04	4.69E-02	4.74E-03	1.53E-05	6.17E-04	6.44E-04	1.70E-01	2.66E-03	3.41E-06	1.28E-04	1.77E-07	183.39
95%	7.73	-204	14.20	0.3349	1.41E-01	2.97E-03	8.54E-02	1.59E-02	2.59E-05	1.81E-03	1.81E-03	2.44E-01	8.07E-03	1.31E-05	1.29E-04	1.40E-06	251.62
99.9%	7.89	-186	18.94	0.4503	1.51E-01	3.22E-03	1.15E-01	1.73E-02	3.91E-05	2.94E-03	3.05E-03	3.29E-01	8.73E-03	1.43E-05	1.30E-04	2.87E-06	335.26
Max=	8.00	-155	20.16	0.4744	1.54E-01	3.30E-03	1.21E-01	1.77E-02	5.32E-05	3.97E-03	4.12E-03	3.48E-01	8.95E-03	1.47E-05	1.31E-04	4.66E-06	356.47

Temperate period — 5000 AD

	pH	Eh	TDS (g/L)	Ionic Str	Na	K	Ca	Mg	Fe	Alk	C	Cl	S(VI)	S(-II)	Si	P	£qM*°
Min=	6.54	-243	1.12	0.0171	1.28E-02	1.64E-04	7.92E-04	1.60E-04	7.47E-07	2.31E-04	2.20E-04	6.21E-03	4.06E-04	6.88E-16	1.21E-04	3.29E-08	15.43
0.1%	6.61	-241	1.29	0.0205	1.50E-02	1.92E-04	9.89E-04	1.99E-04	9.79E-07	2.46E-04	2.36E-04	9.25E-03	4.51E-04	1.47E-12	1.22E-04	3.66E-08	18.52
5%	6.77	-231	2.90	0.0524	3.60E-02	2.51E-04	1.85E-03	4.80E-04	1.52E-06	3.00E-04	2.97E-04	3.61E-02	6.28E-04	1.41E-07	1.25E-04	5.13E-08	47.31
Median=	7.33	-215	9.29	0.1987	7.52E-02	9.37E-04	3.49E-02	4.51E-03	1.95E-05	1.10E-03	1.18E-03	1.51E-01	2.66E-03	2.83E-06	1.28E-04	4.84E-07	163.24
95%	7.52	-181	13.17	0.3094	1.09E-01	2.13E-03	7.74E-02	1.13E-02	3.90E-05	5.82E-03	6.22E-03	2.26E-01	5.85E-03	8.78E-06	1.33E-04	7.94E-06	233.40
99.9%	7.63	-132	17.02	0.4051	1.24E-01	2.55E-03	1.04E-01	1.36E-02	5.98E-05	6.87E-03	7.30E-03	2.95E-01	6.96E-03	1.11E-05	1.34E-04	9.84E-06	301.49
Max=	7.72	-94	17.79	0.4257	1.28E-01	2.64E-03	1.11E-01	1.41E-02	7.16E-05	7.09E-03	7.47E-03	3.09E-01	7.22E-03	1.15E-05	1.34E-04	1.04E-05	315.16

Temperate period — 9000 AD

	pH	Eh	TDS (g/L)	Ionic Str	Na	K	Ca	Mg	Fe	Alk	C	Cl	S(VI)	S(-II)	Si	P	£qM*°
Min=	6.48	-238	1.06	0.0158	1.20E-02	1.44E-04	7.73E-04	2.96E-04	7.01E-07	2.66E-04	2.58E-04	5.16E-03	6.06E-04	1.37E-19	1.21E-04	4.17E-08	14.29
0.1%	6.50	-234	1.07	0.0160	1.21E-02	1.47E-04	7.94E-04	3.00E-04	7.37E-07	2.95E-04	2.88E-04	5.36E-03	7.12E-04	2.59E-19	1.23E-04	4.96E-08	14.49
5%	6.57	-226	1.21	0.0189	1.38E-02	1.66E-04	9.62E-04	3.69E-04	1.41E-06	7.03E-04	7.55E-04	7.87E-03	8.90E-04	6.55E-16	1.26E-04	2.16E-07	17.02
Median=	7.08	-199	6.94	0.1469	6.00E-02	7.09E-04	2.23E-02	3.24E-03	1.94E-05	2.67E-03	3.24E-03	1.10E-01	2.08E-03	1.39E-06	1.30E-04	2.26E-06	120.31
95%	7.51	-128	11.13	0.2569	8.35E-02	1.40E-03	6.12E-02	7.17E-03	5.74E-05	6.89E-03	7.32E-03	1.88E-01	3.92E-03	4.85E-06	1.34E-04	9.84E-06	196.11
99.9%	7.56	-69	14.30	0.3336	1.01E-01	1.96E-03	8.14E-02	1.03E-02	7.74E-05	7.10E-03	7.50E-03	2.45E-01	5.40E-03	7.90E-06	1.35E-04	1.03E-05	252.76
Max=	7.57	-66	15.53	0.3617	1.08E-01	2.19E-03	8.69E-02	1.16E-02	8.17E-05	7.12E-03	7.51E-03	2.66E-01	6.00E-03	9.20E-06	1.35E-04	1.04E-05	274.46

Submerged seawater — 3000BC

	pH	Eh	TDS (g/L)	Ionic Str	Na	K	Ca	Mg	Fe	Alk	C	Cl	S(VI)	S(-II)	Si	P	£qM*°
Min=	7.22	-259	5.33	0.1078	3.36E-02	1.22E-04	3.04E-03	1.14E-04	3.49E-07	2.04E-04	1.90E-04	8.50E-02	3.07E-04	9.29E-08	1.23E-04	2.64E-08	94.47
0.1%	7.24	-253	5.78	0.1269	3.66E-02	1.39E-04	3.81E-03	1.17E-04	4.87E-07	2.05E-04	1.91E-04	9.53E-02	3.13E-04	1.04E-07	1.24E-04	2.69E-08	102.12
5%	7.34	-247	7.34	0.1625	4.31E-02	1.54E-04	5.65E-03	1.35E-04	6.69E-07	2.27E-04	2.14E-04	1.22E-01	3.60E-04	1.38E-07	1.26E-04	3.23E-08	129.97
Median=	7.57	-230	9.69	0.2178	5.66E-02	2.05E-04	5.39E-02	2.79E-04	9.42E-06	2.81E-04	2.75E-04	1.63E-01	5.38E-04	1.02E-06	1.28E-04	4.67E-08	171.41
95%	7.77	-216	11.98	0.2862	1.40E-01	2.95E-03	7.44E-02	1.58E-02	2.17E-05	1.63E-03	1.63E-03	2.07E-01	8.00E-03	1.54E-05	1.30E-04	1.16E-06	212.78
99.9%	7.93	-209	14.76	0.3532	1.57E-01	3.37E-03	9.21E-02	1.81E-02	2.57E-05	1.80E-03	1.78E-03	2.56E-01	9.14E-03	1.94E-05	1.32E-04	1.47E-06	261.96
Max=	8.03	-207	15.88	0.3799	1.59E-01	3.40E-03	9.91E-02	1.83E-02	2.66E-05	1.82E-03	1.80E-03	2.76E-01	9.22E-03	2.03E-05	1.33E-04	1.51E-06	281.55

A4.2 Temperate period: hydrological variant cases. All concentrations and the ionic strength are in mol/L, and the Eh is reported in mV.

Temperate - Extended Heterogeneity — 2000 AD

	pH	Eh	TDS (g/L)	Ionic Str	Na	K	Ca	Mg	Fe	Alk	C	Cl	S(VI)	S(-II)	Si	P	£qM*
Min=	7.11	-263	6.85	0.1498	4.08E-02	1.56E-04	2.82E-03	1.29E-04	2.95E-07	2.15E-04	2.02E-04	1.13E-01	3.38E-04	7.97E-08	1.20E-04	2.90E-08	121.36
0.1%	7.13	-254	7.35	0.1625	4.42E-02	1.62E-04	3.45E-03	1.39E-04	6.55E-07	2.18E-04	2.06E-04	1.22E-01	3.50E-04	8.75E-08	1.20E-04	2.99E-08	130.17
5%	7.24	-243	8.52	0.1871	5.09E-02	1.84E-04	5.56E-03	1.80E-04	9.78E-07	2.69E-04	2.62E-04	1.42E-01	4.73E-04	1.37E-07	1.25E-04	4.28E-08	151.19
Median=	7.45	-223	10.37	0.2212	7.51E-02	8.04E-04	4.53E-02	3.73E-03	1.08E-05	5.32E-04	5.48E-04	1.69E-01	2.17E-03	1.16E-05	1.28E-04	1.38E-07	182.63
95%	7.75	-210	12.99	0.3044	1.42E-01	2.98E-03	7.84E-02	1.60E-02	2.47E-05	1.71E-03	1.71E-03	2.21E-01	8.13E-03	1.84E-05	1.29E-04	1.27E-06	229.59
99.9%	7.95	-201	18.62	0.4430	1.52E-01	3.24E-03	1.13E-01	1.74E-02	3.00E-05	2.13E-03	2.15E-03	3.23E-01	8.80E-03	2.39E-05	1.30E-04	1.81E-06	329.75
Max=	8.10	-200	19.29	0.4586	1.56E-01	3.35E-03	1.17E-01	1.80E-02	3.08E-05	2.55E-03	2.58E-03	3.35E-01	9.08E-03	2.47E-05	1.32E-04	2.41E-06	341.49

Temperate - Extended Heterogeneity — 3000 AD

	pH	Eh	TDS (g/L)	Ionic Str	Na	K	Ca	Mg	Fe	Alk	C	Cl	S(VI)	S(-II)	Si	P	£qM*
Min=	7.05	-258	6.47	0.1217	4.28E-02	1.62E-04	2.91E-03	1.35E-04	4.11E-07	2.17E-04	2.05E-04	9.47E-02	3.47E-04	7.52E-08	1.20E-04	2.96E-08	110.94
0.1%	7.08	-249	7.46	0.1547	4.58E-02	1.70E-04	3.63E-03	1.52E-04	7.44E-07	2.24E-04	2.12E-04	1.20E-01	3.73E-04	9.72E-08	1.20E-04	3.11E-08	131.57
5%	7.16	-240	8.62	0.1839	5.30E-02	1.96E-04	5.65E-03	1.97E-04	1.08E-06	2.76E-04	2.71E-04	1.41E-01	4.96E-04	1.75E-07	1.23E-04	4.44E-08	152.17
Median=	7.42	-221	10.33	0.2198	8.39E-02	9.88E-04	4.53E-02	1.68E-03	1.25E-05	6.13E-04	6.41E-04	1.68E-01	2.64E-03	1.17E-05	1.28E-04	1.74E-07	181.58
95%	7.72	-206	15.12	0.3578	1.39E-01	2.93E-03	9.08E-02	1.57E-02	2.68E-05	1.80E-03	1.80E-03	2.61E-01	7.95E-03	2.07E-05	1.29E-04	1.36E-06	267.97
99.9%	7.88	-198	19.36	0.4531	1.49E-01	3.17E-03	1.11E-01	1.70E-02	3.24E-05	2.88E-03	3.00E-03	3.33E-01	8.60E-03	2.65E-05	1.30E-04	2.77E-06	342.06
Max=	8.01	-196	19.56	0.4612	1.54E-01	3.31E-03	1.20E-01	1.78E-02	3.34E-05	3.93E-03	4.07E-03	3.37E-01	8.97E-03	2.74E-05	1.31E-04	4.57E-06	345.80

Temperate - Extended Heterogeneity — 5000 AD

	pH	Eh	TDS (g/L)	Ionic Str	Na	K	Ca	Mg	Fe	Alk	C	Cl	S(VI)	S(-II)	Si	P	£qM*
Min=	6.69	-243	1.17	0.0181	1.36E-02	1.69E-04	8.10E-04	1.58E-04	7.73E-07	2.33E-04	2.22E-04	7.08E-03	4.13E-04	1.30E-09	1.21E-04	3.33E-08	16.37
0.1%	6.70	-241	1.50	0.0247	1.75E-02	1.86E-04	1.25E-03	1.85E-04	9.92E-07	2.46E-04	2.36E-04	1.28E-02	4.47E-04	5.57E-09	1.21E-04	3.67E-08	22.21
5%	6.86	-233	3.29	0.0604	3.98E-02	2.34E-04	2.60E-03	3.60E-04	1.52E-06	2.94E-04	2.91E-04	4.29E-02	5.75E-04	3.32E-07	1.23E-04	4.95E-08	54.35
Median=	7.32	-215	9.40	0.2045	7.63E-02	9.44E-04	3.93E-02	4.42E-03	1.92E-05	9.78E-04	1.05E-03	1.54E-01	2.63E-03	1.12E-05	1.28E-04	3.94E-07	165.63
95%	7.51	-185	14.59	0.3393	1.06E-01	2.04E-03	8.38E-02	1.07E-02	3.68E-05	5.33E-03	5.79E-03	2.49E-01	5.60E-03	3.02E-05	1.33E-04	6.84E-06	257.89
99.9%	7.61	-153	17.32	0.4123	1.23E-01	2.52E-03	1.06E-01	1.34E-02	5.36E-05	6.57E-03	7.06E-03	3.00E-01	6.86E-03	4.59E-05	1.34E-04	9.19E-06	306.69
Max=	7.72	-147	18.19	0.4318	1.27E-01	2.62E-03	1.10E-01	1.40E-02	5.50E-05	7.04E-03	7.42E-03	3.15E-01	7.12E-03	4.72E-05	1.34E-04	1.03E-05	321.75

Temperate - Extended Heterogeneity — 9000 AD

	pH	Eh	TDS (g/L)	Ionic Str	Na	K	Ca	Mg	Fe	Alk	C	Cl	S(VI)	S(-II)	Si	P	£qM*
Min=	6.58	-239	1.07	0.0160	1.20E-02	1.43E-04	7.85E-04	3.08E-04	7.18E-07	2.61E-04	2.52E-04	5.36E-03	5.42E-04	8.45E-15	1.22E-04	4.02E-08	14.49
0.1%	6.59	-235	1.12	0.0171	1.27E-02	1.57E-04	8.76E-04	3.73E-04	8.56E-07	2.82E-04	2.75E-04	6.37E-03	5.98E-04	1.30E-14	1.23E-04	4.60E-08	15.44
5%	6.67	-223	1.47	0.0243	1.66E-02	1.99E-04	1.54E-03	5.40E-04	2.15E-06	4.39E-04	4.52E-04	1.27E-02	9.38E-04	6.11E-11	1.25E-04	9.74E-08	21.72
Median=	7.11	-201	7.52	0.1631	6.03E-02	6.24E-04	2.97E-02	2.78E-03	1.98E-05	1.99E-03	2.37E-03	1.22E-01	1.88E-03	9.85E-06	1.29E-04	1.35E-06	132.10
95%	7.43	-141	12.46	0.2911	8.40E-02	1.33E-03	7.14E-02	6.75E-03	5.18E-05	6.36E-03	6.93E-03	2.13E-01	3.73E-03	4.44E-05	1.34E-04	8.65E-06	220.55
99.9%	7.54	-110	15.01	0.3544	1.00E-01	1.94E-03	8.97E-02	1.02E-02	6.63E-05	6.97E-03	7.39E-03	2.58E-01	5.33E-03	5.85E-05	1.34E-04	1.00E-05	265.86
Max=	7.58	-110	15.36	0.3625	1.08E-01	2.17E-03	9.22E-02	1.15E-02	6.70E-05	7.10E-03	7.48E-03	2.64E-01	5.94E-03	5.92E-05	1.35E-04	1.03E-05	271.62

Temperate - Hydrogeological variant case 5 — 2000AD

	pH	Eh	TDS (g/L)	Ionic Str	Na	K	Ca	Mg	Fe	Alk	C	Cl	S(VI)	S(-II)	Si	P	£qM*
Min=	7.11	-258	7.50	0.1596	4.31E-02	1.67E-04	3.21E-03	1.31E-04	4.24E-07	2.14E-04	2.01E-04	1.22E-01	3.38E-04	8.95E-08	1.22E-04	2.86E-08	132.49
0.1%	7.13	-255	7.71	0.1702	4.64E-02	1.73E-04	3.41E-03	1.48E-04	5.29E-07	2.20E-04	2.08E-04	1.29E-01	3.54E-04	1.14E-07	1.23E-04	3.04E-08	137.05
5%	7.21	-245	8.60	0.1864	5.29E-02	1.96E-04	4.97E-03	2.24E-04	1.03E-06	2.78E-04	2.72E-04	1.42E-01	4.98E-04	2.63E-07	1.26E-04	4.53E-08	152.43
Median=	7.42	-222	10.35	0.2170	8.59E-02	1.25E-03	3.90E-02	6.23E-03	1.14E-05	7.21E-04	7.56E-04	1.67E-01	3.39E-03	1.19E-05	1.28E-04	2.34E-07	181.84
95%	7.80	-209	12.39	0.2813	1.46E-01	3.08E-03	7.02E-02	1.65E-02	2.51E-05	1.72E-03	1.72E-03	2.08E-01	8.35E-03	1.89E-05	1.29E-04	1.31E-06	218.71
99.9%	7.97	-201	14.86	0.3433	1.55E-01	3.30E-03	8.40E-02	1.77E-02	2.99E-05	2.00E-03	2.00E-03	2.53E-01	8.95E-03	2.38E-05	1.30E-04	1.67E-06	262.72
Max=	8.01	-200	15.66	0.3637	1.57E-01	3.37E-03	8.95E-02	1.81E-02	3.10E-05	2.19E-03	2.19E-03	2.68E-01	9.15E-03	2.49E-05	1.30E-04	1.95E-06	276.93

Temperate - Hydrogeological variant case 9 — 2000AD

	pH	Eh	TDS (g/L)	Ionic Str	Na	K	Ca	Mg	Fe	Alk	C	Cl	S(VI)	S(-II)	Si	P	£qM*
Min=	7.10	-272	6.19	0.1190	4.25E-02	1.67E-04	2.26E-03	1.43E-04	1.71E-07	2.23E-04	2.10E-04	9.44E-02	3.69E-04	8.97E-08	1.22E-04	3.13E-08	108.60
0.1%	7.13	-264	7.28	0.1424	4.64E-02	1.74E-04	2.75E-03	1.68E-04	3.33E-07	2.34E-04	2.34E-04	1.13E-01	3.98E-04	1.08E-07	1.23E-04	3.39E-08	127.93
5%	7.22	-242	8.63	0.1855	5.36E-02	2.08E-04	5.44E-03	3.00E-04	1.09E-06	2.88E-04	2.83E-04	1.42E-01	5.46E-04	4.46E-07	1.26E-04	4.84E-08	152.66
Median=	7.40	-220	10.32	0.2136	9.06E-02	1.41E-03	3.57E-02	7.12E-03	1.05E-05	7.90E-04	8.34E-04	1.66E-01	3.84E-04	1.19E-05	1.28E-04	2.75E-07	181.46
95%	7.77	-209	12.31	0.2767	1.41E-01	2.98E-03	6.73E-02	1.60E-02	2.52E-05	1.70E-03	1.70E-03	2.06E-01	8.10E-03	1.90E-05	1.29E-04	1.26E-06	217.13
99.9%	8.11	-201	15.29	0.3560	1.51E-01	3.22E-03	8.55E-02	1.73E-02	3.00E-05	2.00E-03	2.01E-03	2.61E-01	8.73E-03	2.38E-05	1.32E-04	1.69E-06	270.65
Max=	8.23	-199	16.00	0.3801	1.55E-01	3.32E-03	9.68E-02	1.78E-02	3.13E-05	2.37E-03	2.39E-03	2.77E-01	9.00E-03	2.51E-05	1.34E-04	2.17E-06	283.78

A4.3 Glacial cycle. Base Case. All concentrations and the ionic strength are in mol/L, and the Eh is reported in mV.

Temperate — 0

	pH	Eh	TDS (g/L)	Ionic Str	Na	K	Ca	Mg	Fe	Alk	C	Cl	S(VI)	S(-II)	Si	P	£qM⁴⁺
Min=	6.44	-231	0.76	0.0107	6.87E-03	1.44E-04	7.98E-04	2.83E-04	7.80E-07	3.37E-03	5.17E-03	1.76E-04	7.92E-04	1.21E-20	1.26E-04	3.95E-06	9.22
0.1%	6.46	-231	0.76	0.0107	6.87E-03	1.44E-04	7.98E-04	2.85E-04	7.80E-07	3.43E-03	5.25E-03	1.76E-04	8.01E-04	2.54E-20	1.27E-04	4.08E-06	9.22
5%	6.50	-211	0.87	0.0132	7.54E-03	1.45E-04	1.44E-03	2.91E-04	1.81E-06	3.60E-03	5.44E-03	2.64E-04	8.22E-04	2.40E-19	1.29E-04	4.44E-06	11.19
Median=	6.67	-172	3.20	0.0676	1.93E-02	1.66E-04	1.60E-02	3.02E-04	1.07E-05	4.24E-03	5.95E-03	4.58E-02	8.60E-04	5.47E-06	1.32E-04	5.52E-06	52.05
95%	7.32	-68	6.94	0.1574	3.75E-02	1.99E-04	3.99E-02	3.09E-04	7.29E-05	6.54E-03	7.22E-03	1.12E-01	8.84E-04	6.43E-05	1.34E-04	8.71E-06	118.11
99.9%	7.53	-58	8.99	0.2069	4.75E-02	2.17E-04	5.31E-02	3.09E-04	8.38E-05	7.03E-03	7.48E-03	1.49E-01	8.86E-04	7.52E-05	1.35E-04	9.80E-06	154.44
Max=	7.53	-54	9.84	0.2273	5.16E-02	2.25E-04	5.85E-02	3.09E-04	8.80E-05	7.03E-03	7.48E-03	1.64E-01	8.86E-04	7.93E-05	1.35E-04	9.80E-06	169.40

Glacial (advance) — Ia

	pH	Eh	TDS (g/L)	Ionic Str	Na	K	Ca	Mg	Fe	Alk	C	Cl	S(VI)	S(-II)	Si	P	£qM⁴⁺
Min=	6.37	-224	0.81	0.0118	7.16E-03	1.28E-04	1.07E-03	2.50E-04	1.10E-06	3.06E-03	4.71E-03	1.23E-03	7.14E-04	1.12E-21	1.22E-04	3.20E-06	10.05
0.1%	6.38	-220	0.83	0.0123	7.30E-03	1.31E-04	1.21E-03	2.54E-04	1.35E-06	3.09E-03	4.77E-03	1.76E-03	7.23E-04	1.60E-21	1.22E-04	3.29E-06	10.47
5%	6.41	-192	1.35	0.0239	1.00E-02	1.48E-04	4.34E-03	2.76E-04	1.86E-06	3.26E-03	5.02E-03	1.21E-02	7.69E-04	9.15E-21	1.25E-04	3.69E-06	19.42
Median=	6.55	-166	5.43	0.1212	3.02E-02	1.86E-04	3.03E-02	2.94E-04	2.87E-06	3.77E-03	5.58E-03	8.57E-02	8.34E-04	8.39E-08	1.30E-04	4.74E-06	91.52
95%	6.98	-53	11.71	0.2723	6.06E-02	2.41E-04	7.05E-02	3.07E-04	8.96E-05	5.44E-03	6.65E-03	1.97E-01	8.79E-04	8.10E-05	1.34E-04	7.11E-06	202.33
99.9%	7.38	-45	15.01	0.3521	7.66E-02	2.70E-04	9.17E-02	3.09E-04	1.01E-04	6.70E-03	7.31E-03	2.55E-01	8.85E-04	9.28E-05	1.34E-04	9.01E-06	260.71
Max=	7.43	-43	15.86	0.3726	8.07E-02	2.78E-04	9.71E-02	3.09E-04	1.04E-04	6.81E-03	7.36E-03	2.71E-01	8.85E-04	9.56E-05	1.35E-04	9.24E-06	275.75

Glacial (advance) — IIa

	pH	Eh	TDS (g/L)	Ionic Str	Na	K	Ca	Mg	Fe	Alk	C	Cl	S(VI)	S(-II)	Si	P	£qM⁴⁺
Min=	6.34	-302	0.30	0.0067	1.47E-03	1.66E-05	1.73E-03	1.25E-05	9.08E-09	3.01E-04	2.65E-04	4.58E-03	2.91E-05	5.00E-22	1.18E-04	6.02E-08	4.96
0.1%	6.35	-293	0.33	0.0074	1.61E-03	1.72E-05	1.92E-03	1.37E-05	1.51E-08	3.27E-04	2.93E-04	5.11E-03	3.23E-05	6.00E-22	1.19E-04	6.83E-08	5.48
5%	6.38	-206	2.26	0.0482	1.30E-02	6.39E-05	1.15E-02	6.86E-05	1.57E-06	1.32E-03	1.46E-03	3.24E-02	1.87E-04	1.71E-21	1.22E-04	6.13E-07	37.06
Median=	6.46	-165	8.79	0.2023	4.65E-02	2.15E-04	5.18E-02	2.77E-04	6.15E-06	3.27E-03	5.03E-03	1.46E-01	7.72E-04	1.05E-06	1.27E-04	3.72E-06	150.96
95%	7.16	-45	15.30	0.3592	7.80E-02	2.73E-04	9.36E-02	2.99E-04	1.01E-04	4.07E-03	5.80E-03	2.61E-01	8.51E-04	9.23E-05	1.34E-04	5.21E-06	265.95
99.9%	8.49	-40	19.29	0.4556	9.73E-02	3.08E-04	1.19E-01	3.05E-04	1.09E-04	4.75E-03	6.27E-03	3.31E-01	8.71E-04	1.01E-04	1.41E-04	6.22E-06	336.31
Max=	8.54	-39	19.89	0.4701	1.00E-01	3.13E-04	1.23E-01	3.05E-04	1.11E-04	4.87E-03	6.33E-03	3.42E-01	8.73E-04	1.03E-04	1.42E-04	6.38E-06	347.02

Glacial (advance) — IIIa

	pH	Eh	TDS (g/L)	Ionic Str	Na	K	Ca	Mg	Fe	Alk	C	Cl	S(VI)	S(-II)	Si	P	£qM⁴⁺
Min=	6.36	-348	0.11	0.0023	4.37E-04	1.18E-05	5.95E-04	5.92E-06	7.51E-10	2.01E-04	1.37E-04	1.42E-03	1.04E-05	8.01E-22	1.20E-04	2.73E-08	1.65
0.1%	6.37	-342	0.12	0.0025	4.92E-04	1.20E-05	6.55E-04	6.20E-06	1.00E-09	2.03E-04	1.40E-04	1.60E-03	1.12E-05	1.49E-21	1.21E-04	2.78E-08	1.83
5%	6.48	-311	0.25	0.0055	1.19E-03	1.49E-05	1.41E-03	9.62E-06	8.79E-09	2.39E-04	1.97E-04	3.70E-03	2.07E-05	4.00E-19	1.27E-04	4.06E-08	4.08
Median=	7.57	-233	1.26	0.0291	6.49E-03	3.80E-05	7.45E-03	3.98E-05	5.45E-06	8.58E-04	8.82E-04	2.04E-02	1.06E-04	4.52E-07	1.36E-04	2.92E-07	21.56
95%	8.74	-72	8.68	0.2002	4.56E-02	2.08E-04	5.15E-02	2.86E-04	6.92E-05	3.56E-03	5.32E-03	1.44E-01	8.05E-04	6.08E-05	1.45E-04	4.29E-06	149.36
99.9%	9.21	-44	16.01	0.3763	8.12E-02	2.77E-04	9.81E-02	3.02E-04	1.02E-04	4.29E-03	5.97E-03	2.73E-01	8.60E-04	9.34E-05	1.62E-04	5.57E-06	278.44
Max=	9.27	-41	17.29	0.4071	8.76E-02	2.90E-04	1.06E-01	3.04E-04	1.07E-04	4.63E-03	6.15E-03	2.96E-01	8.68E-04	9.84E-05	1.65E-04	5.96E-06	301.01

Glacial (advance) — IVa

	pH	Eh	TDS (g/L)	Ionic Str	Na	K	Ca	Mg	Fe	Alk	C	Cl	S(VI)	S(-II)	Si	P	£qM⁴⁺
Min=	6.67	-372	0.05	0.0007	6.71E-05	1.06E-05	2.07E-04	4.61E-06	3.05E-10	1.87E-04	1.31E-04	1.90E-04	6.71E-06	5.45E-18	1.27E-04	2.47E-08	0.51
0.1%	6.70	-366	0.05	0.0007	7.91E-05	1.07E-05	2.09E-04	4.85E-06	3.61E-10	1.98E-04	1.33E-04	1.90E-04	7.39E-06	1.84E-17	1.28E-04	2.56E-08	0.51
5%	6.94	-327	0.16	0.0033	7.21E-04	1.33E-05	8.38E-04	7.77E-06	5.10E-09	2.23E-04	1.69E-04	2.12E-03	1.56E-05	2.77E-12	1.32E-04	3.44E-08	2.48
Median=	7.87	-254	0.99	0.0229	4.98E-03	2.87E-05	5.92E-03	2.33E-05	4.82E-06	5.05E-04	2.30E-03	1.62E-02	5.88E-05	3.67E-07	1.37E-04	1.36E-07	16.94
95%	8.99	-161	3.66	0.0851	1.90E-02	9.01E-05	2.20E-02	1.11E-04	2.70E-05	1.91E-03	2.30E-03	6.08E-02	3.07E-04	1.96E-05	1.52E-04	1.22E-06	63.15
99.9%	9.60	-98	7.65	0.1809	3.86E-02	1.40E-04	4.73E-02	1.82E-04	5.11E-05	2.84E-03	3.69E-03	1.31E-01	5.13E-04	4.34E-05	1.97E-04	2.60E-06	133.39
Max=	9.63	-90	8.96	0.2118	4.50E-02	1.52E-04	5.54E-02	2.50E-04	5.54E-05	3.78E-03	5.05E-03	1.53E-01	7.10E-04	4.74E-05	2.01E-04	4.30E-06	156.19

Glacial (advance) Va

	pH	Eh	TDS (g/L)	Ionic Str	Na	K	Ca	Mg	Fe	Alk	C	Cl	S(VI)	S(-II)	Si	P	£qM⁴⁺
Min=	7.15	-374	0.04	0.0006	4.15E-05	1.05E-05	1.86E-04	4.60E-06	2.86E-10	1.54E-04	1.01E-04	9.79E-05	6.71E-06	2.73E-11	1.34E-04	1.54E-08	0.43
0.1%	7.21	-365	0.05	0.0009	1.07E-04	1.08E-05	2.40E-04	4.79E-06	4.18E-10	1.58E-04	1.10E-04	3.03E-04	7.20E-06	3.50E-04	1.34E-04	1.71E-08	0.61
5%	7.40	-326	0.17	0.0036	7.75E-04	1.36E-05	9.16E-04	7.59E-06	5.21E-09	1.97E-04	1.48E-04	2.33E-03	1.48E-05	3.59E-08	1.35E-04	2.64E-08	2.65
Median=	7.98	-262	0.88	0.0203	4.38E-03	2.57E-05	5.28E-03	1.94E-05	4.48E-06	4.33E-04	4.11E-04	1.44E-02	4.77E-05	3.67E-07	1.37E-04	1.01E-07	15.00
95%	8.99	-217	1.78	0.0415	8.96E-03	4.56E-05	1.08E-02	5.10E-05	1.72E-05	1.09E-03	1.14E-03	2.95E-02	1.38E-04	9.94E-06	1.52E-04	4.34E-07	30.64
99.9%	9.57	-185	2.28	0.0534	1.15E-02	5.85E-05	1.39E-02	8.01E-05	2.22E-05	1.66E-03	1.79E-03	3.82E-02	2.22E-04	1.48E-05	1.93E-04	8.73E-07	39.39
Max=	9.66	-171	2.32	0.0543	1.18E-02	6.51E-05	1.41E-02	1.02E-04	2.46E-05	2.10E-03	2.32E-03	3.87E-02	2.87E-04	1.71E-05	2.06E-04	1.30E-06	40.12

Glacial (retreat) Vr

	pH	Eh	TDS (g/L)	Ionic Str	Na	K	Ca	Mg	Fe	Alk	C	Cl	S(VI)	S(-II)	Si	P	£qM⁴⁺
Min=	6.97	-357	0.10	0.0020	3.60E-04	1.12E-05	5.39E-04	4.67E-06	5.44E-10	1.22E-04	8.38E-05	1.24E-03	6.79E-06	4.07E-14	1.32E-04	9.94E-09	1.46
0.1%	7.04	-342	0.16	0.0034	6.62E-04	1.20E-05	9.03E-04	4.94E-06	1.24E-09	1.24E-04	8.63E-05	2.30E-03	7.39E-06	6.39E-13	1.32E-04	1.03E-08	2.49
5%	7.22	-293	0.80	0.0189	3.91E-03	2.12E-05	4.94E-03	8.83E-06	4.66E-08	1.64E-04	1.30E-04	1.36E-02	1.63E-05	3.10E-10	1.33E-04	1.83E-08	13.87
Median=	7.69	-244	2.62	0.0622	1.29E-02	4.42E-05	1.63E-02	2.10E-05	4.59E-06	4.06E-04	3.93E-04	4.49E-02	4.90E-05	4.06E-07	1.35E-04	8.54E-08	45.64
95%	8.42	-190	3.81	0.0905	1.89E-02	6.56E-05	2.37E-02	5.19E-05	2.22E-05	1.01E-03	1.09E-03	6.54E-02	1.38E-04	1.50E-05	1.40E-04	3.88E-07	66.52
99.9%	9.20	-155	4.41	0.1049	2.19E-02	7.87E-05	2.75E-02	8.04E-05	2.86E-05	1.51E-03	1.70E-03	7.58E-02	2.20E-04	2.12E-05	1.61E-04	7.73E-07	77.07
Max=	9.38	-139	4.53	0.1080	2.24E-02	8.47E-05	2.84E-02	1.02E-04	3.28E-05	1.84E-03	2.16E-03	7.83E-02	2.83E-04	2.53E-05	1.74E-04	1.12E-06	79.25

Glacial (retreat) IVr

	pH	Eh	TDS (g/L)	Ionic Str	Na	K	Ca	Mg	Fe	Alk	C	Cl	S(VI)	S(-II)	Si	P	£qM⁴⁺
Min=	6.82	-326	0.59	0.0139	2.81E-03	1.65E-05	3.68E-03	5.24E-06	3.22E-09	1.14E-04	7.23E-05	1.00E-02	7.46E-06	2.46E-16	1.27E-04	7.93E-09	10.19
0.1%	6.94	-321	0.62	0.0146	2.96E-03	1.68E-05	3.87E-03	5.46E-06	4.26E-09	1.19E-04	7.83E-05	1.06E-02	7.99E-06	9.84E-15	1.28E-04	9.12E-09	10.71
5%	7.11	-288	1.41	0.0335	6.89E-03	2.69E-05	8.83E-03	8.97E-06	6.94E-08	1.50E-04	1.19E-04	2.43E-02	1.58E-05	5.40E-12	1.30E-04	1.54E-08	24.58
Median=	7.64	-242	3.67	0.0876	1.81E-02	5.54E-05	2.30E-02	2.13E-05	5.08E-06	3.81E-04	3.69E-04	6.34E-02	4.79E-05	7.41E-07	1.34E-04	7.62E-08	64.24
95%	8.32	-170	7.64	0.1829	3.76E-02	1.03E-04	4.82E-02	5.31E-05	2.66E-05	9.51E-04	1.04E-03	1.33E-01	1.36E-04	1.95E-05	1.39E-04	3.53E-07	134.11
99.9%	8.82	-136	9.75	0.2335	4.79E-02	1.26E-04	6.15E-02	8.07E-05	3.55E-05	1.40E-03	1.63E-03	1.70E-01	2.17E-04	2.82E-05	1.47E-04	7.04E-07	171.22
Max=	8.87	-114	10.30	0.2470	5.06E-02	1.28E-04	6.51E-02	1.01E-04	4.34E-05	1.61E-03	1.98E-03	1.80E-01	2.73E-04	3.59E-05	1.48E-04	9.27E-07	180.99

Glacial (retreat) IIr

	pH	Eh	TDS (g/L)	Ionic Str	Na	K	Ca	Mg	Fe	Alk	C	Cl	S(VI)	S(-II)	Si	P	£qM⁴⁺
Min=	6.92	-360	0.09	0.0018	3.05E-04	1.10E-05	4.81E-04	4.23E-06	4.79E-10	1.16E-04	7.68E-05	1.07E-03	5.51E-06	4.43E-15	1.27E-04	8.63E-09	1.29
0.1%	7.02	-354	0.11	0.0022	4.08E-04	1.13E-05	6.00E-04	4.40E-06	6.10E-10	1.17E-04	7.86E-05	1.42E-03	5.90E-06	1.18E-13	1.28E-04	8.90E-09	1.63
5%	7.18	-325	0.37	0.0086	1.73E-03	1.44E-05	2.28E-03	5.61E-06	7.49E-09	1.37E-04	9.30E-05	6.17E-03	8.87E-06	1.13E-10	1.30E-04	1.22E-08	6.32
Median=	7.91	-260	2.30	0.0547	1.13E-02	3.84E-05	1.44E-02	1.53E-05	4.78E-06	2.76E-04	2.53E-04	3.96E-02	3.26E-05	4.02E-07	1.36E-04	4.51E-08	40.11
95%	8.92	-187	7.53	0.1802	3.71E-02	9.92E-05	4.75E-02	4.53E-05	2.37E-05	8.17E-04	8.74E-04	1.31E-01	1.14E-04	1.66E-05	1.50E-04	2.71E-07	132.17
99.9%	9.36	-149	10.07	0.2417	4.94E-02	1.25E-04	6.37E-02	6.51E-05	3.18E-05	1.14E-03	1.30E-03	1.76E-01	1.71E-04	2.46E-05	1.72E-04	4.92E-07	177.01
Max=	9.43	-130	11.10	0.2663	5.44E-02	1.35E-04	7.02E-02	8.48E-05	3.68E-05	1.42E-03	1.69E-03	1.94E-01	2.28E-04	2.94E-05	1.78E-04	7.34E-07	195.04

Submerged glacial lake Or

	pH	Eh	TDS (g/L)	Ionic Str	Na	K	Ca	Mg	Fe	Alk	C	Cl	S(VI)	S(-II)	Si	P	£qM⁴⁺
Min=	7.01	-334	0.41	0.0096	1.92E-03	1.45E-05	2.54E-03	4.70E-06	2.01E-09	1.03E-04	6.25E-05	6.87E-03	6.10E-06	7.22E-14	1.32E-04	6.19E-09	7.02
0.1%	7.11	-329	0.51	0.0120	2.41E-03	1.55E-05	3.17E-03	4.97E-06	2.79E-09	1.05E-04	6.55E-05	8.63E-03	6.65E-06	4.64E-12	1.32E-04	6.64E-09	8.77
5%	7.36	-304	1.33	0.0316	6.44E-03	2.48E-05	8.32E-03	6.73E-06	2.60E-08	1.16E-04	7.96E-05	2.29E-02	1.01E-05	1.35E-08	1.33E-04	8.72E-09	23.14
Median=	7.91	-260	2.92	0.0698	1.43E-02	4.42E-05	1.84E-02	1.45E-05	4.80E-06	2.48E-04	2.25E-04	5.07E-02	2.96E-05	6.18E-07	1.35E-04	3.75E-08	51.15
95%	8.57	-213	4.31	0.1030	2.12E-02	6.43E-05	2.71E-02	3.67E-05	1.91E-05	7.08E-04	7.36E-04	7.48E-02	9.29E-05	1.20E-05	1.42E-04	2.12E-07	75.54
99.9%	8.93	-168	5.15	0.1231	2.53E-02	7.96E-05	3.24E-02	5.75E-05	2.63E-05	1.05E-03	1.16E-03	8.94E-02	1.51E-04	1.91E-05	1.50E-04	4.18E-07	90.27
Max=	8.99	-145	5.25	0.1255	2.58E-02	8.74E-05	3.30E-02	7.32E-05	3.18E-05	1.29E-03	1.48E-03	9.12E-02	1.96E-04	2.45E-05	1.52E-04	6.08E-07	92.03

A4.4 Glacial cycle. Variant case: glacier advance N-S. All concentrations and the ionic strength are in mol/L, and the Eh is reported in mV.

Glacial N-S — Temperate 0

	pH	Eh	TDS (g/L)	Ionic Str	Na	K	Ca	Mg	Fe	Alk	C	Cl	S(VI)	S(-II)	Si	P	£qMq*
Min=	6.44	-231	0.76	0.0107	6.87E-03	1.44E-04	7.98E-04	2.83E-04	7.80E-07	3.37E-03	5.17E-03	1.76E-04	7.92E-04	1.21E-20	1.26E-04	3.95E-06	9.22
0.1%	6.46	-231	0.76	0.0107	6.87E-03	1.44E-04	7.98E-04	2.85E-04	7.80E-07	3.43E-03	5.25E-03	1.76E-04	8.01E-04	2.54E-20	1.27E-04	4.08E-06	9.22
5%	6.50	-211	0.87	0.0132	7.54E-03	1.45E-04	1.44E-03	2.91E-04	1.81E-06	3.60E-03	5.44E-03	2.64E-03	8.22E-04	2.40E-19	1.29E-04	4.44E-06	11.19
Median=	6.67	-172	3.20	0.0676	1.93E-02	1.66E-04	1.60E-02	3.02E-04	1.07E-05	4.24E-03	5.95E-03	4.58E-02	8.60E-04	5.47E-06	1.32E-04	5.52E-06	52.05
95%	7.32	-68	6.94	0.1574	3.75E-02	1.99E-04	3.99E-02	3.09E-04	7.29E-05	6.54E-03	7.22E-03	1.12E-01	8.84E-04	6.43E-05	1.34E-04	8.71E-06	118.11
99.9%	7.53	-58	8.99	0.2069	4.75E-02	2.17E-04	5.31E-02	3.09E-04	8.38E-05	7.03E-03	7.48E-03	1.49E-01	8.86E-04	7.52E-05	1.35E-04	9.80E-06	154.44
Max=	7.53	-54	9.84	0.2273	5.16E-02	2.25E-04	5.85E-02	3.09E-04	8.80E-05	7.03E-03	7.48E-03	1.64E-01	8.86E-04	7.93E-05	1.35E-04	9.80E-06	169.40

Glacial N-S — IIa

	pH	Eh	TDS (g/L)	Ionic Str	Na	K	Ca	Mg	Fe	Alk	C	Cl	S(VI)	S(-II)	Si	P	£qMq*
Min=	6.34	-331	0.10	0.0019	4.65E-04	1.41E-05	4.71E-04	1.17E-05	1.60E-09	3.38E-04	2.76E-04	1.05E-03	2.72E-05	5.36E-22	1.19E-04	8.14E-08	1.44
0.1%	6.35	-307	0.15	0.0028	7.65E-04	1.70E-05	6.54E-04	1.75E-05	7.00E-09	4.54E-04	4.08E-04	1.52E-03	4.38E-05	6.72E-22	1.19E-04	1.29E-07	2.14
5%	6.38	-224	0.72	0.0143	4.50E-03	5.29E-05	3.02E-03	8.58E-05	1.52E-06	1.84E-03	1.98E-03	7.88E-03	2.41E-04	1.91E-21	1.22E-04	1.05E-06	11.01
Median=	6.50	-165	6.89	0.1562	3.73E-02	1.99E-04	3.96E-02	2.83E-04	5.71E-06	3.44E-03	5.22E-03	1.12E-01	7.95E-04	6.28E-07	1.29E-04	4.07E-06	117.22
95%	7.46	-46	15.32	0.3596	7.81E-02	2.73E-04	9.37E-02	3.02E-04	1.00E-04	4.36E-03	6.01E-03	2.61E-01	8.62E-04	9.15E-05	1.36E-04	5.65E-06	266.20
99.9%	8.70	-41	18.83	0.4444	9.51E-02	3.04E-04	1.16E-01	3.07E-04	1.08E-04	5.69E-03	6.78E-03	3.23E-01	8.81E-04	9.99E-05	1.44E-04	7.43E-06	328.28
Max=	9.04	-40	19.44	0.4593	9.80E-02	3.09E-04	1.20E-01	3.08E-04	1.10E-04	6.02E-03	6.95E-03	3.34E-01	8.82E-04	1.02E-04	1.53E-04	7.88E-06	339.06

Glacial N-S — IVa

	pH	Eh	TDS (g/L)	Ionic Str	Na	K	Ca	Mg	Fe	Alk	C	Cl	S(VI)	S(-II)	Si	P	£qMq*
Min=	6.44	-372	0.05	0.0007	5.54E-05	1.06E-05	1.96E-04	4.68E-06	2.97E-10	2.16E-04	1.53E-04	1.42E-04	6.94E-06	1.12E-20	1.26E-04	3.16E-08	0.47
0.1%	6.44	-343	0.10	0.0018	4.04E-04	1.24E-05	4.36E-04	7.43E-06	9.80E-10	2.31E-04	1.70E-04	9.47E-04	1.47E-05	1.54E-20	1.27E-04	3.73E-08	1.34
5%	6.55	-309	0.17	0.0035	8.29E-04	1.57E-05	8.38E-04	1.29E-05	1.61E-08	3.30E-04	2.86E-04	2.03E-03	3.03E-05	3.41E-18	1.28E-04	7.26E-08	2.57
Median=	7.03	-196	2.35	0.0529	1.27E-02	8.10E-05	1.33E-02	1.04E-04	5.10E-06	1.83E-03	2.18E-03	3.67E-02	2.87E-04	3.73E-07	1.33E-04	1.13E-06	39.64
95%	8.74	-86	7.72	0.1793	4.01E-02	1.84E-04	4.63E-02	2.76E-04	5.88E-05	3.60E-03	5.23E-03	1.29E-01	7.80E-04	5.06E-05	1.45E-04	4.21E-06	133.13
99.9%	9.20	-55	9.66	0.2230	5.07E-02	2.23E-04	5.74E-02	3.01E-04	8.66E-05	4.84E-03	6.13E-03	1.61E-01	8.59E-04	7.80E-05	1.61E-04	6.11E-06	166.20
Max=	9.64	-54	9.97	0.2305	5.22E-02	2.26E-04	5.99E-02	3.06E-04	8.84E-05	5.34E-03	6.43E-03	1.66E-01	8.74E-04	7.98E-05	2.03E-04	6.63E-06	171.71

A4.5 Glacial cycle. Glacier advance over a frozen soil (permafrost) and periglacial period. All concentrations and the ionic strength are in mol/L, and the Eh is reported in mV.

Periglacial

	pH	Eh	TDS (g/L)	Ionic Str	Na	K	Ca	Mg	Fe	Alk	C	Cl	S(VI)	S(-II)	Si	P	$\sum qM^{q+}$
Min=	6.52	-199	1.28	0.0224	9.74E-03	1.49E-04	3.88E-03	2.93E-04	1.84E-06	3.68E-03	5.52E-03	1.07E-02	8.29E-04	2.50E-19	1.30E-04	4.59E-06	18.26
0.1%	6.52	-199	1.29	0.0225	9.78E-03	1.49E-04	3.93E-03	2.93E-04	1.84E-06	3.69E-03	5.52E-03	1.08E-02	8.29E-04	2.70E-19	1.30E-04	4.60E-06	18.40
5%	6.55	-194	1.41	0.0253	1.04E-02	1.50E-04	4.67E-03	2.95E-04	1.86E-06	3.79E-03	5.61E-03	1.31E-02	8.37E-04	1.36E-18	1.30E-04	4.78E-06	20.50
Median=	6.68	-163	3.10	0.0651	1.88E-02	1.65E-04	1.53E-02	3.02E-04	1.67E-06	4.28E-03	5.97E-03	4.39E-02	8.61E-04	1.14E-05	1.32E-04	5.57E-06	50.22
95%	6.96	-76	5.39	0.1202	3.00E-02	1.86E-04	3.00E-02	3.07E-04	6.59E-05	5.37E-03	6.61E-03	8.50E-02	8.78E-04	5.73E-05	1.34E-04	7.02E-06	90.79
99.9%	7.01	-69	6.18	0.1390	3.38E-02	1.93E-04	3.50E-02	3.07E-04	7.24E-05	5.54E-03	6.70E-03	8.89E-02	8.80E-04	6.38E-05	1.34E-04	7.25E-06	104.61
Max=	7.01	-68	6.21	0.1397	3.40E-02	1.93E-04	3.52E-02	3.07E-04	7.28E-05	5.56E-03	6.71E-03	9.94E-02	8.80E-04	6.41E-05	1.34E-04	7.26E-06	105.15

Permafrost (glacier advance I)

	pH	Eh	TDS (g/L)	Ionic Str	Na	K	Ca	Mg	Fe	Alk	C	Cl	S(VI)	S(-II)	Si	P	$\sum qM^{q+}$
Min=	6.33	-190	2.15	0.0447	1.33E-02	1.25E-04	1.04E-02	2.23E-04	1.67E-06	2.83E-03	4.31E-03	2.92E-02	6.34E-04	4.00E-22	1.17E-04	2.64E-06	34.57
0.1%	6.33	-184	2.49	0.0522	1.51E-02	1.32E-04	1.23E-02	2.37E-04	1.83E-06	2.85E-03	4.33E-03	3.48E-02	6.74E-04	4.30E-22	1.17E-04	2.68E-06	40.27
5%	6.36	-171	5.72	0.1280	3.16E-02	1.89E-04	3.21E-02	2.59E-04	2.24E-06	2.97E-03	4.56E-03	9.08E-02	7.10E-04	9.80E-22	1.20E-04	2.99E-06	96.54
Median=	6.42	-143	11.65	0.2710	6.04E-02	2.41E-04	7.01E-02	2.77E-04	2.13E-05	3.26E-03	5.02E-03	1.96E-01	7.74E-04	1.56E-05	1.25E-04	3.70E-06	201.39
95%	6.54	-42	17.91	0.4222	9.06E-02	2.96E-04	1.10E-01	2.94E-04	1.05E-04	3.74E-03	5.56E-03	3.07E-01	8.33E-04	9.67E-05	1.30E-04	4.69E-06	312.00
99.9%	6.79	-39	21.21	0.5021	1.07E-01	3.25E-04	1.32E-01	3.01E-04	1.12E-04	4.24E-03	5.94E-03	3.65E-01	8.59E-04	1.04E-04	1.33E-04	5.50E-06	370.43
Max=	6.84	-38	21.56	0.5104	1.08E-01	3.28E-04	1.34E-01	3.03E-04	1.13E-04	4.39E-03	6.05E-03	3.71E-01	8.64E-04	1.05E-04	1.33E-04	5.73E-06	376.53

Permafrost (glacier advance II)

	pH	Eh	TDS (g/L)	Ionic Str	Na	K	Ca	Mg	Fe	Alk	C	Cl	S(VI)	S(-II)	Si	P	$\sum qM^{q+}$
Min=	6.33	-208	1.31	0.0273	7.86E-03	7.92E-05	6.37E-03	1.38E-04	1.32E-06	2.60E-03	3.03E-03	1.73E-04	3.89E-04	3.70E-22	1.17E-04	1.97E-06	20.96
0.1%	6.33	-199	1.58	0.0334	9.51E-03	8.66E-05	7.87E-03	1.48E-04	1.47E-06	2.76E-03	3.24E-03	2.16E-02	4.20E-04	4.04E-22	1.17E-04	2.18E-06	25.58
5%	6.35	-172	5.64	0.1265	3.11E-02	1.82E-04	3.18E-02	2.55E-04	2.19E-06	2.93E-03	4.47E-03	8.97E-02	6.95E-04	8.53E-22	1.19E-04	2.88E-06	95.37
Median=	6.42	-163	11.61	0.2702	6.01E-02	2.38E-04	6.99E-02	2.69E-04	1.44E-05	3.21E-03	4.89E-03	1.96E-01	7.50E-04	8.86E-06	1.25E-04	3.57E-06	200.73
95%	6.55	-42	18.85	0.4449	9.52E-02	3.04E-04	1.16E-01	2.89E-04	1.06E-04	3.62E-03	5.42E-03	3.24E-01	8.17E-04	9.78E-05	1.30E-04	4.44E-06	328.59
99.9%	7.03	-38	21.72	0.5143	1.09E-01	3.29E-04	1.35E-01	2.97E-04	1.13E-04	3.91E-03	5.71E-03	3.74E-01	8.45E-04	1.05E-04	1.34E-04	4.99E-06	379.40
Max=	7.12	-38	22.24	0.5270	1.12E-01	3.34E-04	1.38E-01	2.98E-04	1.14E-04	3.95E-03	5.74E-03	3.84E-01	8.47E-04	1.06E-04	1.34E-04	5.05E-06	388.63

Permafrost (glacier advance IV)

	pH	Eh	TDS (g/L)	Ionic Str	Na	K	Ca	Mg	Fe	Alk	C	Cl	S(VI)	S(-II)	Si	P	$\sum qM^{q+}$
Min=	6.45	-365	0.05	0.0009	1.21E-04	1.10E-05	2.38E-04	4.79E-06	3.68E-10	1.85E-04	1.23E-04	3.07E-04	7.17E-06	9.38E-21	1.23E-04	2.25E-08	0.62
0.1%	6.56	-355	0.07	0.0013	2.27E-04	1.13E-05	3.32E-04	5.33E-06	5.62E-10	1.90E-04	1.26E-04	6.31E-04	8.67E-06	3.04E-19	1.24E-04	2.35E-08	0.92
5%	6.82	-297	0.34	0.0075	1.65E-03	1.68E-05	1.90E-03	1.15E-05	4.96E-08	2.77E-04	2.37E-04	5.01E-03	2.61E-05	4.89E-15	1.29E-04	5.05E-08	5.55
Median=	7.30	-214	2.06	0.0479	1.06E-02	5.20E-05	1.24E-02	5.64E-05	5.14E-06	1.14E-03	1.23E-03	3.39E-02	1.53E-04	3.85E-07	1.34E-04	4.75E-07	35.46
95%	8.53	-130	6.98	0.1648	3.52E-02	1.22E-04	4.30E-02	1.09E-04	3.66E-05	1.76E-03	2.17E-03	1.19E-01	2.98E-04	2.91E-05	1.42E-04	1.08E-06	121.54
99.9%	9.42	-77	12.85	0.3041	6.45E-02	2.05E-04	7.96E-02	1.62E-04	6.73E-05	2.17E-03	2.98E-03	2.21E-01	4.40E-04	5.94E-05	1.76E-04	1.64E-06	224.28
Max=	9.54	-55	14.62	0.3464	7.33E-02	2.30E-04	9.08E-02	2.40E-04	8.79E-05	2.92E-03	4.36E-03	2.52E-01	6.64E-04	7.95E-05	1.90E-04	2.96E-06	255.34